Macroevolutionary Dynamics of Vertebral Column Evolution in African Cichlids

Callum Vincent Bucklow

A thesis submitted in fulfilment of the requirements
for the degree of Doctor of Philosophy
at the University of Oxford

Corpus Christi College

Hilary 2025

Dedication

In loving memory of Michelle Wilkinson, my secondary school biology teacher who ignited my passion and love of biology

"*Very truly I tell you, the one who believes has eternal life*" (John 6:47)

Abstract

African cichlids comprise over 1,800 species of freshwater teleosts, with spectacular adaptive radiations in Lakes Tanganyika, Malawi, and Victoria giving rise to extraordinary morphological diversity. However, the evolution of the cichlid axial skeleton has remained largely overlooked, despite the importance of the axial skeleton in the diversification of other teleostean clades. Here, we show that elongation of the fusiform body has been critical for adaptation in multiple African cichlid lineages. Although occupation of axial morphospace broadly correlates with the age of the lacustrine radiations, rates of vertebral count evolution are still higher in older lineages, suggesting constraints have limited axial evolution in the lacustrine radiations of African cichlids. Intriguingly, while vertebral addition contributes to body elongation, we find that intraspecific variation in vertebral count has been strongly canalised during African cichlid diversification. Therefore, despite vertebral counts being highly evolvable somitic fidelity has not undergone selection during African cichlid diversification. Furthermore, individuals with increased vertebral counts exhibit no detectable differences in body aspect ratio, indicating that intraspecific variation in vertebral number is decoupled from macroevolutionary patterns of elongation, where the addition of vertebrae has driven body elongation. Within Lake Malawi, we show that vertebral shape modification correlates with ecological divergence. However, much of the identified shape variation is likely being driven by elongation of the body. In addition, neither vertebral centra elongation nor increased intervertebral spacing appears to contribute to overall body elongation, suggesting that these traits have not evolved to modulate vertebral column flexibility. Collectively, our findings demonstrate the importance of comparative approaches to elucidate axial morphological evolution and highlight African cichlid fishes as a powerful model for investigating the evolutionary and developmental dynamics of the teleostean vertebral column. Future work will focus on dissecting the genetic mechanisms underpinning axial evolution in Lake Malawi cichlid hybrid crosses using quantitative trait locus (QTL) analysis.

Acknowledgements

I end all of my public talks making the joke that it takes a village to raise a doctoral student, and my research would not have been possible without the help and support of a large number of people.

I must first thank my primary supervisor Dr Berta Verd for her continual support and for her willingness to let me pursue my own interests and to push my research into the directions I wished to follow. I look forward to continuing to work with you in the future, both as a member of your lab and beyond. I have been extremely lucky to find a supervisor with whom I just 'click'. My second thanks must go to my co-supervisor Professor Roger Benson, whose patience throughout my DPhil has been greatly appreciated. Without his guidance much of the analysis herein would not have been possible. In addition, his expertise in generating the μCT-scan data has been invaluable. I note that I started this project not even being aware of cichlids and with only a basic knowledge of evolutionary biology (my undergraduate degree is in biomedically-focused biochemistry). I therefore appreciate the great patience that both of my supervisors have shown me over the last few years.

I have developed a deep love of cichlids over the past few years and this would not have been possible without the aide of multiple different people. Both Professor Martin Genner and Professor George Turner were instrumental in providing specimens for the μCT-scan dataset that we released, but an additional, special thanks must go to both of them for patiently answering the vast number of questions I have asked them over the years. I thank Walter Salzburger too, for providing access to his research collections so that I could increase my sampling of riverine haplochromines and also Fabrizia Ronco for her dataset of 2D X-rays of Lake Tanganyikan cichlids. A final thanks goes to both Dr Michael Oliver and Professor Melanie Stiassny whose passion for African cichlids was infectious and greatly appreciated.

I thank Dr Emília Santos for providing the *Astatotilapia callitpera* '*mbaka*' consistute half of the hybrid crosses, and also for her support and guidance in fish husbandry. A great thanks must be extended to the fish technicians, Christine Soper, Helen Sanders and Allex Turner who I know I have driven completely insane the past few years with my poor planning and my chaotic approach to fish work. Whilst my hybrids do not feature in my thesis (albeit for future work), raising these lines has been, by some margin, the

most fun and the most definitely the part I am most proud and it would not have been possible without the dedication and care of the technicians.

Thank you to all members of the Verd lab, both past and present who had to deal with my chaos, including James Hammond, Shannon Taylor and Georgina Stooke-Vaughan, who have helped me immensely during my DPhil. A special thank you to James, in particular, for his his continued friendship and fantastic sense of humour, who has been a source of great amusement and perhaps more importantly, great intellectual discussion.

A great thank you to my partner Jeff, who none of this would have been possible without. I love you deeply and cannot imagine my life without you. Your patience, fortitude and warmth continues to amaze me, much as it did when I first met you. On the matter of warmth, a thank you to my writing partner and living hot water bottle, Oreo, who was by my side every night of writing.

Contents

1 Introduction

1.1 Background and Motivation

The vertebral column, the defining anatomical feature of all vertebrate animals, is critical for movement, not only facilitating muscle attachment to support locomotion, but also providing a protective casing for the spinal cord and nerve roots required for the transduction of the central and peripheral signals essential for movement [Ford, 1937]. Teleosts (infraclass Teleostei) are the largest group within Actinopterygii, commonly known as ray-finned fishes, and account for more than 50% of all described vertebrate species [Near and Thacker, 2024]. Therefore, elucidating the dynamics of macroevolutionary change in the structure of the teleost vertebral column is central to understanding morphological and functional diversification in a large group.

Unlike in tetrapods, that are defined by the presence of five well defined vertebral types: cervical, thoracic, lumbar, sacral and caudal (tail) [Cerbus et al., 2024], the teleostean vertebral column has traditionally been divided into two domains: the precaudal and caudal [Oliver, 2024, Woltering et al., 2018]. Precaudal vertebrae are defined by the presence of ventrolateral basapophyses for the attachment of ribs, which protect the viscera and provide points of attachment for muscle and tendons. Caudal vertebrae, in contrast, are defined by the presence of a closed haemal arch formed by haemal spines, which provide important points of articulation with the anal and caudal fins required for swimming [Ford, 1937]. Teleosts and other ray-finned fishes (actinopterygians) have been the subject of multiple macroevolutionary studies examining the evolution of the vertebral column [Ward and Brainerd, 2007, Ward and Mehta, 2010, Mehta et al., 2010]. Whilst these studies have identified patterns of macroevolutionary change across teleosts, spanning many orders and families, little is known about the evolutionary dynamics of vertebral column evolution on smaller phylogenetic scales that contribute to these larger scale patterns.

African cichlids (Ovalentaria, Cichliformes, Cichlidae, Pseudocrenilabrinae) are an extremely speciose and morphologically diverse subfamily of teleosts found throughout the rivers and freshwater lakes of Africa and the Middle East [Astudillo-Clavijo et al., 2023]. The subfamily includes the adaptive radiations of the Great Rift Valley lakes of

Tanganyika, Malawi and Victoria, where the vast majority of their species diversity has arisen [McGee et al., 2020]. Pseudocrenilabrinae diverged from the rest of Cichlidae approximately 64–58 mya [Friedman et al., 2013, McGee et al., 2020, Svardal et al., 2021] and have evolved remarkable phenotypic diversity [Malinsky et al., 2018, Ronco et al., 2021]. Aided by developments in whole-genome sequencing technologies [Svardal et al., 2021], it has been possible to considerably improve our understanding of the phylogenetic relationships among cichlids [Meier et al., 2017, Ronco et al., 2021, Malinsky et al., 2018, McGee et al., 2020, Astudillo-Clavijo et al., 2023]. Previously intractable macroevolutionary studies, such as the convergent evolution of hypertrophied lips [Masonick et al., 2022] can now take advantage of relatively robust phylogenies based on whole-genome sequences.

African cichlids have evolved remarkable diversity in the total number and relative proportions of precaudal and caudal vertebrae [Oliver, 2024] and in body shape [Malinsky et al., 2018, Ronco et al., 2021]. Therefore, there are now opportunities to take advantage of the high phylogenetic resolution to investigate the evolution of the axial and appendicular skeleton, that is of key importance in teleost diversification [Price et al., 2015, Baxter et al., 2022]. However, the evolution of the vertebral column (and more broadly the axial skeleton) has been overlooked in African cichlids [Oliver, 2024] and no macroevolutionary study on the axial skeleton has been conducted in African cichlids, despite the presence of well-defined phylogenies for individual lake radiations [Genner and Turner, 2012, Malinsky et al., 2018, Ronco et al., 2021, Masonick et al., 2022] and for the wider subfamily [McGee et al., 2020, Astudillo-Clavijo et al., 2023], as well as extensive taxonomic sampling in museum collections [Bucklow et al., 2024], representing a significant gap in our understanding of the evolution of Pseudocrenilabrinae.

The diverse life history of Pseudocrenilabrinae, including multiple, independent, adaptive radiations into lacustrine systems, featuring extremely rapid diversification [Malinsky et al., 2018, Ronco et al., 2021, Meier et al., 2017], and the existence of relatively stable, basal riverine lineages, provides a powerful comparative model to investigate the macroevolutionary dynamics of trait evolution on multiple scales. This is particularly curious given that multiple, extensive and rapid adaptive radiations, as well as relatively basal riverine lineages are nestled within Pseudocrenilabrinae. Therefore, African cichlids provide a powerful natural experiment to elucidate how factors such as ecological opportunity, divergence time, speciation rates [McGee et al., 2020], or developmental constraint influence phenotypic evolution. Therefore, I wanted to investigate the following: determine whether evolutionary modification of the vertebral column has occurred within distinct ecological niches, characterise the broad morphological diversity of axial phenotypes across the subfamily, and to investigate and compare the macroevolutionary dynamics that underpin vertebral evolution. Together, these aims allow us to assess whether common evolutionary processes govern the diversification of the vertebral column

across the major African cichlid radiations, as well as the riverine lineages that connect the radiations, and ultimately decipher the generalisable macroevolutionary patterns of trait evolution that emerge across large clades and adaptive radiations.

Vertebral counts and identity are ultimately determined by the embryonic process of somitogenesis and subsequent anterior–posterior patterning directed by *Hox* genes [Iimura et al., 2009]. Differences in the number and type of vertebrae among adults (and other post-embryonic stages) of different species provide evidence of both somitic and homeotic changes in development since their divergence from a common ancestor [Cerbus et al., 2024]. When extrapolated to broader phylogenetic scales, these differences offer valuable insights into the macroevolutionary dynamics of somitogenesis and vertebral regionalisation across clades [Soul and Benson, 2017, Mehta et al., 2010, Narita and Kuratani, 2005]. Although many macroevolutionary studies have explored the evolution of the vertebral column, most have focused on tetrapods [Jones et al., 2018a,b, Cerbus et al., 2024], while comparatively few have examined vertebral count and identity in ray-finned fishes (Actinopterygii), including teleosts [Ward and Brainerd, 2007, Mehta et al., 2010]. Our interest in examining the evolution of total vertebral counts and the relative proportions of their identity in African cichlids stems from a broader aim to understand how the mechanisms underlying somitogenesis and axial patterning have evolved across a diverse vertebrate clade. This approach provides an opportunity to infer causative links between developmental processes and macroevolutionary patterns of vertebral change. In addition, despite the emphasis on interspecific patterns of vertebral count evolution, relatively few studies have investigated intraspecific variation, even though such variation is well documented across vertebrates [Slijepčević et al., 2015, Hu et al., 2016, Sosa and Hospitaleche, 2024], including teleost fishes [Yamahira et al., 2006, Tibblin et al., 2016, Oliver, 2024]. Exploring intraspecific variation in vertebral number could provide important insights into the degree of canalisation in somitic counts and, by extension, the evolutionary fidelity of somitogenesis as a large vertebrate clade has diversified.

1.2 Literature Review

1.2.1 Origin of Cichlids

Cichlids (family Cichlidae) emerged as a distinct lineage approximately 80–100 million years ago during the Late Cretaceous period [Malabarba et al., 2014, Matschiner, 2019, Matschiner et al., 2020]. Today, there are an estimated 3,000–4,000 cichlid species, accounting for roughly 10% of all extant bony fishes [Salzburger, 2018]. The family Cichlidae is divided into several subfamilies, which are largely distinguished by their geographic distribution. Cichlinae and Pseudocrenilabrinae are endemic to Central/South America and Africa, respectively [Matschiner, 2019]. In addition, a few isolated lineages are found in

southern India, Iran, and along the eastern Mediterranean coast (see Figure 1.1A). Most of the family's species richness is concentrated within Cichlinae and Pseudocrenilabrinae, which together diverged from other cichlids approximately 78–72 million years ago [Matschiner, 2019]. Pseudocrenilabrinae itself diverged somewhat later, around 64–58 million years ago [Friedman et al., 2013, McGee et al., 2020, Svardal et al., 2021] (Figure 1.1B). Notably, divergence times between major cichlid lineages, such as the African and South American clades, occurred well after the breakup of Gondwana, with a temporal gap of about 40 million years [Matschiner, 2019]. This timing challenges a strict vicariance model. The earliest fossil cichlids date to the Eocene (∼46 mya) [Murray, 2001b,a], long after the Gondwanan fragmentation, and molecular clock estimates place the origin of the family in the Paleocene (approximately 65–57 mya) [Friedman et al., 2013], further supporting a post-Gondwanan origin. Therefore, the dispersion of cichlids cannot be fully explained by vicariance alone. Instead, transoceanic dispersal or other mechanisms likely played a role in their current distribution [Matschiner, 2019], alongside more recent and rapid diversification events [McGee et al., 2020].

1.2.2 Diversification of Pseudocrenilabrinae

African cichlids are an extremely speciose and morphologically diverse subfamily of teleost fishes distributed across the rivers and freshwater lakes of Africa, the Levant and the Middle East [Astudillo-Clavijo et al., 2023]. The group includes the iconic adaptive radiations of the Great Rift Valley lakes Tanganyika, Malawi, and Victoria (Figure 1.1C), which together account for the majority of the subfamily's species diversity [McGee et al., 2020]. The subfamily is subdivided into multiple tribes, although the exact number remains debated [Astudillo-Clavijo et al., 2023, Oliver, 2024]. Tribal-level phylogenetic relationships were most recently resolved by Astudillo-Clavijo et al. [2023], who also provides an excellent and thorough discussion on the taxonomic and phylogenetic relationships of African cichlids. Nonetheless, we provide a brief overview of various African tribes here.

Within Pseudocrenilabrinae, early divergences gave rise to the predominantly riverine West and Central African tribes: Heterochromini, Tylochromini, Chromidotilapiini, Pelmatochromini, and Hemichromini. The placement of Heterochromini within Pseudocrenilabrinae was initially challenged by morphological [Stiassny, 1987, 1990] and some molecular studies [Farias et al., 1999, Keck and Hulsey, 2014]; however, most molecular evidence now supports its position as the sister group to all other extant African lineages [Friedman et al., 2013, Astudillo-Clavijo et al., 2023]. Among these early-diverging groups, Chromidotilapiini is particularly notable for the extremely elongate, rheophilic genus *Teleogramma*, native to the Western Congo River basin. These fishes are distinguished by their elongated heads and uninterrupted lateral line, a feature atypical among cichlids [Stiassny and Alter, 2015].

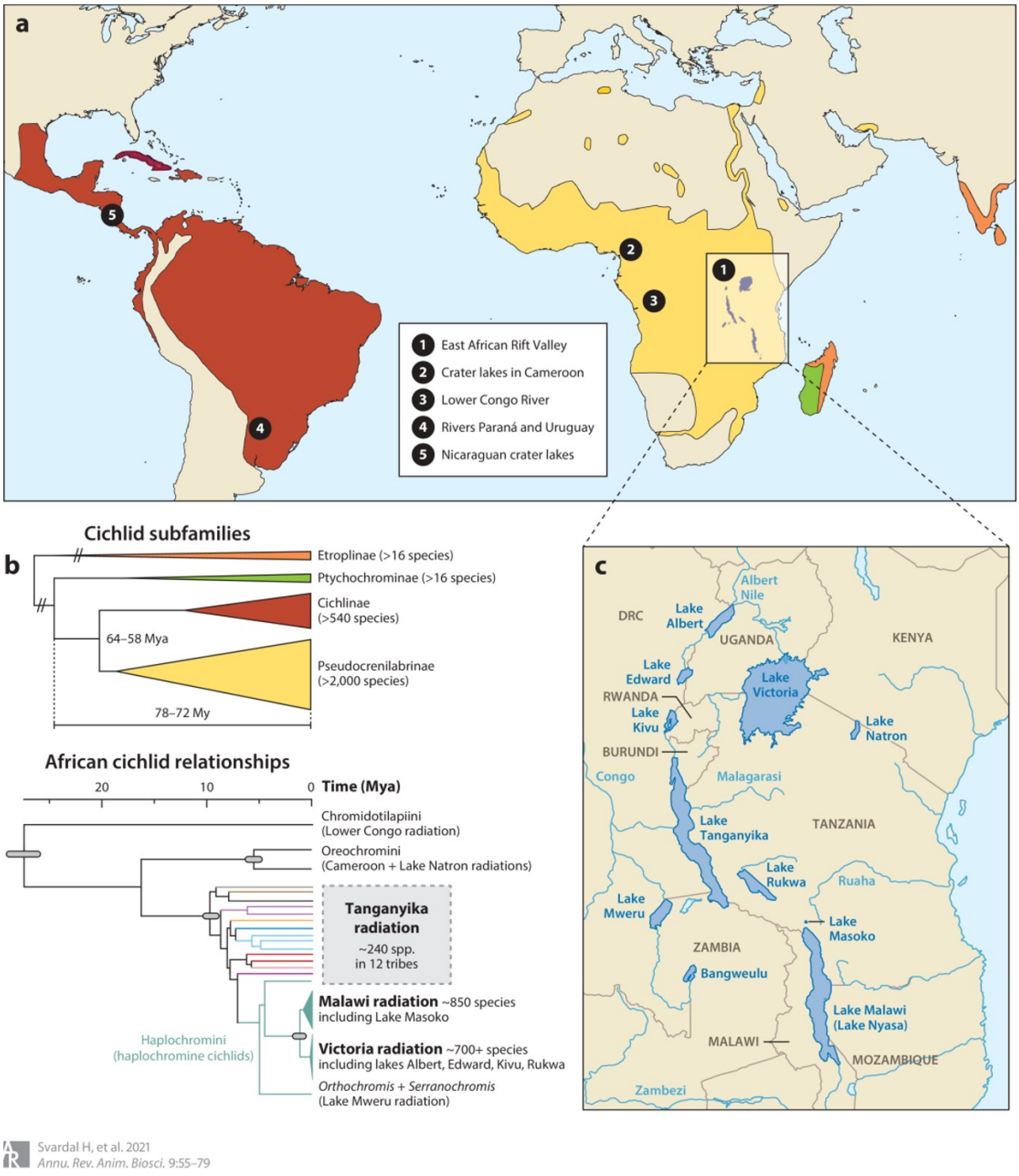

Figure 1.1: Distribution of cichlids. (A) Global distribution of cichlid fishes. Colours indicate subfamily affiliation and correspond to those shown in the phylogeny in (B). (B) Cladogram showing estimated divergence times of the major cichlid subfamilies, including Cichlinae (American cichlids) and Pseudocrenilabrinae (African cichlids), based on estimates from Matschiner [2019], Matschiner et al. [2020]. The lower ultrametric tree provides a simplified view of relationships among major Pseudocrenilabrinae lineages, with divergence times following Ronco et al. [2021]. (C) Map of East Africa highlighting the major lakes and river systems of the Great Rift Valley, which harbours the majority of cichlid species diversity. Figure adapted from Svardal et al. [2021].

Later divergences gave rise to additional riverine tribes, many of which were formerly grouped under the catch-all 'Tilapiini' [Poll, 1986]. The grouping was redefined by Dunz and Schliewen [2013], but their interrelationships nonetheless remain poorly resolved [Astudillo-Clavijo et al., 2023]. Major tribes include Oreochromini, which includes commercially important food fishes such as *Sarotherodon galilaeus* and *Oreochromis niloticus*, as well as Steatocranini and Gobiocichlini. The latter two include elongate rheophilic clades native to the rapids of the Congo River. Members of Gobiocichla are especially notable for losing the articulation of the anal fin with the caudal vertebral domain and for possessing an elongated swim bladder, accommodated by an expansion of the precaudal vertebral region [Oliver, 2024].

The remaining tribes, part of the East African Radiation (EAR) are limited to East Africa. Approximately 12 tribes are endemic to Lake Tanganyika [Ronco et al., 2020]. Lake Tanganyika was likely colonised by cichlids approximately 9-12 mya [Irisarri et al., 2018, Ronco et al., 2021], coinciding with the geological formation of the lake [Cohen et al., 1993]. Tribes include: Bathybatini, Benthochromini, Boulengerochromini, Cyphotilapiini, Cyprichromini, Ectodini, Eretmodini, Lamprologini, Limnochromini, Perissodini, Trematocarini and Tropheini, the latter of which is a haplochromine subtribe [Oliver, 2024]. Phylogenetic relationships between the Lake Tanganyika endemic tribes were recently resolved by Ronco et al. [2021], who also previously provided a detailed taxonomic discussion of the species endemic to the radiation [Ronco et al., 2020].

1.2.3 Origin and Divergence of Haplochromines

Haplochromini is the most speciose tribe within the subfamily Pseudocrenilabrinae, comprising at least 1,000 species [Turner et al., 2001]. Unlike the adaptive radiation of Lake Tanganyika, which involves multiple cichlid tribes [Ronco et al., 2020, Svardal et al., 2021], the radiations of Lakes Malawi and Victoria are composed exclusively of haplochromines [Meier et al., 2017, Malinsky et al., 2018]. All haplochromines are maternal mouthbrooders, a trait they share with several other African cichlid lineages [Duponchelle et al., 2008]. Molecular evidence places Haplochromini as the sister clade to Eretmodini [Meyer et al., 2017, Irisarri et al., 2018, Ronco et al., 2021], a tribe endemic to Lake Tanganyika [Ronco et al., 2020]. The so-called 'modern haplochromines' [Salzburger et al., 2005] are specifically recovered as sister to a clade comprising *Orthochromis* (sometimes referred to as 'Orthochromini'), as well as *Ctenochromis*, and Haplochromini *sensu lato*, including the Tanganyikan tribe Tropheini [Astudillo-Clavijo et al., 2023].

Two contrasting and contentious hypotheses have been proposed regarding the origin of Haplochromini. The '*Out of Tanganyika*' hypothesis suggests that the tribe originated within Lake Tanganyika around 5–6 million years ago and subsequently dispersed into East African rivers, where they seeded the major radiations of Lakes Malawi and

Victoria, as well as other radiations associated with the broader Lake Victoria region [Salzburger et al., 2005, Koblmüller et al., 2008]. In contrast, the '*Melting Pot [of] Tanganyika*' hypothesis [Weiss et al., 2015] posits that the origin of Haplochromini predates the formation of Lake Tanganyika, potentially diverging from other Pseudocrenilabrinae lineages as early as 22 million years ago [Schedel et al., 2019]. Support for this older origin includes putative haplochromine fossils dated to 9–10 million years ago from a paleolake in the Central Kenyan Rift, north-east of Lake Tanganyika. This fossil suggests that haplochromines were present outside the lake well before the timeline proposed by the '*Out of Tanganyika*' hypothesis [Altner et al., 2020]. Nonetheless, extensive molecular evidence, including the nested placement of haplochromines within the Lake Tanganyika radiation, continues to support the view that extant haplochromines ultimately derive from Tanganyikan endemics, with 'modern haplochromines' arising from a riverine ancestor that later recolonised Lake Tanganyika [Salzburger et al., 2005, Ronco et al., 2021].

The haplochromine cichlids of Lakes Malawi and Victoria represent two sister radiations that likely diverged from riverine ancestors in the Great Ruaha River approximately 4 million years ago (3.2-3.9 mya) [Irisarri et al., 2018, Svardal et al., 2020, Genner et al., 2015, Turner et al., 2021], and between themselves approximately one million years later (2.0-2.9 mya) [Svardal et al., 2020]. Early mtDNA-based phylogenies placed riverine haplochromines native to the [Great] Ruaha river, such as *Astatotilapia sp.* 'Ruaha blue', as sister taxa to the Lake Malawi radiation [Genner et al., 2015]. However, genome-wide analyses have since shown that *A. gigliolii* and *A. sp.* 'Ruaha blue', themselves sister taxa, form a clade that is sister to both the Malawi and Victoria radiations [Svardal et al., 2020]. This revised topology likely reflects an ancient hybridisation event involving the common ancestor of both lake radiations prior to their diversification (see Figure 1.2), but nonetheless suggests that ancestral hybridisation events may have been critical in driving the explosive haplochromine adaptive radiations of Lakes Malawi and Victoria. Nonetheless, extensive work is currently underway to better characterise the riverine haplochromines, particularly the polyphyletic genus *Astatotilapia* [Turner et al., 2021], and future research will likely further clarify the connection between riverine haplochromines and the Lake Malawi and Victoria radiations.

1.2.4 Lake Malawi Cichlids

Lake Malawi haplochromine cichlids represent a particularly speciose and phenotypically diverse adaptive radiation of lacustrine fishes. This diversity, comprising approximately 850 species, is the most extensive adaptive radiation of vertebrates so far identified [Turner et al., 2001, Genner and Turner, 2012]. Molecular clock analyses estimate the radiation to be approximately 800 thousand years old [Malinsky et al., 2018]. Despite their high phenotypic diversity, genetic variation between Lake Malawi cichlids is extremely low.

Whole genomic comparisons of representatives from all seven distinct ecomorphological groups within Lake Malawi, estimated an average DNA sequence divergence of just 0.19-0.27% [Malinsky et al., 2018] – a range comparable to that within human populations [Svardal et al., 2021]. In addition, a relatively low DNA mutation rate; that alone cannot account for the estimated divergence time of Lake Malawi cichlids [Malinsky et al., 2018, Svardal et al., 2021] and overlapping distributions of inter- and intraspecific (heterozygosity) genetic variation [Malinsky et al., 2018] only further complicates our understanding of this enigmatic adaptive radiation.

1.2.5 Distinct Ecomorphological Groups in Lake Malawi

The radiation is divided into seven distinct groups, which cluster both genetically and broadly according to ecology, such as feeding behaviour, preference along the benthic-pelagic axis and depth preference [Malinsky et al., 2018]. These groups include: the riverine generalist (*Astatotilapia calliptera*) [Turner et al., 2021], the rock-dwelling 'mbuna' [Genner and Turner, 2005], the benthics (shallow and deep); the zooplanktivorous utaka [Turner et al., 2022] and the pelagic-limnetic zone-preferring *Diplotaxodon* and *Rhamphochromis* (see Figure 1.2). Oliver [2024] recently subdivided the haplochromines of Lake Malawi into three subtribes, Rhamphochromina (*Rhamphochromis*, *Diplotaxodon* and *Pallidochromis*), Pseudotropheina (Mbuna) and Cyrtocarina (the benthics). However, despite these recent taxonomic refinements, we retain the broader ecological groupings used in earlier studies, as they more clearly reflect functional and morphological divergence across the radiation. I therefore provide a brief breakdown of each ecomorphological group below.

Diplotaxodon* and *Rhamphochromis

The *Diplotaxodon* and *Rhamphochromis* groups are two reciprocally monophyletic diverging lineages of Lake Malawi cichlids [Malinsky et al., 2018] that have adapted to the pelagic-limnetic zone of Lake Malawi [Hahn et al., 2017]. Notably, it also includes the monotypic genus *Pallidochromis* (represented by *Pallidochromis tokolosh*), however little is known about the species as it has not been observed in the wild [Oliver, 2024]. The majority of species in *Diplotaxodon* and *Rhamphochromis* (and *Pallidochromis*) are piscivorous, although several species, including *Diplotaxodon limnothrissa* are predominantly zooplanktivorous [Turner, 1994]. Large-bodied *Rhamphochromis* primarily feed on Lake Malawi sardines (usipa; *Engraulicypris sardella*) and endemic cichlids (e.g. utaka). Members of *Diplotaxodon* and *Rhamphochromis* are among the deepest-living of all Lake Malawi cichlids, with representatives of both being caught at depths exceeding 200 metres – the 'twilight zone' where light is almost completely absent [Hahn et al., 2017].

Remarkable size variation is present particularly within *Rhamphochromis*. *Rham-*

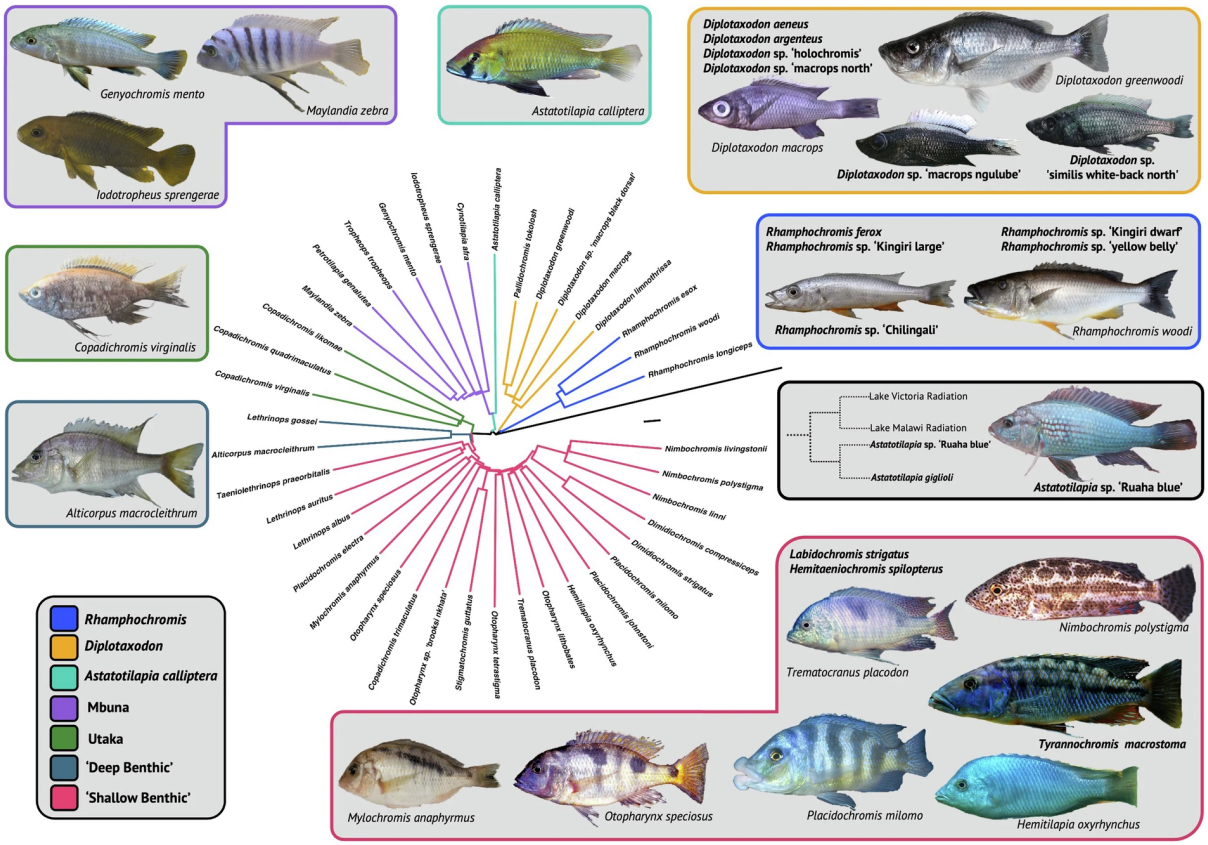

Figure 1.2: Phylogeny of Lake Malawi cichlids. Branches of the tree are coloured according to the seven ecomorphological groups. Representative species, including images, are indicated for each group where box colours match the tree branches. A cladogram depicting the relationship between the Lake Victoria, Lake Malawi and the *Astatotilapia* species native to the Great Ruaha River is indicated in the black box. Black bar: 2×10^{-4} substitutions per base pair. Fish images used with permission from Ad Konings (*Alticorpus macrocleithrum*, *Diplotaxodon greenwoodi*, *Genyochromis mento*, *Hemitilapia oxyrhynchus*, *Iodotrophesus sprengerae*, *Nimbochromis polystigma*, *Placidochromis milomo* and *Trematocranus placodon*), George F. Turner (*Astatotilapia sp.* 'Ruaha blue' [Turner et al., 2021], *Diplotaxodon macrops*, *Mylochromis anaphyrmus*, *Otopharynx speciosus* and *Rhamphochromis woodi*), Martin J. Genner (*Diplotaxodon sp.* 'similis white-back north', *Diplotaxodon sp.* 'macrops ngulube' and *Rhamphochromis sp.* 'Chilingali'), Hannes Svardal (*Copadichromis virginalis*) and Callum V. Bucklow (*Maylandia zebra*). Fish images are not to scale. Figure adapted from Bucklow et al. [2024].

phochromis woodi is considered to be one of the largest Lake Malawi cichlids, measuring a standard length (SL) of up to 40 cm [Turner et al., 2004]. In contrast, the smallest known member of *Rhamphochromis*, *Rhamphochromis sp. 'Kingiri dwarf'*, endemic to the crater lake Kingiri, do not exceed 7.5 cm SL in the wild [Turner et al., 2019]. Similarly, wild caught *Rhamphochromis* sp. 'Chilingali' are also small bodied, with maximum observed standard length of 10.6 cm [Genner et al., 2007], which makes them relatively amenable to laboratory study. Its elongate body, supported by relatively high vertebral counts, has made it a useful model in evolutionary developmental biology [Santos et al., 2023], particularly for the study of somitogenesis [Marconi et al., 2023], the developmental process that gives rise to the vertebral precursors. Their usefulness as a model for the study of somitogenesis partly stems from the genus also evolving relatively high vertebral counts (35-40 [Bucklow et al., 2024]). The genus contains *Rhamphochromis esox*, which has evolved a maximum number of 40 vertebrae, tied with the maximum number recorded for the subfamily in *Bathybates fasciatus* [Stiassny, 1981, Oliver, 2024], a pelagic piscivore endemic to Lake Tanganyika [Ronco et al., 2020].

Deep and Shallow Benthics

Oliver [2024] groups the shallow and deep benthics into the subtribe Cyrtocarina without defining any morphological synapomorphies. However, they do suggest that they can broadly be differentiated by their preference for demersal or epibenthic, over sand, mud, rocky or intermediate habitats. Deep-water benthic species are found below 50m, a 'twilight' zone with very little visible light. The group includes genera such as *Alticorpus* whose members are characterised by the presence of greatly enlarged cranial sensory openings and lateral line canals that they use to detect prey in the sediment. Together, the shallow and deep benthic species group represent hundreds of species, the majority of which are shallow preferring, inhabiting inshore habitats of Lake Malawi, such as the sand or mud lake floor, or sand-rock transitional zones [Malinsky et al., 2018]. It includes large, deep-bodied ambush predators, such as those in the genus *Nimbochromis*. These remarkable 'sleepers' bury themselves in sandy substrate and snatch unsuspecting prey attracted by the disturbed sediment [Konings, 2016]. The group also includes active, elongate pursuit piscivores, such as those belonging to *Dimidiochromis* and *Champsochromis*. In addition, it contains trophic specialists like the molluscivores *Mylochromis anaphyrmus* and *Trematocranus placodon*. Trematocranus placodon, in particular, is notable for helping to regulate populations of the gastropods *Bulinus nyassanus* and *Melanoides tuberculata*, which serve as intermediate hosts for *Schistosoma* flukeworms [Evers et al., 2006].

A recent phylogeny constructed by Blumer et al. [2025] further argues that the deep and shallow benthics are monophyletic groups [Malinsky et al., 2018], but also suggests

that they can be broadly distinguished by the frequencies of five large chromosomal inversions on chromosomes 2, 9-11 and 13, that were previously reported to be present within the 'benthics' sub-radiation [Kumar et al., 2025]. The chromosomal inversions were likely introduced into the sub-radiation via three primary ancestral hybridisation events. Inversions on chromosomes 9 and 11 were transferred to the 'benthics' via an admixture event between the *Diplotaxodon* lineage, with further hybridisation events between an '*A. calliptera-like*' lineage and a non-endemic haplochromine lineage transferring the remaining chromosomal inversions. Fixation of these inversions is likely to have been important for adaptation along a depth gradient. Protein-coding genes within these chromosomal inversions were found to be under positive selection (dN/dS) and whose zebrafish (*Danio rerio*) orthologs have been associated with vision, mechanoreception and nervous system function [Blumer et al., 2025], all of which have previously been shown to be important in adaptation along a depth gradient in cichlids [Hahn et al., 2017].

Mbuna

The mbuna group dominates the rocky shores of Lake Malawi and has long served as a model system for studying rapid speciation and adaptive radiation [Albertson, 2008, Conith and Albertson, 2021, Genner and Turner, 2005]. Like the shallow-benthic cichlids, the mbuna comprise hundreds of species, many of which remain undescribed [Konings, 2016, Genner and Turner, 2005]. Genera within this group are typically distinguished by differences in dentition. For example, *Cynotilapia*, which is unusual among mbuna for its planktivorous diet, possesses relatively simple unicuspid (conical) teeth [Konings, 2016, Ribbink et al., 1983, Kassam et al., 2005]. In contrast, more typical mbuna such as *Maylandia* (also referred to as *Metriaclima* [Stauffer Jr et al., 1997], a junior synonym [Scharpf, 2025]), *Tropheops*, and *Iodotropheus* have multiple rows of closely packed bicuspid teeth. *Petrotilapia* exhibits an even more complex dentition, with a mix of tri- and unicuspid teeth [Marsh, 1983]. These dental morphologies are well-suited for scraping and pulling epilithic algae from the rocky substrates that define their preferred habitats [Ribbink et al., 1983, Holzberg, 1978].

Among the mbuna, *Genyochromis mento* stands out as a highly specialised lepidophage (scale-eater), targeting the caudal and anal fins of other cichlids in rocky habitats [Ribbink et al., 1983, Konings, 2016, Takeuchi et al., 2019]. Intriguingly, individuals exhibit a striking lateral bias: right-leaning and left-leaning individuals preferentially attack the corresponding side of their prey, a behaviour that correlates with asymmetry in the dentary. However, this jaw laterality, as judged by the angle of laterality, is less pronounced in *G. mento* than in *Perissodus microlepis* [Takeuchi et al., 2019], a lepidophage endemic to Lake Tanganyika [Ronco et al., 2020]. This difference is likely a result of phylogenetic constraint from their shorter evolutionary history and their herbivorous ancestors

[Takeuchi et al., 2019], highlighting that constraint can arise as a consequence of short evolutionary timescales and ancestral condition.

Astatotilapia calliptera

Astatotilapia is polyphyletic and current members of the genus are widespread across East and North Africa [Genner et al., 2015, Svardal et al., 2021, Turner et al., 2021]. Only one species of *Astatotilapia* is native to Lake Malawi, *Astatotilapia calliptera*, which is also found in East African rivers flowing eastward to the Indian Ocean, from the Rovuma River in the north, to the Save River in the south. Populations of *A. calliptera* differ in life history strategies [Parsons et al., 2017] and are also undergoing sympatric speciation along a depth gradient in at least one location (Lake Masoko) [Genner et al., 2007], where littoral and benthic *A. calliptera* ecomorphs have diverged in multiple characteristics, including body shape and trophic specialism, in approximately 1000 years [Genner et al., 2007]. Given the wide distribution of the species, it is perhaps unsurprising that intraspecific genetic variation within the species is comparable to that of the whole Lake Malawi radiation [Malinsky et al., 2018, Svardal et al., 2020]. Despite their wide distribution and relatively large intraspecific genetic variation, they phylogenetically cluster within the Lake Malawi radiation (Figure 1), forming a sister clade to the mbuna, with which they share an excess of alleles [Malinsky et al., 2018, Genner and Turner, 2012]. This pattern, alongside a perceived riverine 'generalist' lifestyle, has led to the hypothesis that either Lake Malawi cichlids radiated from an *A. calliptera-like* ancestor or that *A. calliptera* is the sympatric ancestor of all Lake Malawi cichlids [Malinsky et al., 2018, Turner et al., 2021, Svardal et al., 2021].

Utaka

Zooplankton-feeding, shoaling cichlids which are commonly referred to as 'utaka'. Utaka is primarily made up of species belonging to *Copadichromis* [Anseeuw et al., 2012], with a small number of species also belonging to *Mchenga* and *Nyassachromis* [Stauffer and Konings, 2006]. Utaka feed in the water column, and can be commonly found close to the shore [Konings, 2016]. *Copadichromis* are generally characterised by their relatively small, highly protrusible mouths, that they use to suck zooplankton into their mouths, as well as numerous long gill rakers which strain plankton from the water that enters their mouths as a result of their sucking feeding mechanism [Konings, 2016, Turner et al., 2022].

1.2.6 Structure of the Teleostean Vertebral Column

The vertebral column, a defining anatomical feature of all vertebrate animals, is critical for movement, not only facilitating muscle attachment to support locomotion, but also

providing a protective casing for the spinal cord and nerve roots required for the transduction of the central and peripheral signals essential for movement [Ford, 1937]. The vertebral column of vertebrates consists of two features: vertebral centra, which form around the notochord and form the central axis of the trunk skeleton, and the neural and haemal arches, which attach to the centra dorsally and ventrally, respectively, enveloping the axial blood vessels and the spinal cord [Fleming et al., 2015]. The teleostean vertebral column has traditionally been divided into two domains: the precaudal and caudal (Figure 1.3A). Precaudal vertebrae are characterised by ventrolateral basapophyses that serve as attachment sites for pleural ribs (Figure 1.3C), which protect the viscera and provide anchorage for muscles and tendons. Caudal vertebrae, in contrast, are defined by the presence of a closed haemal arch formed by haemal spines (Figure 1.3D), which provide articulation points for the anal and caudal fins required for swimming [Ford, 1937].

Division of the vertebral column into just two domains is partly because of the relatively homogenous vertebral shape present along the anterior-posterior axis [De Clercq et al., 2017]. Constraints placed on the structure of the vertebral column due to a fully aquatic environment may be responsible for this homogenisation. Both skates and cetaceans also have what appear to be relatively homogenised vertebral columns. However, landmarked-based geometric morphometric quantification of vertebral shape variation has demonstrated the presence of multiple domains nested within the precaudal and caudal domains, with the number of regions being comparable to tetrapods [Criswell et al., 2021, Gillet et al., 2024].

Consistent with this, previous studies have suggested that the teleostean vertebral column has more than two distinct regions. Anatomical and histological characterisation of vertebral morphology in juvenile Chinook salmon (*Oncorhynchus tshawytscha*) identified at least six distinct domains: (1) post-cranial vertebrae, (2) ribless vertebrae immediately posterior to the cranium, (3) precaudal vertebrae, (4) transitional vertebrae, a highly variable region exhibiting features of both precaudal and caudal vertebrae, where vertebrae may possess rudimentary haemal spines while still being associated with pleural ribs and ventrolateral basapophyses, (5) caudal vertebrae, and (6) preural and ural vertebrae [De Clercq et al., 2017]. This regional pattern appears to be consistent across salmonoids, where a more recent study demonstrated that vertebral length alone was sufficient to define five regions in the vertebral column (minus the ural domain) in six additional species of salmonoid [Sankar et al., 2024]. The number of subdivision of domains is comparable to cichlids. Quantification of vertebral lengths and heights in *Coptozon zillii* and *Oreocrhomis aureus*, members of the Coptodoini and Oreochromini tribes, respectively, identified six domains in the adult vertebral column [Jawad et al., 2018] broadly aligning with those identified in Chinook salmon (see Figure 1.3B), domains also identified following characterisation of the skeletal ontogeny of the haplochromine

Astatotilapia burtoni [Woltering et al., 2018]. However, despite the previous efficacy of geometric morphometrics of 3D vertebral shape to define regions along the vertebral column [Criswell et al., 2021, Gillet et al., 2024], it has not yet been attempted in teleosts.

1.2.7 Evolution of Vertebral Column in Teleosts

The number, type, relative proportions and shapes of vertebrae, have been extensively modified in teleosts. *Mola mola* (Ocean sunfish), adapted to float on the ocean surface, has just 17 vertebrae and the caudal fin has been lost in the closely related *Mola tecta* [Britz and Johnson, 2005], whereas the extremely elongate deep sea *Nemichthys scolopaceus* (slender snipe eel) has upwards of 740 vertebrae [Deniz and Ağilkaya, 2018]. In syngnathidids (seahorses, pipefishes, and seadragons), pleural ribs and epicentrals, associated with precaudal vertebrae and which act as attachment points for tendons and muscle [Liem and Sanderson, 1986], have been secondarily lost [Small et al., 2016, Schneider et al., 2023].

The structure of the vertebral column has been the focus of macroevolutionary studies too. Ward and Brainerd [2007] previously demonstrated that precaudal and caudal vertebral counts have evolved independently of one another in actinopterygians and elasmobranchs (cartilaginous fishes), permitting clades to independently modulate the number of precaudal and caudal vertebrae. Anguilliformes, for example, have disproportionally added caudal vertebrae to support their elongate bodies. In contrast, however, Polypteriformes (bichirs, reed or ropefishes) have dramatically increased the number of precaudal vertebrae relative to caudal vertebrae [Ward and Brainerd, 2007, Ward and Kley, 2012], a dramatic shift in vertebral column regionalisation which may aid in their demersal lifestyle [Ward and Kley, 2012]. The evolutionary modification of vertebral shape has also been implicated in adaptation along the benthic-pelagic axis. Benthic species (e.g., flounders) possess larger notochordal foramina and shorter centra for enhanced flexibility, which may enable substrate manoeuvring and ambush behaviours, while pelagic species have narrower foramina and shorter centra, the latter of which may increase vertebral column flexibility, permitting optimisation of swimming at pelagic depths [Baxter et al., 2022].

In elopomorphs (tarpons, ladyfishes, and eels), increasing the total number of vertebrae has been important in driving the extreme elongation present in the clade [Mehta et al., 2010]. Indeed, elongation of the whole body appears to be the primary axis of body shape diversification across a number of teleostean clades [Claverie and Wainwright, 2014]. However, additional mechanisms are clearly important for the elongation of the teleostean body. Although cranial elongation is typically associated with an increase in overall body aspect ratio, it does not correlate with total vertebral count [Mehta et al., 2010]. In addition, fast predatory fish such as barracuda or Scombriformes have

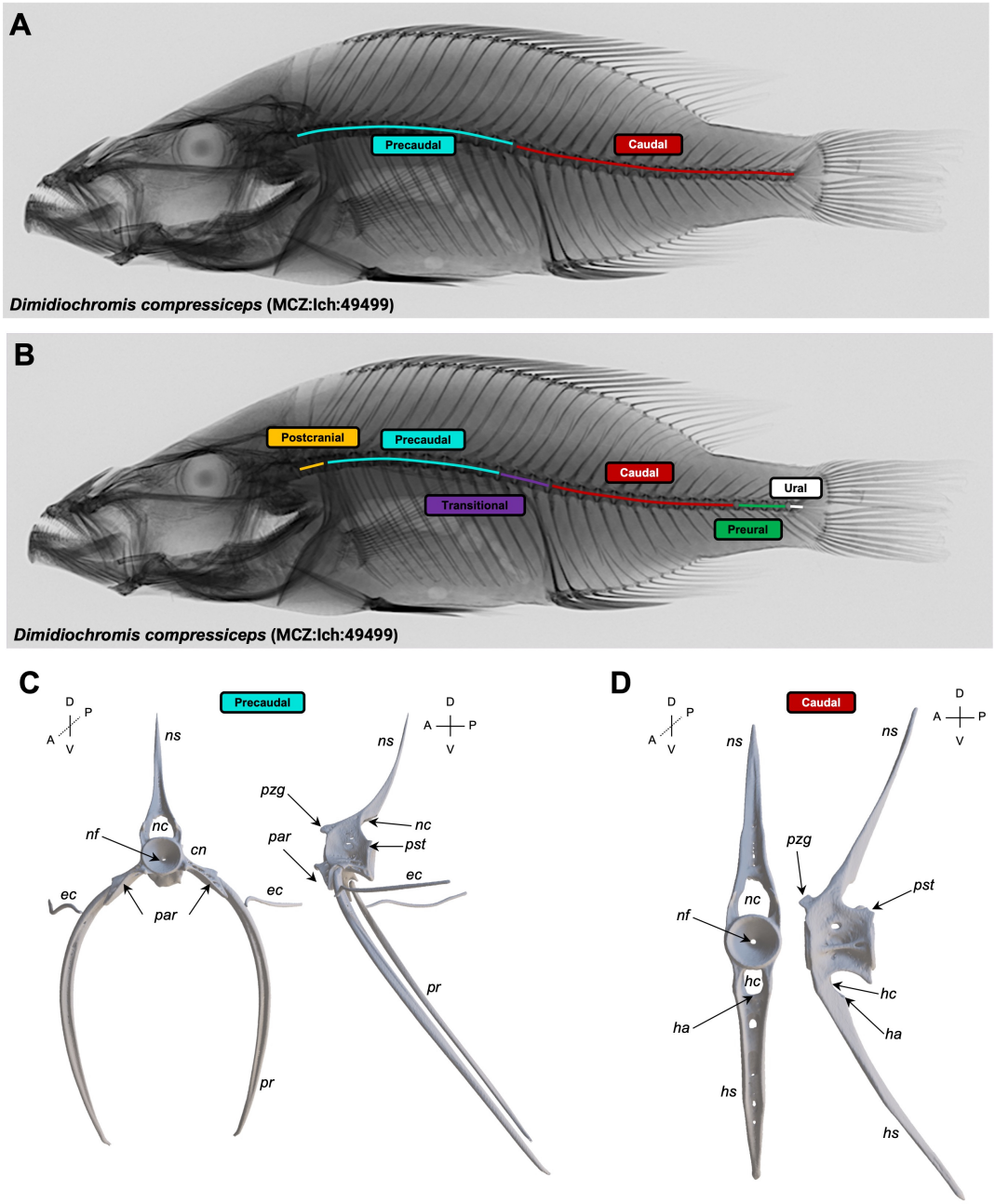

Figure 1.3: The teleostean vertebral column is divided into two domains. (A) lateral whole body x-ray of *Dimidiochromis compressiceps*, a species endemic to Lake Malawi, with the traditional precaudal and caudal domains indicated. (B) The same x-ray of *Dimidiochromis compressiceps*, instead marked with the six regions identified by Jawad et al. [2018] and Woltering et al. [2018]. Labelled precaudal (C) and caudal vertebrae (D) from *Maylandia zebra*. Note that the two vertebral types are differentiated by the presence (caudal) or absence (precaudal) of a haemal arch (*ha*) formed by a haemal spine (*hs*). Orientations are indicated as compasses for each image. Abbreviations are as follows: centrum (*cn*); epicentrals (*ec*); haemal canal (*hc*); neural canal (*nc*); neural foramen (*nf*); neural spine (*ns*); parapophyses (*par*); pleural ribs (*pr*); postzygapophysis (*pst*); prezygapophysis (*pzg*).

relatively few vertebrae compared with other similarly elongate fish [Mehta et al., 2010], opting instead to modulate the vertebral aspect ratio to generate fewer but more elongate vertebrae, which may stiffen their body axis, providing better propulsion when pursuing prey [Jimenez et al., 2023]. Therefore, body elongation in teleosts has also been shaped by mechanisms other than changes in vertebral number but nonetheless demonstrates the importance of the vertebral column on elongation of the body. However, the evolutionary relationship between vertebral counts and body elongation has not been investigated in African cichlids.

1.2.8 Somitogenesis and Regionalisation

Vertebral precursors and by extension vertebrae, arise from somites, paired transient embryonic segments that rhythmically bud from the presomitic mesoderm (PSM) during axial elongation during somitogenesis [Christ and Ordahl, 1995, Morin-Kensicki et al., 2002, Maroto et al., 2012]. The number of somites is partially controlled by the frequency of an intracellular oscillator known as the segmentation clock, which synchronises differentiation of cells in the PSM and thus controls the timing of the regular budding of cells out of the PSM to form the somites [Cooke and Zeeman, 1976, Palmeirim et al., 1997, Gomez et al., 2008]. Concurrent with somite formation, anterior-posterior (AP) patterning of the somitic mesoderm is directed by overlapping expression domains of *Hox* genes, which specify vertebral identity along the axis [Iimura et al., 2009]. This mechanism is deeply conserved across vertebrates [Morin-Kensicki et al., 2002, Böhmer et al., 2015, Criswell et al., 2021]. *Hox* genes are typically arranged in linear clusters within the genome, and their sequential activation during development reflects the serial organization of the vertebral column [Iimura et al., 2009]. This phenomenon, known as *Hox* colinearity, spatially and temporally regulates AP patterning of the vertebrate body axis [Ye and Kimelman, 2020]. Thus, evolutionary changes to both vertebral number and regional identity can arise through modifications to the rate of somite formation or shifts in the expression boundaries of *Hox* genes [Cohn and Tickle, 1999].

Homeotic transformations, for example the development of one type of vertebrae at the expense of another due to aberrant *Hox* gene expression, is well documented [Iimura et al., 2009]. In mice, for instance, *HoxA11* mutations lead to double homeotic transformations, forming two lumbar vertebrae in place of a thoracic and a lumbar vertebra, respectively [Small and Potter, 1993], with similar homeotic transformations being reported for mutations in multiple other *Hox* paralagous groups including: *Hox8* [Akker et al., 2001], *Hox9* [Fromental-Ramain et al., 1996], and *Hox10* [Carapuço et al., 2005, Hostikka et al., 2009, Rijli et al., 1995]. Evolutionary modulation of both somitogenesis and anterior-posterior *Hox* patterning has been critical to the evolution of variation in the vertebrate body plan [Naganathan and Oates, 2020]. Shifts in *Hox* patterning have

been linked to the considerable variability present in vertebral column regionalisation in archosaurs [Böhmer et al., 2015] aligning with morphological domains present in the avian vertebral column [Marek et al., 2021]. In mammals, homeotic shifts are sufficient to explain variation in lumbar and thoracic proportions [Narita and Kuratani, 2005] and indeed in the proportions of all post-cervical vertebral counts [Cerbus et al., 2024]. In addition, to homeotic shifts, changes in vertebral proportions can be brought about by increasing the rate of somitogenesis relative to the *hox* 'timer'. In Python embryos, for example, an increased rate of somitic budding leads to the formation of a greater number of smaller somites relative to chicken embryos [Gomez et al., 2008, Woltering et al., 2009]. In order to support their elongated axes, an anterior shift of *HoxC6* and *HoxC8* in the lateral plate mesoderm prevents forelimb formation, specifying instead the development of thoracic (chest, rib-bearing) vertebrae to support their elongate bodies [Cohn and Tickle, 1999].

Elucidating anterior-posterior patterning during teleostean development is particularly difficult due to the presence of seven/eight *hox* clusters [Crow et al., 2006, Hoegg et al., 2007], where overlapping expression of many paralogous genes, often with functional redundancy [Adachi et al., 2024], makes identifying the key *hox* genes difficult. *hox6* paralogs have been implicated in determining precaudal vertebral identity in *Danio rerio* (zebrafish) and the anterior-expression limits of *hoxC10a* and *hoxD12a* correlate with the somites that go on to contribute to vertebrae at the precaudal-caudal boundary [Morin-Kensicki et al., 2002, Hayward et al., 2015]. There is little reason, however, to assume that the specific *hox* genes involved are conserved across teleosts. Subfunctionalisation of *hox* rhombomere patterning has occurred multiple times in teleosts [Scemama et al., 2006], including in cichlids [Le Pabic et al., 2007]. Moreover, the identity of *hox* genes which specify fin formation [Sordino et al., 1995] are also not conserved in teleosts [Adachi et al., 2024]. In addition, epigenetic regulation of *hox* expression may play a role in teleosts. Dysregulation of *hox* methylation due to the loss of maternally-expressed factors has been shown to lead to homeotic transformations in zebrafish [Xue et al., 2022]. Even in tetrapods, the *Hox* code doesn't seem to be particularity conserved, paralogous groups 9-11 have been implicated in patterning the transition of different domains across the AP axis [Cerbus et al., 2024].

1.2.9 Development of the Cichlid Vertebral Column

Woltering et al. [2018] provides an exceptionally detailed and thorough account of vertebral column development and ossification in *Astatotilapia burtoni*. Although the development of other cichlids has also been characterised, including *Oreochromis niloticus* (Nile tilapia) [Fujimura and Okada, 2007], *Astatotilapia calliptera*, *Rhamphochromis sp.* 'Chilingali', and *Tropheus sp.* 'mauve' [Marconi et al., 2023], these studies are not strongly

focused on skeletal ontogeny or the development of the axial skeleton. As such, their utility for understanding the developmental origins of axial regionalisation and variation in vertebral morphology across cichlid lineages is limited. We briefly outline here the developmental basis of the vertebral column in cichlids, which in key respects appears to be consistent with broader teleostean patterns [Woltering et al., 2018].

In vertebrates, the number of vertebrae is determined by the number of embryonic somite pairs formed during early development [Morin-Kensicki et al., 2002]. This relationship is especially direct in teleosts. Unlike in tetrapods and cartilaginous fishes, where resegmentation occurs, a process in which adjacent rostral and caudal somitic halves merge to form vertebral precursors [Ewan and Everett, 1992, Ward et al., 2017, Criswell et al., 2017a], teleosts do not undergo resegmentation following somite development. The anterior-most somites contribute to the formation of the basioccipital region of the skull [Patterson and Johnson, 1995, Morin-Kensicki et al., 2002], which appears to be the case in *Astatotilapia burtoni*. Woltering et al. [2018] reports the identification of three myotomal segments, consistent with observations in other anamniotes (craniates that have a completely aquatic egg stage) [Piekarski and Olsson, 2007, 2014], that form the posterior region of the skull [Woltering et al., 2018]. With the remaining somites (specifically the sclerotome) contributing to the development of the vertebrae [Woltering et al., 2018]. Consequently, the number of somitic pairs formed during development is typically three greater than the number of vertebrae observed in the adult, reflecting the contribution of the anterior somites to the skull.

In *A. burtoni*, the first vertebral elements to form are the chondral condensations of the neural and haemal arches, which appear as paired structures and develop in an anterior to posterior sequence, with ossification of the vertebral centra following shortly after [Woltering et al., 2009]. As in all other teleosts [Dietrich et al., 2020], vertebrae are directly ossified from the notochord sheath, an ossification layer around the notochord, via intramembranous ossification, where mesenchymal cells directly differentiate into osteoblasts, bypassing the need for a cartilaginous intermediate [Apschner et al., 2011]. However, the ribs, which form after the ossification of the centra first form as cartilagenous elements that later become ossified [Woltering et al., 2018]. Curiously, ribs are only present on the third vertebrae in adult cichlids (see Figure 1.3A), however, Woltering et al. [2018] reports detecting presumptive cartilage formation (Alcian blue staining) in somites anterior to the somites corresponding to the third vertebrae, suggesting possible initiation of cryptic rib formation which is later shutdown. The final vertebral elements to form are the epicentrals (see Figure 1.3C), which form much later during development, appearing on the first vertebrae, forming sequentially on each vertebrae in the precaudal domain anterior to posterior [Woltering et al., 2018]. As directly developing animals, cichlids do not undergo metamorphosis and instead develop directly from embryo to adult [Woltering et al., 2018, Marconi et al., 2023]. They hatch as miniature versions of adults,

with the vertebral column fully formed, and post-hatching, the body grows allometrically, likely scaling in size as they age [Fujimura and Okada, 2008], which is presumably the case for the vertebrae and its associated elements.

1.3 Aims

This study aims to investigate the evolution and regionalisation of the vertebral column in African cichlids, with a particular focus on morphological variation, macroevolutionary dynamics, and the evolution of developmental mechanisms. As a first step, we seek to characterise the axial morphological diversity present across the group and assess whether modification of the vertebral column has contributed to the diversification of the subfamily. To evaluate whether axial morphology represents an adaptive trait, we will examine correlations between vertebral structure and ecological niche occupation, and test for macroevolutionary patterns consistent with adaptation. For example, does the rate of vertebral count evolution vary across the phylogeny? Are different lineages being driven to adopt different trait optima in vertebral counts, proportions, or body elongation? In addition, we use vertebral counts and proportions as proxies to investigate how the developmental processes of somitogenesis and anterior–posterior patterning have evolved during the radiation of Pseudocrenilabrinae. This raises important questions: can evolutionary changes in axial patterning occur independently of changes to somitogenesis? And if so, what does this imply about the modularity and evolution of anterior–posterior patterning mechanisms? Finally, we aim to determine whether vertebral shape itself is an adaptive trait in Lake Malawi cichlids, and to quantitatively characterise the number and structure of axial regions present within the cichlid vertebral column.

2 African Cichlid Lake Radiations Recapitulate Riverine Axial Morphologies Through Repeated Exploration of Morphospace

2.1 Motivation and Novelty of Manuscript

Understanding the macroevolutionary dynamics underpinning the evolution of the axial skeleton, particularly vertebral counts, is essential for explaining how body shape diversity has evolved in African cichlids. Although much attention has been given to the spectacular diversification of lacustrine radiations, the broader landscape of axial morphological variation across both riverine and lacustrine species, and indeed across the entire subfamily, remains poorly understood. Until now, no macroevolutionary study had systematically examined the evolution of the axial skeleton in African cichlids, despite the availability of well-resolved phylogenies for individual lake radiations [Genner and Turner, 2012, Malinsky et al., 2018, Ronco et al., 2021, Masonick et al., 2022] and for the wider subfamily [McGee et al., 2020, Astudillo-Clavijo et al., 2023], as well as extensive taxonomic sampling in museum collections [Bucklow et al., 2024]. Vertebral counts and body proportions are often used as meristic traits to distinguish species or genera [Stiassny, 1981, Oliver, 2024], but no one had yet compiled a comparative dataset of axial traits suitable for macroevolutionary analysis. This gap was partially bridged by the availability of a large dataset of lateral x-rays from cichlids endemic to Lake Tanganyika [Ronco et al., 2021], but a broader dataset spanning the subfamily was needed. This effort was aided by the whole-body μCT-scan dataset I generated for Lake Malawi cichlids [Bucklow et al., 2024], but still required extensive additional sampling. A substantial portion of this project involved expanding taxon coverage through fieldwork and research visits to museum collections in Switzerland and the United States, as well as systematic manual searches through natural history databases. Ultimately, I compiled a comprehensive dataset including total, precaudal, and caudal vertebral counts, as well as

whole-body, cranial, and postcranial aspect ratios. The dataset includes 4544 individuals representing approximately 583 species of Pseudocrenilabrinae, spanning all 26 currently recognised tribes [Astudillo-Clavijo et al., 2023], and captures the full extent of ecological and morphological variation within the group. While the compilation of this dataset was essential for the present study, it also forms the basis for an additional manuscript, which is the focus of my second results chapter.

To investigate the evolutionary dynamics of the axial skeleton, I used this dataset to characterise the axial morphospace of African cichlids. Using phylogenetic comparative methods, I show that riverine species occupy a broader and more variable axial morphospace than lacustrine species. However, lacustrine species have repeatedly and independently evolved more elongate bodies supported by higher total vertebral counts. This pattern is driven, at least in part, by a higher stochastic rate of total vertebral count evolution in riverine lineages, which exceeds that observed in any lacustrine radiation. Within lakes, elongation of the body, supported by increased vertebral numbers, has played a key role in adaptation to pelagic, demersal, and piscivorous niches. Despite this, many lacustrine forms appear to have re-evolved axial morphologies already present in riverine lineages. Curiously, however, increased occupation of axial morphospace correlates with the age of the respective lacustrine radiations but their divergence times alone and not sufficient to explain this pattern, suggesting that individual lake dynamics have contributed to the evolution of axial morphologies within the lake radiations despite the convergence of form. Finally, my ancestral state reconstructions suggest that the common ancestor of all African cichlids occupied an axial morphospace more typical of modern riverine species, indicating that the lineage originated from a deep-bodied ancestor with relatively few vertebrae and I note that the ancestral reconstruction of all of the traits may be helpful with the phylogenetic placement of fossils, which is particularly challenging for cichlids [Murray, 2001a,b, Altner et al., 2020]. In this study, I highlight the importance of stochastic processes in shaping vertebral evolution and emphasise the need to expand comparative frameworks beyond well-studied lacustrine radiations. Doing so is critical to fully understanding the evolutionary and ecological drivers of morphological innovation in this iconic group.

African Cichlid Lake Radiations Recapitulate Riverine Axial Morphologies Through Repeated Exploration of Morphospace

Pages 29–62

Interactive features (e.g. links) are disabled in this embedded version.
For the fully functional version, visit `https://shorturl.at/pKfCS`.

Author contributions are included at the end of the manuscript.

African Cichlid Lake Radiations Recapitulate Riverine Axial Morphologies Through Repeated Exploration of Morphospace

Callum V. Bucklow[1,2,*], Emanuell Duarte Ribeiro[3], Fabrizia Ronco[3], Nathan Vranken[4,5,6], Michael K. Oliver[7], Walter Salzburger[3], Melanie Stiassny[8], Roger Benson[2,9,*], and Berta Verd[1,*]

[1]**Evolutionary Biology Section, Department of Biology, University of Oxford, Oxford, UK**
[2]**Paleobiology Group, Department of Earth Sciences, University of Oxford, Oxford, UK**
[3]**Department of Environmental Science, University of Basel, Switzerland**
[4]**Section Vertebrates, Biology Department, Royal Museum for Central Africa, Tervuren, Belgium**
[5]**Laboratory of Fish Diversity and Conservation, Department of Biology, University of Leuven, Leuven, Belgium**
[6]**Research Group Zoology: Biodiversity and Toxicology, Centre for Environmental Sciences, Hasselt University, Diepenbeek, Belgium**
[7]**Peabody Museum of Natural History, Yale University, New Haven, USA**
[8]**Department of Ichthyology, American Museum of Natural History, New York City, USA**
[9]**Division of Paleontology, American Museum of Natural History, New York City, USA**
[*]**Co-corresponding authors: Callum V Bucklow (callum.bucklow@biology.ox.ac.uk); Roger Benson (rbenson@amnh.org); Berta Verd (berta.verdfernandez@biology.ox.ac.uk)**

ABSTRACT

African cichlids comprise more than 1800 species of freshwater fishes, with remarkable adaptive radiations in Lakes Tanganyika, Malawi, and Victoria that have given rise to extraordinary morphological diversity. However, the evolution of the cichlid axial skeleton has been largely overlooked, despite its high variation and functional significance for locomotion. Here, we present the first macroevolutionary study of axial morphology in African cichlids, based on phylogenetic comparative analyses of 4861 individuals from 583 species. Adaptation to demersal, pelagic, and piscivorous niches has led to the evolution of elongate bodies with high vertebral counts in lacustrine cichlids, emphasising the role of the fusiform body shape in ecological adaptation. However, riverine species occupy a broader axial morphospace than lacustrine species, which is partly explained by a higher stochastic rate of vertebral count evolution in riverine lineages. In addition, the occupied axial morphospace broadly correlates with the estimated age of the lacustrine radiations, suggesting that exploration of axial morphospace is a function of divergence time. However, rates of vertebral count evolution are not the same across the lake radiations. Therefore, accumulated variation in vertebral counts (and more broadly axial morphospace) is not solely a function of divergence time. Finally, we show that the common ancestor of African cichlids possessed a distinctly riverine axial morphology, indicating that the exploration of axial morphospace radiated outward from this ancestral riverine form. These findings highlight the importance of a comparative approach to studying cichlid evolution and underscore the value of African cichlids as a model for investigating the evolutionary and developmental dynamics of the teleostean vertebral column.

Keywords: macroevolution, cichlids, teleosts, adaptation, axial skeleton, vertebral column, vertebrae, ray-finned fish

INTRODUCTION

The vertebral column, a defining anatomical feature of all vertebrates, is critical for movement, not only facilitating muscle attachment to support locomotion, but also providing a protective casing for the spinal cord and nerve roots required for the transduction of the central and peripheral signals essential for movement (Ford, 1937). Teleosts (infraclass Teleostei) are the largest group within Actinopterygii, commonly known as ray-finned fishes, and account for more than 50% of all described vertebrate species (Near and Thacker, 2024). Therefore, elucidating the dynamics of macroevolutionary change in the structure of the teleost vertebral column is central to understanding morphological and functional diversification in a large group.

The teleostean vertebral column is regionalised into precaudal and caudal vertebral series. Precaudal vertebrae are defined by the ventrolateral basapophyses for the attachment of ribs, which protect the viscera and provide points of attachment for muscle and tendons. Caudal vertebrae, in contrast, are defined by the presence of a closed haemal arch formed by haemal spines (see Figure 1A) and provide important points of articulation with the anal and caudal fins required for swimming (Ford, 1937). The number, type, relative proportions and shapes of vertebrae, have been extensively modified in ray-finned fishes. *Mola mola* (Ocean sunfish), adapted to float on the ocean surface, has just 17 vertebrae and the caudal fin has been lost in the closely related *Mola tecta* (Britz and Johnson, 2005), whereas the extremely elongate deep sea *Nemichthys scolopaceus* (slender snipe eel) has upwards of 740 vertebrae (Deniz and Ağilkaya, 2018). In syngnathidids (seahorses, pipefishes, and seadragons), pleural ribs and epicentrals, associated with precaudal vertebrae and which act as attachment points for tendons and muscle (Liem and Sanderson, 1986), have been secondarily lost (Small et al., 2016; Schneider et al., 2023).

Teleosts and other ray-finned fishes (actinopterygians) have been the subject of multiple macroevolutionary studies examining the evolution of the vertebral column. Ward and Brainerd (2007) previously demonstrated that precaudal and caudal vertebral counts have evolved independently of one another in actinopterygians and elasmobranchs (cartilaginous fishes), permitting clades to independently modulate the number of precaudal and caudal vertebrae. Anguilliformes (eels and morays), for example, have disproportionally added caudal vertebrae to support their elongate bodies. In contrast, however, Polypteriformes (bichirs and reed- or ropefish) have dramatically increased the number of precaudal vertebrae relative to caudal vertebrae (Ward and Brainerd, 2007; Ward and Kley, 2012), a dramatic shift in vertebral column regionalisation which may aid in their demersal lifestyle (Ward and Kley, 2012). In elopomorphs (tarpons, ladyfishes, and eels), increasing the total number of vertebrae has been important in driving the extreme elongation present in the clade (Mehta et al., 2010). Indeed, elongation of the whole body appears to be the primary axis of body shape diversification across a number of teleostean clades (Claverie and Wainwright, 2014). However, additional mechanisms are clearly important for the elongation of the teleostean body. Although cranial elongation is typically associated with an increase in overall body aspect ratio, it does not correlate with total vertebral count (Mehta et al., 2010). This suggests that body elongation in teleosts has also been shaped by mechanisms other than changes in vertebral number. Whilst these studies have identified patterns of macroevolutionary change across teleosts, spanning many orders and families, little is known about the evolutionary dynamics of vertebral column evolution on smaller phylogenetic scales that contribute to these larger scale patterns.

African cichlids (Ovalentaria, Cichliformes, Cichlidae, Pseudocrenilabrinae) are an extremely species-rich and morphologically diverse subfamily of teleosts found throughout the rivers and freshwater lakes of Africa and in the Middle East (Astudillo-Clavijo et al., 2023). The subfamily includes the adaptive radiations of the Great Rift Valley Lakes Tanganyika, Malawi and Victoria, where the vast majority of their species diversity has arisen (Salzburger, 2018; McGee et al., 2020). Pseudocrenilabrinae diverged

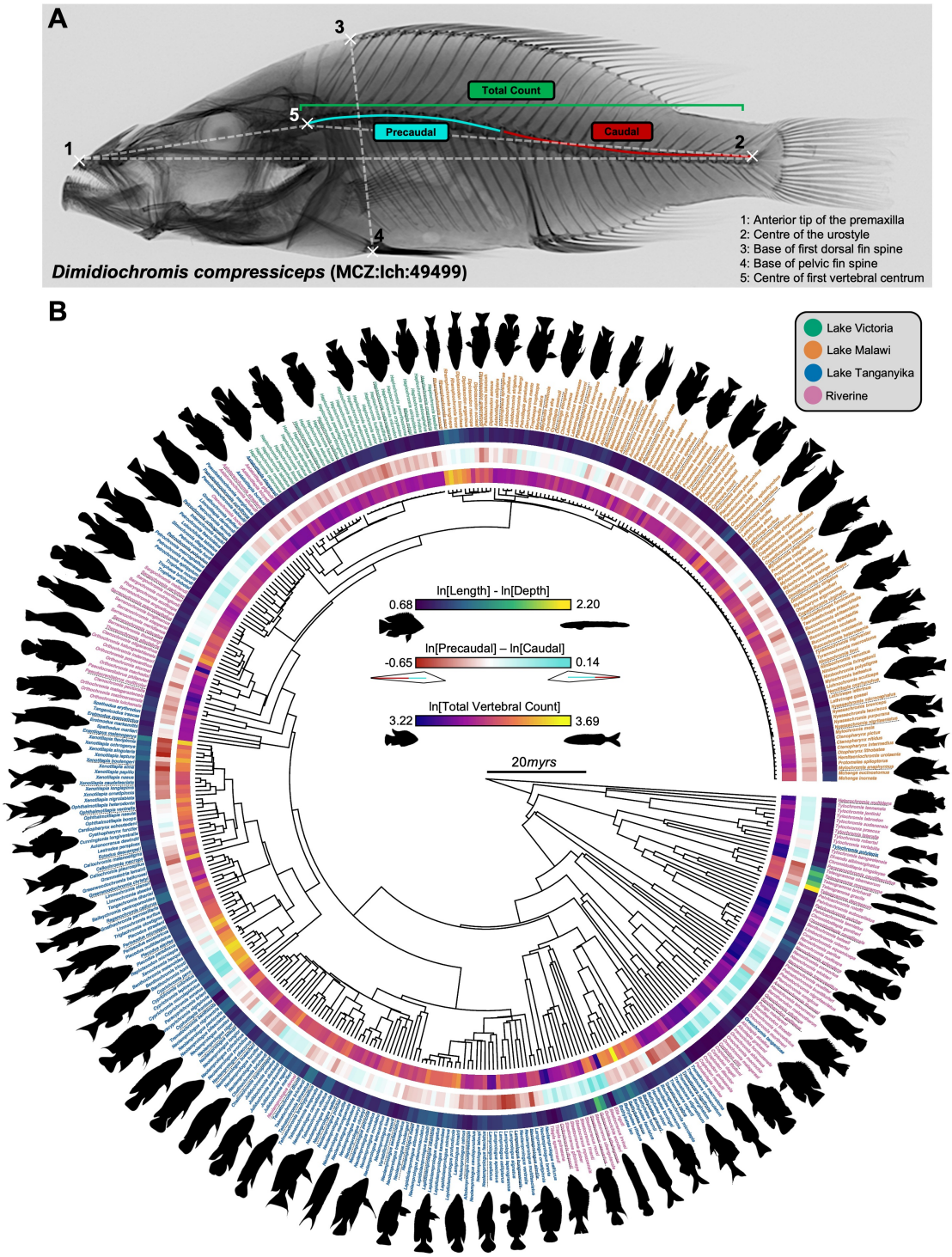

Figure 1. (A) Landmarks used in the study, as previously published (Ronco et al., 2021). Dashed lines indicate straight lines used for the calculation of the three respective aspect ratios used in the study. Precaudal vertebrae are indicated in blue and the caudal vertebrae in red. The total vertebral count (green) is the summation of the precaudal and caudal vertebral counts. The specimen data record can be accessed here. (B) Phylogeny from McGee et al. (2020) pruned to species present in the dataset. The respective ln[Total Count] (inner circle), ln[Precaudal] - ln[Caudal] (ratio of precaudal to caudal vertebrae, middle circle) and ln[Length] - ln[Depth] (body aspect ratio, outer circle) are indicated for each species as a heatmap (see legend). Silhouettes to demonstrate body shape diversity are shown for select species (dashed lines). Coloured tips indicate the water system occupancy of extant species (see legend). See Supplementary Materials for image acknowledgments.

from the rest of Cichlidae approximately 64–58 mya (Matschiner et al., 2020) and have evolved diversity in the total number and relative proportions of precaudal and caudal vertebrae (Oliver, 2024) and in body shape (Malinsky et al., 2018; Ronco et al., 2021) (Figure 1B). The diverse evolutionary history of Pseudocrenilabrinae, including multiple, independent, adaptive radiations into lacustrine systems, featuring extremely rapid diversification rates (Malinsky et al., 2018; Ronco et al., 2021; Meier et al., 2017), and the existence of relatively stable, basal riverine lineages, provides a powerful comparative model to investigate the macroevolutionary dynamics of vertebral column evolution on multiple scales.

To date, however, no macroevolutionary study on the axial skeleton has been conducted in African cichlids, despite the presence of well-defined phylogenies for individual lake radiations (Genner and Turner, 2012; Malinsky et al., 2018; Ronco et al., 2021; Masonick et al., 2022; Meier et al., 2023) and for the wider subfamily (McGee et al., 2020; Astudillo-Clavijo et al., 2023), as well as extensive taxonomic sampling in museum collections (Bucklow et al., 2024). To address this, we compiled a dataset including total, precaudal, and caudal vertebral counts, as well as whole-body, cranial, and postcranial aspect ratios. Our dataset spans 583 species of Pseudocrenilabrinae, representing all 26 currently recognised tribes (Astudillo-Clavijo et al., 2023), including both riverine lineages and the major lacustrine radiations. Using phylogenetic comparative methods, we show that riverine cichlids occupy a wider axial morphospace than lacustrine species, but that lacustrine species are repeatedly and independently being driven to adopt more elongate bodies supported by greater total vertebral counts. This pattern is driven, at least in part, by the higher stochastic rate of total vertebral count evolution in riverine lineages — a rate that exceeds that of any lacustrine radiation. Within the lacustrine radiations, elongation of the body, supported by high vertebral counts, has been important for adaptation to pelagic, demersal, and piscivorous niches. However, lacustrine species have largely re-evolved axial morphologies already present in riverine lineages. Finally, our ancestral reconstructions suggest that the common ancestor of all African cichlids occupied an axial morphospace characteristic of riverine species, indicating that the lineage originated from a deep-bodied ancestor with relatively few vertebrae. Our analysis clearly indicates the importance of stochastic processes in the evolution of the vertebral column, also highlighting the need for careful, considerate comparative studies of the evolution of African cichlids and the necessity of including riverine species within future analyses.

METHODS AND MATERIALS

Collating X-Ray Library

We collated a library of 2D-lateral images of 4544 individuals of Pseudocrenilabrinae. Of the 4544, 3633 were from previously published studies or generated ourselves. This included: 2D lateral X-rays (n=2183) of cichlids from the Lake Tanganyika basin (Ronco et al., 2021); whole-body 2D lateral x-rays of specimens part of the American Museum of Natural History (AMNH) ichthyology collection (n=764); haplochromine riverine specimens part of the research collection at the University of Basel (n=310); 132 individuals of 2D whole-body lateral x-rays generated by Michael Oliver (Oliver, 2024); 131 Lake Victoria haplochromines generated by Nathan Vranken; lateral images generated from whole-body volume renderings or 3D models of the whole skeleton of μCT-scans (n=113) of Lake Malawi haplochromines (Bucklow et al., 2024) and whole-body volume renderings from μCT-scans (n=9) of Lake Malawi cichlids from the Durbin Lab (University of Cambridge) that are part of the Museum of Zoology, University of Cambridge (CAMZM) collection.

The remaining images (n=911) were collated from an extensive online search for each genus belonging to Pseudocrenilabrinae (see below), initially on the Natural History Museum, London (NHMUK) data portal (Scott et al., 2019). This was subsequently expanded to GBIF, which included all the museum

connections linked to the resource, allowing a much larger sampling for images. A search for each of the 166 currently recognised genera (see below) that constitute Pseudocrenilabrinae was made on GBIF and was filtered to just consider records with associated images. Radiographs were downloaded and landmarked (see below). An additional manual search for each genus was also made on the AMNH's ichthyology collection using their own data portal, which can be accessed here. Species names were initially taken from the museum record for the specimen(s) and the recorded species name was checked on FishBase (Froese and Pauly, 2000) and updated to the senior synonym, if required. For Lake Malawi haplochromines, this was also supplemented by the curated species list available on malawi.si, accessible here. X-rays with multiple images/skeletons were presumed to all be individuals unless explicitly stated, or unless it was clear that two images were from the same specimen (e.g. by having identical specimen damage). Individuals were cropped manually from each image from left-right and up-down (wherever possible) and labelled A-Z, unless individual numbers were recorded with each individual within the image in which case these numbers were used instead.

Vertebral Counts and Landmarking

Individual cropped images were manually landmarked using the multi point tool in FIJI (Schindelin et al., 2012), a GUI for ImageJ (Schneider et al., 2012). For landmarks used see Figure 1A. Vertebral centra were counted anterior to posterior, starting with the anterior-most, ribless vertebrae, finishing and including the urostyle, the vertebra that articulates with the caudal-fin, and has a highly modified centrum (Woltering et al., 2018; Di'Biagio et al., 2022). The total number of centra was then recorded as the total vertebral count of that specimen (Oliver, 2024). Where fused centra were visible, we instead counted the number of neural spines (Supplementary Figure 1A). The precaudal count, included the two most anterior vertebrae, which are not associated with pleural ribs, as well as the rib-associated precaudal vertebrae (with zygapophyses) (Ford, 1937). The caudal vertebrae included all vertebrae posterior of the last rib-bearing precaudal vertebrae which have haemal spines (and therefore a haemal arch). The presence of 'transitional' vertebrae (Supplementary Figure 1B, C), bearing the morphology of both precaudal and caudal vertebrae which differs between individuals (De Clercq et al., 2017) made defining the final precaudal and the first caudal vertebrae difficult. Since inter- and intraspecific morphological variation was high, we instead defined the transitional vertebrae as caudal unless it very clearly had *fully formed* pleural ribs (Supplementary Figure 1B). The presence of a haemal spine (and therefore haemal arch), no matter how rudimentary, overrode the classification regardless of the presence of pleural ribs (Supplementary Figure 1C). In order to compare regionalisation of the vertebral column between species with drastically different vertebral counts, we also calculated a ratio of the two counts (ln[Precaudal] - ln[Caudal], whereby 0.00 is precaudal = caudal) to consider the relative proportions of the two vertebral types. All vertebral counts can be found in the supplementary material.

To examine the relationship between vertebral counts and body elongation we calculated three body aspect ratios, a whole body aspect ratio quantifying the relationship between anteroposterior length and dorsoventral depth of the whole body, an anterior body aspect ratio (broadly quantifying elongation of the head) and a posterior body aspect ratio (quantifying postcranial elongation), using previously described landmarks (Ronco et al., 2021), see Figure 1A. Since many of the radiographs lacked scale bars, we calculated raw pixel lengths and widths from the coordinates of the landmarks for the body aspect ratio and calculated a ratio between the log-transformed measures. All whole body aspect ratios were positive, indicating that every specimen in the dataset is longer than deep. In contrast, anterior body aspect ratios were both negative and positive, indicating that specimens with craniums wider than they are long were common. Not all specimens could have a ratio calculated (missing from 71 specimens) because of missing craniums, dorsal fin rays etc. Specimens with missing values were filtered from any analysis that

included the body aspect ratio (including the PPCA). All landmarked individual images are available in the Supplementary Materials.

Taxonomic Considerations and Defining Water Systems

We wanted to sample the Pseudocrenilabrinae as widely as possible. Therefore, we focused on maximising the sampling of every tribe and genus within these tribes. We used the detailed discussion of Pseudocrenilabrinae taxonomy of Astudillo-Clavijo et al. (2023) to collate a list of genera that belong to each tribe not endemic to Lake Tanganyika including: Chromidotilapiini, Coptodonini, Gobiocichlini, Hemichromini, Heterochromini, Oreochromini, Pelmatochromini, Pelmatolapiini, Steatocranini, Tilapiini and Tylochromini. For Lake Tanganyika endemic tribes, we instead used the detailed taxonomic discussion of endemics and native species to Lake Tanganyika (Ronco et al., 2020), as well as the phylogeny constructed by Ronco et al. (2021), which resolved the phylogenetic relationships between all tribes of Pseudocrenilabrinae that are endemic or native to Lake Tanganyika or the wider basin, respectively. Tribes endemic or native to Lake Tanganyika included: Bathybatini, Benthochromini, Boulengerochromini, Cyphotilapiini, Cyprichromini, Ectodini, Eretmodini, Lamprologini, Limnochromini, Perissodini, Trematocarini, Tropheini (Lake Tanganyika endemic haplochromines) and haplochromines endemic to the wider basin, but not part of the Lake Victoria or Malawi radiations. All species belonging to any of the Lake Tanganyika endemic tribes were classified as belonging to the Lake Tanganyika water system, besides *Telmatochromis devosi*, formerly *Neolamprologus* (Indermaur et al., 2024), a Lamprologini, a species found in the lower Malagarasi river, an inlet of Lake Tanganyika (Schelly et al., 2003).

All haplochromine genera belonging to the Lake Malawi radiation, were classified as such, including species endemic to satellite lakes of Lake Malawi (Turner et al., 2019). *Astatotilapia calliptera* is distributed across the rivers flowing eastward to the Indian Ocean, from the Rovuma River in the north, to the Save River in the south (Turner et al., 2021) and despite its exceptionally wide distribution and riverine ecology, it clusters phylogenetically within the Lake Malawi radiation (Malinsky et al., 2018). Therefore, all specimens of *Astatotilapia calliptera* were categorised as being part of the Lake Malawi system and not riverine. Similar exceptions were made for *Astatotilapia burtoni* and *Astatotilapia stappersii*, non-Tropheini haplochromines native to Lake Tanganyika and its wider catchment, including its connecting waterways (Turner et al., 2021). Other *Astatotilapia* species included: *A. gigliolii*, part of the '[Great] Ruaha [River] catchment' that belongs to a sister lineage to the haplochromine radiations of Lake Malawi and Lake Victoria (Svardal et al., 2020); *A. bloyeti*, a species distributed in the Wami River system, the Malagarasi, the Pangani and the catchments of Lake Manyara and Eyasi and associated lakes; *A.* (*Haplochromis*) *paludinosa*, whose distribution overlaps with that of *A. bloyeti* (Turner et al., 2021) were all classified as 'Riverine' species. Haplochromines that do not belong to either the Lake Malawi or Lake Victoria radiations were classified as riverine. For example, *Serranochromis robustus* belongs to one of the two genera, *Serranochromis* and *Sargochromis*, collectively referred to as 'serranochromines', which are native to Lake Malawi but not endemic to it (Turner et al., 2019). Phylogenetic analyses show that serranochromines do not cluster within the Lake Malawi radiation (McGee et al., 2020; Astudillo-Clavijo et al., 2023), and members of the group are found throughout East African river systems (Thorstad et al., 2005). This, along with evidence suggesting that the group originated in a now extinct lake before colonising nearby rivers (Joyce et al., 2005), supports their classification as riverine.

All haplochromine species belonging to the Lake Victoria Region Superflock (LVRS) were grouped into the 'Lake Victoria' system. This includes all haplochromine species endemic to Lakes Victoria, Albert, Edward, George and Kivu (Meier et al., 2017), as well as Lake Kyoga whose endemics were not considered by Meier et al. (2017). However, Lake Kyoga is nonetheless directly connected to Lake Victoria by the White (Victoria) Nile (Mwanja et al., 2001) and more recent evidence suggests

that the Lake Kyoga endemics are indeed part of the LVRS (Meier et al., 2023). Only eight total specimens (three species) were from Lake Kyoga, including the holotype of *Haplochromis worthingtoni*, NHMUK 1929.1.24.334; six syntypes of *Haplochromis latifasciatus* from NHMUK 1929.1.24.335-339; and a specimen of *Paralabidochromis sp.* "black" from the Museum of Comparative Zoology (MCZ), MCZ:Ich:137961, the latter of which was not present on the phylogeny and not included in any phylogenetic analysis.

Phylogenetic Comparative Methods

All analyses were conducted in R (v4.2.0) (R Core Team, 2022). Phylogenetic analyses used the cichlid phylogeny constructed by McGee et al. (2020) as the tree is ultrametric, time-calibrated and includes all three of the major lacustrine radiations of African cichlids (Lake Tanganyika, Lake Malawi and Lake Victoria), as well as representatives from every currently recognised tribe in the African subfamily (see above). After pruning the tree and subsetting our dataset, we were left with data for 429 species (131 genera) of Pseudocrenilabrinae, with representatives from all tribes within the subfamily.

Phylogenetic Principal Component Analysis

To identify the primary axes of variation within our dataset and quantify the occupied axial morphospace of the species within our dataset, we used phylogenetic principal component analysis (PPCA), a phylogenetic modification of PCA which corrects for phylogenetic autocorrelation (Revell, 2009). We input our count data (ln[Total Count], ln[Precaudal] and ln[Caudal]) and transformed body aspect ratios (anterior, posterior and whole) into the *phyl.pca* function in the R package *phytools* (v2.1.1) (Revell, 2024) with a correlation matrix derived from Brownian motion (method = 'BM'). Loadings for each principal component can be found in Table Supplementary Table 1. PC scores for each species can be found in the supplementary materials. Previous evidence suggested that adaptation to lacustrine environments was a key driver of morphological evolution in African cichlids (Malinsky et al., 2018; Ronco et al., 2021; Meier et al., 2017), therefore we clustered species according to their respective lacustrine (Lake Tanganyika, Lake Malawi or Lake Victoria) or riverine system occupation (see Figure 1B), their placement on the benthic-pelagic axis and for diet preference (piscivore versus non-piscivore). For visualisation, the 95% CI for group was calculated, the area of which we considered to be the occupied axial morphospace for each respective group. To quantify overlap in axial morphospace between lacustrine and riverine species, we generated 100,000 random points within the lacustrine morphospace using *mvrnorm* (*MASS* v7.3.58.2) (Venables and Ripley, 2002). Points were sampled based on the lacustrine centroid (mean PC1 and PC2 scores) and covariance matrix. We then calculated each point's Mahalanobis distance (T^2) from the riverine centroid and classified points as within the riverine morphospace if $T^2 \leq 5.991$, the 95% confidence threshold for a Chi-square (χ^2) distribution with 2 degrees of freedom. The percentage overlap was defined as the proportion of lacustrine points within this boundary. A multivariate analysis of variance (MANOVA) was used to test for significant differences in axial morphospace between groups. This was implemented using the *procD.lm* function in the R package *geomorph* (v4.0.6) (Baken et al., 2021), which performs MANOVA via residual randomization, as provided by the *RRPP* package (Collyer and Adams, 2018). Where more than two groups were present, pairwise comparisons were made using the *pairwise* function in *geomorph*.

Ancestral Continuous Trait Reconstruction

We estimated the ancestral states of five of the seven univariate traits: the total vertebral count (ln[Total Count], see Supplementary Figure 2); the precaudal:caudal ratio (ln[Precaudal]-ln[Caudal]), the whole body aspect ratio (ln[Length]-ln[Depth]) as well as the anterior and posterior body aspect ratios. Although in principle total vertebral count is count data, a discrete trait, intraspecific variation exists within species

such that mean vertebral counts can be treated as a continuous trait. To estimate the root trait value (Z_0) for Pseudocrenilabrinae, we fit single rate BM models in which the variance parameter (σ^2) is an estimate of the rate of evolution (Hansen, 1997) to the trait data using *fitContinuousMCMC* in the R package *geiger* (v2.0.10) (Pennell et al., 2014). Using the ancestral reconstruction of the ln[Total Count] and ln[Precaudal]-ln[Caudal] ratio we inferred the possible combinations of precaudal and caudal vertebrae, rather than ancestrally reconstructing these two additional traits, by calculating the possible combinations of precaudal and caudal vertebrae given the ancestrally reconstructed ln[Total Count] count and ln[Precaudal]-ln[Caudal] ratio. Chain mixing and convergence was assessed in the R package *coda* (v0.19.4.1) (Plummer et al., 2006). For each analysis (i.e., for each univariate trait) we combined the results from five independent Markov chains that ran for 2 million generations and discarded the first 10% as burn-in. Effective sample sizes were all greater than 250.

We identified two extant species that closely resembled the reconstructed common ancestor, one of which most closely matched in axial morphology alone, and another that most closely matched in terms of both axial morphology and in discrete traits that we had also ancestrally reconstructed for the common ancestor (see below, riverine, benthopelagic, non-piscivore and substrate brooder). For the former, we took the median (Z_0) for each of the five univariate traits that we ancestrally reconstructed and calculated the Euclidean distance between the ancestor and each extant species using the mean for each of the five reconstructed traits. For the inclusion of the discrete traits, we calculated the Gower distance between the ancestral and extant species using the *daisy* function in the R package, *cluster* (v2.1.4) (Maechler et al., 2025). To quantify the similarity of these species with the common ancestor we also calculated similarity scores ($1 - D_{min}/D_{max}$), where D_{lowest}/D_{max} represents the ratio between the lowest (most similar) distance and highest (least similar) distance score within the extant species.

Ancestral Discrete Trait Reconstruction

Discrete traits, including water system occupancy, presence on the benthic-pelagic axis and piscivory were ancestrally reconstructed using the *fitDiscrete* function in the R package *geiger* (v2.0.10) (Pennell et al., 2014). To allow more comparisons downstream, we pruned the tree to the '*minimal tree*', that is, the tree with the lowest number of species with complete data (i.e. species for which we had a complete ecological dataset), leaving us with a tree with 415 tips. We compared the fit using AICc values of an equal rates (ER) model, where a single parameter governs all transition rates, an all-rates-different (ARD) model, where each transition has a unique rate parameter and a symmetric (SYM) model, where forward and reverse transitions share the same parameter. For piscivory versus non-piscviory, as well as riverine versus lacustrine, we did not fit a SYM model as a SYM model collapses to an ER model when the number of parameters (k) = 2 (Pagel, 1994; Lewis, 2001). As determined by comparison of the AIC for each model fit, for all but the Haplochromini, versus Lake Tanganyika endemics and basal riverine lineages, which reported an ER model as the best fit, an ARD model was the best model fit. To account for uncertainty in the model fit, we simulated the best fitting model 10,000 times on the minimal tree with all branch lengths scaled to 1 using *make.simmap* also in *geiger* (v2.0.10) (Pennell et al., 2014).

Modelling ln[Total Count] Evolution

Total vertebral count is ultimately determined during somitogenesis, the developmental process that establishes the number of somites and, consequently, vertebral precursors (Morin-Kensicki et al., 2002). Increasing vertebral count is important during evolutionary elongation of teleosts, including Pseudocrenilabrinae (see results) (Ward and Brainerd, 2007; Ward and Mehta, 2010; Mehta et al., 2010). Additionally, ln[Total Count] contributes positively to both PC1 and PC2, which together explain 88.30% of axial morphological variation in our dataset (see results). Therefore, ln[Total Count] evolution provides not only a useful proxy for body elongation but better opportunity for the inference of causative explanations of

vertebral changes via development. We tested multiple hypotheses about the evolution of ln[Total Counts] during Pseudocrenilabrinae diversification.

Since pelagic and piscivorous species have convergently evolved elongated bodies supported by increased vertebral counts (Stiassny, 1981; Vranken et al., 2023), and we found that demersal, pelagic, and piscivorous species were more elongate than benthopelagic or non-piscivorous species (see results), we hypothesised that variation in ln[Total Count] may reflect adaptation to these ecological niches. Specifically, we hypothesised that strong selection on ln[Total Count] may be driving body elongation in these environments. In addition, we wanted to test whether the evolution of ln[Total Count] could be a function of divergence time. Multiple adaptive radiations are nested within Pseudocrenilabrinae, each having occurred independently (Ronco et al., 2021; Malinsky et al., 2018; Meier et al., 2017). These radiations, along with more basal riverine lineages, provide a natural experiment for investigating how total vertebral counts have evolved over time. If ln[Total Count] evolution is entirely a function of divergence time, we would expect riverine, and all three lacustrine systems to have the same evolutionary rate. However, if the rates differ it would suggest that each system accumulates variation at its own rate, potentially reflecting differences in ecological opportunity, selection pressure, or developmental constraints. Finally, given the exceptionally high speciation rate in haplochromines (McGee et al., 2020), which constitute the entirety of both the Lake Malawi and Lake Victoria adaptive radiations, as well as a more recent radiation within Lake Tanganyika (Tropheini) (Ronco et al., 2020, 2021), we also tested whether the evolution of ln[Total Count] was a function of increased speciation rates by considering haplochromines (including riverine haplochromines) as a single regime compared to riverine and Lake Tanganyika endemic tribes.

To test these hypotheses, we employed a series of comparative analyses, comparing the fit of BM and OU models of continuous trait evolution on regimes that we ancestrally reconstructed on the phylogeny. Rates of ln[Total Count] evolution were estimated amongst different discrete regimes that we had ancestrally reconstructed on the tree. A set of 100 trees randomly sampled from our multiSimmap (the same set was used for each regime) with branch lengths returned to their original, time-calibrated scale. The fit of multiple BM and OU models was tested amongst our regimes in *OUwie* (Beaulieu and O'Meara, 2022). This included a single rate (σ^2) and multi-rate Brownian motion (BM) model (BMS), in which each regime is permitted its own σ^2, as well as the comparison of multiple Ornstein-Uhlenbeck (OU) models, where the attraction (α), rate (σ^2) and trait optima (θ) parameters are constant or permitted to be variable between regimes. The AICc weights were used to select the best fitting model within a regime and the best fitting model *overall* was identified by comparison of the median AICc value for each regimes best fitting model (see Table 1).

Phylogenetic Generalised Least Squares Analysis

Since our PPCA analysis had already determined a positive correlation between the total number of vertebrae and the whole body aspect ratio (see biplot inset Figure 2A), we wanted to further investigate the evolutionary dynamics of the relationship between vertebral counts and body elongation. Therefore, we fit multiple linear models to determine the relationship between the total count and the body aspect ratio to examine how these traits have evolved across the African cichlid phylogeny (see Table 2). We used phylogenetic generalised least squares (PGLS) to evaluate the relationships between individual continuous variables using the R package *caper* (v1.0.1) (Orme et al., 2018) using the *pgls* function. To account for phylogenetic signal in the trait covariance, we estimated Pagel's λ branch transformation parameter (Pagel, 1997, 1999) by maximum likelihood. Pagel's λ measures the influence of phylogeny on trait covariance, where $\lambda = 1$ suggests that the covariance evolves according to Brownian motion along the phylogenetic tree. Values between 0 and 1 indicate varying degrees of phylogenetic influence, with higher

values reflecting stronger phylogenetic signal in the trait covariance.

Phylogenetic ANOVA and Residual Variance Analysis

To test for significant differences in means between univariate groups, we used the *phylANOVA* function in the R package phytools (v2.1.1) (Revell, 2024), which implements the simulation-based phylogenetic ANOVA of Garland Jr et al. (1993). Each test was run with 10,000 simulations, and multiple testing was accounted for using a Holm–Bonferroni correction. To test whether the variance in ln[Total Counts] between riverine and lacustrine species was significant, we initially fitted an intercept only model (ln[Total Count] ~ 1.00) using the *pgls* function from the R package *caper* (v1.0.1) (Orme et al., 2018). Phylogenetic signal in the residuals was estimated to be very high ($\lambda = 0.949$ 95% CI: [0.925, 0.965]), indicating strong phylogenetic dependence. Given this high phylogenetic signal, rather than using raw variances we instead tested whether there was any significant difference in the variance between phylogenetically-corrected riverine and lacustrine residuals. Significance was tested using a Levene's test in the *leveneTest* function in the R package *car* (Fox and Weisberg, 2019). To quantify the relative difference in variance, we calculated a variance ratio by dividing the variance of the riverine ln[Total Count] residuals by the variance of the lacustrine residuals, where a ratio greater than 1.00 suggests that the riverine variance is larger than lacustrine variance.

Data and Code Availability

All code used in the analysis has been deposited on GitHub and can be accessed here. All radiographs, count and body shape data has been deposited on Zenodo (Bucklow et al., 2025), where it can be freely downloaded, shared and utilised in further studies.

RESULTS

Riverine cichlids occupy a broader axial morphospace, encompassing most lacustrine morphospace

The first principal component (PC) axis explains 66.40% of the variation axial morphospace in Pseudocrenilabrinae, representing a linear combination of all seven variables (see Table Supplementary Table 1). Species loading positively on PC1 have higher total, precaudal and caudal vertebral counts, with relatively elongate heads and postcranial bodies. Therefore, PC1 can be considered a proxy for elongation, where loadings more positively on PC1 represent more elongate body shapes. PC2 explains 21.90% of the variation in axial morphospace and positive values of PC2 correspond to high caudal vertebral counts and low precaudal:caudal ratios, whilst species with more negative values of PC2 have lower absolute caudal vertebral counts (Figure 2A). The most negative extremes of PC1 and PC2 are occupied by the riverine '*dwarf*' cichlids *Anomalochromis thomasi* and *Chromidotilapia cavalliensis* and are contrasted in both PC1 and PC2 by lacustrine species, such as the pelagic piscivore, *Bathybates fasciatus* (PC1) and demersal, sand-dwelling *Enatiopus melanogenys* (PC2) both of which are endemic to Lake Tanganyika (Ronco et al., 2020). Notably, however, the absolute positive extreme of PC1 is occupied by the rheophile *Gobiocichla ethelwynnae*, which along with its relatively high vertebral counts has also evolved an expanded precaudal vertebral domain.

The considerable majority of lacustrine axial morphospace (90.43%) is co-occupied by riverine species, leaving just 9.57% of lacustrine axial morphospace unique to lake-endemic species. Therefore, only a small fraction of lacustrine species exhibit axial morphologies not present in riverine lineages. In contrast, only 50.04% of riverine morphospace is occupied by lacustrine species, with the remaining 49.96% of riverine morphospace scoring negatively along both PC1 and PC2, representing a region of axial morphospace that is distinctly riverine. This region of axial morphospace is primarily occupied by

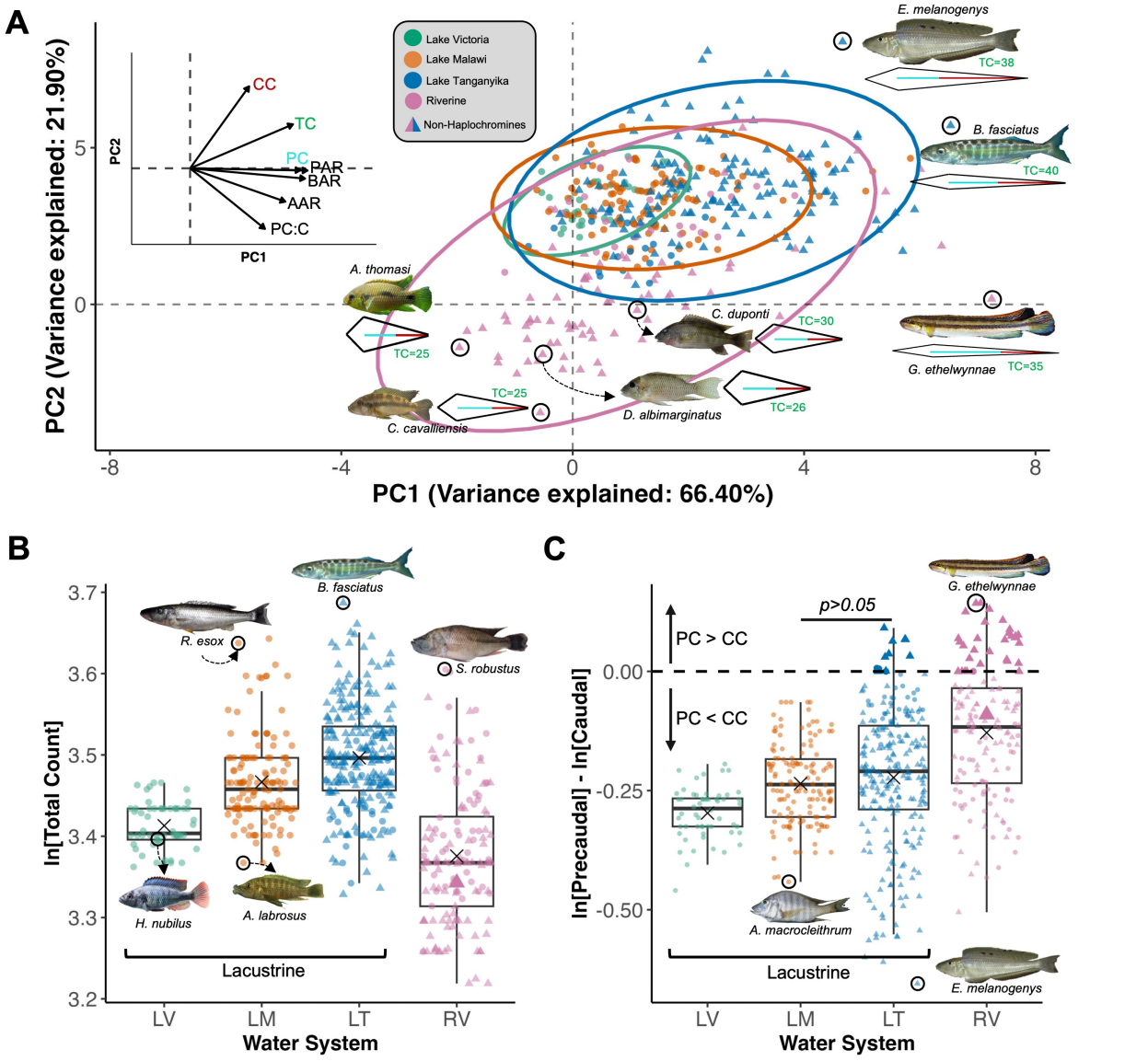

Figure 2. (A) Phylogenetic PCA plotting PC1 against PC2. The variance explained by each respective PC is indicated on the axes. A loading plot on the same axes is displayed in the upper-left corner. Species representing the extremes of each PC are indicated, and extant species that closely resemble the ancestral axial phenotype of the common ancestor of Pseudocrenilabrinae, along with a graphical representation of their axial phenotype. Modal total vertebral counts for each species are indicated in green. Spheres around each water system cluster represent the 95% CI. Distribution of ln[Total Counts] (B) and ln[Precaudal]-ln[Caudal] ratio (C) by water system. Means are indicated with a cross. All mean differences were significant (p¿0.001), besides the ln[Precaual]-ln[Caudal] ratio of Lake Tanganyika and Lake Malawi. See Supplementary Materials for image credits. Genera omitted: A, *Anomlochromis* (*thomasi*), *Abactochromis* (*labrosus*), *Alticorpus* (*macrocleithrum*); B, *Bathybates*; C, *Chilochromis* (*duponti*), *Chromidotilapia* (*cavallensis*); D, *Divandu*; E, *Enantiopus*, G, *Gobiocichla*; R, *Rhamphochromis*; S, *Serranochromis*

two relatively basal Pseudocrenilabrinae groups: large, deep-bodied riverine cichlids, with relatively few total vertebrae (Supplementary Figure 2) many of which were formerly grouped as catch-all Tilapiines (Poll, 1986), including Oreochromini, Coptodonini, Tilapiini, and Pelmatolapiini from Africa and the Middle East, and smaller species (Chromidotilapiini, Pelmatochromini) native to western and central Africa (Astudillo-Clavijo et al., 2023). Notably, just two species of riverine haplochromines fell into this distinct region of axial morphology (*Pseudocrenilbarus multicolor* and *Ctenochromis oligacanthus*), suggesting that the majority of riverine haplochromines have retained axial morphologies more similar to lacustrine species. A broad pattern of disparity in morphospace occupation between riverine and lacustrine cichlids persists along PC3 and PC4, reinforcing the broader axial diversity of riverine species relative to their lacustrine counterparts (see Supplementary Figure 3).

Despite having considerable overlapping occupation of axial morphospace lacustrine species, on average, are more elongate (PC1) and have larger counts of caudal vertebrae (PC2) than riverine species (MANOVA, d= 2.742, Z=8.218, p$<$0.0001). Consistent with this, riverine species have, on average, significantly fewer total vertebrae (Figure 2B) and a higher precaudal:caudal ratio (Figure 2C) than members of the lacustrine radiations, including the Lake Tanganyika species flock, the oldest of the East African adaptive radiations and more comparable to riverine lineages in terms of tribe-level diversity (Astudillo-Clavijo et al., 2023). However, despite the observed differences between riverine and lacustrine cichlids, we found no evidence that adaptation to riverine or lacustrine environments *alone* was responsible for driving the differences observed in ln[Total Counts] (see Table 1). Therefore, the increased vertebral counts in lacustrine systems are likely being driven by more complex regimes.

Higher stochastic rates lead to greater vertebral diversity in riverine cichlids

Consistent with riverine species occupying a broader axial morphospace than lacustrine species, the variance of residual ln[Total Count] is significantly greater in extant riverine species when phylogeny is accounted for (Levene's Test: F = 10.747, p = 0.00113, $d.f.$ = 427), nearly twice that observed in lacustrine species (variance ratio = 1.78). This pattern is likely a consequence of underlying differences in the rate of ln[Total Count] evolution. Among the models tested for the evolution of ln[Total Count], the best-supported was a modified Brownian motion model (BMS), in which ln[Total Count] evolves under distinct stochastic rates (σ^2) in riverine environments and within each lacustrine radiation. Under this model, ln[Total Count] in riverine lineages evolves at a median stochastic rate of 0.001520 ln[Total Count]/myr—more than twice the median rates estimated for the lacustrine radiations (0.000344-0.000736 ln[Total Count]/myr). This indicates that riverine lineages accumulate variation in total vertebral counts more rapidly than any lacustrine radiation. Accordingly, the elevated variance and broader axial morphospace occupation observed in riverine species appears to be driven by an accelerated evolutionary rate (σ^2) (see Table 1).

Individual lacustrine stochastic rates correlate with the age of the respective radiations, with older lakes exhibiting higher evolutionary rates. Lake Tanganyika, the oldest, shows a median rate of 0.000736 ln[Total Count]/myr; Lake Malawi, intermediate in age, exhibits a slightly lower rate of 0.000586 ln[Total Count]/myr; and the youngest, Lake Victoria, has the lowest rate at 0.000344 ln[Total Count]/myr. Since stochastic rates correlate with the relative ages of the lacustrine radiations, the accumulated variance in ln[Total Count] (Figure 2B), and indeed axial morphology (Figure 2A), is not simply a function of divergence time. Rather, it also reflects differences in evolutionary rate (σ^2), suggesting that young radiations like Lake Victoria also exhibit slower trait evolution than older radiations. Moreover, we found no evidence that shared ancestry among haplochromine lineages, which have radiated independently in Lake Tanganyika (Tropheini) (Ronco et al., 2021) and in riverine systems, as well as in Lake Malawi and Victoria, accounts for observed differences between lacustrine lineages. Instead, the differences in evolutionary rate appear to be shaped primarily by environmental context rather than phylogenetic

relatedness.

Demersal, pelagic, and piscivorous lineages have evolved elongate bodies with high vertebral counts

We observed distinct differences in axial morphospace occupancy among species occupying different positions along the bentho-pelagic axis. Pelagic and demersal species are generally more elongate (PC1) and exhibit relatively higher caudal vertebral counts (PC2) than benthopelagic species (Figure 3A), suggesting that elongation of the body axis and the addition of caudal vertebrae represent key adaptations to demersal and pelagic lifestyles, both across the subfamily and within lacustrine radiations (for MANOVA results, see Supplementary Figure 5). Similarly, piscivorous species have more positive PC1 and PC2 scores than non-piscivores (Figure 3B; MANOVA, d = 1.446, Z = 4.935, p $<$ 0.0001), indicating that body elongation has also been important in the evolution of piscivorous lineages. Consistent with this, piscivores, on average, possess significantly more vertebrae than non-piscivores (Figure 3C). Although mean ln[Total Count] does not differ significantly between benthopelagic and demersal species overall (Figure 3D), among lacustrine species, demersal species are more elongate than their benthopelagic counterparts (Figure Supplementary Figure 5B). Together, these results suggest that pelagic, demersal, and piscivorous species have independently evolved elongated body axes supported by increased total and caudal vertebral counts.

Whilst OU models provided the best fit for both the benthic-pelagic axis and piscivory regime comparisons, we found no evidence of strong selection within any regime (Table 1). Estimated attraction (α) parameters were extremely low, approaching zero, indicating very weak, if any, attraction toward trait optima (θ). Therefore, phylogenetic half-lives ($ln(2)/\alpha$), or the time required in millions of years for half of the phylogenetic covariance to be erased between sister taxa, are exceptionally large, far exceeding the age of the lacustrine radiations. For example, ln[Total Count] in piscivorous lineages reported the highest α parameter of $0.03156\,\mathrm{Myr}^{-1}$. As a consequence, it would take approximately 22 million years for ln[Total Count] to move towards its long term optimum, nearly twice the age of the Lake Tanganyika radiation (Ronco et al., 2021) and 22 times the age of the Lake Malawi radiation (Malinsky et al., 2018). In addition, when $\alpha \sim 0$, OU models behave similarly to Brownian motion models with a directional trend ($\mu = \alpha\theta$), representing the estimated rate of directional change per million years (Hansen, 1997). ln[Total Counts] in pelagic lineages are estimated to change more rapidly than in demersal or benthopelagic lineages, which may contribute to the higher total counts present in pelagic species (Figure 3C). Notably, however, piscivorous lineages were estimated to have the highest μ (0.11098 [0.00000, 0.15360] ln[Total Count]/myr), approximately seven times greater than the μ estimated for pelagic lineages (0.01577 [0.01039, 0.02146] ln[Total Count]/myr), suggesting a much steeper directional increase in ln[Total Count] in piscivorous lineages than any of the benthic-pelagic regimes. However, model comparisons indicated that adaptation along the benthic-pelagic axis or to piscivory poorly explained the evolution of ln[Total Count], despite the observed differences in trait values across these regimes.

The addition of vertebrae is important but is not the only driver of body elongation

Whole body aspect ratio is weakly, but nonetheless significantly, positively correlated with total vertebral counts (Figure 4A, R^2 = 0.238, β_1 = 1.475, λ = 0.918, $p > 0.0001$, *d.f.* = 427). Since the slope coefficient (β_1) is greater than 1.00, both vertebral count and body aspect have scaled non-linearly as African cichlids diversified, with the magnitude of the increase in body aspect ratio decreasing in lineages with already relatively high vertebral counts ($Y = e^{-4.109} * X^{1.511}$). A high λ value (0.918) suggests that the covariance between ln[Total Count] and ln[Length] - ln[Depth] is strongly constrained by shared ancestry. Nonetheless, ln[Total Count] explains only a small portion of the variation in ln[Length] - ln[Depth] (R^2 = 0.238), indicating that additional mechanisms likely contributed to body elongation during the

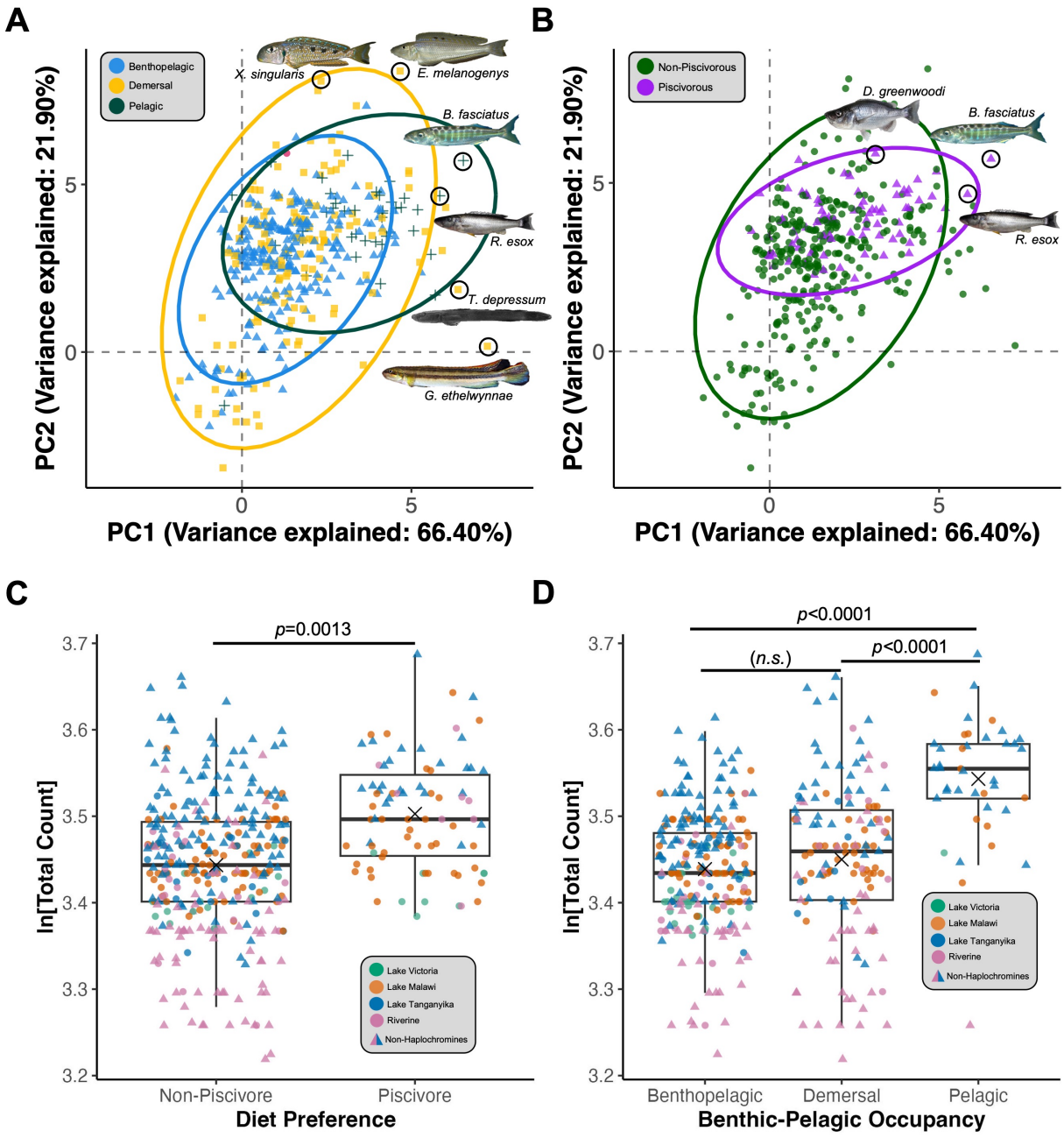

Figure 3. Phylogenetic PCA plotting PC1 against PC2. The variance explained by PC1 and PC2 is indicated on the axes, see Figure 2A for loadings. Species have been grouped according to their occupation along the benthic-pelagic axis (A) or piscivory (B). Spheres around each group cluster represent the 95% CI. Distributions of ln[Total Count] by depth preference (C) and piscivory (D) for all species. The water system each species belongs to is indicated by the key. Means for each group are indicated with a black cross. Whether means between groups is indicated by horizontal bars. Means were compared with a phylogenetic ANOVA (see Methodology), the significance of each mean difference is indicated.

diversification of African cichlids.

Both *Gobiocichla* and *Teleogramma* are rheophilic genera composed of highly elongate species, but they have fewer vertebrae than would be expected for such elongate species (Figure 4A, dotted black box). The most elongate species in the dataset, *Teleogramma depressum*, is on average 9.05 times as long as it is wide but has only 33.68 vertebrae, approximately 50% fewer vertebrae than would be predicted by our model (65.18). Coincidentally, both genera exhibit extremely elongate anterior (primarily the cranial region) and post-cranial bodies, consistent with the strong positive correlation we found between the anterior and posterior body aspect ratios (Figure 4B, $R^2 = 0.618$, $\beta_1 = 0.688$, $\lambda = 0.738$, $p < 0.0001$, *d.f.* = 427) across the whole subfamily. This suggests that elongation of the post-cranial body is typically accompanied by elongation of the head as well. Notably, the relationship between cranial and posterior elongation is less strongly tied to phylogenetic structure ($\lambda = 0.738$, 95% CI: [0.582, 0.847]), suggesting greater evolutionary flexibility and modularity in these traits, allowing for independent modification among sister taxa. Interestingly, cranial elongation is only weakly correlated with increases in total vertebral counts (Table 2, $R^2 = 0.061$, $\beta_1 = 0.741$, $\lambda = 0.933$, $p < 0.0001$, *d.f.* = 427). Therefore, while vertebral addition has been important for body elongation, other mechanisms independent of vertebral count also contribute to the evolution of this trait.

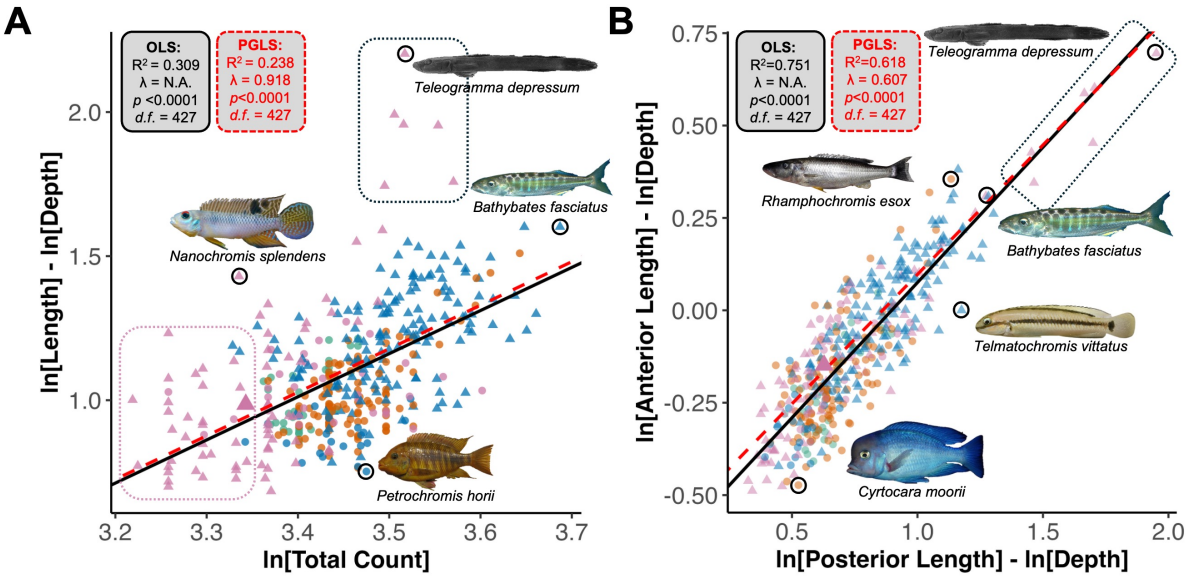

Figure 4. Scatterplots of whole body aspect ratio (ln[Length] - ln[Depth]) and ln[Total Count] (A) and anterior aspect ratio (ln[Anterior Length] - ln[Depth]) and post-cranial body aspect ratio (ln[Posterior Length] - ln[Depth]) (B). Regression lines for the OLS (black) and PGLS (red, dashed) are shown for the best fitting model (see Table 2). Residual *d.f.* for each model fit are indicated. *Teleogramma* and *Gobiocichla* are indicated by the dotted black box. A distinct region of riverine axial morphology (deep bodied with fewer vertebrae is indicated in the dotted pink box. Note that such a region is not found in (B). See Supplementary Materials for image credits.

The common ancestor of Pseudocrenilabrinae had a distinctly riverine axial morphology

We found that the common ancestor of all African cichlids was probably a riverine species (Supplementary Figure 4), preferring relatively shallow, benthopelagic environments (Supplementary Figure 6), and likely preferred a non-piscivorous diet (Supplementary Figure 7). As previously suggested (Oliver, 2024), our models predict that the common ancestor of African cichlids had relatively few vertebrae (ln[Total Count],

$\bar{x}$=3.343 (28.30), 95% CI [3.340, 3.346]) compared to extant members of Pseudocrenilabrinae (z-score = -1.36), a value within the range of the standard error associated with the estimated Z_0 of the BMS model of ln[Total Count] (see Table 1) and below the mean for extant riverine species (Figure 2B, large pink triangle). Consistent with having relatively few vertebrae, the ancestor was inferred to be fairly deep-bodied (ln[Length] - ln[Depth], $\bar{x}$=0.986 (2.68), 95% CI [0.972, 0.999], z-score = -0.476), which along with the relatively low ln[Total Count] places it within a broad region of axial morphospace only occupied by riverine species (Figure 4A, large pink triangle). The species is predicted to have had a high precaudal-caudal ratio (ln[Precaudal] - ln[Caudal], $\bar{x}$=-0.091, 95% CI [-0.096, -0.086], z-score = 0.896), the latter of which places it above the average for extant riverine taxa and considerably higher than any of the lacustrine radiations (Figure 2C, large pink triangle).

Consistent with the estimation of a relatively low whole body aspect ratio (see Table 2), the common ancestor of all African cichlids likely had a fairly wide but short cranial region (ln[Anterior Length] - ln[Depth], $\bar{x}$=-0.148 (0.862), 95% CI [-0.164, -0.133], z-score = -0.189) and a fairly laterally compressed posterior (ln[Posterior Length] - ln[Depth], $\bar{x}$=0.628 (1.874), 95% CI [0.614, 0.642], z-score = -0.509). Comparisons of the reconstructed ancestral traits with extant distributions indicate that the common ancestor of Pseudocrenilabrinae occupied a position in axial morphospace exclusively associated with riverine species. *Divandu albimarginatus* (based on axial traits alone, using Euclidean distance, 94.09% similar) and *Chilochromis duponti* (based on both axial and qualitative traits, using Gower distance, 95.02%) represent the closest matches to the reconstructed traits of the common ancestor of Pseudocrenilabrinae and both occupy the region of axial morphospace unique to riverine species (Figure 2A). These findings reinforce that riverine species exhibit a broader range of axial morphologies than lacustrine species and suggests that all axial phenotypes found in African cichlids have evolved from a region of axial morphospace that is exclusively occupied by riverine species.

DISCUSSION

A fairly deep-bodied, benthopelagic riverine cichlid with relatively few vertebrae diverged from the rest of Cichlidae approximately 64–58 mya (Friedman et al., 2013; McGee et al., 2020; Matschiner et al., 2020), giving rise to Pseudocrenilabrinae, which diversified into hundreds of species spread across the rivers and lakes of Africa. Early in the diversification of Pseudocrenilabrinae, species adapted to various riverine environments, modifying their axial morphologies as they did. Extreme elongation would go on to evolve in some rheophilic lineages, however, many other riverine lineages would go on to evolve even deeper bodies, losing vertebrae in the process. These riverine ancestors would later seed the lacustrine radiations (Ronco et al., 2021; Malinsky et al., 2018; Meier et al., 2017), where their descendants rapidly diversified, adapting to lacustrine niches and further modifying their axial morphologies in the process. In particular, pelagic, demersal and piscivorous lineages would go on to elongate their bodies by the addition of vertebrae, emphasising the importance of a fusiform body for the adaptation to these niches. Ultimately, however, lacustrine lineages evolved by repeatedly and independently evolving axial morphologies that had already been explored by riverine lineages.

Previous evidence has shown that body shape underwent an early burst within the Lake Tanganyika cichlid radiation (Ronco et al., 2021) and we assumed total vertebral counts should have been subject to the same dynamics, given that modification of vertebral counts are important in elongation of the body (this study). This discrepancy may partly reflect the relatively weak correlation between ln[Total Count] and body elongation. Nonetheless, the elevated evolutionary rate in Lake Tanganyika suggests that increased variance in vertebral counts, and more broadly, axial morphology, is not simply a consequence of increased time available for diversification in Lake Tanganyika. In contrast to Lake Tanganyika, the

cichlid radiations of Lakes Malawi and Victoria are considerably younger, estimates place both radiations on the scale of several hundred thousand years old (Malinsky et al., 2018), if not younger (Meier et al., 2017). Uyeda et al. (2011) previously demonstrated that whilst rapid, short term ($<$1 myrs) trait evolution can occur, and our analysis clearly indicates vertebral counts have evolved in Lake Malawi, the rates may be constrained, where neither of the radiations have had sufficient time to accumulate variation. Over longer intervals ($>$1 myrs), such as that of Lake Tanganyika, this pattern of bounded evolution capitulates to a pattern of increasing divergence with time. Preliminary evidence did suggest that the best fitting model for ln[Total Count], ln[length]-ln[Depth] and ln[Precaudal]-ln[Caudal] evolution within Lake Malawi was the exponentially accelerating model of Blomberg et al. (2003) (data not shown), suggesting that axial morphospace in Lake Malawi is still being explored. Whilst our analysis demonstrates that total vertebral count evolution has evolved under different stochastic rates, individual lacustrine dynamics are more complex than a single stochastic rate. Therefore, more considerate comparisons between the radiations, particularly between Lake Malawi and Lake Tanganyika, could better capture the dynamics of axial evolution in African cichlids.

Whilst we have paid great attention to the axial morphospace explored by African cichlids, the regions of axial morphospace not explored are interesting too. For example, we do not see anguilliform African cichlids, nor do we see African cichlids that are deeper than they are longer. Species falling outside of the 95% CIs for their respective water systems' axial morphospace have extreme phenotypes, 'monsters' (Alberch, 1989), may be indicative of constraints on the evolution and development of the vertebral column and provide important models to study the evolution and development of the axial skeleton. Species within the demersal Ectodini tribe (such as *Enantiopus melanogenys*, see Figure 2A) are endemic to Lake Tanganyika and have evolved elongate bodies, supported by many caudal vertebrae, occupying the 10% of lacustrine morphospace absent of any riverine species. Presumably, the elongate caudal domains provide an elongate posterior and tail that is beneficial for its substrate burying habits. Additional 'monsters', such as *Gobiocichla* and *Cyprichromis*, have convergently evolved unique axial morphologies characterised by the expansion of the precaudal vertebral domain, loss of articulation of the anal fin with the caudal domain and an anterior shift in the positioning of the anal fin (Oliver, 2024) and could provide powerful models to study the evolution and development of body plan patterning in teleosts. American cichlids (Subfamily: Cichlinae) have evolved multiple axial morphologies not observed in Pseudocrenilabrinae. For example, species belonging to *Symphysodon* (Discus fish) and *Pterophyllum* (Angelfish), are deeper than they are long and elongate members of *Crenicichla* (Pike cichlids) have large numbers of vertebrae with relatively high precaudal counts (Varella et al., 2023), a phenotype not seen in any active, predatory piscivores in African cichlids. Moreover, in contrast to African cichlids, the vast majority of species diversity within Cichlinae is riverine (Sparks and Smith, 2004; Leo Smith et al., 2008). Therefore, expansion of the analysis to the whole family would provide a full understanding of the axial morphology occupied within Cichlidae, providing a better understanding of the constraints present on the evolution of the vertebral column and help parse impact of adaptation to riverine environments on axial morphology.

The addition of vertebrae is a common means of elongation within teleosts (Ward and Brainerd, 2007; Mehta et al., 2010; Ward and Mehta, 2010). However, the real axis of change is that of elongation of the whole body. Much of the body shape diversity present in tropical reef fishes, for example, has primarily been driven by diversification along an axis of body elongation (Claverie and Wainwright, 2014), which is also the case for African cichlids. Consistent with other teleostean clades, evolving an elongate body has also been important for piscivores and pelagic species, where a more elongate fusiform body likely ensures predators can move through the water column more efficiently (Mehta et al., 2010). It is perhaps unsurprising, therefore, that the highest extreme of the total vertebral count distributions is occupied by species that are both pelagic and piscivorous, such as those belonging to Tanganyikan *Bathybates* and

Malawian *Rhamphochromis*, which despite being in different lacustrine radiations and subject to different stochastic rates, have convergently evolved the highest vertebral counts in the subfamily (Stiassny, 1981) and occupy the same region of axial morphospace. Whilst our data does suggest that piscivores tend to be more elongate (and have relatively higher caudal vertebral counts) than non-piscivores, a fusiform body allows for fast movement, which is essential for active predators. Across the subfamily we see multiple examples of piscivorous species that have average vertebral counts. Ambush predators such as those belonging to *Nimbochromis* and *Cyphotilapia*, endemic to Lake Malawi and Lake Tanganyika, respectively, are relatively deep bodied with average vertebral counts. Presumably, since they are not actively involved in the sustained pursuit of prey they have not needed to evolve an elongate body form.

Vertebral counts have not co-evolved with cranial elongation, but an extended cranium is usually accompanied by increased posterior body aspect ratio, a pattern consistent with the extremely slender forms of elopomorphs (Mehta et al., 2010), suggesting these trends may be widespread among teleosts. Whilst the addition of vertebrae has been important in elongating the body in African cichlids, it is clear that additional mechanisms are also contributing to elongation of the whole body. Fast predatory fish such as barracuda and Scombriformes are known to have relatively few vertebrae compared with other similarly elongate fish (Mehta et al., 2010), opting instead to modulate the vertebral aspect ratio to generate fewer but more elongate vertebrae which may stiffen their body axis, providing better propulsion when pursuing prey (Jimenez et al., 2023). It is possible that different lineages may be modulating their vertebral shape to contribute to elongation of the body in cichlids too, which could explain the relatively fewer than expected vertebrae in *Teleogramma* and *Gobiocichla*. Given that both genera are demersal and rheophilic having a stiff vertebral column with relatively few vertebrae could be advantageous. In contrast, the increased flexibility presumably provided by the addition of vertebrae may explain why the addition of vertebrae has a diminishing effect on the whole body aspect ratio. The active and sustained pursuit of prey is critical for the success of *Rhamphochromis* and *Bathybates* and the added flexibility provided by vertebral addition (and more elongate body) is presumably maladaptive to this lifestyle (to a certain limit). Therefore, the addition of vertebral aspect ratios and quantification of intervertebral distances, which have been modified during teleostean diversification (Baxter et al., 2022), may help dissect the relationship between vertebral column flexibility, whole body elongation and the number of vertebrae.

Little is known about early cichlid evolution and inferences can only be made through macroevolutionary studies, the study of fossils or their incorporation into macroevolutionary studies. Cichlid fossils have been identified (Murray, 2001a,b; Altner et al., 2020) and have been important in setting a minimum age for the origin of cichlids (Friedman et al., 2013). However, their placement within the current subfamily tree is difficult to determine and relies upon taxonomic comparison with extant tribes and placement within the tribe it shares the most characters with (Altner et al., 2020). For this reason, we did not include any fossil data within our analysis, despite it providing useful node priors in ancestral state reconstruction (Barba-Montoya et al., 2017; Mongiardino Koch et al., 2021). Along with previously released datasets (Bucklow et al., 2024; Oliver, 2024), we have generated a very large dataset of multiple axial traits and ancestrally reconstructed multiple axial phenotypes across Pseudocrenilabrinae, This may improve confidence in placing fossils within the subfamily, particularly when axial traits are combined with other characters that vary more markedly between clades and offer stronger resolution for clade-level identification.

Here we have presented the first macroevolutionary study of axial morphology in African cichlids. Our analysis clearly indicates the importance of careful, considerate comparative studies of the evolution of African cichlids and the necessity of including riverine species within these analyses. Large quantities of morphological (Ronco et al., 2021; Haberthür et al., 2023; Bucklow et al., 2024), genomic (Meier et al., 2017; Malinsky et al., 2018; McGee et al., 2020; Ronco et al., 2021; Meier et al., 2023; Astudillo-Clavijo

et al., 2023) and behavioural (Johnson et al., 2020; Sommer-Trembo et al., 2024) data has been generated and collated across African cichlids, particularly for the lacustrine radiations. Whilst the radiations of Lakes Tanganyika, Malawi and Victoria are impressive model systems, and much important work has been completed to elucidate the genomic mechanisms occurring within each radiation. Integrated approaches to understand how phenotypic variation has arisen across the subfamily remain scarce. Now is the time to integrate these data across radiations. Only through a comparative approach, across macroevolutionary and microevolutionary scales, can we begin to elucidate the generalisable dynamics that have been critical to the evolution of African cichlids.

TABLES

Trait	Regime	Model	Median AICc	AICc Weight	Median Parameters (Range)				
					Stochastic Rate (σ^2)	Attraction (α) [Half-Life]	Optima (θ) or Root (Z_0)	*s.e.* of θ or Z_0	Trend Coefficient (μ)*
ln[Total Count]	Riverine	OUMV	-1039.959	0.983	0.0521 (0.0520, 0.0523)	6.0934 (6.0924, 6.0934) [0.11375]	3.3841 (3.3834, 3.3847)	0.0083 (0.0083, 0.0084)	-
	Lacustrine				0.0855 (0.0847, 0.0864)		3.4829 (3.4827, 3.4832)	0.0040 (0.0040, 0.0040)	-
ln[Total Count]	Basal Riverine	OUMVA*	-1375.888	0.992	0.001485 (0.001469, 0.001510)	1.24E-09 (1.00E-09, 2.76E-09)	3.3221 (3.3159, 3.3230)	0.0309 (0.0308, 0.0313)	-
	Lake Tanganyika^				0.000035 (0.000031, 0.000458)	0.0349 (0.0050, 0.0359)	3.4869 (3.4762, 4.1828)	0.0502 (0.0490, 0.4252)	-
	Haplochromini^				0.000746 (0.000746, 0.000763)	3.54E-09 (1.04E-09, 1.12E-08)*	N.A.*	-	0.00560 (0.00000, 0.006456)
ln[Total Count]	**Riverine**	**BMS**	**-1380.227**	**0.905**	**0.001520 (0.001487, 0.016080)**	**-**	**3.3162 (3.3161, 3.3163)**	**0.0317 (0.0313, 0.0326)**	**-**
	Lake Tanganyika				**0.000736 (0.000694, 0.000753)**				
	Lake Malawi				**0.000586 (0.000583, 0.000591)**				
	Lake Victoria				**0.000344 (0.000343, 0.000352)**				
ln[Total Count]	Benthopelagic	OUM*	-1356.217	0.449	0.00084 (0.00083, 0.00085)	1.68E-08 (6.54E-09, 2.37E-07)*	N.A.*	-	0.00283 (0.00000, 0.00515)
	Demersal						N.A.*	-	0.00662 (0.00000, 0.00955)
	Pelagic						N.A.*	-	0.01577 (0.01039, 0.02146)
ln[Total Count]	Benthopelagic	OUMV*	-1356.175	0.279	0.00072 (0.00062, 0.00086)	1.01E-08 (4.61E-09, 2.60E-07)*	N.A.*	-	0.00307 (0.00000, 0.00532)
	Demersal				0.00102 (0.00081, 0.00119)		N.A.*	-	0.00691 (0.00000, 0.00997)
	Pelagic				0.00107 (0.00093, 0.00126)		N.A.*	-	0.01778 (0.01118, 0.02330)
ln[Total Count]	Non-Piscivore	OUMVA*	-1364.904	0.988	0.00096 (0.00072, 0.00113)	0.00000 (0.00000, 0.00255)	N.A.*	-	0.00000 (0.00000, 0.00845)
	Piscivore				0.00003 (0.00001, 0.00080)	0.03156 (0.00000, 0.04405)	N.A.*	-	0.11098 (0.00000, 0.15360)

Table 1. The parameters of models with non-negligible support for ln[Total Count] evolution during African cichlid diversification are shown. Results are drawn from single and multi-regime Brownian motion (BM) and Ornstein-Uhlenbeck (OU) models. Parameters were estimated from 100 trees with ancestral reconstruction of the indicated regime (see Methodology). The median Akaike's information criteria for finite sample sizes (AICc) and the Median AICc weight (within regime) is indicated for each model. An OUMV model is a model where the trait optima of ln[Total Count] (θ) and the stochastic rate of change in ln[Total Count] per million years is permitted to vary between regimes but the strength of stabilising selection (α) remains the same. Phylogenetic half-life ($ln(2)/\alpha$) is time taken in millions of years for half of the phylogenetic covariance to be erased between sister taxa. A BMS model is a modified BM model where the stochastic rate (σ^2) of ln[Total Count] varies between regimes. *When $\alpha \sim 0$, the OU model behaves similarly to a BM model with a linear directional trend coefficient ($\mu = \alpha\theta$) which represents the change in ln[Total Count] per million years. ^Lake Tanganyika includes all tribes endemic to the lake (excluding Tropheini) and Haplochromini includes all haplochromine lineages, including those endemic to Lake Tanganyika and riverine lineages. The model with the highest support amongst all model fits is shown in bold.

Variables		Non-Phylogenetic (OLS)		Phylogenetic (PGLS)		
Explanatory Variable	Response Variable	R^2	β_1 (%)	R^2	β_1 (%)	Branch Transformation (λ [95% CI]
ln[Total Count]	ln[Length] - ln[Depth]	0.309	1.497	0.250	1.511	0.918 [0.879, 0.945]
ln[Total Count]	ln[Anterior Length] - ln[Depth]	0.204	1.083	0.085	0.861	0.815 [0.729, 0.876]
ln[Total Count]	ln[Posterior Length] - ln[Depth]	0.326	1.619	0.311	1.789	0.933 [0.901, 0.955]
ln[Posterior Length] - ln[Depth]	ln[Anterior Length] - ln[Depth]	0.751	0.732	0.609	0.700	0.607 [0.436, 0.734]
ln[Anterior Length] - ln[Depth]	ln[Length] - ln[Depth]	0.854	1.038	0.740	0.872	0.819 [0.735, 0.877]
ln[Posterior Length] - ln[Depth]	ln[Length] - ln[Depth]	0.977	0.937	0.959	0.924	0.526 [0.326, 0.678]

Table 2. Univariate OLS and PGLS model fits are indicated for each relationship tested and based on data from 429 species retained on the McGee et al. (2020) phylogeny. Adjusted R^2 values for each model fit are shown. Since all variables are natural log-transformed, the slope (m) represents the approximate percentage change in the response variable for a 1% increase in the explanatory variable (elasticity). Maximum likelihood (ML) estimates for λ branch transformation are indicated along with their 95% confidence intervals. AIC weights for each PGLS model are indicated. Note that these weight values refer to the weight of the respective model fit for that relationship. All model fits were highly significant ($p<0.0001$).

SUPPLEMENTARY FIGURES AND TABLES

Variable	Abbreviation	PC1	PC2	PC3	PC4	PC5	PC6
ln[Precaudal Count]	PC	0.9127	-0.0199	-0.4071	0.0282	0.0012	0.0070
ln[Caudal Count]	CC	0.4883	0.8718	0.0237	0.0302	0.0015	0.0085
ln[Total Count]	TC	0.8511	0.4679	-0.2349	0.0365	-0.0012	-0.0135
ln[Precaudal] - ln[Caudal]	PC:C	0.6192	-0.6443	-0.4488	0.0083	0.0001	0.0014
ln[Length] - ln[Depth]	BAR	0.9512	-0.1097	0.2812	-0.0519	-0.0367	0.0007
ln[Anterior Length] - ln[Depth]	AAR	0.7876	-0.3548	0.4864	0.1305	0.0115	0.0000
ln[Posterior Length] - ln[Depth]	PAR	0.9714	-0.0237	0.1927	-0.1340	0.0257	-0.0005
Variance Explained (%)		66.4011	21.8992	11.0820	0.5828	0.0306	0.0044
Cumulative Variance Explained (%)		66.4011	88.3003	99.3823	99.9651	99.9956	≈ 100

Supplementary Table 1. Phylogenetically-corrected principle component loading's for 429 species belonging to all tribes within Pseudocrenilabrinae. Abbreviations refer to those used in Figure 1 for each respective variable. Loadings for PC1 have been multiplied by -1 to make them positive (and consistent with Figure 2). The contributions of PC7 are negligible and have been omitted.

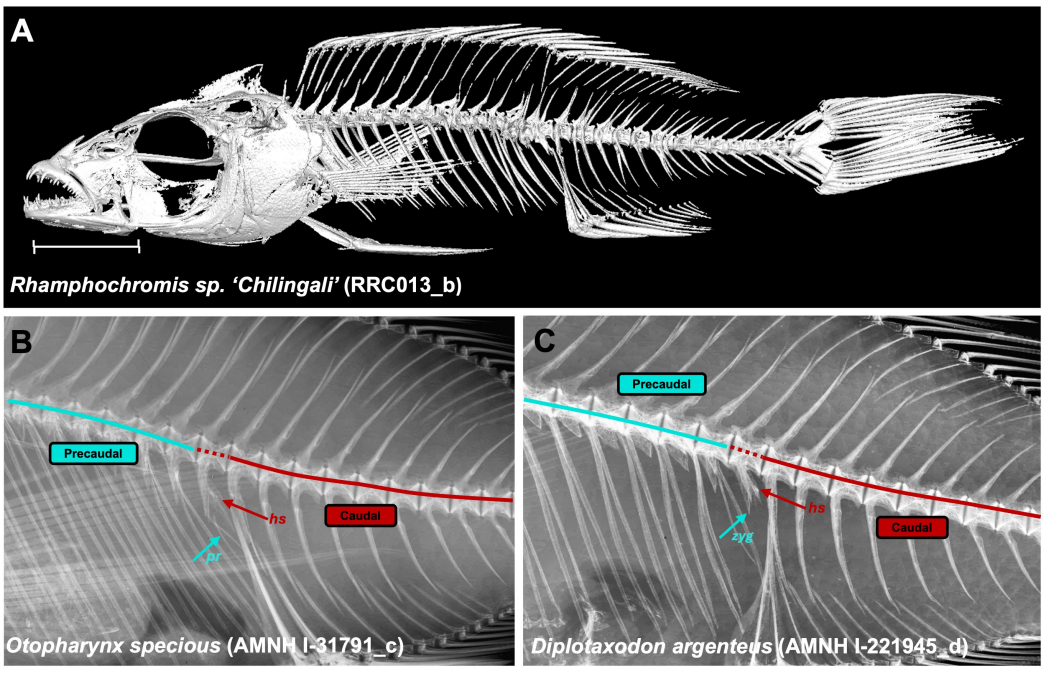

Supplementary Figure 1. Counting Vertebrae and Defining Precaudal-Caudal Boundary (A) A specimen of *Rhamphochromis sp.* 'Chilingali' with a deformed vertebral column with multiple instances of fused vertebrae. Note that each fused centra still retains a neural spine. Scale is 1cm. The threshold value used to generate the model was not high enough to resolve the epineural bone but it is indeed present in the specimen. (B) A transitional vertebrae bearing both rudimentary pleural ribs (pr) (blue arrow) and a haemal spine (hs) and therefore a haemal arch. Specimen references are indicated for each image. (C) An example of a transitional vertebrae that bears zygapophyses (zyg) resembling a precaudal vertebrae (blue arrow) but has a rudimentary haemal spine (hs) and therefore a haemal arch. See Supplementary Materials for images matching these specimens.

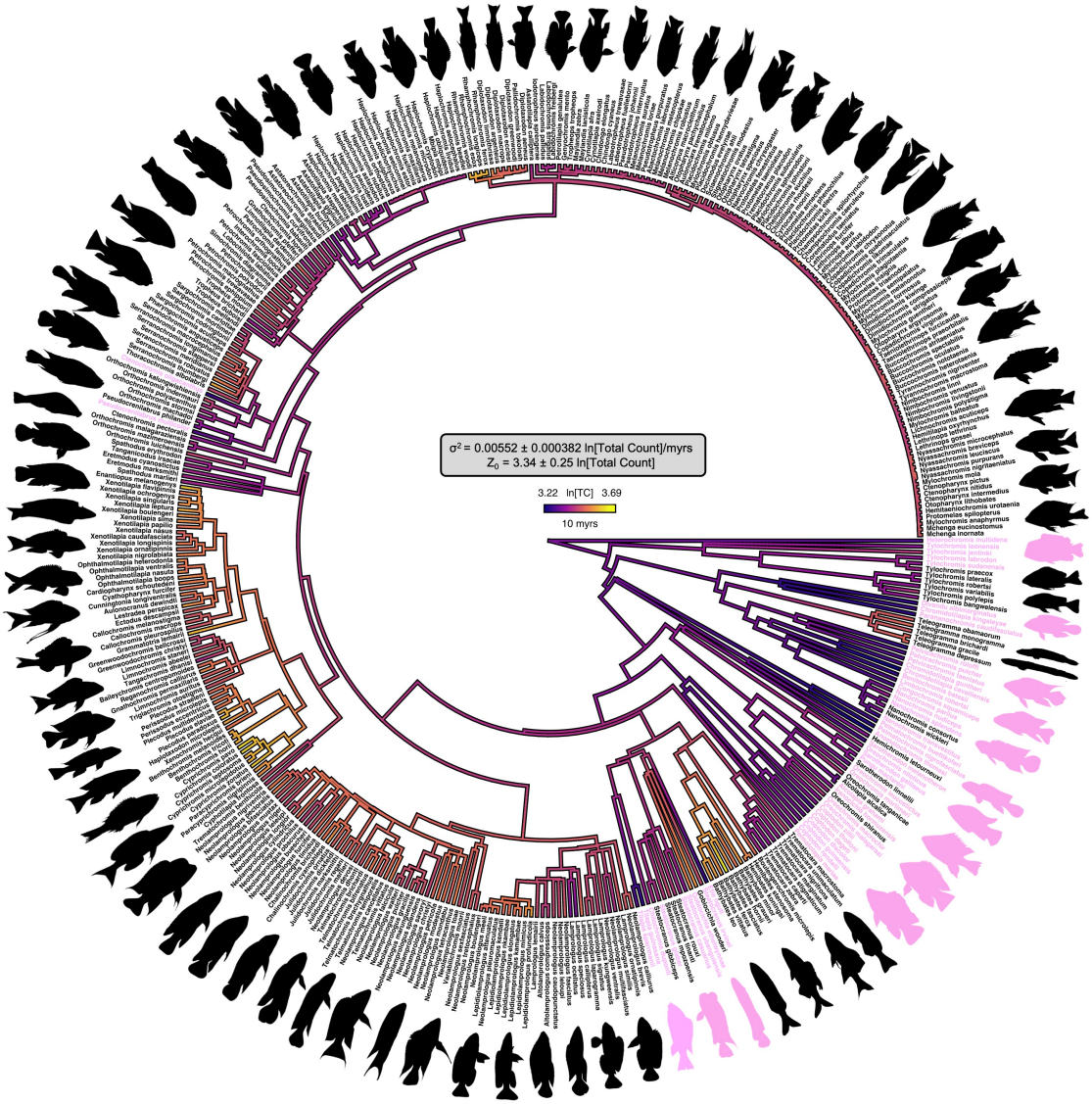

Supplementary Figure 2. Ancestral reconstruction of ln[Total Count] in Pseudocrenilabrinae. A single rate Brownian motion model was fit to the subfamily tree as per the methodology. $\bar{x} \pm \text{SD}$ is shown for the estimated stochastic rate (σ^2) and the root trait value (Z_0). Species present within the distinct riverine axial morphospace are shown as pink tips, the body shape of some of these species is also shown as pink silhouettes. Note that the majority of the species within this distinct region of axial morphospace are predicted to have undergone losses in ln[Total Counts] (dark blue) and are relatively basal on the tree.

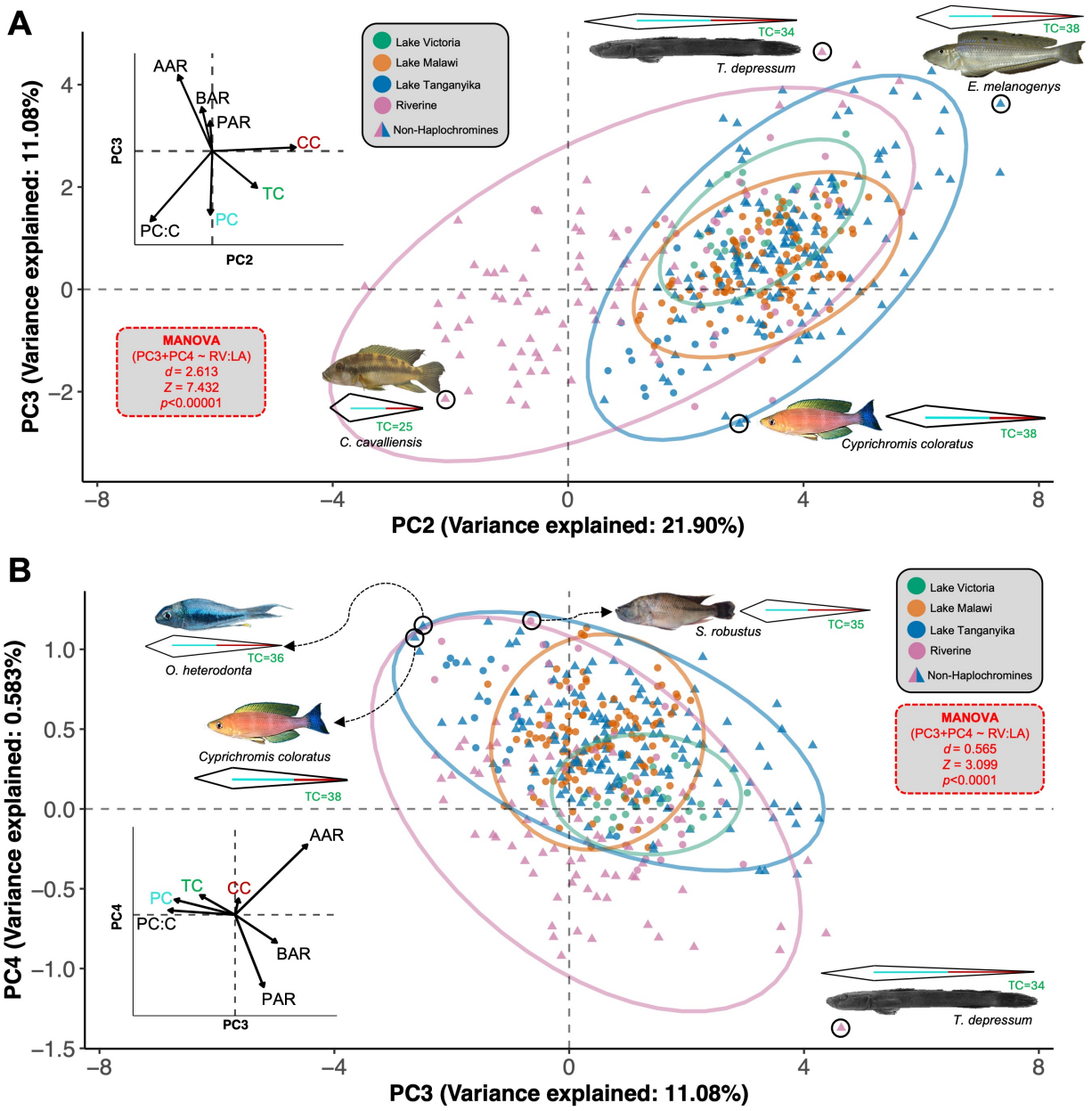

Supplementary Figure 3. Phylogenetic PCA plotting PC2 against PC3 (A) and PC3 against PC4 (B). The variance explained by each PC is indicated on the axes. A loading plot on the same axes is displayed for both plots. Species representing the extremes of each PC are indicated, along with a graphical representation of their axial phenotype. Modal total vertebral counts for each species are indicated in green. Spheres around each water system cluster represent the 95% CI. MANOVA results are indicated in a dashed red box and test for significant differences in the occupation in PC2+PC3 or PC3+PC4 between riverine (RV) and lacustrine (LA, Lake Victoria, Lake Malawi and Lake Tanganyika) species.

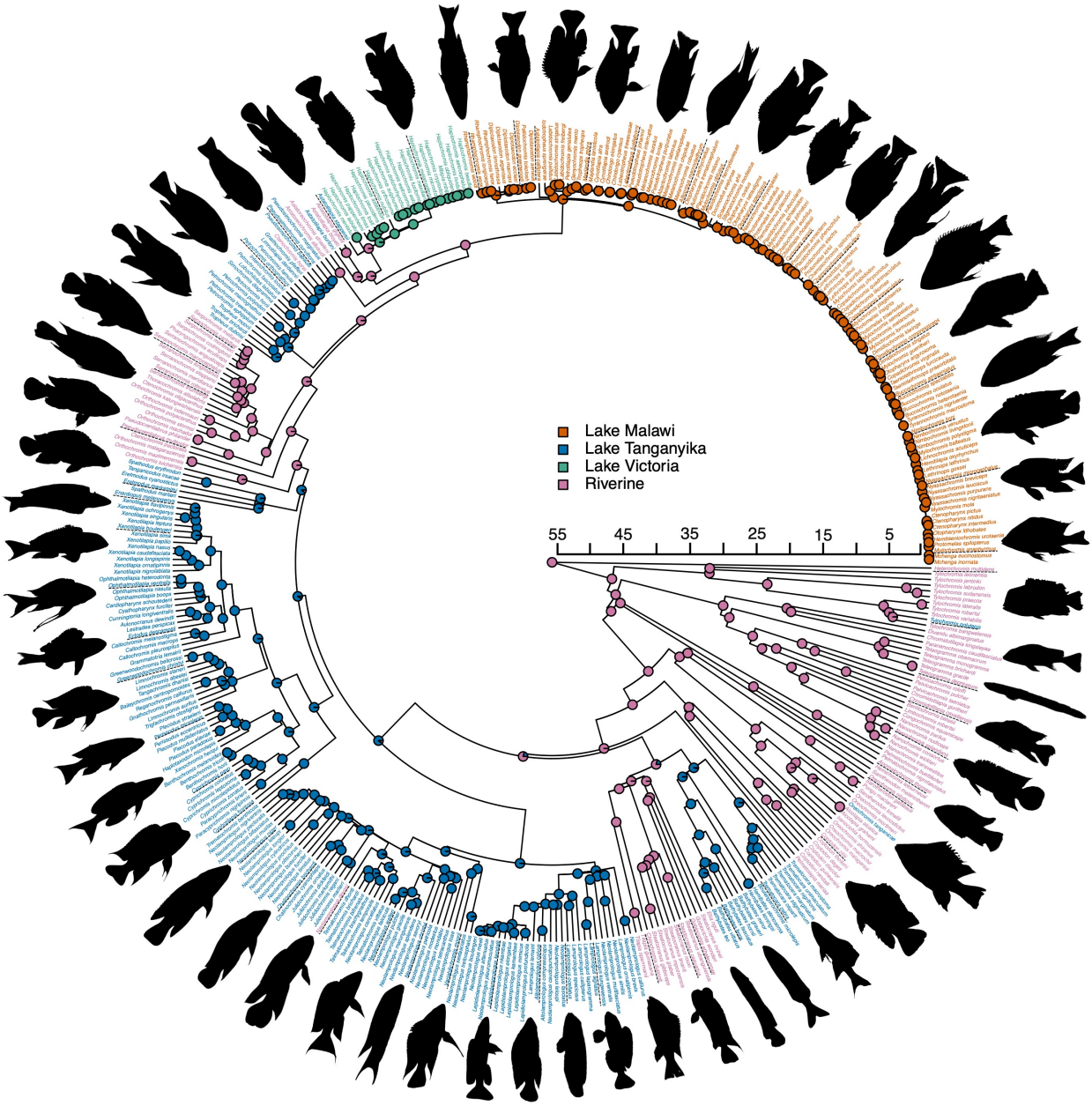

Supplementary Figure 4. Ancestral reconstruction of water system occupancy estimated by maximum likelihood. Uncertainty in node prediction is shown in the form of a pie chart for each node from 10000 simulations (see Methodology). Tips are coloured according to their water system occupancy. Silhouettes of select extant species are shown. Scale is in millions of years. See Supplementary Materials for image credits.

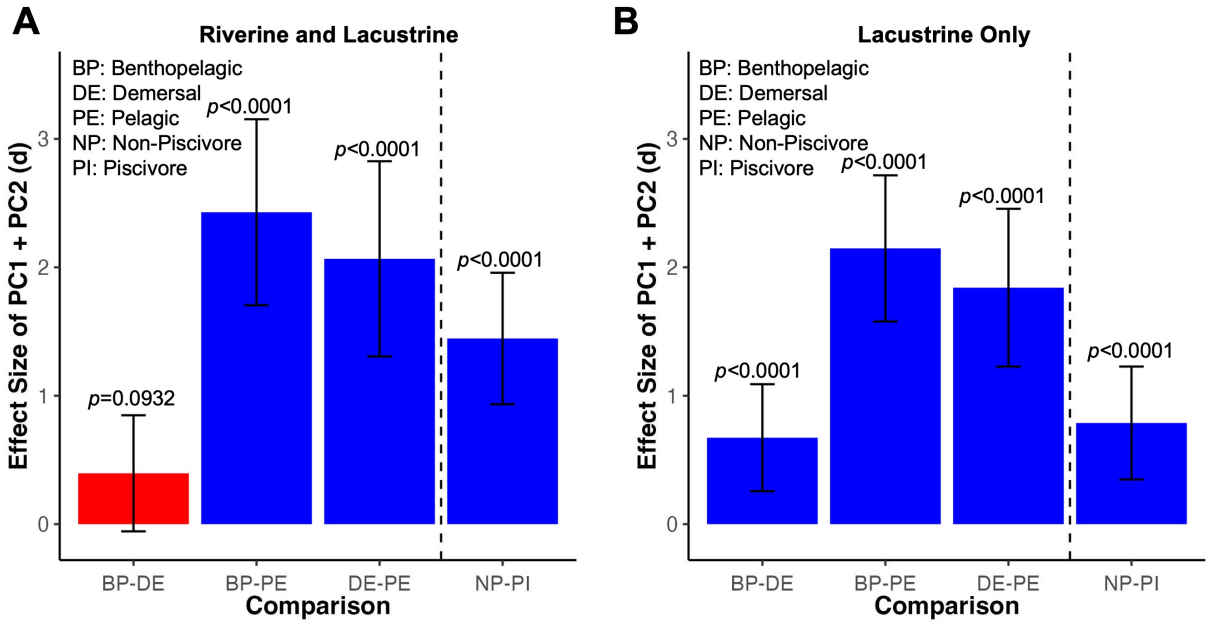

Supplementary Figure 5. Effect sizes (*d*) from a MANOVA on PC1 and PC2 for occupation of species along the benthic-pelagic axis and piscivory are shown for all species (Riverine and Lacustrine, (A) and for Lacustrine species alone (B). Comparisons are indicated (see legend for full details). Significant effects are shown in blue, while non-significant effects are shown in red. Error bars represent the 95% confidence intervals for the effect sizes. P-values for each effect are indicated.

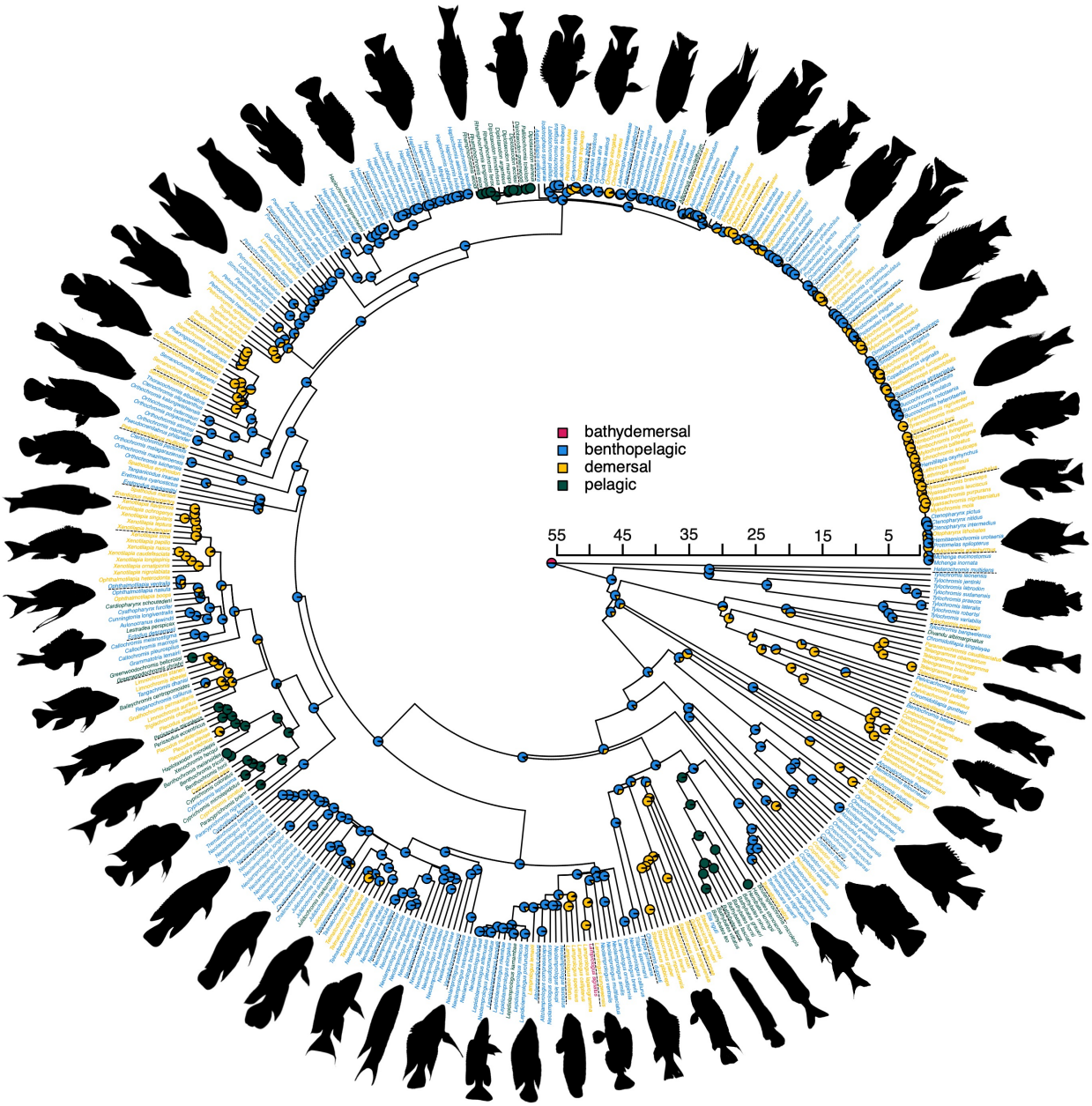

Supplementary Figure 6. Ancestral reconstruction of occupation along benthic-pelagic axis estimated by maximum likelihood. Uncertainty in node prediction is shown in the form of a pie chart for each node from 10000 simulations (see Methodology). Tips are coloured according to their water system occupancy. Silhouettes of select extant species are shown. Scale is in millions of years. See Supplementary Materials for image credits.

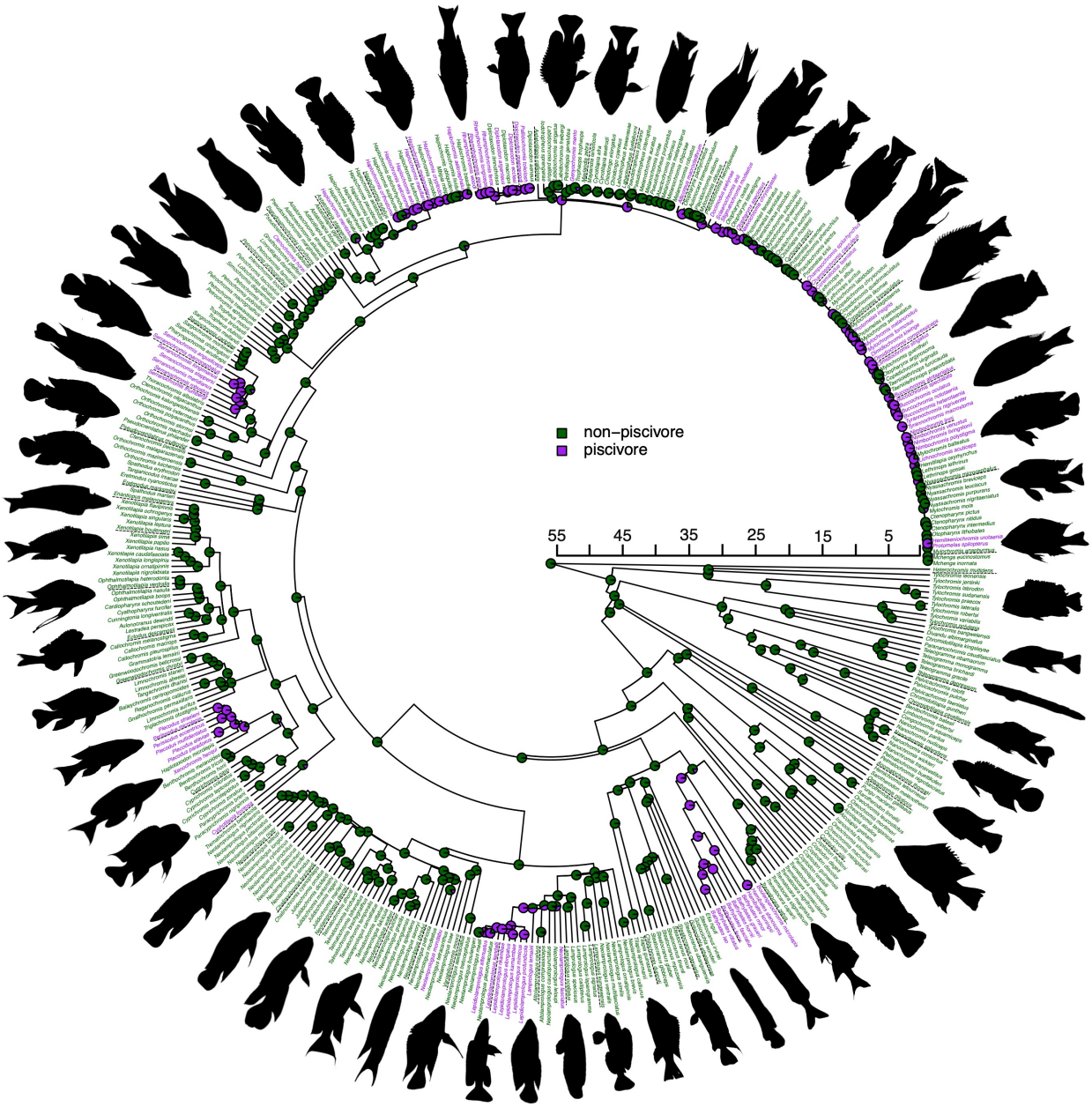

Supplementary Figure 7. Ancestral reconstruction of piscivory estimated by maximum likelihood. Uncertainty in node prediction is shown in the form of a pie chart for each node from 10000 simulations (see Methodology). Tips are coloured according to their water system occupancy. Silhouettes of select extant species are shown. Scale is in millions of years. See Supplementary Materials for image credits.

AUTHOR CONTRIBUTIONS

C.V.B, B.V and R.B conceived the study. C.V.B. collated the data and performed the data analysis. C.V.B, B.V and R.B helped interpret results. E.D.R helped with digitisation of x-rays. F.R., M.K.O, C.V.B and N.V provided x-ray images of specimens. M.S. and W.S. provided access to their respective collections for data collection. C.V.B wrote the manuscript. B.V. and R.B. edited the manuscript. All authors reviewed the manuscript.

ACKNOWLEDGMENTS

This research was funded by a Biotechnology and Biological Sciences Research Council (BBSRC) studentship (Grant Number: 2445747) and by a Swiss National Science Foundation (SNSF) grant (Grant Numbers: 176039 and 208002). Thank you to Richard Durbin for providing whole-body μCT-scans for nine Lake Malawi cichlid specimens. Most of the fish images presented in the figures were taken by just three individuals, Ad Konings, George Turner and Adrian Indermaur and we thank them greatly for the images. Thank you to the fishes whose lives were sacrificed for this work.

REFERENCES

Alberch, P. (1989). The logic of monsters: evidence for internal constraint in development and evolution. *Geobios*, 22:21–57.

Altner, M., Ruthensteiner, B., and Reichenbacher, B. (2020). New haplochromine cichlid from the upper miocene (9–10 mya) of central kenya. *BMC Evolutionary Biology*, 20:1–26.

Astudillo-Clavijo, V., Stiassny, M. L., Ilves, K. L., Musilova, Z., Salzburger, W., and López-Fernández, H. (2023). Exon-based phylogenomics and the relationships of african cichlid fishes: tackling the challenges of reconstructing phylogenies with repeated rapid radiations. *Systematic Biology*, 72(1):134–149.

Baken, E. K., Collyer, M. L., Kaliontzopoulou, A., and Adams, D. C. (2021). geomorph v4. 0 and gmshiny: Enhanced analytics and a new graphical interface for a comprehensive morphometric experience. *Methods in Ecology and Evolution*, 12(12):2355–2363.

Barba-Montoya, J., Dos Reis, M., and Yang, Z. (2017). Comparison of different strategies for using fossil calibrations to generate the time prior in bayesian molecular clock dating. *Molecular Phylogenetics and Evolution*, 114:386–400.

Baxter, D., Cohen, K. E., Donatelli, C. M., and Tytell, E. D. (2022). Internal vertebral morphology of bony fishes matches the mechanical demands of different environments. *Ecology and Evolution*, 12(11):e9499.

Beaulieu, J. M. and O'Meara, B. (2022). *OUwie: Analysis of Evolutionary Rates in an OU Framework*. R package version 2.10.

Blomberg, S. P., Garland Jr, T., and Ives, A. R. (2003). Testing for phylogenetic signal in comparative data: behavioral traits are more labile. *Evolution*, 57(4):717–745.

Britz, R. and Johnson, G. D. (2005). Occipito-vertebral fusion in ocean sunfishes (teleostei: Tetraodontiformes: Molidae) and its phylogenetic implications. *Journal of Morphology*, 266(1):74–79.

Bucklow, C., Duarte-Ribeiro, E., Ronco, F., Vranken, N., Oliver, M., Stiassny, M., Salzburger, W., Benson, R., and Verd, B. (2025). African cichlid lake radiations recapitulate riverine axial morphologies through repeated exploration of morphospace. *Zenodo*.

Bucklow, C. V., Genner, M. J., Turner, G. F., Maclaine, J., Benson, R., and Verd, B. (2024). A whole-body micro-ct scan library that captures the skeletal diversity of lake malawi cichlid fishes. *Scientific Data*, 11(1):984.

Claverie, T. and Wainwright, P. C. (2014). A morphospace for reef fishes: elongation is the dominant axis of body shape evolution. *PloS one*, 9(11):e112732.

Collyer, M. L. and Adams, D. C. (2018). Rrpp: An r package for fitting linear models to high-dimensional data using residual randomization. *Methods in Ecology and Evolution*, 9(7):1772–1779.

De Clercq, A., Perrott, M. R., Davie, P. S., Preece, M. A., Wybourne, B., Ruff, N., Huysseune, A., and Witten, P. E. (2017). Vertebral column regionalisation in chinook salmon, oncorhynchus tshawytscha. *Journal of anatomy*, 231(4):500–514.

Deniz, A. and Ağilkaya, G. Ş. (2018). New record of the slender snipe eel, nemichthys scolopaceus (richardson, 1848), from the north-eastern mediterranean sea (büyükeceli coast). *Mediterranean Fisheries and Aquaculture Research*, 1(2):87–91.

Di'Biagio, C., Dellacqua, Z., Martini, A., Huysseune, A., Scardi, M., Witten, P. E., and Boglione, C. (2022). A baseline for skeletal investigations in medaka (oryzias latipes): The effects of rearing density on the postcranial phenotype. *Frontiers in Endocrinology*, 13:893699.

Ford, E. (1937). Vertebral variation in teleostean fishes. *Journal of the marine biological association of the United Kingdom*, 22(1):1–60.

Fox, J. and Weisberg, S. (2019). *An R Companion to Applied Regression*. Sage, Thousand Oaks CA, third

edition.

Friedman, M., Keck, B. P., Dornburg, A., Eytan, R. I., Martin, C. H., Hulsey, C. D., Wainwright, P. C., and Near, T. J. (2013). Molecular and fossil evidence place the origin of cichlid fishes long after gondwanan rifting. *Proceedings of the Royal Society B: Biological Sciences*, 280(1770):20131733.

Froese, R. and Pauly, D. (2000). *FishBase 2000: concepts designs and data sources*, volume 1594. WorldFish.

Garland Jr, T., Dickerman, A. W., Janis, C. M., and Jones, J. A. (1993). Phylogenetic analysis of covariance by computer simulation. *Systematic biology*, 42(3):265–292.

Genner, M. J. and Turner, G. F. (2012). Ancient hybridization and phenotypic novelty within lake malawi's cichlid fish radiation. *Molecular Biology and Evolution*, 29(1):195–206.

Haberthür, D., Law, M., Ford, K., Häsler, M., Seehausen, O., and Hlushchuk, R. (2023). Microtomographic investigation of a large corpus of cichlids. *Plos one*, 18(9):e0291003.

Hansen, T. F. (1997). Stabilizing selection and the comparative analysis of adaptation. *Evolution*, 51(5):1341–1351.

Indermaur, A., Schedel, F. D., and Ronco, F. (2024). Morphological diversity of the genus telmatochromis from the lake tanganyika drainage with the description of a new riverine species and the generic reassignment of the malagarasi river lamprologine. *Journal of Fish Biology*.

Jimenez, Y. E., Lucas, K. N., Long Jr, J. H., and Tytell, E. D. (2023). Flexibility is a hidden axis of biomechanical diversity in fishes. *Journal of Experimental Biology*, 226(Suppl_1):jeb245308.

Johnson, Z. V., Moore, E. C., Wong, R. Y., Godwin, J. R., Streelman, J. T., and Roberts, R. B. (2020). Exploratory behaviour is associated with microhabitat and evolutionary radiation in lake malawi cichlids. *Animal Behaviour*, 160:121–134.

Joyce, D. A., Lunt, D. H., Bills, R., Turner, G. F., Katongo, C., Duftner, N., Sturmbauer, C., and Seehausen, O. (2005). An extant cichlid fish radiation emerged in an extinct pleistocene lake. *Nature*, 435(7038):90–95.

Leo Smith, W., Chakrabarty, P., and Sparks, J. S. (2008). Phylogeny, taxonomy, and evolution of neotropical cichlids (teleostei: Cichlidae: Cichlinae). *Cladistics*, 24(5):625–641.

Lewis, P. O. (2001). A likelihood approach to estimating phylogeny from discrete morphological character data. *Systematic biology*, 50(6):913–925.

Liem, K. F. and Sanderson, S. L. (1986). The pharyngeal jaw apparatus of labrid fishes: a functional morphological perspective. *Journal of Morphology*, 187(2):143–158.

Maechler, M., Rousseeuw, P., Struyf, A., Hubert, M., and Hornik, K. (2025). *cluster: Cluster Analysis Basics and Extensions*. R package version 2.1.8.1 — For new features, see the 'NEWS' and the 'Changelog' file in the package source).

Malinsky, M., Svardal, H., Tyers, A. M., Miska, E. A., Genner, M. J., Turner, G. F., and Durbin, R. (2018). Whole-genome sequences of malawi cichlids reveal multiple radiations interconnected by gene flow. *Nature ecology & evolution*, 2(12):1940–1955.

Masonick, P., Meyer, A., and Hulsey, C. D. (2022). Phylogenomic analyses show repeated evolution of hypertrophied lips among lake malawi cichlid fishes. *Genome Biology and Evolution*, 14(4):evac051.

Matschiner, M., Böhne, A., Ronco, F., and Salzburger, W. (2020). The genomic timeline of cichlid fish diversification across continents. *Nature communications*, 11(1):5895.

McGee, M. D., Borstein, S. R., Meier, J. I., Marques, D. A., Mwaiko, S., Taabu, A., Kishe, M. A., O'Meara, B., Bruggmann, R., Excoffier, L., et al. (2020). The ecological and genomic basis of explosive adaptive radiation. *Nature*, 586(7827):75–79.

Mehta, R. S., Ward, A. B., Alfaro, M. E., and Wainwright, P. C. (2010). Elongation of the body in eels. *Integrative and Comparative Biology*, 50(6):1091–1105.

Meier, J. I., Marques, D. A., Mwaiko, S., Wagner, C. E., Excoffier, L., and Seehausen, O. (2017). Ancient hybridization fuels rapid cichlid fish adaptive radiations. *Nature communications*, 8(1):14363.

Meier, J. I., McGee, M. D., Marques, D. A., Mwaiko, S., Kishe, M., Wandera, S., Neumann, D., Mrosso, H., Chapman, L. J., Chapman, C. A., et al. (2023). Cycles of fusion and fission enabled rapid parallel adaptive radiations in african cichlids. *Science*, 381(6665):eade2833.

Mongiardino Koch, N., Garwood, R. J., and Parry, L. A. (2021). Fossils improve phylogenetic analyses of morphological characters. *Proceedings of the Royal Society B*, 288(1950):20210044.

Morin-Kensicki, E. M., Melancon, E., and Eisen, J. S. (2002). Segmental relationship between somites and vertebral column in zebrafish. *Development*.

Murray, A. M. (2001a). Eocene cichlid fishes from tanzania, east africa. *Journal of Vertebrate Paleontology*, 20(4):651–664.

Murray, A. M. (2001b). The oldest fossil cichlids (teleostei: Perciformes): indication of a 45 million-year-old species flock. *Proceedings of the Royal Society of London. Series B: Biological Sciences*, 268(1468):679–684.

Mwanja, W. W., Armoudlian, A. S., Wandera, S. B., Kaufman, L., Wu, L., Booton, G. C., and Fuerst, P. A. (2001). The bounty of minor lakes: the role of small satellite water bodies in evolution and conservation of fishes in the lake victoria region, east africa. *Hydrobiologia*, 458:55–62.

Near, T. J. and Thacker, C. E. (2024). Phylogenetic classification of living and fossil ray-finned fishes (actinopterygii). *Bulletin of the Peabody Museum of Natural History*, 65(1):3–302.

Oliver, M. K. (2024). African cichlid fishes: morphological data and taxonomic insights from a genus-level survey of supraneurals, pterygiophores, and vertebral counts (ovalentaria, blenniiformes, cichlidae, pseudocrenilabrinae). *Biodiversity Data Journal*, 12:e130707.

Orme, D., Freckleton, R., Thomas, G., Petzoldt, T., Fritz, S., Isaac, N., and Pearse, W. (2018). *caper: Comparative Analyses of Phylogenetics and Evolution in R*. R package version 1.0.1.

Pagel, M. (1994). Detecting correlated evolution on phylogenies: a general method for the comparative analysis of discrete characters. *Proceedings of the Royal Society of London. Series B: Biological Sciences*, 255(1342):37–45.

Pagel, M. (1997). Inferring evolutionary processes from phylogenies. *Zoologica Scripta*, 26(4):331–348.

Pagel, M. (1999). Inferring the historical patterns of biological evolution. *Nature*, 401(6756):877–884.

Pennell, M. W., Eastman, J. M., Slater, G. J., Brown, J. W., Uyeda, J. C., FitzJohn, R. G., Alfaro, M. E., and Harmon, L. J. (2014). geiger v2. 0: an expanded suite of methods for fitting macroevolutionary models to phylogenetic trees. *Bioinformatics*, 30(15):2216–2218.

Plummer, M., Best, N., Cowles, K., and Vines, K. (2006). Coda: Convergence diagnosis and output analysis for mcmc. *R News*, 6(1):7–11.

Poll, M. (1986). Classification des cichlidae du lac tanganika. tribus, genres et espèces. *Académie Royale de Belgique. Mémoires de la Classe des Sciences.*, 45:1–163.

R Core Team (2022). *R: A Language and Environment for Statistical Computing*. R Foundation for Statistical Computing, Vienna, Austria.

Revell, L. J. (2009). Size-correction and principal components for interspecific comparative studies. *Evolution*, 63(12):3258–3268.

Revell, L. J. (2024). phytools 2.0: an updated R ecosystem for phylogenetic comparative methods (and other things). *PeerJ*, 12:e16505.

Ronco, F., Büscher, H. H., Indermaur, A., and Salzburger, W. (2020). The taxonomic diversity of the cichlid fish fauna of ancient lake tanganyika, east africa. *Journal of Great Lakes Research*, 46(5):1067–1078.

Ronco, F., Matschiner, M., Böhne, A., Boila, A., Büscher, H. H., El Taher, A., Indermaur, A., Malinsky, M., Ricci, V., Kahmen, A., et al. (2021). Drivers and dynamics of a massive adaptive radiation in cichlid

fishes. *Nature*, 589(7840):76–81.

Salzburger, W. (2018). Understanding explosive diversification through cichlid fish genomics. *Nature Reviews Genetics*, 19(11):705–717.

Schelly, R., Stiassny, M. L., and Seegers, L. (2003). Neolamprologus devosi sp. n., a new riverine lamprologine cichlid (teleostei, cichlidae) from the lower malagarasi river, tanzania. *Zootaxa*, 373(1):1–11.

Schindelin, J., Arganda-Carreras, I., Frise, E., Kaynig, V., Longair, M., Pietzsch, T., Preibisch, S., Rueden, C., Saalfeld, S., Schmid, B., et al. (2012). Fiji: an open-source platform for biological-image analysis. *Nature methods*, 9(7):676–682.

Schneider, C. A., Rasband, W. S., and Eliceiri, K. W. (2012). Nih image to imagej: 25 years of image analysis. *Nature methods*, 9(7):671–675.

Schneider, R. F., Woltering, J. M., Adriaens, D., and Roth, O. (2023). A comparative analysis of the ontogeny of syngnathids (pipefishes and seahorses) reveals how heterochrony contributed to their diversification. *Developmental Dynamics*, 252(5):553–588.

Scott, B., Baker, E., Woodburn, M., Vincent, S., Hardy, H., and Smith, V. S. (2019). The natural history museum data portal. *Database*, 2019:baz038.

Small, C., Bassham, S., Catchen, J., Amores, A., Fuiten, A., Brown, R., Jones, A., and Cresko, W. (2016). The genome of the gulf pipefish enables understanding of evolutionary innovations. *Genome biology*, 17:1–23.

Sommer-Trembo, C., Santos, M. E., Clark, B., Werner, M., Fages, A., Matschiner, M., Hornung, S., Ronco, F., Oliver, C., Garcia, C., et al. (2024). The genetics of niche-specific behavioral tendencies in an adaptive radiation of cichlid fishes. *Science*, 384(6694):470–475.

Sparks, J. S. and Smith, W. L. (2004). Phylogeny and biogeography of cichlid fishes (teleostei: Perciformes: Cichlidae). *Cladistics*, 20(6):501–517.

Stiassny, M. (1981). Phylogenetic versus convergent relationships between piscivorous cichlid fishes from lakes malawi and tanganyika. *Bulletin of the British Museum (Natural History), Zoology*, 40:67 – 101.

Svardal, H., Quah, F. X., Malinsky, M., Ngatunga, B. P., Miska, E. A., Salzburger, W., Genner, M. J., Turner, G. F., and Durbin, R. (2020). Ancestral hybridization facilitated species diversification in the lake malawi cichlid fish adaptive radiation. *Molecular biology and evolution*, 37(4):1100–1113.

Thorstad, E. B., Hay, C. J., Næsje, T. F., Chanda, B., and Økland, F. (2005). Movements and habitat utilization of nembwe, serranochromis robustus (günther, 1864), in the upper zambezi river. *African Zoology*, 40(2):253–259.

Turner, G., Ngatunga, B. P., and Genner, M. J. (2019). The natural history of the satellite lakes of lake malawi. *EcoEvoRxiv*.

Turner, G., Ngatunga, B. P., and Genner, M. J. (2021). Astatotilapia species (teleostei, cichlidae) from malawi, mozambique and tanzania, excluding the basin of lake victoria. *EcoEvoRxiv*.

Uyeda, J. C., Hansen, T. F., Arnold, S. J., and Pienaar, J. (2011). The million-year wait for macroevolutionary bursts. *Proceedings of the National Academy of Sciences*, 108(38):15908–15913.

Varella, H. R., Kullander, S. O., Menezes, N. A., Oliveira, C., and López-Fernández, H. (2023). Revision of the generic classification of pike cichlids using an integrative phylogenetic approach (cichlidae: tribe geophagini: subtribe crenicichlina). *Zoological Journal of the Linnean Society*, 198(4):982–1034.

Venables, W. N. and Ripley, B. D. (2002). *Modern Applied Statistics with S*. Springer, New York, fourth edition. ISBN 0-387-95457-0.

Vranken, N., Van Steenberge, M., Mbalassa, M., and Snoeks, J. (2023). Just below the surface, the pelagic haplochromine cichlids from the lake edward system. *Hydrobiologia*, 850(14):3173–3195.

Ward, A. B. and Brainerd, E. L. (2007). Evolution of axial patterning in elongate fishes. *Biological*

Journal of the Linnean Society, 90(1):97–116.

Ward, A. B. and Kley, N. J. (2012). Effects of precaudal elongation on visceral topography in a basal clade of ray-finned fishes. *The Anatomical Record: Advances in Integrative Anatomy and Evolutionary Biology*, 295(2):289–297.

Ward, A. B. and Mehta, R. S. (2010). Axial elongation in fishes: using morphological approaches to elucidate developmental mechanisms in studying body shape. *Integrative and Comparative Biology*, 50(6):1106–1119.

Woltering, J. M., Holzem, M., Schneider, R. F., Nanos, V., and Meyer, A. (2018). The skeletal ontogeny of astatotilapia burtoni–a direct-developing model system for the evolution and development of the teleost body plan. *BMC developmental biology*, 18(1):1–23.

3 Somitic Changes Alter Vertebral Regionalisation in African Cichlid Fishes Despite Conserved Somite Counts

3.1 Motivation and Novelty of Manuscript

Our focus in '*African Cichlid Lake Radiations Recapitulate Riverine Axial Morphologies Through Repeated Exploration of Morphospace*' was firstly to determine the regions of axial morphospace occupied by African cichlids, determine how vertebral counts related to elongation of the body and deduce how total vertebral counts had evolved across the subfamily. Therefore, our focus was firmly on elucidating the macroevolutionary dynamics of axial diversification of African cichlids. Our reasoning for focusing just on total vertebral counts, rather than examining how the multivariate principal components have evolved, for example, was because not only did total vertebral counts provide a useful proxy for body elongation but also offered the possibility of inferring causative explanations of vertebral count changes via development. However, whilst we were able to show how and why total vertebral counts had evolved as African cichlids had diversified, we could only offer limited causative explanations for the evolution of this trait.

In 'Somitic Changes Alter Vertebral Regionalisation in African Cichlid Fishes Despite Conserved Somite Counts' we aimed to demonstrate firstly that macroevolutionary studies could be informative of the evolution of developmental mechanisms, as has previously been shown [Ward and Brainerd, 2007, Mehta et al., 2010, Soul and Benson, 2017] but also provide additional, causative explanation to the patterns we had previously described in total vertebral counts, as well as in the relative proportions of precaudal and caudal vertebrae. While our previous work was primarily directed at a comparative and evolutionary audience interested in patterns of morphological diversification, this study is written with a different readership in mind. Here, we aim to engage researchers working at the intersection of evolutionary biology, developmental biology, and evo-devo, partic-

ularly those interested in the developmental underpinnings of macroevolutionary change. Our focus on intraspecific variation, developmental mechanisms, and modes of regionalisation evolution is intended to provide insight into how phenotypic diversity emerges and is constrained at the level of developmental processes.

By analysing phylogenetic patterns of intraspecific variation, this study forms a rare connection between macroevolutionary dynamics and developmental mechanisms in vertebral evolution. First, it explicitly bridges macroevolutionary patterns with developmental mechanisms by leveraging phylogenetic patterns of intraspecific variation, an approach that is rarely applied in studies of vertebrate evolution. We firstly show that precaudal and caudal vertebral counts have evolved independently and that changes in count in both regions are highly variable and lineage specific. Second, building on the framework proposed by Soul and Benson [2017], we define three distinct modes of evolutionary change in vertebral column evolution: pure homeotic shifts, balanced somitic effects, and combined somitic effects. Together, these offer a refined approach to interpreting the evolution of regionalisation at macroevolutionary scales. Third, we demonstrate that despite the large diversity of total counts across species, intraspecific variation is low, lacks phylogenetic structure, and has remained stable during the diversification of African cichlids. Furthermore, vertebral count variability within species does not scale with body elongation, nor does it differ between lineages with divergent total counts. Together, these results indicate that while vertebral numbers and regionalisation have evolved dynamically and extensively across cichlid lineages, intraspecific variability in somitic counts remains strongly constrained and decoupled from macroevolutionary patterns of body shape and vertebral diversification. Therefore, this manuscript attempts to bridge the relatively descriptive evolutionary patterns offered in the first manuscript to mechanistically grounded explanations for the evolution of axial phenotypes, whilst contributing a new perspective on how developmental constraints shape and limit phenotypic evolution in vertebrates.

Somitic Changes Alter Vertebral Regionalisation in African Cichlid Fishes Despite Conserved Somite Counts

Pages 65–92

Interactive features (e.g. links) are disabled in this embedded version.
For the fully functional version, visit `https://shorturl.at/t3IWg`.

Author contributions are included at the end of the manuscript.

Somitic Changes Alter Vertebral Regionalisation in African Cichlid Fishes Despite Conserved Somite Counts

Callum V Bucklow[1,2,*], Emanuell Duarte Ribeiro[3], Roger Benson[2,4], and Berta Verd[1]

[1]**Evolutionary Biology Section, Department of Biology, University of Oxford, Oxford, UK**
[2]**Paleobiology Group, Department of Earth Sciences, University of Oxford, Oxford, UK**
[3]**Department of Environmental Science, University of Basel, Switzerland**
[4]**Division of Paleontology, American Museum of Natural History, New York City, USA**
[*]**Co-corresponding authors: Callum V Bucklow (callum.bucklow@biology.ox.ac.uk); Berta Verd (berta.verdfernandez@biology.ox.ac.uk)**

ABSTRACT

Vertebrae arise from somites, transient embryonic segments that rhythmically bud from the presomitic mesoderm during axial elongation. The number and identity of vertebrae are ultimately determined by somitogenesis and subsequent anterior-posterior regionalisation, largely governed by *hox* gene expression. Interspecific variation in vertebral count and regionalisation therefore reflects evolutionary changes in somite number and homeotic identity following species divergence. While many macroevolutionary studies have examined homeotic and non-homeotic changes in the vertebral column, few have explored these dynamics in teleosts, despite their exceptional species richness. Using African cichlids as a model, we show that shifts in vertebral regionalisation can arise through modifications to anterior-posterior patterning, but that much of the observed variation is driven by changes in somite number, with homeotic effects emerging largely as a by-product of somitic changes. Moreover, low intraspecific variation in vertebral count, lacking phylogenetic structure, suggests that somitic count variation within species is strongly canalised and has remained consistent throughout the diversification of African cichlids. In addition, we find no correlation between intraspecific variation in vertebral counts and mean vertebral counts, and this variation does not consistently scale with body aspect ratio among individuals. Therefore, intraspecific variation is decoupled from both macroevolutionary patterns of vertebral count evolution and body shape diversification. Together, our findings highlight the dynamic interplay between somitogenesis and homeotic transformations in shaping vertebral diversity and underscore the value of cichlids as a model for understanding the developmental basis of axial evolution in teleosts.

Keywords: cichlids, teleosts, somitogenesis, regionalisation, *hox*, vertebrae

INTRODUCTION

The vertebral column, a defining feature of all vertebrates, is critical for locomotion, providing structural support for muscle attachment and protecting the spinal cord and nerve roots that transmit motor and sensory signals (Ford, 1937). Vertebrae arise from somites, transient embryonic segments that rhythmically bud from the presomitic mesoderm during axial elongation during somitogenesis (Maroto et al., 2012). Concurrent with somite formation, anterior-posterior (AP) patterning of the somitic mesoderm is directed by overlapping expression domains of *Hox* genes, which specify vertebral identity along the axis (Iimura et al., 2009), a mechanism deeply conserved across vertebrates (Morin-Kensicki et al., 2002; Böhmer et al., 2015; Criswell et al., 2021). *Hox* genes are typically arranged in linear clusters within the genome,

and their sequential activation during development reflects the serial organisation of the vertebral column (Iimura et al., 2009). This phenomenon, known as *Hox* collinearity, spatially and temporally regulates AP patterning of the vertebrate body axis (Ye and Kimelman, 2020). Thus, evolutionary changes to both vertebral number and regional identity can arise through modifications to the rate of somite formation or shifts in the expression boundaries of *Hox* genes (Cohn and Tickle, 1999).

Evolutionary modulation of both somitogenesis and anterior-posterior *Hox* patterning has been critical to the evolution of variation in the vertebrate body plan (Naganathan and Oates, 2020). Shifts in *Hox* patterning have been linked to the considerable variability present in vertebral column regionalisation in archosaurs (Böhmer et al., 2015) aligning with morphological domains present in the avian vertebral column (Marek et al., 2021). In mammals, homeotic shifts are sufficient to explain variation in lumbar and thoracic proportions (Narita and Kuratani, 2005) and indeed in the proportions of all post-cervical vertebral counts (Cerbus et al., 2024). In addition to homeotic shifts, changes in vertebral proportions can be brought about by increasing the rate of somitogenesis relative to the *hox* 'timer'. In Python embryos, for example, an increased rate of somitic budding leads to the formation of a greater number of smaller somites relative to chicken embryos (Gomez et al., 2008; Woltering et al., 2009). In order to support their elongated axes, an anterior shift of *HoxC6* and *HoxC8* in the lateral plate mesoderm prevents forelimb formation, specifying instead the development of thoracic (chest, rib-bearing) vertebrae to support their elongate bodies (Cohn and Tickle, 1999).

Since the number and type of vertebrae is ultimately determined by somitogenesis and subsequent *Hox* regionalisation, differences in the number and type of vertebrae among adults (and other post-embryonic stages) of different species provide evidence of somitic and homeotic changes in development since divergence from their most recent common ancestor. Extrapolation of this onto a larger scale can provide informative abstractions and unique insights into the macroevolutionary dynamics and evolutionary modification of somitogenesis and regionalisation within and between clades (Narita and Kuratani, 2005; Mehta et al., 2010; Soul and Benson, 2017). Whilst a large number of macroevolutionary studies have examined the evolution of the structure of the vertebral column, most have focused on tetrapods (Narita and Kuratani, 2005; Jones et al., 2018b,a; Cerbus et al., 2024) and few have examined the macroevolutionary patterns of vertebral count and identity in ray-finned fish (Actinopterygii) (Ward and Brainerd, 2007; Mehta et al., 2010).

Ray-finned fish (Actinopterygii) are the most speciose class of extant vertebrates, accounting for over 50% of described species, of which 99% are teleosts (Near and Thacker, 2024). Understanding the macroevolutionary and developmental dynamics of the teleost vertebral column is therefore central to elucidating morphological and functional diversification in a highly diverse group. Unlike in tetrapods, that are defined by the presence of five well defined vertebral types: cervical, thoracic, lumbar, sacral and caudal (tail) (Cerbus et al., 2024), the teleostean vertebral column has traditionally been divided into two domains: the precaudal and caudal. Precaudal vertebrae are characterised by ventrolateral basapophyses that serve as attachment sites for ribs, which protect the viscera and provide anchorage for muscles and tendons. Caudal vertebrae, in contrast, are defined by the presence of a closed haemal arch formed by haemal spines (see Figure 1A), which provide articulation points for the anal and caudal fins required for swimming (Ford, 1937). Therefore, changing proportions of precaudal and caudal vertebrae are a useful proxy to investigate the evolutionary importance of homeotic transformations in teleost evolution.

While most studies of vertebral evolution have focused on interspecific patterns across broad phylogenetic scales, relatively few, if any, have examined patterns of intraspecific variation in vertebral number, despite widespread evidence of such variation across vertebrates (Slijepčević et al., 2015; Hu et al., 2016; Sosa and Hospitaleche, 2024), including in teleosts (Yamahira et al., 2006; Tibblin et al., 2016; Oliver, 2024) (see Figure 1B). Intraspecific variation in total vertebral count necessarily reflects underlying

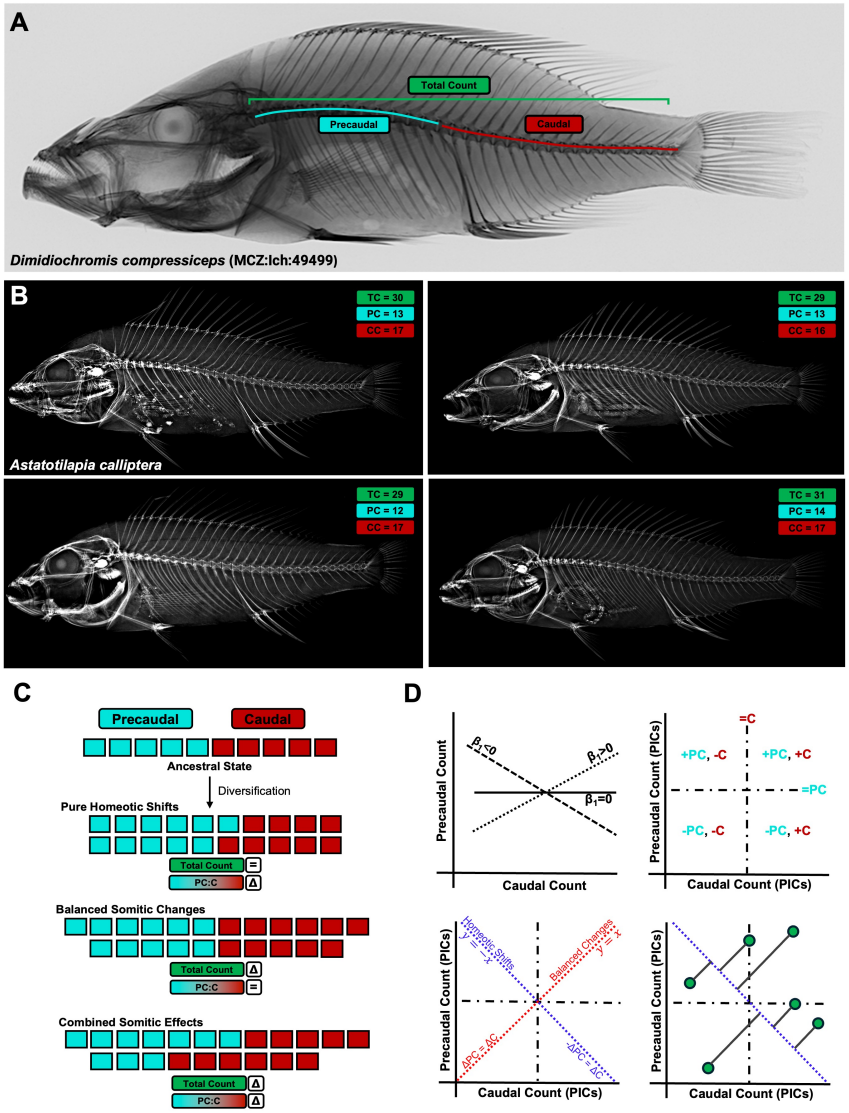

Figure 1. Vertebral column structure in cichlids. (A) X-ray of *Dimidiochromis compressiceps*, showing precaudal, caudal, and total vertebral counts. (B) X-rays of four individuals of *Astatotilapia calliptera*, illustrating intraspecific variation in total vertebral count and proportions of precaudal and caudal vertebrae. (C) Evolutionary changes in vertebral number and regionalisation can arise through three primary modes: Pure Homeotic Shifts, in which the relative proportions of precaudal and caudal vertebrae change without altering the total count, consistent with changes to anterior-posterior patterning independent of somitogenesis; Balanced Somitic Changes, where precaudal and caudal counts increase or decrease proportionally, suggesting changes in somite number without affecting regional identity boundaries; and Combined Somitic Effects, where changes in precaudal and caudal counts are disproportionate, reflecting shifts in regional proportions that arise as a consequence of altered somitogenesis, without necessarily involving changes to anterior-posterior patterning. (D) Schematics clarifying Figure 2. Top left: if precaudal and caudal counts have evolved independently they do not co-vary ($\beta_1 = 0$). Top right: the position of nodes in different quadrants reflects changes in precaudal and caudal proportions relative to the ancestral state. Bottom left: nodes falling along the $y = -x$ and $y = x$ lines represent pure homeotic shifts and balanced somitic changes, respectively. Bottom right: nodes deviating perpendicularly from the $y = -x$ line indicate changes in total vertebral count accompanied by a shift in regionalisation; the greater the perpendicular distance, the greater the magnitude of the somitic change.

variation in somitogenesis, since the number of vertebrae corresponds to the number of embryonic somite pairs formed during early development (Morin-Kensicki et al., 2002). In teleosts, this relationship is particularly direct: because resegmentation does not occur following somite specification, the total number of vertebrae corresponds to the number of somitic pairs minus three, with the anterior-most somites contributing to the basioccipital region of the skull (Woltering et al., 2018). Examining the phylogenetic distribution and structure of intraspecific variation in vertebral counts therefore offers a powerful but unexplored means to investigate how axial patterning and developmental constraint have evolved in vertebrates. However, despite its potential significance, the extent, developmental basis, and evolutionary implications of intraspecific variation in precaudal, caudal and total vertebral counts in teleosts remains poorly understood and represents a key gap in our understanding of vertebrate axial evolution.

African cichlids (Ovalentaria, Cichliformes, Cichlidae, Pseudocrenilabrinae) represent one of the most species-rich and morphologically diverse groups of teleost fishes, found across the rivers and lakes of Africa and the Middle East (Astudillo-Clavijo et al., 2023). Much of this diversity has arisen within the adaptive radiations of the East African Great Lakes Tanganyika, Malawi, and Victoria, which together represent hundreds of endemic species (McGee et al., 2020). The radiations of Lakes Malawi and Victoria, in particular, have diverged rapidly, with estimated ages of approximately 800,000 and 100,000 years, respectively (Malinsky et al., 2018; Meier et al., 2017). Among their many axes of phenotypic diversity, African cichlids exhibit remarkable variation in axial skeletal morphology, including in total vertebral counts, the relative proportions of precaudal and caudal vertebrae, and in elongation of the body (Oliver, 2024; Bucklow et al., 2025b). We previously showed that while total vertebral counts evolve under lineage-specific stochastic rates within each lake radiation, these rates are highest among riverine lineages, contributing to their especially diverse axial morphologies. Moreover, increases in total vertebral counts, often driven by increased caudal counts, are associated with elongation of the body axis, a trait linked to pelagic, demersal, and piscivorous lifestyles (Bucklow et al., 2025b). However, despite investigating the macroevolutionary dynamics of total count evolution, we did not make any inferences about the evolution of the developmental mechanisms that may underlie these evolutionary patterns. Understanding the developmental basis of vertebral variation is therefore essential to fully understand the evolution of axial morphology in African cichlids.

Here we show that across African cichlids, precaudal and caudal vertebral counts evolve largely independently of each other. While variation in total vertebral count is often accompanied by changes in regionalisation, the relationship between precaudal-caudal proportions and total vertebral count is weak, non-linear, and likely highly lineage-specific. We define three distinct modes of evolutionary change in vertebral column evolution (Figure 1C). First, pure homeotic shifts involve proportional changes in precaudal and caudal vertebral counts, shifting the boundary between regions without altering total vertebral number. Second, balanced somitic effects reflect the gain or loss of vertebrae, with precaudal and caudal counts changing in the same direction and proportion. Finally, combined somitic effects involve unbalanced changes in precaudal and caudal counts, altering both total vertebral number and regional identity. We detect examples of all three modes across the African cichlid phylogeny, but find that evolutionary changes to vertebral column structure most often involve combined somitic effects, whereas pure homeotic shifts and balanced somitic changes are comparatively rare. These patterns are especially pronounced within the haplochromine radiations of Lakes Victoria and Malawi, where the highest rates of combined change are observed. In addition, despite the large diversity of total counts across species, intraspecific variation is low, lacks phylogenetic structure, and has remained consistent during the diversification of African cichlids. Furthermore, vertebral count variability within species does not scale with body elongation, nor does it differ between lineages with divergent total counts. Together, these results indicate that while vertebral numbers and regionalisation have evolved dynamically and

extensively across cichlid lineages, intraspecific variability in somitic counts remains strongly constrained and decoupled from macroevolutionary patterns of body shape and vertebral diversification.

METHODS AND MATERIALS

All analyses were conducted in R (v4.2.0) (R Core Team, 2022). Phylogenetic analyses used the cichlid family tree constructed by McGee et al. (2020) as the tree is ultrametric, time-calibrated and includes all three of the major lacustrine radiations of African cichlids (Lake Tanganyika, Lake Malawi and Lake Victoria), as well as representatives from every currently recognised tribe in the African subfamily. All vertebral count data is from a previous study, which includes all necessary information about how the counts were conducted and includes landmarked images of all the specimens (Bucklow et al., 2025b). All code and data have been deposited alongside this manuscript as a self-contained R project.

Testing modularity of precaudal and caudal domains

To explore the macroevolutionary relationship between vertebral column regionalisation and somitogenesis, we first needed to confirm that changes in precaudal and caudal vertebrae could serve as reliable proxies for homeotic and somitic changes. If counts in either domain have changed independently of the other, then changes in the relative numbers of precaudal and caudal vertebrae can be used as a proxy for homeotic shifts (and co-occurring somitic changes). We also examined the relationship between the ratio of precaudal:caudal vertebrae (ln[Precaudal]-ln[Caudal]) and the ln[Total Count], to evaluate whether increases in total vertebral count were associated with shifts in the relative allocation of precaudal versus caudal vertebrae. We used phylogenetic generalised least squares (PGLS) to evaluate the relationship between the univariate traits, using the *pgls* function in the R package *caper* (v1.0.1) (Orme et al., 2018). To account for phylogenetic signal, we estimated λ (Pagel, 1999) for the covariance matrix, with δ and κ fixed at 1. We added a quadratic term to the PGLS model for the ratio of ln[Precaudal] - ln[Caudal] as a function of ln[Total Count], as both the OLS and linear PGLS model fits did not visually capture the data structure well (see Figure 2B). The linear term was marginally non-significant ($\beta_1 = 0.304$, P = 0.055) but the quadratic term was significant ($\beta_2 = 0.460$, $P < 0.001$) and the model overall provided a considerably better fit than the linear PGLS model ($\Delta AIC > 3$).

Identification of pure homeotic shifts, balanced somitic changes and combined somitic effects

To assess the phylogenetic scale of homeotic shifts and test whether their rates varied across the tree, we used standardised phylogenetic independent contrasts (PICs) (Felsenstein, 1985) to quantify changes in precaudal and caudal vertebral counts. PICs were calculated as the difference in the modal raw counts between nodes, standardised by their expected standard deviation, using the R package *ape* (v5.7.1) (Paradis and Schliep, 2019), where the contrast sign indicated the direction of change in vertebral counts at that respective node. We calculated PICs in two ways: first, using the original, time-calibrated branch lengths; and second, with all branch lengths set to 1. The time-calibrated PICs allowed us to investigate the temporal scale at which homeotic and somitic effects could occur, since PICs represent point estimates of the evolutionary rate of change in precaudal and caudal vertebral counts (Freckleton and Harvey, 2006). In contrast, using equal branch lengths enabled us to assess the raw magnitude of changes across the phylogeny, independent of divergence time.

Following Soul and Benson (2017), we defined homeotic shifts as nodes where precaudal and caudal vertebrae contrasts changed disproportionally. Specifically, instances where a predicted loss of precaudal vertebrae was accompanied by a concurrent, equal-magnitude increase in caudal vertebrae were considered ‘pure homeotic shifts’, as they did not alter the total vertebral count (and thus the number of somites). In contrast, we defined ‘balanced somitic changes’ as nodes where precaudal and caudal count contrasts were

predicted to have changed, albeit proportionally, maintaining the ratio of precaudal-caudal vertebrae but not the total vertebral counts. Nodes where precaudal and caudal count contrasts changed disproportionately, implying homeotic shifts with co-occurring somitic changes, were defined as 'combined somitic effects'. For example, if the loss of one precaudal vertebra was accompanied by the addition of two caudal vertebrae, the total vertebral count (and also the number of somites) increased, indicating a co-occurring somitic change (see Figure 1C).

In practical terms, we plotted precaudal count PICs against those of caudal vertebral counts (see Figure 1D for summary). Pure homeotic shifts were identified as nodes falling on the $y = -x$ line, indicating equal and opposite changes in precaudal and caudal counts. Balanced changes were nodes located on the $y = x$ line, where precaudal and caudal counts changed proportionally, preserving their ratio. Nodes deviating perpendicularly from the $y = -x$ line were considered homeotic shifts accompanied by somitic changes, as both vertebral column regionalisation and the number of either precaudal in either both or one vertebrae changed. The magnitude of deviation along this perpendicular axis represented the magnitude of the somitic change for nodes where combined somitic effects were identified. Greater perpendicular distances indicate a larger additive or subtractive somitic effect (i.e. co-occurring somitic change) (Soul and Benson, 2017). For PICs calculated using estimated divergence times, a greater perpendicular deviation indicates that substantial somitic changes occurred over relatively short evolutionary timescales. To quantify the magnitude of co-occurring somitic changes (for 'combined somitic effect' nodes), we calculated the perpendicular distance of each node from the $y = -x$ line, using the formula: $d = \frac{|X_0+Y_0|}{\sqrt{2}}$, where X_0 and Y_0 are the standardised contrasts for caudal and precaudal vertebrae, respectively. A value of $d = 0$ corresponded to pure homeotic shifts, while $d = 1$ (aligned with $y = x$) represents balanced changes. A perpendicular distance $0 < d \neq 1$, indicated homeotic shifts with co-occurring somitic changes.

Quantification of intraspecific variation in vertebral counts

Intraspecific variation in vertebral counts is present in African cichlids (Oliver, 2024). Since the total number of vertebrae is ultimately defined by the number of somite pairs formed during somitogenesis, the presence of intraspecific variation in vertebral counts implies flexibility in somitogenesis which could be the source of interspecific variation in total vertebral counts. We had previously shown that vertebral addition is necessary for elongation of the fusiform body in African cichlids (Bucklow et al., 2025b). If increased vertebral counts evolved through positive selection acting on intraspecific variation in somite number, we would expect lineages with exceptionally high vertebral counts such as *Rhamphochromis*, *Serranochromis*, and *Bathybates* to retain elevated levels of intraspecific variation in vertebral number. Alternatively, if higher vertebral counts arose through a directional shift followed by purifying selection against lower counts (e.g., due to ecological or functional constraints), we would expect this to result in a narrowing of the trait distribution, and thus reduced intraspecific variation within those high-count lineages. To explore this, however, we needed to characterise the intraspecific variation in African cichlids, determine whether it is linked to interspecific vertebral counts and test whether intraspecific variation has been modified over the course of their diversification.

We filtered our dataset of vertebral counts to only include species for which we had at least five individuals, leaving us with 277 species retained on the phylogeny after pruning. Interspecific variation in total counts remained normally distributed in this subset of species (Supplementary Figure 1A, Shapiro-Wilks test, W = 0.995, p = 0.573) and covered the full range of vertebral counts present in African cichlids (Oliver, 2024; Bucklow et al., 2025b). Given that sample sizes were highly variable among species (n = 5–57 individuals), we tested whether species with larger sample sizes exhibited inflated estimates of intraspecific variation. This was particularly important because some specimens, especially from museum collections, may have been misidentified, potentially increasing apparent variation. A linear

model was fit using log-transformed values of the total count standard deviation and sample size to account for potential non-linearity and heteroscedasticity (Supplementary Figure 1B). We found a weak and marginally non-significant positive correlation between intraspecific variation and sample size (R^2 = 0.010, β_1 = 0.04584, p = 0.056, *d.f.* = 267), and highly non-significant results from a non-parametric Spearman's rank correlation test (ρ = 0.054, p = 0.37). Therefore, increased sampling does not systematically inflate observed intraspecific variation.

To quantify intraspecific variation in total vertebral counts, we used the coefficient of variation (CV; $CV = \sigma/\mu$) rather than the standard deviation. Since the standard deviation is an absolute measure, it can be biased by species with higher mean vertebral counts, making cross-species comparisons less meaningful. In contrast, the CV expresses variation relative to the mean, enabling standardised comparisons and providing a clearer assessment of relative developmental variability in vertebral number across species. We did, however, calculate the variance (σ^2) of precaudal and caudal counts to estimate their respective contributions to total vertebral count variance. Total count is the sum of precaudal and caudal counts. Therefore, total variance can be expressed as $\sigma^2_{TC} = \sigma^2_{PC} + \sigma^2_{CC} + 2\mathrm{Cov}(PC, CC)$. However, precaudal and caudal counts did not covary when corrected for phylogeny (Figure 2A). Thus, $2\mathrm{Cov}(PC, CC) \approx 0$, and $\sigma^2_{TC} \approx \sigma^2_{PC} + \sigma^2_{CC}$. Significant differences in the distributions of precaudal and caudal variances thus indicate differential contributions to total vertebral count variation. Nonetheless, we also calculated the CVs for precaudal and caudal counts separately, since in most species the mean caudal count (μ_{CC}) is greater than the mean precaudal count (μ_{PC}), see Figure 2A.

Investigating the evolution of intraspecific variation in vertebral counts

The CV is bounded at zero and sensitive to small means, therefore, the distribution of total count CV was right-skewed and not normally distributed (see Figure 4A), violating the assumption of normality required for PGLS models. In order to to examine whether intraspecific variation in total count could contribute to the evolution of the total vertebral count or had changed across the African phylogeny, we instead used a non-parametric approach. Since the range of vertebrae is 15 (Supplementary Figure 1), we binned mean total vertebral counts into groups of 3 vertebrae to ensure that sample sizes per group were comparable. We applied a permutation-based implementation of the Kruskal-Wallis test to determine whether the medians were significantly different between groups. We simulated total count CV evolution using a single rate (σ^2) Brownian motion model, using the *fastBM* function in the R package *phytools* (v2.1.1) (Revell, 2024). The rate (σ^2) was set as the total count CV variance and CV estimates were bounded between 0 and 1 to avoid the estimation of negative CVs. Model fits were simulated 10,000 times, each of which was used as input for a Kruskal-Wallis test. χ^2 values were extracted, and p-values were estimated from the null distribution using the formula: $p = \frac{\sum_{i=1}^{N}(\chi_i^2 \geq \chi^2_{obs})}{N}$, where N is the total number of simulations.

To assess whether somitic count variability has remained consistent across the phylogeny, we leveraged the unique evolutionary history of African cichlids. Multiple adaptive radiations are nested within Pseudocrenilabrinae, each having occurred independently (Ronco et al., 2021; Malinsky et al., 2018; Meier et al., 2017). These radiations, along with more basal riverine lineages, provide a natural experiment for investigating how trait variability evolves over time. Our previous analyses showed that interspecific variation in vertebral counts correlates with the age of a radiation, where total count evolution in each lacustrine radiation (and riverine lineages) was subject to its own stochastic rate of evolution (σ^2) (Bucklow et al., 2025b). If intraspecific variation in vertebral counts evolved in tandem with shifts in vertebral count disparity, we might expect systematic differences in variability across these independent lineages. Alternatively, if somitic count variability has been maintained at consistent levels, despite shifts in mean vertebral counts, it would suggest that intraspecific variation has remained consistent throughout the

diversification of African cichlids. Consequently, implying a developmental constraint, or canalisation, of the number of somite pairs formed during somitogenesis within a species across clades. To test for significant differences in the intraspecific variation between water systems, we redeployed the permutation-based Kruskal-Wallis test as described above.

As a second approach to investigate the evolution of intraspecific variation in vertebral counts, we quantified the phylogenetic signal in the total, precaudal and caudal count CVs using Pagel's λ (Pagel, 1999) and Blomberg's K (Blomberg et al., 2003). These metrics assess the extent to which closely related species exhibit similar levels of intraspecific variability. If phylogenetic signal in the CV is weak or absent, it would suggest that intraspecific variation (i.e., somitic count variability) is similar between distantly related and closely related lineages, rather than being constrained by shared ancestry. Pagel's λ measures how much trait evolution follows a Brownian motion (BM) model by scaling internal branch lengths of the phylogenetic tree. A λ value of 1 indicates strong phylogenetic dependence, meaning that intraspecific variability evolves in proportion to shared ancestry. In contrast, a λ of 0 suggests no phylogenetic structure, implying that variability arises independently across species. Intermediate values indicate partial phylogenetic influence, where variation is shaped by both ancestry and other evolutionary factors. Blomberg's K compares observed trait variation to expectations under BM. A K value of 0 suggests that the trait varies independently of phylogeny, whilst a value of 1 suggests that variation follows BM exactly. Values of $K < 1$ indicate that closely related species are more different than expected, suggesting weaker phylogenetic constraint. Conversely, $K > 1$ implies that related species are more similar than expected under BM, potentially due to stabilising selection or shared developmental constraints. Both metrics were estimated using the *phylogsig* function in *phytools* (v2.1.1) (Revell, 2024). Significance was assessed through 100,000 simulations. For λ, we examined its likelihood profile, while for K, we compared observed values to simulated null distributions (Supplementary Figure 2).

Testing scaling of intraspecific variation and whole body elongation

We had previously reported that elongation of the fusiform body in African cichlids has partly been driven by the addition of vertebrae (Bucklow et al., 2025b). In addition, prior evidence suggests that intraspecific variation in vertebral counts may enhance individual fitness by providing functional advantages (Swain, 1992; Tibblin et al., 2016). We therefore hypothesised that variation in vertebral count may scale with variation in body aspect ratio, and sought to examine whether this relationship is consistent both within and across African cichlids. To test this hypothesis, we fit within-species regressions (ordinary least squares) of ln[Total Vertebral Count] on ln[Length] – ln[Depth] (body aspect ratio) for species with at least 10 individuals (176 species). Individual species' regression slopes (β_1) were highly variable, generally weak, and noisy (see Results). Therefore, in order to assess the presence of an overall trend, while accounting for slope sampling variances and phylogenetic non-independence, we performed a multivariate phylogenetic meta-analysis (Lajeunesse, 2009) using restricted maximum likelihood (REML) via the *rma.mv* function in the R package *metafor* (v4.8.0) (Viechtbauer, 2010). Species-specific regression slopes were treated as effect sizes and weighted by their respective sampling variances (i.e. the squared standard errors). Species were included as a random effect, allowing each to deviate from the overall mean slope. To account for shared evolutionary history, we included a phylogenetic covariance matrix constructed using the *vcv* function from the R package *ape* (v5.7.1) (Paradis and Schliep, 2019). This approach allowed us to estimate the average relationship between vertebral number and body aspect ratio while accounting for both measurement uncertainty and phylogenetic structure.

Data and Code Availability

All code used in the analysis has been deposited on GitHub and can be accessed here. All radiographs, count and body shape data were previously deposited on on Zenodo (Bucklow et al., 2025a), as part of a

previous study (Bucklow et al., 2025b).

RESULTS

Precaudal and caudal vertebral counts evolve independently across cichlid lineages

We found no significant correlation between ln[Precaudal Count] and ln[Caudal Count] across species (Figure 2A; $R^2 = 0.002$, $\beta_1 = 0.082$, $\lambda = 0.935$, *d.f.* = 427, $p = 0.1884$), suggesting that the number of vertebrae in each region has evolved largely independently. This indicates that lineages have gained or lost vertebrae in one domain without requiring corresponding changes in the other. We found a very weak but significant positive correlation between the relative proportions of precaudal and caudal vertebrae (ln[Precaudal] - ln[Caudal]) and total vertebral count, indicating that the addition of vertebrae may be driven primarily by the addition of precaudal vertebrae (Figure 2B; $R^2 = 0.02$, $\beta_1 = 0.269$, $\lambda = 0.935$, $p < 0.001$, *d.f.* = 427). However, this pattern appears to be influenced by specific genera, such as *Gobiocichla* and *Cyprichromis*, which exhibit relatively high total vertebral counts alongside an unusually large number of precaudal vertebrae (Oliver, 2024; Bucklow et al., 2025b). Incorporating a quadratic term into the PGLS model significantly improved model fit ($\Delta AIC > 3$). Only the quadratic term was significant ($\beta_2 = 0.460, p < 0.001$), suggesting that the relationship between ln[Precaudal] - ln[Caudal] and ln[Total Count] is not constant but varies across the range of total vertebral counts, rather than following a simple power-law relationship. Consistent with previous findings (Bucklow et al., 2025b), different lineages, therefore, have independently modified precaudal-to-caudal proportions and total vertebral counts. In addition, the phylogenetic signal for precaudal and caudal covariance was very high ($\lambda = 0.935$, 95% CI [0.910, 0.955]), indicating that while vertebral counts in each region evolve separately (Figure 2A), their variation remains strongly structured by shared ancestry. Consequently, similar vertebral patterns are found within closely related species, even though the exact number of vertebrae in each region can vary independently (Figure 2B).

Changes in vertebral column regionalisation are usually driven by somitic change

For most points of divergence in the phylogeny (i.e. nodes of the tree), changes in the total number of vertebrae are accompanied by shifts in regionalisation, suggesting a dominant role of combined somitic effects in the evolution of the vertebral column in African cichlids (Figures 2C, D points dispersed across space). Subsequently, changes to the total number of vertebrae (i.e. somitic changes) are rarely present without a concurrent shift in regionalisation. Nodes estimated to have undergone large somitic changes (and homeotic shifts) were predictably present in nodes representing divergences of clades with large differences in total vertebral count (Figure 3, black arrows). The highest rates of combined somitic effects were found exclusively in haplochromines (Figure 2D), specifically within the adaptive radiations of Lake Victoria and Lake Malawi (Supplementary Figure 3), which have undergone extremely rapid diversification in the presence of limited genetic variation (Meier et al., 2017; Malinsky et al., 2018). Therefore, evolutionary modification of vertebral column regionalisation (and co-occurring somitic changes) can occur with relatively little genetic variation and relatively quickly. We nonetheless did identify nodes where pure homeotic shifts (i.e., without co-occurring somitic changes) were predicted to have occurred (Figure 2C, D, blue triangles), indicating that changes in vertebral column regionalisation can occur independently of changes in vertebral count. Balanced somitic changes too were identified (Figures 2C, D, red squares), albeit at notably fewer nodes that either combined somitic effects or pure homeotic shifts (Figure 2E), suggesting that balanced somitic changes have played a minor role in the evolution of the vertebral column. Nonetheless, combined somitic effects, where changes in precaudal and caudal proportions have occurred as a consequence of additive or subtract somitic changes were identified

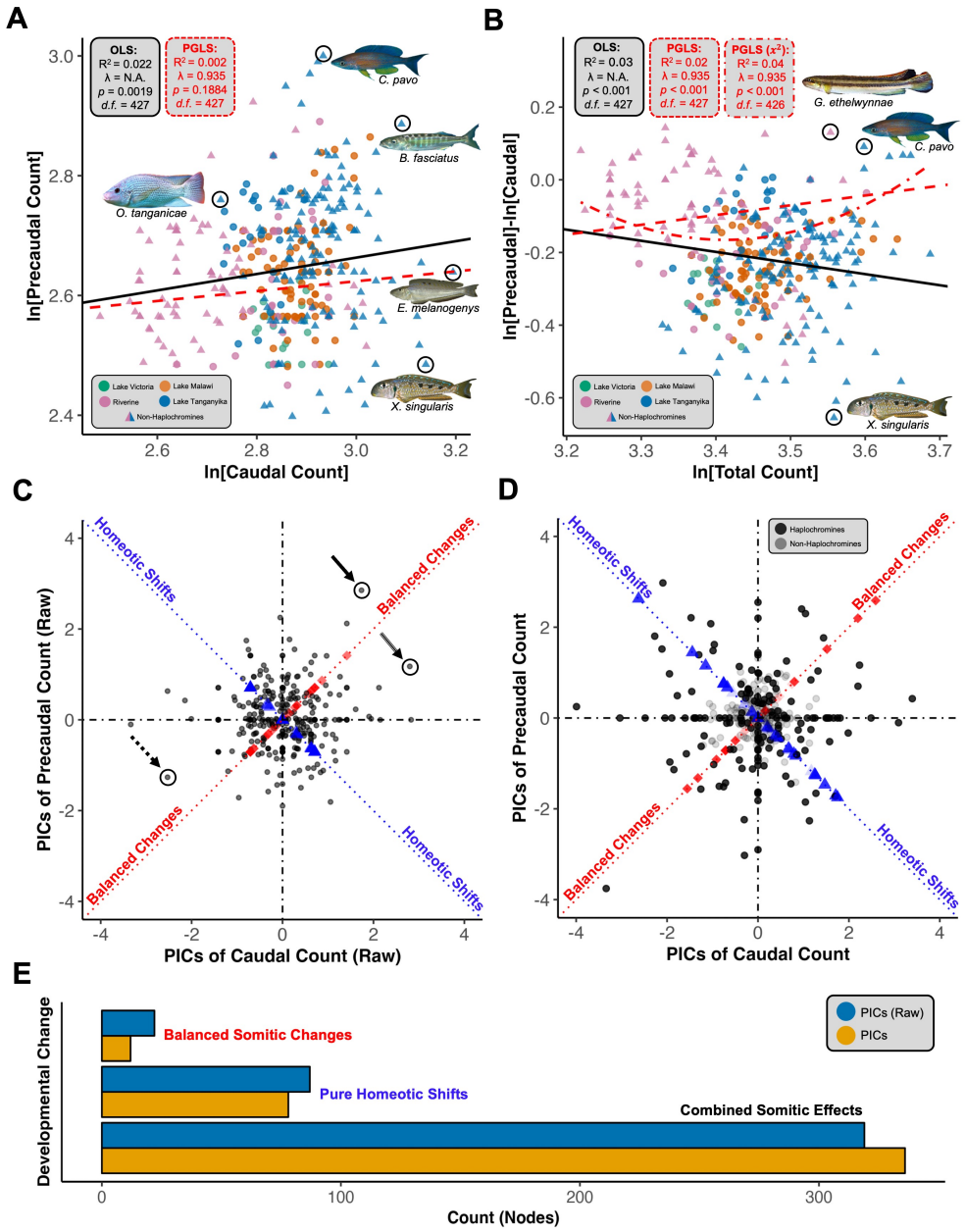

Figure 2. Homeotic and somitic changes in African cichlids. (A) Scatterplot of ln[Precaudal] and ln[Caudal] vertebral counts and (B) ln[Precaudal]-ln[Caudal] (PC:C ratio) with regression lines: black (OLS) and red, dashed (PGLS). Scatterplot of modal, raw (C) and time-calibrated (D) precaudal and caudal vertebral phylogenetic independent contrasts (PICs). Points (blue triangles) on the $y = -x$ line (blue, dotted) indicate pure homeotic shifts, points (red diamonds) on the $y = x$ line (red, dotted) indicate balanced changes, perpendicular deviations from either line represent co-occurring somitic changes. Arrows match nodes exemplified in Figure 3. (E) Bar chart showing the number of nodes where each developmental change (defined in Figure 1) are predicted to have occurred. Blue represents the number of nodes where each developmental change is predicted to have occurred, based on PICs where the branch length is equal to 1 (i.e. the raw magnitude of change) and in orange are the predictions based on the time-corrected PICs. *B*, *Bathybates*; *C*, *Cyprichromis*; *E*, *Enantiopus*; *G*, *Gobiocichla*; *L*, *Lamprologus*; *O*, *Oreochromis*; *X*, *Xenotilapia*. See Supplementary Materials for image credits.

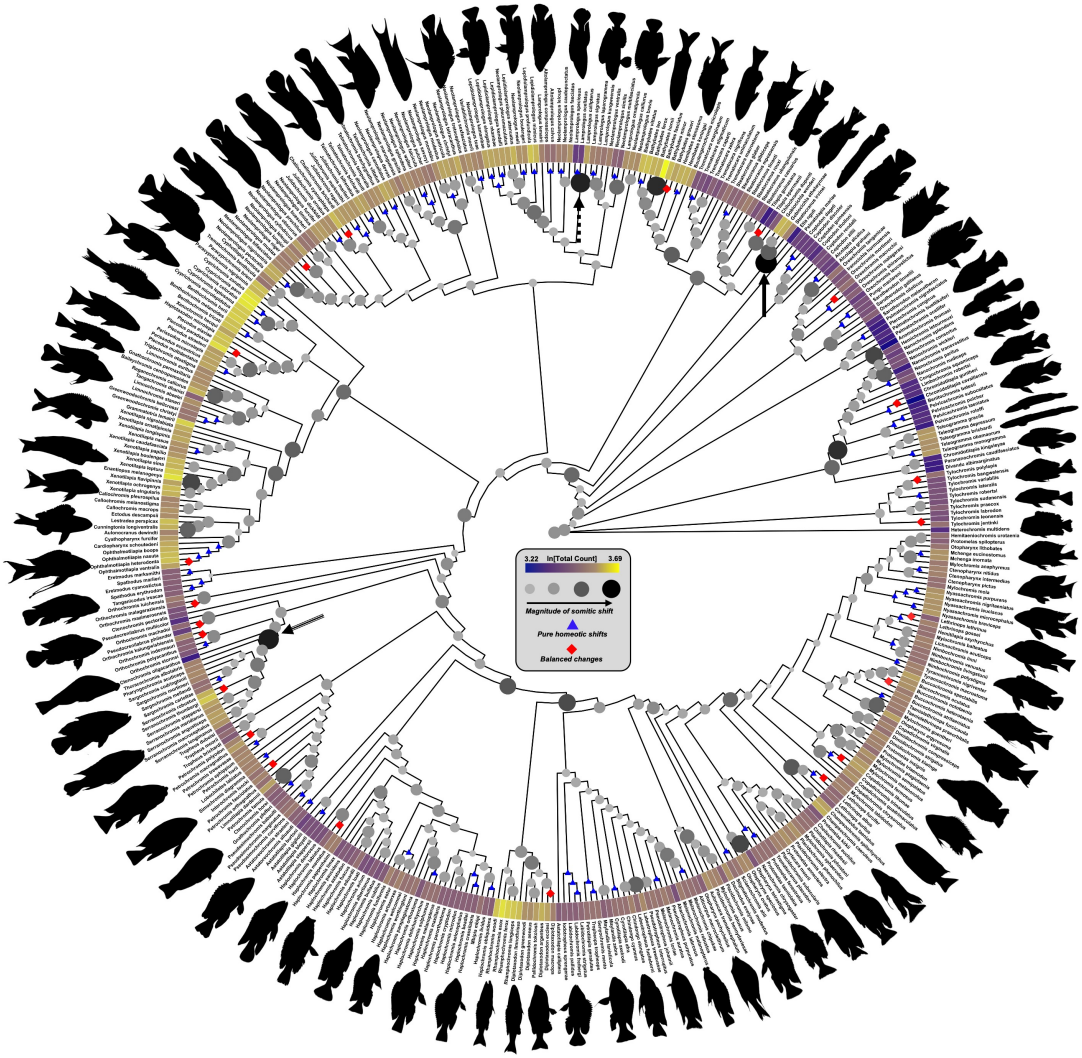

Figure 3. Magnitude of somitic changes in African cichlids. African cichlid cladogram. Node size and colour are scaled to the perpendicular distance (d) of nodes from the $y = -x$ line (i.e. 'pure homeotic shifts', see Figure 2C), where larger, darker nodes represent the raw magnitude of estimated co-occurring somitic change (i.e. combined somitic effects). Blue triangles mark nodes with pure homeotic shifts and red diamonds where balanced somitic changes are predicted to have occurred. ln[Total Count] is plotted as a heatmap at the tips. Arrows match nodes exemplified in Figure 2C. Silhouettes of select cichlid species are displayed around the periphery of the phylogeny for visual reference. See Supplementary Materials for image credits.

at the vast majority of nodes in the phylogeny (Figure 2E), suggesting that the majority of changes in vertebral column regionalisation arise as a result of somitic, rather than homeotic changes.

Intraspecific variation is low and lacks phylogenetic structure

Intraspecific variation in vertebral counts is tightly clustered around the mean for each species (Figure 4A). The median coefficient of variation (CV) is just 1.49%, indicating that for most species, the standard deviations are a small fraction of the mean total vertebral count. This suggests that vertebral counts are dispersed closely around the mean, with intraspecific variation in vertebral counts deviating minimally from the mean count. In real terms, the modal range of intraspecific counts is just $TC \pm 1$. Caudal variance

(σ^2) is significantly higher than precaudal variance (Figure 4B, Wilcoxon Rank Sum, V = 5805.5, $p < 0.001$), suggesting that the loss or gain of caudal vertebrae is more common than that of precaudal vertebrae within species. Moreover, since the total count variance is the sum of the variances of the precaudal and caudal counts (see Methodology), caudal variance may contribute more to total vertebral count intraspecific variation than precaudal. However, we found no significant difference between the CVs for precaudal and caudal vertebral counts (Figure 4B, Wilcoxon Rank Sum, V = 16506, $p = 0.196$). Whilst caudal counts exhibit a larger absolute spread, likely a result of caudal counts generally being larger in African cichlids (see Figure 2B), the relative variation (compared to the mean vertebral count) is similar for both domains. Therefore, intraspecific variation in total vertebral count likely reflects both homeotic (shifts between regions) and somitic (additive or subtractive) effects. Estimates of phylogenetic signal revealed K values indistinguishable from zero (precaudal CV: $K = 0.0089$, $p = 0.49$; caudal CV: $K = 0.0116$, $p = 0.40$), and although λ values were significantly greater than zero (precaudal CV: $\lambda = 0.166$, $p = 0.01$; caudal CV: $\lambda = 0.525$, $p = 0.0004$), the flat likelihood profiles (see Supplementary Figure 2) suggest these results reflect estimation uncertainty rather than meaningful signal. Thus, both K and λ indicate little to no phylogenetic structure in the relative variation of vertebral counts, suggesting that intraspecific variation in precaudal and caudal counts is largely independent of phylogenetic relatedness and is unlikely to be constrained by shared ancestry.

The evolution of vertebral counts is not correlated with changes in intraspecific variation

We found no significant differences between the total count CV and the total vertebral count across any of the tested bins (Figure 4C, Kruskal-Wallis, $\chi^2 = 2.366$, *d.f.* = 4, p = 0.669). Results were consistent with a permutation-based Kruskal-Wallis test to correct for phylogenetic relationships (Figure 4D, n=10,000, p = 0.959), suggesting that accounting for phylogenetic relatedness did not substantially alter any of the group differences. Therefore, somitic count variability does not scale with total vertebral count and is unlikely to have undergone positive or indeed purifying (negative) selection. As a consequence, elongate lineages do not differ in somitic count variability from lineages with more conservative vertebral counts. We did find evidence of difference in the total count CV between water systems (Kruskal-Wallis, $\chi^2 = 13.17$, *d.f.* = 3, p = 0.004), but pairwise comparisons indicated a significant difference only between Lake Tanganyika and Lake Malawi ($p = 0.015$), see Figure 4E. However, a phylogenetic implementation of the Kruskal-Wallis test (see Methodology) found no significant differences in the median CV between any of the respective water systems (Figure 4F, p = 0.912). Consequently, intraspecific variation has remained stable across the phylogeny despite differences in evolutionary dynamics of interspecific total count evolution between water systems (Bucklow et al., 2025b). Consistent with this, we found no evidence of phylogenetic signal in the total count CV. Both λ (0.196, p = 0.197) and K (0.030, p = 0.077) were indistinguishable from 0 (Supplementary Figure 2), suggesting that interspecific variation in intraspecific variability is not strongly structured by phylogenetic relatedness. Therefore, although vertebral counts have evolved extensively, somitic count variability has likely remained consistent across the phylogeny. This suggests that low intraspecific variation in vertebral number results from a conserved developmental constraint that has persisted throughout the diversification of African cichlids.

Intraspecific variation does not scale predictably with body elongation

Despite the importance of vertebral addition in driving body elongation between species (Bucklow et al., 2025b), we found no evidence that individuals with increased vertebral counts exhibit higher body aspect ratios across the full range of body shapes present in African cichlids (Figure 5A). This lack of association held both across species and within them. Within-species regressions of ln[Total Count] on ln[Length] – ln[Depth] (body aspect ratio), produced highly variable and generally weak slopes, with no consistent pattern in direction or magnitude (Figure 5B). The REML estimated mean slope was 0.448 ± 0.401 (z =

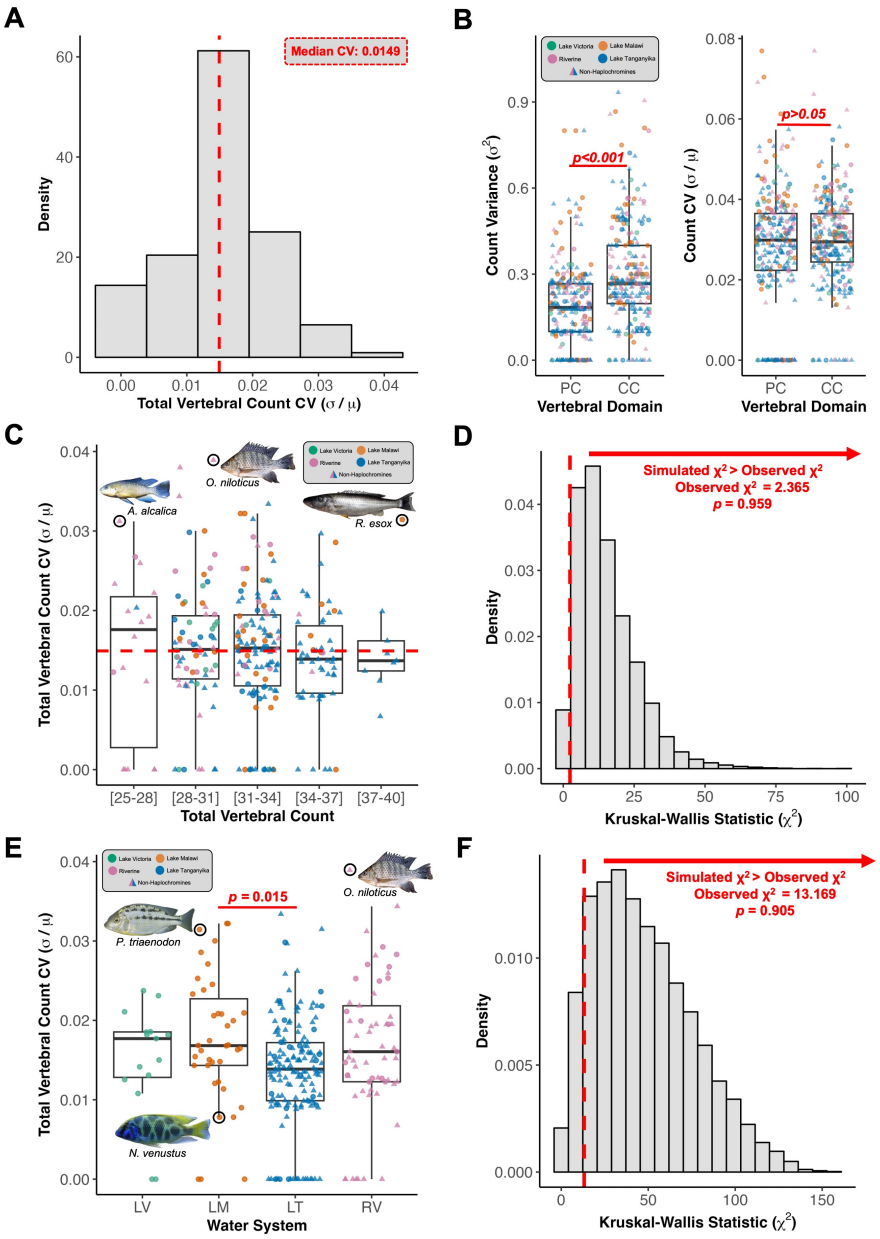

Figure 4. Intraspecific variation in vertebral counts is low. (A) Distribution of the coefficient of variation (CV; σ/μ) for total vertebral count across species. The median is indicated with a dashed red line. (B) Box plots of count variance (σ^2) for precaudal (PC) and caudal (CC) vertebrae (left), and corresponding CV values (right). Group medians are indicated by thick black lines. Differences in variance and CV were tested using a Wilcoxon rank-sum test; significance levels are indicated. Box plot of total count CV grouped by total count (C) and by water system (E), respectively. Overall median CV is indicated with a dashed red line. Permutation-based phylogenetic Kruskal-Wallis null distribution for total count CV by total count (D) and by water system (F), respectively. The observed χ^2 value from the non-phylogenetically corrected test is indicated by a dashed red line. The p-value represents the proportion of permuted χ^2 values greater than the observed value (see Methodology). Genera abbreviations: *A*, *Alcolapia*; *N*, *Nimbochromis*; *O*, *Oreochromis*; *P*, *Protomelas*; *R*, *Rhamphochromis*. Image credits provided in Supplementary Materials.

1.116, $p = 0.264$; 95% CI: –0.338 to 1.234), indicating no significant association between vertebral count and elongation across species (Figure 5C). Despite this, heterogeneity was substantial ($Q(175) = 338.35$, $p < 0.0001$), and the estimated between-species variance was high ($\sigma^2 = 0.811$), suggesting that species differ markedly in the strength and direction of this relationship (including decreases in body aspect ratio being associated with vertebral count increases). Crucially, there is no consistent evidence that individuals with more vertebrae also tend to be more elongate. Therefore, intraspecific variation in vertebral number does not scale predictably with body aspect ratio, and vertebral count variation appears decoupled from large-scale morphological divergence in elongation across species.

DISCUSSION

Modification of the regionalisation of the vertebral column is common in teleosts (Ward and Brainerd, 2007; Ward and Kley, 2012), including in African cichlids (Bucklow et al., 2025b). Our results further support that teleostean clades have independently modified the relative proportions of precaudal and caudal vertebrae (Ward and Brainerd, 2007; Mehta et al., 2010). In addition, our analysis suggests that homeotic shifts can, and likely have, occurred during the diversification of African cichlids, helping to explain some of the variation in vertebral proportions observed across the subfamily. The presence of pure homeotic shifts suggests that AP patterning can be modified without altering somitogenesis. Homeotic transformations are well documented in mutational studies across vertebrates but it is less clear whether these mutations could be maintained across populations (and species). In tetrapods, constraints on vertebral column regionalisation are well documented. Famously, mammals are constrained to have exactly seven cervical vertebrae in developing embryos (Böhmer et al., 2018; Buchholtz and Stepien, 2009), albeit complicated by the early ossification of 'cervical' (thoracic) vertebrae posterior to the seventh cervical vertebrae in sloths (Asher et al., 2011). Cervical vertebral counts in archosaurs, in contrast, are highly variable (Marek et al., 2021). Furthermore, thoracic-to-lumbar transformations are common in mammals (Narita and Kuratani, 2005; Cerbus et al., 2024), indeed homeotic transformations within all domains posterior of the cervical domain can describe much of the vertebral formulae variation in mammals (Cerbus et al., 2024).

Pure homeotic shifts could be driven by changes in the regulation of the *hox* genes responsible for patterning the precaudal-caudal boundary. However, elucidating anterior-posterior patterning during teleostean development is particularly difficult due to the presence of seven/eight *hox* clusters (Crow et al., 2006; Hoegg et al., 2007), where overlapping expression of many paralogous genes, often with functional redundancy (Adachi et al., 2024), makes identifying the key *hox* genes difficult. *hox6* paralogs have been implicated in determining precaudal vertebral identity in *Danio rerio* (zebrafish) and the anterior-expression limits of *hoxC10a* and *hoxD12a* correlate with the somites that go on to contribute to vertebrae at the precaudal-caudal boundary (Morin-Kensicki et al., 2002; Hayward et al., 2015). There is little reason, however, to assume that the specific *hox* genes involved are conserved across teleosts. Subfunctionalisation of *hox* rhombomere patterning has occurred multiple times in teleosts (Scemama et al., 2006), including in cichlids (Le Pabic et al., 2007). Moreover, the identity of *hox* genes which specify fin formation (Sordino et al., 1995) are also not conserved in teleosts (Adachi et al., 2024). Epigenetic regulation of *hox* expression may also play a role in teleosts. Dysregulation of *hox* methylation due to the loss of maternally-expressed factors has been shown to lead to homeotic transformations in zebrafish (Xue et al., 2022). Even in tetrapods, the *Hox* code does not appear to be particularly conserved; paralogous groups 9–11 have been implicated in patterning transitions between different axial domains along the anterior-posterior axis (Cerbus et al., 2024). Therefore, the key genes involved in patterning the precaudal-caudal boundary could vary amongst different teleostean lineages. A systematic, comparative

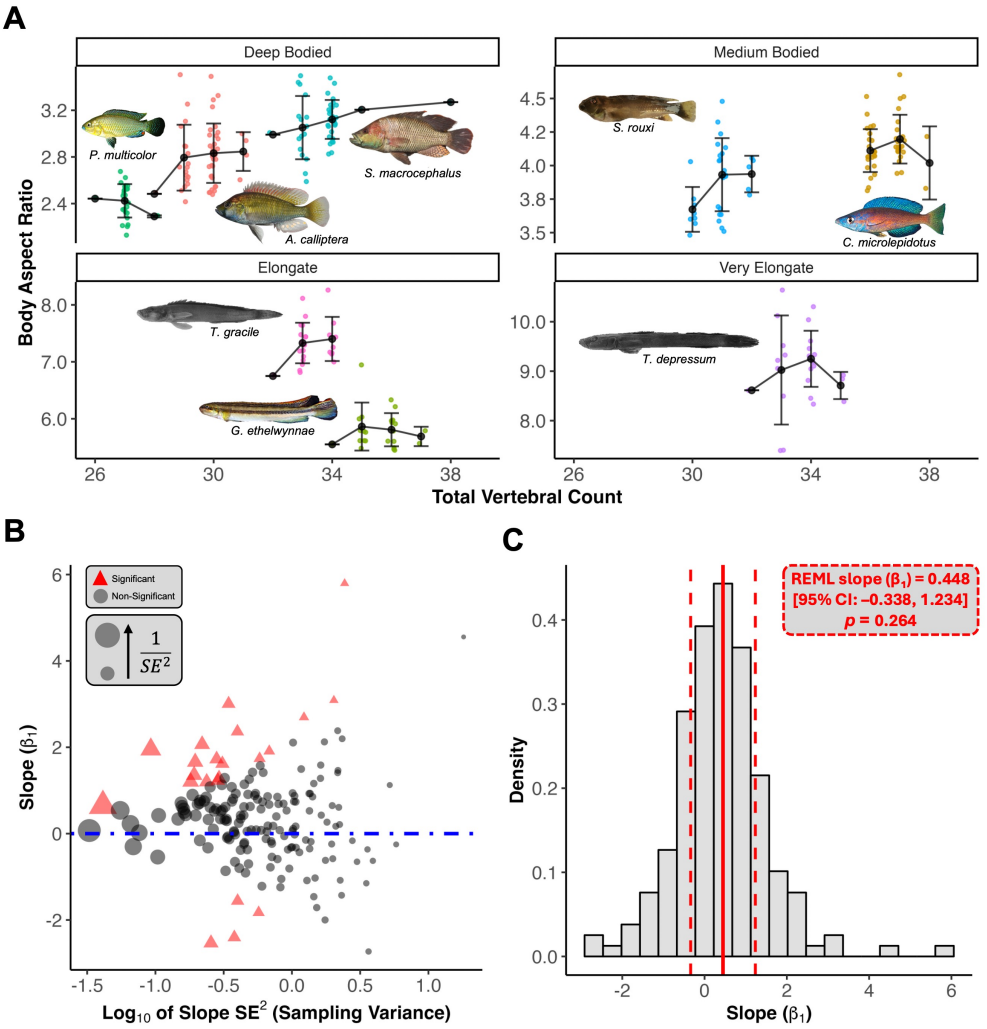

Figure 5. Intraspecific variation does not scale predictably with body elongation. (A) Body aspect ratios plotted against vertebral count for selected species with more than 25 individuals. Panels are faceted by elongation category. Black circles represent the mean body aspect ratio for each vertebral count, with vertical bars indicating the standard deviation. Species images are included for reference. (B) Scatterplot of intraspecific regression slopes (β_1) of ln[Total Vertebral Count] on ln[Length]-ln[Depth] against their respective sampling variances. Point sizes are scaled according to the weights used in the meta-analysis (i.e., inverse of the squared standard error); larger points reflect more precise estimates and thus greater weight. Red triangles indicate slopes significantly different from zero ($p<0.05$). A dot-dashed blue line indicates a slope of zero (i.e., no relationship between ln[Total Count] and ln[Length]-ln[Depth]). (C) Histogram showing the distribution of intraspecific slopes across all species (n=177) with at least ten individuals. The solid red line shows the restricted maximum likelihood (REML) estimate of the mean slope; dashed red lines denote the 95% confidence interval. Note that the confidence interval overlaps zero. Genera abbreviations: *A*, *Astatotilapia*; *C*, *Cyprichromis*; *G*, *Gobiocichla*; *P*, *Pseudocrenilabrus*; *S*, *Serranochromis* (*macrocephalus*), *Steatocranus* (*rouxi*); *T*, *Teleogramma*. Image credits provided in Supplementary Materials.

investigation of *hox* expression across multiple teleost clades will be essential to clarify how these regional boundaries are established and how they have evolved.

We have considered homeotic transformations in just two domains but previous studies have suggested that the teleostean vertebral column has more than two distinct regions (De Clercq et al., 2017; Jawad et al., 2018), however, unlike in terrestrial tetrapods these regions are difficult to visually distinguish due to the relatively homogenous vertebral shape present along the anterior-posterior axis (De Clercq et al., 2017), prohibiting large scale comparative studies such as those that can be more easily conducted in tetrapods (Carapuço et al., 2005; Asher et al., 2011; Cerbus et al., 2024). Constraints placed on the structure of the vertebral column due to a fully aquatic environment may be responsible for this homogenisation. Skates and cetaceans both have what appear to be relatively homogenised vertebral columns. However, landmarked-based geometric morphometric quantification of vertebral shape variation demonstrates the presence of multiple domains nested within the precaudal and caudal domains, with the number of regions being comparable to tetrapods (Criswell et al., 2021; Gillet et al., 2024). Systematic quantification of vertebral shape within teleosts along the AP axis is likely to identify the presence of multiple, nested domains within the precaudal and caudal domains. Once these nested domains have been defined, counting the number of vertebrae within each domain could provide novel insights into the evolution of vertebral column regionalisation, such as the non-homeotic positive correlation recently reported in vertebral counts between the distal cervical and sacral domains in birds (Cerbus et al., 2024).

The dominance of combined somitic effects suggests that much of the variation in the African cichlid vertebral column can be attributed to changes in somite number. Importantly, this also implies that most shifts in vertebral proportions arise as a by-product of somitic changes, rather than through direct modification of axial patterning mechanisms like the *Hox* genes. In other words, homeotic transformations could occur without requiring evolutionary changes in the *Hox* regulatory network itself. In teleosts, anterior *Hox* genes are expressed even prior to gastrulation (Stevens et al., 1996; Amali et al., 2013). While they are not essential for initiating gastrulation, these genes do help organise mesodermal derivatives during development (Nowicki and Burke, 2000; Iimura and Pourquié, 2007). Later-acting *Hox13* genes have also been implicated in regulating the neuromesodermal progenitor (NMP) niche (Ye and Kimelman, 2020), as well as controlling mesodermal cell movements out of the tailbud in tetrapods (Denans et al., 2015). However, if the rate of somite formation changes, producing more or fewer somites in the same amount of time, the overall *Hox* 'timer' may remain unchanged. In this scenario, the *hox* pattern shifts as a consequence of changing the number of somites. In Lake Malawi cichlids, an increased somitic rate, relative to *Astatotilapia calliptera* which forms fewer somites, has been shown to contribute towards the increased somite counts observed in *Rhamphochromis sp.* 'Chilingali' (Marconi et al., 2023). Thus, altering the rate or duration of somitogenesis may be sufficient to drive both changes in total vertebral count and regionalisation, without necessitating changes to the underlying *Hox* code. This could also explain why balanced somitic changes where both the somitic rate and *Hox* timer evolve in tandem to preserve proportions appear to be relatively rare: such changes would require coincident modifications affecting both somitogenesis and *Hox* regulation, which appears to be evolutionarily unlikely.

Given the increased rates observed in haplochromines, very little genetic variation appears to be required in order to drive these somitic changes (and indeed homeotic changes), reinforcing the utility of haplochromines as powerful models in evolutionary developmental biology (Santos et al., 2023). Lake Malawi cichlids, for example, are extremely closely related, more so than human populations (Malinsky et al., 2018). CTCCC-binding factor (CTCF) has been implicated in the regulation of *hox* timing. Genomic CTCF-binding sites act as anchor points for the formation of chromatin loops, which can alter the rate of *hox* transcription (Deschamps and Duboule, 2017; Rekaik et al., 2023). Modification of CTCF-binding sites has even been shown to trigger homeotic transformations (Narendra et al., 2016; Rekaik et al.,

2023). Therefore, the evolutionary modification of CTCF-binding sites in the *hox* clusters could act as a mechanism to modulate the *Hox* 'timer'. Therefore, relatively small genetic mutations between closely related animals could alter CTCF-binding sites in the *Hox* clusters. Larger intragenic distances (proxy for number of CTCF-binding sites) between *Hox* clusters do not appear to correlate with shifts in regionalisation across tetrapods, at least when corrected for phylogeny. However, significant clade specific differences were identified, such as a positive correlation between the number of thoracic vertebrae and HoxD1-HoxD3 intergenic distances in amphibians (Cerbus et al., 2024). Therefore, smaller scale effects may be possible. Many axial phenotypes have now been characterised in haplochromine cichlids (Oliver, 2024; Bucklow et al., 2025b) and we now have robust whole genomes for many haplochromines (Meier et al., 2017; Malinsky et al., 2018; Masonick et al., 2022). An analysis of *Hox* intergenic distances and their correlation with multiple axial phenotypes in haplochromines could provide a powerful model system to investigate this further.

Strong developmental constraints are likely maintaining vertebral number within a narrow range, preventing intraspecific variation in vertebral counts to fluctuate within a species. This stability across the phylogeny implies that selection or genetic/developmental constraints prevent vertebral count from varying significantly within species, suggesting strong canalisation of intraspecific variation in the number of somitic pairs formed during somitogenesis. Intraspecific variation in vertebral counts has been identified across vertebrates (Yamahira et al., 2006; Slijepčević et al., 2015; Tibblin et al., 2016), including in humans (Hu et al., 2016; Yan et al., 2022). Both common garden experiments, as well as heritability estimates derived from quantitative genetic studies, have shown that intraspecific variation in vertebral counts has an additive and heritable genetic basis (Leary et al., 1985; Manier et al., 2007; Alho et al., 2011). This raises the question of why somitogenesis is canalised so strongly. At least in teleosts, it may partly be a consequence of needing to buffer against environmentally-induced phenotypic plasticity. Changes in salinity, light, and temperature have all been shown to lead to changes in vertebral counts (Fowler, 1970; Tibblin et al., 2016; Campbell et al., 2021). Therefore, canalisation of the intraspecific somitic count variability would minimise the production of maladaptive phenotypes, particularly in ecological contexts where axial morphology may be linked to locomotory performance, predator avoidance, or habitat use (Swain, 1992; Tibblin et al., 2016).

It was nonetheless surprising that we found no relationship between intraspecific variation in total vertebral counts and body aspect ratio, given the well-established role of vertebral addition in driving interspecific body elongation, across teleosts (Ward and Brainerd, 2007; Ward and Mehta, 2010; Mehta et al., 2010), including in African cichlids (Bucklow et al., 2025b). If intraspecific variation is indeed important in generating intraspecific differences in phenotypes (Swain, 1992; Tibblin et al., 2016), it does not seem to affect elongation of the body on the level of individuals. In cichlids, body shape is known to be highly polygenic, with quantitative trait locus (QTL) analyses of hybrids revealing contributions from many loci (Husemann et al., 2017; DeLorenzo et al., 2023). Indeed, it appears that hybridisation is sufficient to lead to the emergence of transgressive body shapes (Husemann et al., 2017; Selz and Seehausen, 2019), including vertebral count in other teleostean lineages (Seleit et al., 2024). Many of these loci are likely involved in multiple developmental pathways throughout growth and development. In Central American cichlids (*Amphilophus* spp.), vertebral counts and lateral line scale numbers not only covary phenotypically but also co-segregate genomically, suggesting shared developmental control and tight linkage of the underlying genomic regions (Ehemann et al., 2024). In African cichlids, we have previously shown that evolutionary changes in posterior body elongation are tightly coupled to changes in cranial elongation. However, cranial elongation appears to occur without corresponding increases in vertebral number (Bucklow et al., 2025b). Therefore, body elongation in cichlids could arise through the reuse or modification of developmental programs other than those controlling axial segmentation. QTL

analysis focused specifically on identifying genomic and phenotypic covariation in interspecific hybrids differing in multiple axial phenotypes, including total numbers of vertebrae, proportions of precaudal and caudal vertebrae and body shape may help further elucidate the complex relationship between the axial skeleton and body shape evolution.

In summary, our findings highlight the dynamic interplay between homeotic transformations and somitic changes in shaping the vertebral column of African cichlids. While shifts in vertebral regionalisation can arise through modification of anterior-posterior patterning, our results suggest that much of the observed variation is likely driven by changes in somitogenesis, with homeotic effects emerging as a by-product rather than a direct target of selection. The developmental processes governing somite formation and regionalisation in cichlids are likely highly canalised, limiting intraspecific variation even as interspecific diversity evolves. Future work integrating comparative developmental genetics, quantitative morphology, and genomics, particularly leveraging the exceptional diversity and genomic resources of haplochromine cichlids, holds considerable promise for disentangling the relative roles of somitogenesis and homeotic regulation in vertebral evolution. Ultimately, understanding how these processes interact across clades will shed new light on the origins of vertebral regionalisation and its evolutionary flexibility in vertebrates.

SUPPLEMENTARY FIGURES

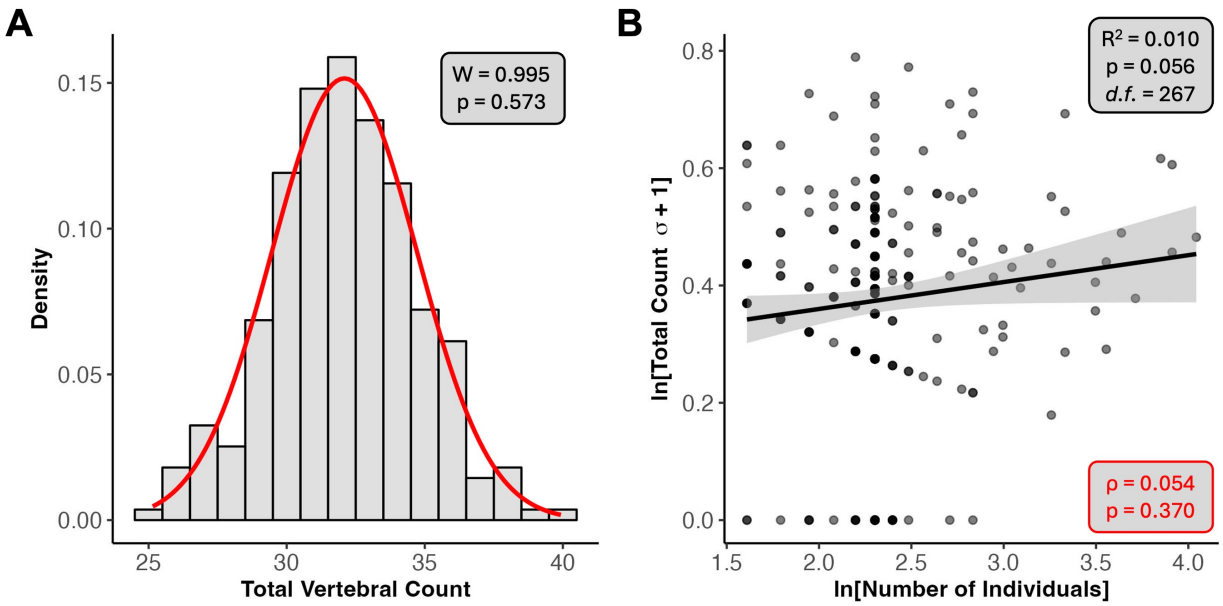

Supplementary Figure 1. (A) Distribution of total vertebral counts for species represented by ≥ 5 individuals and included in the phylogeny (n = 277). The observed range (25–40 vertebrae) is consistent with previous reports for African cichlids (Oliver, 2024; Bucklow et al., 2025b). A red curve shows an idealised normal distribution. Results of a Shapiro-Wilk test for normality are provided in the black box. (B) Relationship between ln-transformed total vertebral count standard deviation (σ) and ln-transformed sample size. To accommodate zero values, one was added to all standard deviations prior to transformation. The black line shows the ordinary least squares (OLS) regression fit, with shaded regions indicating standard error. Results of a Spearman rank correlation are shown in red.

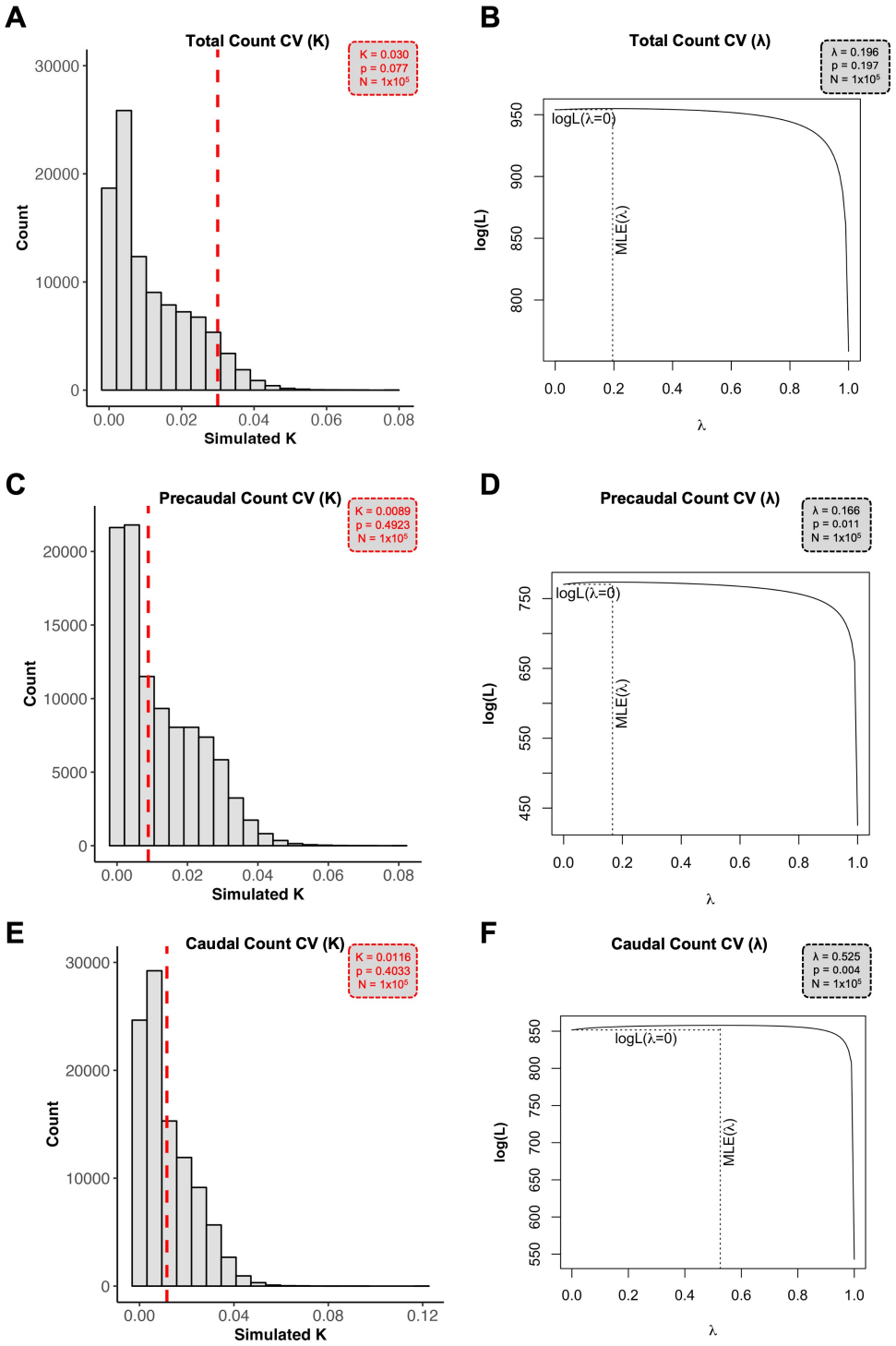

Supplementary Figure 2. Null distributions of Blomberg's K estimates (left) and likelihood profiles of Pagel's λ estimates (right) for (A, B) total count CV, (C, D) precaudal count CV, and (E, F) caudal count CV. Observed K values are shown as red dashed lines. The maximum likelihood estimate (MLE) for λ is shown as a black dotted line. Results of hypothesis tests for $H_0 : K, \lambda > 0$ are shown in red (K) and black (λ), respectively. The number of simulations is indicated in each panel. Note that although significant p-values were obtained for $\lambda > 0$ in precaudal and caudal CV, the likelihood profiles are very flat, suggesting these may represent false positives.

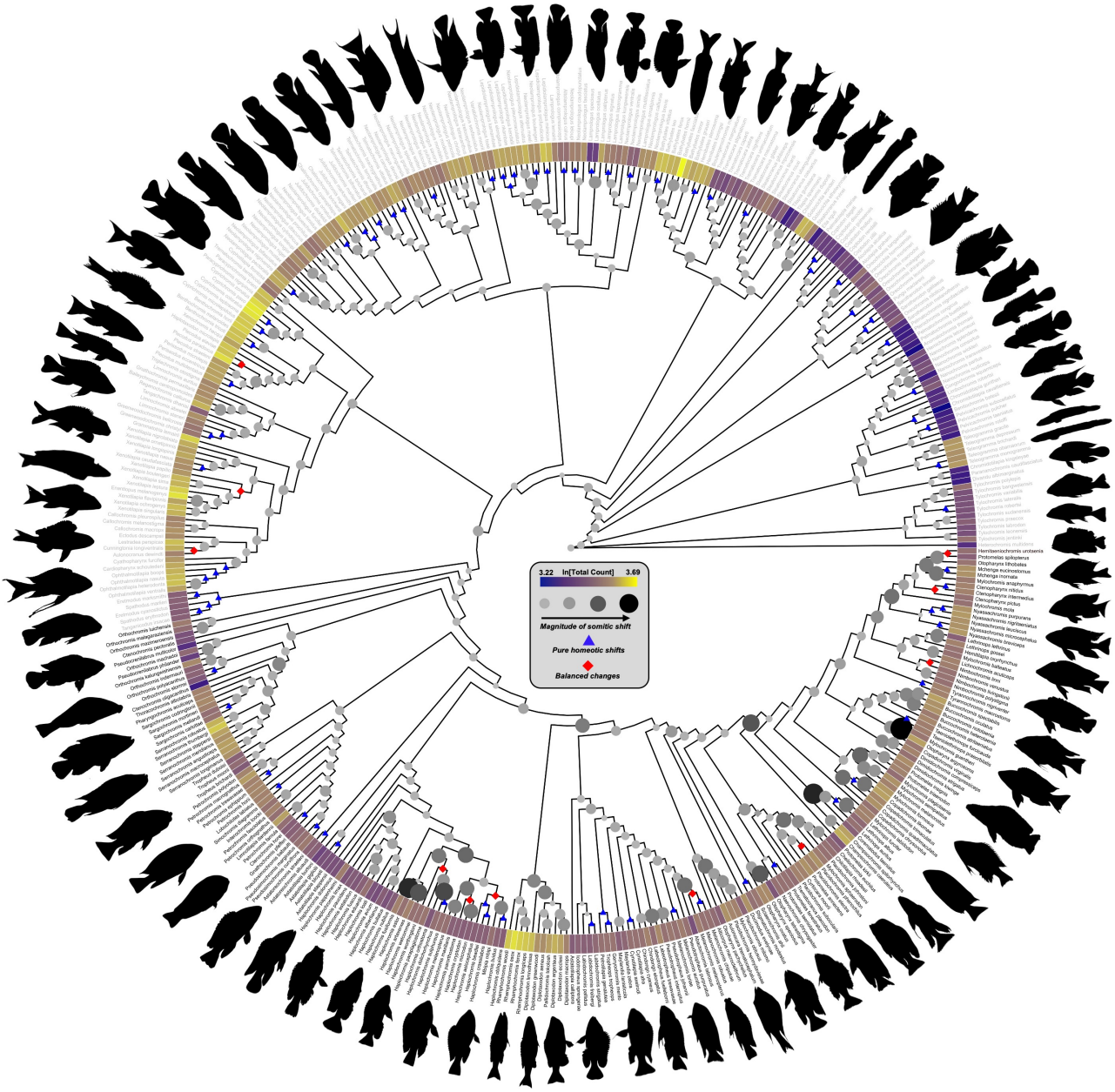

Supplementary Figure 3. All branch lengths are fixed at 1 for visualisation purposes, as many internal branches are too short to display clearly alongside node labels. However, perpendicular distances were derived from phylogenetic independent contrasts (PICs) calculated using the original, time-calibrated branch lengths (see Methodology). Tip labels in black correspond to haplochromine species. Larger, darker internal nodes indicate elevated rates of co-occurring somitic change (i.e., combined precaudal and caudal effects). Nodes marked with blue triangles indicate inferred pure homeotic shifts, while red diamonds mark nodes where balanced somitic changes are predicted. ln[Total Count] (log-transformed total vertebral count) is plotted as a heatmap at the tips of the tree. Silhouettes of select cichlid species are displayed around the periphery of the phylogeny for visual reference. See Supplementary Materials for image credits.

AUTHOR CONTRIBUTIONS

C.V.B, B.V. and R.B. conceived the study. E.D.R helped with phylogenetic generalised least squares analysis of precaudal and caudal counts. C.V.B wrote the manuscript. B.V. and R.B. edited the manuscript. All authors reviewed the manuscript.

DECLARATION OF INTERESTS

The authors declare no competing interests.

ACKNOWLEDGMENTS

This research was funded by a Biotechnology and Biological Sciences Research Council (BBSRC) studentship (Grant Number: 2445747). We thank Laura Soul for her original work describing the methodology to identify homeotic and somitic effects on phylogenetic scales. We thank James Hammond for helpful discussion regarding the evolvability of somitogenesis. Thank you to the fishes whose lives were sacrificed for this work.

REFERENCES

Adachi, U., Koita, R., Seto, A., Maeno, A., Ishizu, A., Oikawa, S., Tani, T., Ishizaka, M., Yamada, K., Satoh, K., et al. (2024). Teleost hox code defines regional identities competent for the formation of dorsal and anal fins. *Proceedings of the National Academy of Sciences*, 121(25):e2403809121.

Alho, J. S., Leinonen, T., and Merilä, J. (2011). Inheritance of vertebral number in the three-spined stickleback (gasterosteus aculeatus). *PLoS One*, 6(5):e19579.

Amali, A. A., Sie, L., Winkler, C., and Featherstone, M. (2013). Zebrafish hoxd4a acts upstream of meis1. 1 to direct vasculogenesis, angiogenesis and hematopoiesis. *PLoS One*, 8(3):e58857.

Asher, R., Lin, K., Kardjilov, N., and Hautier, L. (2011). Variability and constraint in the mammalian vertebral column. *Journal of Evolutionary Biology*, 24(5):1080–1090.

Astudillo-Clavijo, V., Stiassny, M. L., Ilves, K. L., Musilova, Z., Salzburger, W., and López-Fernández, H. (2023). Exon-based phylogenomics and the relationships of african cichlid fishes: tackling the challenges of reconstructing phylogenies with repeated rapid radiations. *Systematic Biology*, 72(1):134–149.

Blomberg, S. P., Garland Jr, T., and Ives, A. R. (2003). Testing for phylogenetic signal in comparative data: behavioral traits are more labile. *Evolution*, 57(4):717–745.

Böhmer, C., Amson, E., Arnold, P., van Heteren, A. H., and Nyakatura, J. A. (2018). Homeotic transformations reflect departure from the mammalian 'rule of seven'cervical vertebrae in sloths: inferences on the hox code and morphological modularity of the mammalian neck. *BMC Evolutionary Biology*, 18:1–11.

Böhmer, C., Rauhut, O. W., and Wörheide, G. (2015). Correlation between hox code and vertebral morphology in archosaurs. *Proceedings of the Royal Society B: Biological Sciences*, 282(1810):20150077.

Buchholtz, E. A. and Stepien, C. C. (2009). Anatomical transformation in mammals: developmental origin of aberrant cervical anatomy in tree sloths. *Evolution & development*, 11(1):69–79.

Bucklow, C., Duarte-Ribeiro, E., Ronco, F., Vranken, N., Oliver, M., Stiassny, M., Salzburger, W., Benson, R., and Verd, B. (2025a). African cichlid lake radiations recapitulate riverine axial morphologies through repeated exploration of morphospace. *Zenodo*.

Bucklow, C. V., Ribeiro, E. D., Ronco, F., Vranken, N., Oliver, M. K., Salzburger, W., Stiassny, M., Benson, R., and Verd, B. (2025b). African cichlid lake radiations recapitulate riverine axial morphologies through repeated exploration of morphospace. *bioRxiv*.

Campbell, C. S., Adams, C. E., Bean, C. W., Pilakouta, N., and Parsons, K. J. (2021). Evolvability under climate change: Bone development and shape plasticity are heritable and correspond with performance in arctic charr (salvelinus alpinus). *Evolution & Development*, 23(4):333–350.

Carapuço, M., Nóvoa, A., Bobola, N., and Mallo, M. (2005). Hox genes specify vertebral types in the presomitic mesoderm. *Genes & development*, 19(18):2116–2121.

Cerbus, R. T., Hiratani, I., and Kawaguchi, K. (2024). Homeotic and nonhomeotic patterns in the tetrapod vertebral formula. *Proceedings of the National Academy of Sciences*, 121(47):e2411421121.

Cohn, M. J. and Tickle, C. (1999). Developmental basis of limblessness and axial patterning in snakes. *Nature*, 399(6735):474–479.

Criswell, K. E., Roberts, L. E., Koo, E. T., Head, J. J., and Gillis, J. A. (2021). hox gene expression predicts tetrapod-like axial regionalization in the skate, leucoraja erinacea. *Proceedings of the National Academy of Sciences*, 118(51):e2114563118.

Crow, K. D., Stadler, P. F., Lynch, V. J., Amemiya, C., and Wagner, G. P. (2006). The "fish-specific" hox cluster duplication is coincident with the origin of teleosts. *Molecular Biology and Evolution*, 23(1):121–136.

De Clercq, A., Perrott, M. R., Davie, P. S., Preece, M. A., Wybourne, B., Ruff, N., Huysseune, A., and

Witten, P. E. (2017). Vertebral column regionalisation in chinook salmon, oncorhynchus tshawytscha. *Journal of anatomy*, 231(4):500–514.

DeLorenzo, L., Mathews, D., Brandon, A. A., Joglekar, M., Carmona Baez, A., Moore, E. C., Ciccotto, P. J., Roberts, N. B., Roberts, R. B., and Powder, K. E. (2023). Genetic basis of ecologically relevant body shape variation among four genera of cichlid fishes. *Molecular ecology*, 32(14):3975–3988.

Denans, N., Iimura, T., and Pourquié, O. (2015). Hox genes control vertebrate body elongation by collinear wnt repression. *Elife*, 4:e04379.

Deschamps, J. and Duboule, D. (2017). Embryonic timing, axial stem cells, chromatin dynamics, and the hox clock. *Genes & development*, 31(14):1406–1416.

Ehemann, N., Franchini, P., Meyer, A., and Hulsey, C. D. (2024). Meristic co-evolution and genomic co-localization of lateral line scales and vertebrae in central american cichlid fishes. *Ecology and Evolution*, 14(9):e70266.

Felsenstein, J. (1985). Phylogenies and the comparative method. *The American Naturalist*, 125(1):1–15.

Ford, E. (1937). Vertebral variation in teleostean fishes. *Journal of the marine biological association of the United Kingdom*, 22(1):1–60.

Fowler, J. A. (1970). Control of vertebral number in teleosts - an embryological problem. *The Quarterly Review of Biology*, 45(2):148–167.

Freckleton, R. P. and Harvey, P. H. (2006). Detecting non-brownian trait evolution in adaptive radiations. *PLoS biology*, 4(11):e373.

Gillet, A., Jones, K. E., and Pierce, S. E. (2024). Repatterning of mammalian backbone regionalization in cetaceans. *Nature Communications*, 15(1):7587.

Gomez, C., Özbudak, E. M., Wunderlich, J., Baumann, D., Lewis, J., and Pourquié, O. (2008). Control of segment number in vertebrate embryos. *Nature*, 454(7202):335–339.

Hayward, A. G., Joshi, P., and Skromne, I. (2015). Spatiotemporal analysis of zebrafish hox gene regulation by cdx4. *Developmental Dynamics*, 244(12):1564–1573.

Hoegg, S., Boore, J. L., Kuehl, J. V., and Meyer, A. (2007). Comparative phylogenomic analyses of teleost fish hox gene clusters: lessons from the cichlid fish astatotilapia burtoni. *BMC genomics*, 8:1–16.

Hu, Z., Zhang, Z., Zhao, Z., Zhu, Z., Liu, Z., and Qiu, Y. (2016). A neglected point in surgical treatment of adolescent idiopathic scoliosis: variations in the number of vertebrae. *Medicine*, 95(34):e4682.

Husemann, M., Tobler, M., McCauley, C., Ding, B., and Danley, P. D. (2017). Body shape differences in a pair of closely related malawi cichlids and their hybrids: Effects of genetic variation, phenotypic plasticity, and transgressive segregation. *Ecology and Evolution*, 7(12):4336–4346.

Iimura, T., Denans, N., and Pourquié, O. (2009). Establishment of hox vertebral identities in the embryonic spine precursors. *Current topics in developmental biology*, 88:201–234.

Iimura, T. and Pourquié, O. (2007). Hox genes in time and space during vertebrate body formation. *Development, growth & differentiation*, 49(4):265–275.

Jawad, L. A., Habbeb, F. S., and Al-Mukhtar, M. A. (2018). Some osteological studies of coptodon zillii (gervais 1848) and oreochromis aureus (steindachner 1864) collected shatt al-arab river, basrah, iraq. *International Journal of Marine Science*, 8(4):26.

Jones, K. E., Angielczyk, K. D., Polly, P. D., Head, J. J., Fernandez, V., Lungmus, J. K., Tulga, S., and Pierce, S. E. (2018a). Fossils reveal the complex evolutionary history of the mammalian regionalized spine. *Science*, 361(6408):1249–1252.

Jones, K. E., Benitez, L., Angielczyk, K. D., and Pierce, S. E. (2018b). Adaptation and constraint in the evolution of the mammalian backbone. *BMC evolutionary biology*, 18:1–13.

Lajeunesse, M. J. (2009). Meta-analysis and the comparative phylogenetic method. *The American Naturalist*, 174(3):369–381.

Le Pabic, P., Stellwag, E. J., Brothers, S. N., and Scemama, J.-L. (2007). Comparative analysis of hox paralog group 2 gene expression during nile tilapia (oreochromis niloticus) embryonic development. *Development genes and evolution*, 217:749–758.

Leary, R. F., Allendorf, F. W., and Knudsen, K. L. (1985). Inheritance of meristic variation and the evolution of developmental stability in rainbow trout. *Evolution*, 39(2):308–314.

Malinsky, M., Svardal, H., Tyers, A. M., Miska, E. A., Genner, M. J., Turner, G. F., and Durbin, R. (2018). Whole-genome sequences of malawi cichlids reveal multiple radiations interconnected by gene flow. *Nature ecology & evolution*, 2(12):1940–1955.

Manier, M., Seyler, C., and Arnold, S. (2007). Adaptive divergence within and between ecotypes of the terrestrial garter snake, thamnophis elegans, assessed with f st-q st comparisons. *Journal of Evolutionary Biology*, 20(5):1705–1719.

Marconi, A., Yang, C. Z., McKay, S., and Santos, M. E. (2023). Morphological and temporal variation in early embryogenesis contributes to species divergence in malawi cichlid fishes. *Evolution & Development*, 25(2):170–193.

Marek, R. D., Falkingham, P. L., Benson, R. B., Gardiner, J. D., Maddox, T. W., and Bates, K. T. (2021). Evolutionary versatility of the avian neck. *Proceedings of the Royal Society B*, 288(1946):20203150.

Maroto, M., Bone, R. A., and Dale, J. K. (2012). Somitogenesis. *Development*, 139(14):2453–2456.

Masonick, P., Meyer, A., and Hulsey, C. D. (2022). Phylogenomic analyses show repeated evolution of hypertrophied lips among lake malawi cichlid fishes. *Genome Biology and Evolution*, 14(4):evac051.

McGee, M. D., Borstein, S. R., Meier, J. I., Marques, D. A., Mwaiko, S., Taabu, A., Kishe, M. A., O'Meara, B., Bruggmann, R., Excoffier, L., et al. (2020). The ecological and genomic basis of explosive adaptive radiation. *Nature*, 586(7827):75–79.

Mehta, R. S., Ward, A. B., Alfaro, M. E., and Wainwright, P. C. (2010). Elongation of the body in eels. *Integrative and Comparative Biology*, 50(6):1091–1105.

Meier, J. I., Marques, D. A., Mwaiko, S., Wagner, C. E., Excoffier, L., and Seehausen, O. (2017). Ancient hybridization fuels rapid cichlid fish adaptive radiations. *Nature communications*, 8(1):14363.

Morin-Kensicki, E. M., Melancon, E., and Eisen, J. S. (2002). Segmental relationship between somites and vertebral column in zebrafish. *Development*.

Naganathan, S. R. and Oates, A. C. (2020). Patterning and mechanics of somite boundaries in zebrafish embryos. In *Seminars in cell & developmental biology*, volume 107, pages 170–178. Elsevier.

Narendra, V., Bulajić, M., Dekker, J., Mazzoni, E. O., and Reinberg, D. (2016). Ctcf-mediated topological boundaries during development foster appropriate gene regulation. *Genes & development*, 30(24):2657–2662.

Narita, Y. and Kuratani, S. (2005). Evolution of the vertebral formulae in mammals: a perspective on developmental constraints. *Journal of Experimental Zoology Part B: Molecular and Developmental Evolution*, 304(2):91–106.

Near, T. J. and Thacker, C. E. (2024). Phylogenetic classification of living and fossil ray-finned fishes (actinopterygii). *Bulletin of the Peabody Museum of Natural History*, 65(1):3–302.

Nowicki, J. L. and Burke, A. C. (2000). Hox genes and morphological identity: axial versus lateral patterning in the vertebrate mesoderm. *Development*, 127(19):4265–4275.

Oliver, M. K. (2024). African cichlid fishes: morphological data and taxonomic insights from a genus-level survey of supraneurals, pterygiophores, and vertebral counts (ovalentaria, blenniiformes, cichlidae, pseudocrenilabrinae). *Biodiversity Data Journal*, 12:e130707.

Orme, D., Freckleton, R., Thomas, G., Petzoldt, T., Fritz, S., Isaac, N., and Pearse, W. (2018). *caper: Comparative Analyses of Phylogenetics and Evolution in R*. R package version 1.0.1.

Pagel, M. (1999). Inferring the historical patterns of biological evolution. *Nature*, 401(6756):877–884.

Paradis, E. and Schliep, K. (2019). ape 5.0: an environment for modern phylogenetics and evolutionary analyses in R. *Bioinformatics*, 35:526–528.

R Core Team (2022). *R: A Language and Environment for Statistical Computing*. R Foundation for Statistical Computing, Vienna, Austria.

Rekaik, H., Lopez-Delisle, L., Hintermann, A., Mascrez, B., Bochaton, C., Mayran, A., and Duboule, D. (2023). Sequential and directional insulation by conserved ctcf sites underlies the hox timer in stembryos. *Nature genetics*, 55(7):1164–1175.

Revell, L. J. (2024). phytools 2.0: an updated R ecosystem for phylogenetic comparative methods (and other things). *PeerJ*, 12:e16505.

Ronco, F., Matschiner, M., Böhne, A., Boila, A., Büscher, H. H., El Taher, A., Indermaur, A., Malinsky, M., Ricci, V., Kahmen, A., et al. (2021). Drivers and dynamics of a massive adaptive radiation in cichlid fishes. *Nature*, 589(7840):76–81.

Santos, M. E., Lopes, J. F., and Kratochwil, C. F. (2023). East african cichlid fishes. *EvoDevo*, 14(1):1.

Scemama, J.-L., Vernon, J. L., and Stellwag, E. J. (2006). Differential expression of hoxa2a and hoxa2b genes during striped bass embryonic development. *Gene expression patterns*, 6(8):843–848.

Seleit, A., Brettell, I., Fitzgerald, T., Vibe, C., Loosli, F., Wittbrodt, J., Naruse, K., Birney, E., and Aulehla, A. (2024). Modular control of vertebrate axis segmentation in time and space. *The EMBO Journal*, 43(18):4068–4091.

Selz, O. M. and Seehausen, O. (2019). Interspecific hybridization can generate functional novelty in cichlid fish. *Proceedings of the Royal Society B*, 286(1913):20191621.

Slijepčević, M., Galis, F., Arntzen, J. W., and Ivanović, A. (2015). Homeotic transformations and number changes in the vertebral column of triturus newts. *PeerJ*, 3:e1397.

Sordino, P., van der Hoeven, F., and Duboule, D. (1995). Hox gene expression in teleost fins and the origin of vertebrate digits. *Nature*, 375(6533):678–681.

Sosa, M. A. and Hospitaleche, C. A. (2024). Vertebral formula and numerical variations in the spine of the antarctic and southern south american penguins (aves: Sphenisciformes). *Vertebrate Zoology*, 74:209–219.

Soul, L. C. and Benson, R. B. (2017). Developmental mechanisms of macroevolutionary change in the tetrapod axis: a case study of sauropterygia. *Evolution*, 71(5):1164–1177.

Stevens, C., Samallo, J., Schipper, H., Stroband, H., and Te Kronnie, G. (1996). Expression of hoxb-1 during gastrulation and segmentation stages of carp (cyprinus carpio). *International Journal of Developmental Biology*, 40(2):463–470.

Swain, D. P. (1992). The functional basis of natural selection for vertebral traits of larvae in the stickleback gasterosteus aculeatus. *Evolution*, 46(4):987–997.

Tibblin, P., Berggren, H., Nordahl, O., Larsson, P., and Forsman, A. (2016). Causes and consequences of intra-specific variation in vertebral number. *Scientific Reports*, 6(1):26372.

Viechtbauer, W. (2010). Conducting meta-analyses in R with the metafor package. *Journal of Statistical Software*, 36(3):1–48.

Ward, A. B. and Brainerd, E. L. (2007). Evolution of axial patterning in elongate fishes. *Biological Journal of the Linnean Society*, 90(1):97–116.

Ward, A. B. and Kley, N. J. (2012). Effects of precaudal elongation on visceral topography in a basal clade of ray-finned fishes. *The Anatomical Record: Advances in Integrative Anatomy and Evolutionary Biology*, 295(2):289–297.

Ward, A. B. and Mehta, R. S. (2010). Axial elongation in fishes: using morphological approaches to elucidate developmental mechanisms in studying body shape. *Integrative and Comparative Biology*, 50(6):1106–1119.

Woltering, J. M., Holzem, M., Schneider, R. F., Nanos, V., and Meyer, A. (2018). The skeletal ontogeny of astatotilapia burtoni–a direct-developing model system for the evolution and development of the teleost body plan. *BMC developmental biology*, 18(1):1–23.

Woltering, J. M., Vonk, F. J., Müller, H., Bardine, N., Tuduce, I. L., de Bakker, M. A., Knöchel, W., Sirbu, I. O., Durston, A. J., and Richardson, M. K. (2009). Axial patterning in snakes and caecilians: evidence for an alternative interpretation of the hox code. *Developmental biology*, 332(1):82–89.

Xue, S., Ly, T. T. N., Vijayakar, R. S., Chen, J., Ng, J., Mathuru, A. S., Magdinier, F., and Reversade, B. (2022). Hox epimutations driven by maternal smchd1/lrif1 haploinsufficiency trigger homeotic transformations in genetically wildtype offspring. *Nature Communications*, 13(1):3583.

Yamahira, K., Lankford Jr, T. E., and Conover, D. O. (2006). Intra-and interspecific latitudinal variation in vertebral number of menidia spp.(teleostei: Atherinopsidae). *Copeia*, 2006(3):431–436.

Yan, Y.-z., Wang, B., Huang, X.-q., Ru, X., Wang, X.-y., and Qu, H.-b. (2022). Variation in global spinal sagittal parameters in asymptomatic adults with 11 thoracic vertebrae, four lumbar vertebrae, and six lumbar vertebrae. *Orthopaedic Surgery*, 14(2):341–348.

Ye, Z. and Kimelman, D. (2020). Hox13 genes are required for mesoderm formation and axis elongation during early zebrafish development. *Development*, 147(22):dev185298.

4 Geometric Morphometrics of Vertebral Shape in Lake Malawi Cichlids

4.1 A whole-body micro-CT scan library that captures the skeletal diversity of Lake Malawi cichlid fishes

4.2 Motivation and Novelty of Paper

Our focus on Lake Malawi cichlids primarily, as opposed to the wider subfamily as for the other chapters was multifactorial. Initially, our focus was just on Lake Malawi cichlids, and the macroevolutionary analysis was initially going to focus on the Lake Malawi radiation. However, this quickly increased to encompass the whole subfamily as systematic mining for 2D x-ray data had uncovered more than I had anticipated. Part of my desire for focusing on just one radiation was to examine the macroevolutionary and morphological patterns common to adaptive radiations [Streelman and Danley, 2003, Gavrilets and Losos, 2009], including Lake Malawi. Previous evidence had already suggested that across teleostean families, the evolutionary modification of vertebral shape has been linked to changing swimming kinematics, body shape and habitat preference [Donatelli et al., 2021], including adapting to pelagic environments [Baxter et al., 2022]. However, it was less obvious whether the modification of vertebral shape could occur rapidly, and in the presence of very little genetic variation (as is the case for Lake Malawi cichlids [Malinsky et al., 2018]). I had established that the axial skeleton played a major role in shaping body elongation and form in African cichlids. However, whether vertebral shape itself could act as an axis of evolutionary variation remained undetermined. After examining several thousand 2D x-rays, it became clear that the shape of vertebrae, including associated ribs and spines, was likely being modified in different lineages. In addition, it was clear that regionalisation of the vertebral column was more complex than just

the traditional precaudal and caudal regions. Previous studies have suggested that the teleostean vertebral column has more than two distinct regions [De Clercq et al., 2017, Jawad et al., 2018, Sankar et al., 2024], however, these regions are difficult to visually distinguish due to the relatively homogenous vertebral shape present along the anterior-posterior axis [De Clercq et al., 2017], particularly when compared to tetrapods [Gillet et al., 2024], prohibiting large scale comparative studies. These observations prompted us to ask whether vertebral shape constitutes a source of adaptive substrate in Lake Malawi cichlids, and whether the number and boundaries of vertebral regions vary in association with ecological or morphological axes. Addressing these questions rigorously, nonetheless, required a large dataset of high-resolution, whole-body μCT scans.

It quickly became evident that the presence of high-quality whole-body μCT scans for Lake Malawi cichlids, especially of the whole body, were relatively rare. The diversity of feeding habits of Lake Malawi cichlids, and the ability to causally link morphological differences in craniofacial morphology to these ecological niches, has enabled integrative genetic and morphological studies examining the evolution of these traits [Albertson and Kocher, 2001, Adams et al., 2004, Hulsey et al., 2019, Conith and Albertson, 2021]. This meant that much of the μCT-scan data available for Lake Malawi cichlids was limited to the cranium. Moreover, there had been no attempts to centralise a database for μCT-scan data for Lake Malawi cichlids and it was evident that a methodology to efficiently μCT-scan multiple specimens simultaneously; reducing scanning time and financial cost, was lacking for cichlids (and indeed more broadly for similarly sized teleosts). Before we could investigate vertebral shape as a source of variation in Lake Malawi cichlids, however, we needed to generate a dataset of high-resolution X-ray micro-computed tomography (μCT) scans of Lake Malawi cichlids. Subsequently, we collated an extensive dataset of 3D data on skeletal morphology for the whole body of 56 species of Lake Malawi cichlid across 26 genera. In total these data comprise 116 individuals from all seven recognised ecomorphological groupings [Malinsky et al., 2018], contrasting in multiple aspects of morphology, size, behaviour, and habitat preference. In the paper we demonstrate the resolution and utility of the dataset by illustrating 3D whole-body renderings of several species, and of several skeletal regions of interest, as well as suggest possible macroevolutionary studies that could be conducted with these data.

Notably, our dataset now joins two other East African adaptive radiation datasets, including the recent haplochromine Lake Victoria library [Haberthür et al., 2023] and an extensive μCT-scan dataset of Lake Tanganyika cichlid fishes [Ronco et al., 2021]. All scans and metadata are publicly accessible via MorphoSource, supporting transparency and reuse. Importantly, the dataset introduces a workflow for multi-specimen scanning of small teleosts that may be useful beyond cichlids. Although the manuscript is a dataset descriptor and does not contain formal statistical analyses or results, it represents a substantial and novel contribution to the field. It provides, for the first time, a resource

that enables the study of vertebral morphology and axial regionalisation in Lake Malawi cichlids on a macroevolutionary scale. The data generated here form the foundation for the analyses presented further within this chapter, where I provide preliminary results investigating the evolution of vertebral regionalisation and axial shape variation in relation to ecology and body form. Generating this dataset, including processing all of the images, preparing the database and writing the manuscript was a particularly large and time consuming undertaking. By making this dataset freely available, we hope to facilitate broader comparisons across cichlid radiations, encourage new lines of inquiry into postcranial morphology, and set a precedent for whole-body μCT scanning as a standard in cichlid morphological research.

A whole-body micro-CT scan library that captures the skeletal diversity of Lake Malawi cichlid fishes

Pages 96–113

Interactive features (e.g. links) are disabled in this embedded version.
For the fully functional version, visit
https://doi.org/10.1038/s41597-024-03687-1.

Author contributions are included at the end of the manuscript.

scientific data

Check for updates

OPEN

DATA DESCRIPTOR

A whole-body micro-CT scan library that captures the skeletal diversity of Lake Malawi cichlid fishes

Callum V. Bucklow[1,2], Martin J. Genner[3], George F. Turner[4], James Maclaine[5], Roger Benson[2,6] ✉ & Berta Verd[1] ✉

Here we describe a dataset of freely available, readily processed, whole-body μCT-scans of 56 species (116 specimens) of Lake Malawi cichlid fishes that captures a considerable majority of the morphological variation present in this remarkable adaptive radiation. We contextualise the scanned specimens within a discussion of their respective ecomorphological groupings and suggest possible macroevolutionary studies that could be conducted with these data. In addition, we describe a methodology to efficiently μCT-scan (on average) 23 specimens per hour, limiting scanning time and alleviating the financial cost whilst maintaining high resolution. We demonstrate the utility of this method by reconstructing 3D models of multiple bones from multiple specimens within the dataset. We hope this dataset will enable further morphological study of this fascinating system and permit wider-scale comparisons with other cichlid adaptive radiations.

Background & Summary

Cichlids are one of the most speciose families of vertebrates, with over 1000 species in the African Rift Valley alone[1,2]. Multiple, independent, adaptive radiations of these fishes have evolved in the Great Lakes of East Africa, their associated satellite water bodies, as well as their connecting riverine systems. The radiations of these fishes (Subfamily: Pseudocrenilabrinae[3]), particularly those associated with Lakes Malawi, Victoria and Tanganyika, have become powerful models for the study of macroevolutionary processes[4–10], behaviour and physiology[11–15], and have emerged more recently as models in evolutionary developmental biology[16–19].

Lake Malawi haplochromine cichlids represent a particularly speciose and phenotypically diverse adaptive radiation of lacustrine fishes. This diversity, comprising approximately 850 species of maternal mouthbrooders, is the most extensive adaptive radiation of vertebrates so far identified[1,9]. Molecular clock analyses estimate the radiation to be approximately 800 thousand years old[4], a relatively young radiation when compared to the older system of Lake Tanganyika (~10myr) which contains just 250 species[7,20]. Despite their high phenotypic diversity, genetic variation between Lake Malawi cichlids is extremely low. Whole genomic comparisons of representatives from all seven distinct ecomorphological groups within Lake Malawi, estimated an average DNA sequence divergence of just 0.19–0.27%[4] - a range comparable to that within human populations[6]. In addition, a relatively low DNA mutation rate; that alone cannot account for the estimated divergence time of Lake Malawi cichlids[4,6] and overlapping distributions of inter- and intraspecific (heterozygosity) genetic variation[4] only further complicates this enigmatic adaptive radiation.

East African cichlids, including those belonging to the Lake Malawi radiation, have recently emerged as powerful models in evolutionary developmental biology[16–19]. Evolutionary modification of embryological mechanisms drives the evolution of novel adaptations and requires genetic variation[21]. Thus, comparing the embryological development of cichlids, which have limited genetic variation, can enable us to identify specific cases where evolution has modified developmental mechanisms[17]. The diversity of feeding habits of Lake Malawi cichlids, and the ability to causally link morphological differences in craniofacial morphology to these ecological niches, has enabled integrative genetic and morphological studies examining the evolution of these traits[22–25].

[1]University of Oxford, Department of Biology, OX1 3SZ, Oxford, United Kingdom. [2]University of Oxford, Department of Earth Sciences, OX1 3AN, Oxford, United Kingdom. [3]University of Bristol, School of Biological Sciences, Bristol, BS8 1TQ, United Kingdom. [4]Bangor University, School of Natural Sciences, Bangor, LL57 2UR, United Kingdom. [5]Natural History Museum, London, SW7 5BD, United Kingdom. [6]American Museum of Natural History, New York City, NY 10024, USA. ✉e-mail: rbenson@amnh.org; berta.verdfernandez@biology.ox.ac.uk

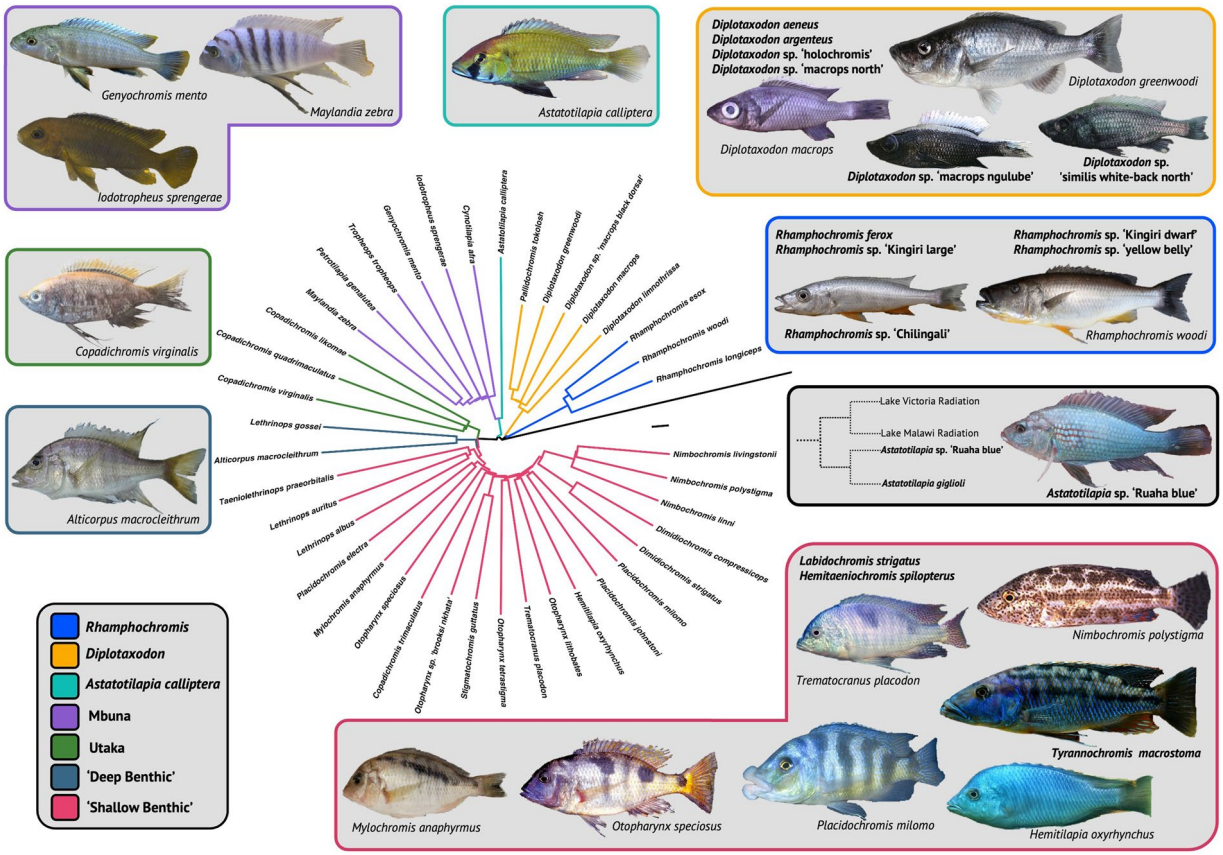

Fig. 1 A summary of the μCT-scan dataset. We were able to sample species from all seven ecomorphological groups in the Lake Malawi haplochromine radiation. The phylogenetic relationships between the majority of the species scanned is indicated and coloured according to the respective ecomorphology. The tree is a pruned version of the full (no intermediates) neighbour-joining tree published by Malinsky *et al.*[4], which is rooted to *Neolamprologous brichardi*, a non-haplochromine cichlid endemic to Lake Tanganyika[20]. Longer terminal branches reflect a higher ratio of within-species to between-species variation. A cladogram depicting the relationship between the Lake Victoria, Lake Malawi and the *Astatotilapia* species native to the Great Ruaha River is indicated in the black box. We also scanned 18 species of cichlid whose phylogenetic relationships are not resolved in the phylogeny shown. The names of these species, most of which are undescribed, are indicated in their respective ecomorphological group in bold. Pictures (not to scale) of example species belonging to each ecomorphological group are also shown. Black bar: 2×10^{-4} substitutions per base pair. Fish images used with permission from Ad Konings (*Alticorpus macrocleithrum*, *Diplotaxodon greenwoodi*, *Genyochromis mento*, *Hemitilapia oxyrhynchus*, *Iodotrophesus sprengerae*, *Nimbochromis polystigma*, *Placidochromis milomo* and *Trematocranus placodon*), George F. Turner (*Astatotilapia sp.* 'Ruaha blue'[183], *Diplotaxodon macrops*, *Mylochromis anaphyrmus*, *Otopharynx speciosus* and *Rhamphochromis woodi*), Martin J. Genner (*Diplotaxodon sp.* 'similis white-back north', *Diplotaxodon sp.* 'macrops ngulube' and *Rhamphochromis sp.* 'Chilingali'), Hannes Svardal (*Copadichromis virginalis*) and Callum V. Bucklow (*Maylandia zebra*). Fish images are not to scale.

More recent studies have expanded the scope beyond craniofacial phenotypes, including pigmentation patterning[26–28]; body and fin shape[19,29] and axial elongation[18]. In parallel, aided by developments in whole-genome sequencing technologies[6], it has been possible to considerably improve our understanding of the phylogenetic relationships among Lake Malawi cichlids[4,9,30,31]. Previously intractable macroevolutionary studies, such as the convergent evolution of hypertrophied lips[32] can now take advantage of relatively robust phylogenies based on whole-genome sequences. Moreover, there are now opportunities to use this new phylogenetic information to focus on the evolution of other traits, such as the axial and appendicular skeleton, that is of key importance in teleost diversification[33,34]. However, a whole-body μCT-scan dataset of Lake Malawi cichlid fishes that captures the skeletal diversity present in the adaptive radiation has not yet been described.

Here we present a new database of high-resolution X-ray micro-computed tomography (μCT) scans of Lake Malawi cichlids, providing 3D data on skeletal morphology for the whole body of 56 species across 26 genera. In total these data comprise 116 individuals (56 species, 26 genera) from seven recognized ecomorphological groupings[4] (Fig. 1, Table 1), contrasting in multiple aspects of morphology, size, behaviour, and habitat preference. We demonstrate the resolution and utility of our dataset by illustrating 3D whole-body renderings of several species, and of several skeletal regions of interest. Our dataset now joins two other East African adaptive radiation datasets, including the recent haplochromine Lake Victoria library[35] and extensive μCT-scan

Ecomorphology	Genera Sampled	Genera Sampled (%)	Species Sampled	Species Sampled (%)
Astatotilapia (calliptera)	1 of 1	100%	3*	N/A
Deep Benthic	2 of 5	40%	3 (5[†]) of 150	2.00% (3.33%)
Diplotaxodon	2 of 2[‡]	100%	9 of 19	47.37%
Mbuna	7 of 12	58.33%	7 of 328	2.13%
Rhamphochromis	1 of 1	100%	10 of 14	71.43%
Shallow Benthic	12 of 32	37.50%	20 of 287	6.97%
Utaka	1 of 1	100%	4[§]of 55	7.27%
Total	**26 of 54**	**48.15%**	**56 of 856**	**6.54%**

Table 1. Genera and species represented within the dataset. The number of genera and species for each ecomorphological group are the same as those used in Malinsky *et al.*[4]. **Astatotilapia calliptera*, *Astatotilapia* sp. 'Ruaha blue' and *Astatotilapia gigliolli*. [†]If considering the addition of *Lethrinops albus* and *Lethrinops auritus* that cluster within the 'shallow benthics'. [‡]Includes *Pallidochromis*. [§]Includes *Copadichromis trimaculatus* which clusters within the shallow benthics in the phylogeny depicted in Fig. 1.

dataset of Lake Tanganyika cichlid fishes[7], permitting the examination of macroevolutionary patterns common to adaptive radiations[36,37] and the macroevolutionary dynamics of convergent evolution. We also describe a methodology to efficiently μCT-scan multiple specimens simultaneously; reducing scanning time and financial cost, whilst maintaining scan quality and demonstrate the utility of this method by reconstructing 3D-models of multiple bones from multiple specimens within our dataset. We hope the availability of these data will inspire others to address some of the many questions still left to understand this remarkable adaptive radiation, permit wider-scale comparisons with other cichlid adaptive radiations, and set a precedent to make whole-body μCT scans the automatic standard for any sampling efforts involving cichlids.

Methods

Sample Selection. There are an estimated 850 species of Lake Malawi cichlid fishes[4]. Many of which have not been described, preserved in museum collections or are available on phylogenies based on whole genome evidence. Therefore, to maximise the utility and morphological variation captured by our dataset, we focused on species present in published phylogenies[4,9,24], and sought to include as many genera as possible. Moreover, we prioritised scanning the type species for genera, and avoided inclusion of species which already had whole body scans available on Morphosource. We were able to sample 26 of the 53 (49.05%) endemic genera listed on the curated species list on malawi.si[38], or 48.15% of the 54 genera previously cited[4] (see Table 1). Our specimens were sourced from the collections at the Natural History Museum in London (NHMUK), from the School of Biological Sciences of the University of Bristol (Martin J. Genner) and from the School of Natural Sciences of Bangor University (George F. Turner). In total we scanned 116 specimens from 56 species (Supplementary Table S1). Of these, 99 were wild-caught and 17 were laboratory-reared. Laboratory-reared specimens included *Astatotilapia calliptera* (Mbaka River, n=10), *Maylandia zebra* (Boadzulu island, n=5) and *Rhamphochromis* sp. 'Chilingali' (n=2), all of which died naturally or were compassionately euthanised by anaesthetic overdose [Schedule 1; Animals (Scientific Procedures) Act 1986]. All animal work was conducted following approval by the Departmental Animal Welfare Ethical Review Body (AWERB) for the Department of Biology at the University of Oxford.

μCT-Scanning. A flowchart describing all the necessary decisions and required processing steps is provided in Fig. 2. Since there was already a large collection of specimens present at the Natural History Museum in London (NHMUK) and in the extensive research collections of Martin J Genner (School of Biological Sciences, University of Bristol) and George F Turner (School of Natural Sciences, Bangor University) we decided to take advantage of the scanners present in the CT facility of NHMUK and at the XTM Facility based in the Paleobiology Research Group at the University of Bristol, respectively. Of the total 116 individuals scanned (56 species), 56 specimens (28 species) were scanned at the NHMUK Imaging and Analysis Centre and 60 specimens (28 species) were scanned at the XTM Facility at the University of Bristol.

Scanning Arrangement. To maximise the utility of our time and the number of species scanned, multiple specimens were scanned in each individual scan (Fig. 3). Each batch of specimens was fit to the width of the scan field of view to maximise resolution, and multiple scans were conducted along a the vertical axis in order to scan the full body length of each specimen. Therefore, batches of similarly sized fish were packaged together prior to scanning to ensure multiple individuals could be simultaneously captured within the field of view during scanning. Batch sizes varied between two and five specimens, with the number of each batch ultimately dependent upon the overall size of the specimens within the batch. Of the 32 batches scanned: 20 were comprised of four specimens; nine of three specimens, and two and one batch(es) of one and five specimens, respectively. Since multiple individuals of different species were often scanned together (Fig. 3A,B) it was critical that individuals of the same species could be readily identified. Therefore, unique, low density objects such as plastic bricks, pipette tips and rubber bands were placed in physical proximity to each specimen, to act as recognisable markers (Fig. 3C) which would readily resolve in the reconstructed image stacks (see Post-Scanning Processing). These objects were attached to each individual specimen-containing bag, and the specimens were bundled together,

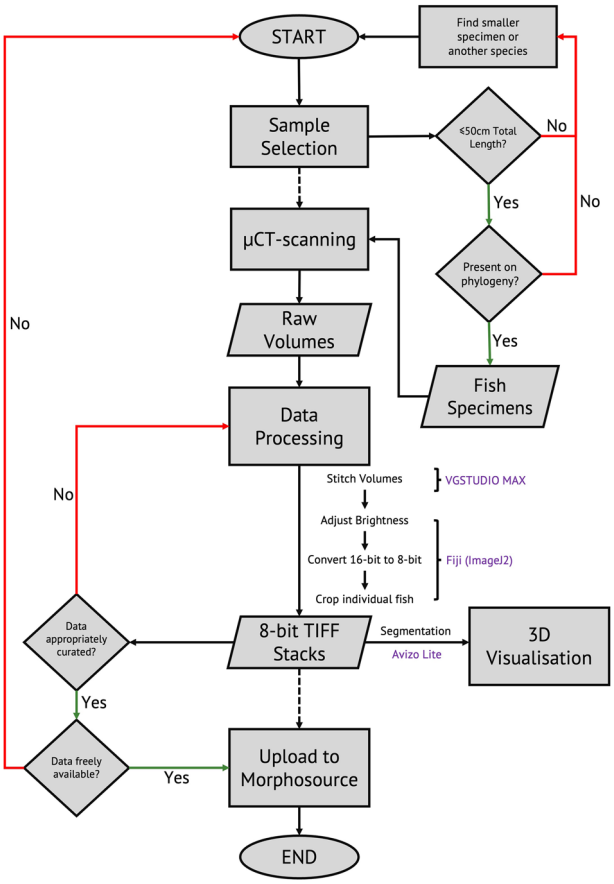

Fig. 2 Flowchart of μCT-scanning, image processing and segmentation methodology. The flowchart outlines the necessary decisions that were made during collation of the described μCT scan dataset. Rectangles represent processes; parallelograms represent inputs or outputs; diamonds represent decisions. It is sufficiently generalised that it can be reused for future data collection. We were focused on generating data for a specific macroevolutionary study, so we restricted the dataset to species with known phylogenetic placements but this is not strictly necessary. Software associated with data processing steps are indicated in purple. Further information about processing and segmentation is provided in the Usage Notes.

ideally ensuring that the objects faced outwards (Fig. 3D–F). Specimens were tightly packed into plastic containers, sealed with tape, and allowed to rest upright (head-up) for at least ten minutes so the contents could settle to prevent movement during scanning (Fig. 3G–K). We were able to scan, on average, 23 specimens per hour at maximal efficiency, an efficiency that was primarily the result of having two people per scanning visit (one scanning and one packing). The scanning rate could be further increased by packaging specimens in advance of the scanning so that subsequent batches can be scanned with no delay.

Scanning Procedure. Prior to scanning, a visual inspection of the specimens was made following X-ray exposure to check for internal damage (such as damage to the vertebral column). If present, and possible, specimens were switched for another specimen of the same collection. To maximise scan resolution, each batch of fish was scanned using the full width of the scanner field of view. This necessitates that multiple, overlapping scans were conducted along the vertical axis of the scanner (Z-axis) in order to capture the full body length of each fish. The overlapping scans were subsequently stitched together in the processing stage using the software, VGStudio Max 3.2.5 64-bit (see below). The fish scanned ranged in standard length of 3.8cm to 33cm, which meant that scanning parameters varied between batches. The number of projections generated range from 901 to 2001. Exposure times varied between 250 and 500 seconds, with a median of 354 seconds. Similarly, power varied between scans, ranging between 12.480 and 37.995 watts (W) (mode 37.440W). All scanning parameters, for each batch conducted, as well as for each individual scan can be found in the metadata supplied in Supplementary Table S1.

Post-Scanning Processing. All processing and segmentation was conducted on a machine specifically built for image analysis, with the following specifications: 2 x Intel® Xeon® CPU-ES-2640 @2.60GHz, 2601MHz, 8 Core(s) processors, 128GB of dedicated DDR3 RAM running on Microsoft Windows 10 Pro (Build Number: 10.0.19045). Raw, isometric volumes generated from the CT-scanning were imported into VGStudio Max 3.2.5 64-bit and anterior and posterior halves were subsequently stitched together by defining overlapping regions of interest in both the anterior, middle (if applicable) and posterior volumes. 16-bit tiff stacks were exported from

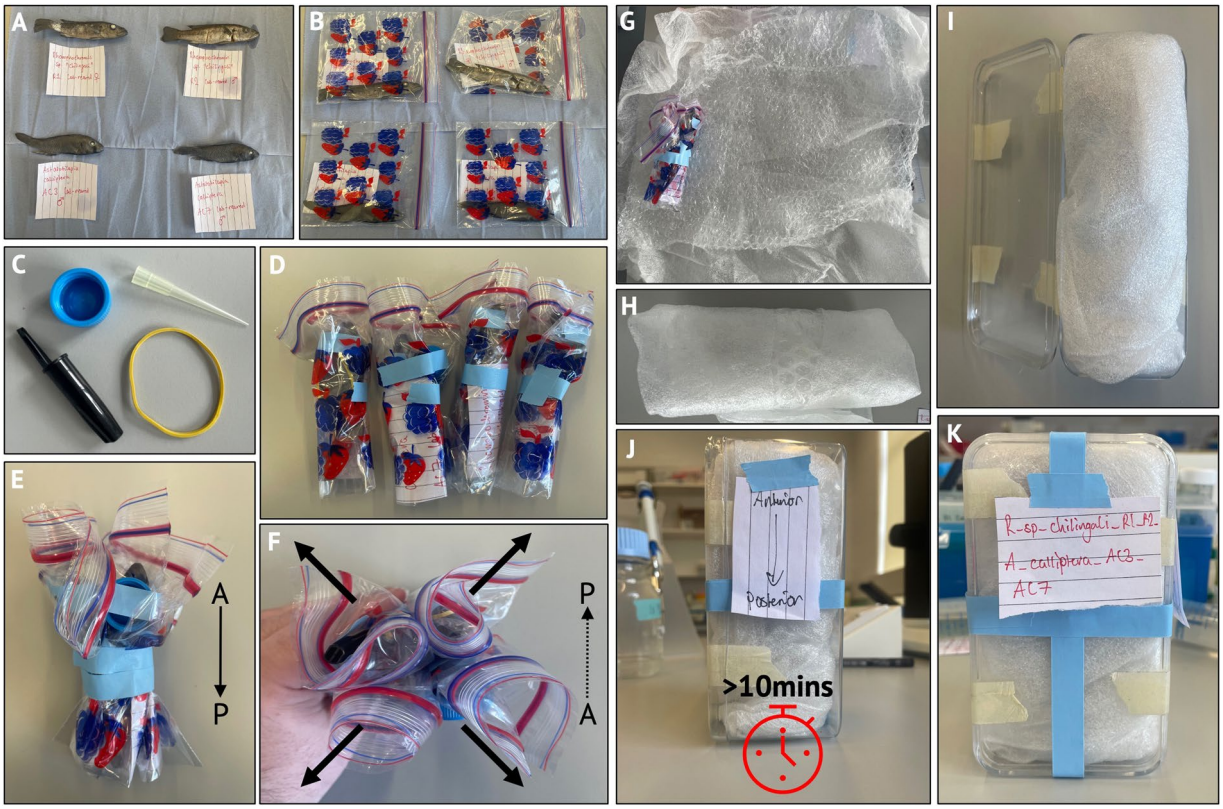

Fig. 3 Specimen preparation for μCT-scanning. Multiple fish were scanned at the same time (**A**). Individual fish were labelled and placed in separate plastic bags so they could be correctly identified and stored after imaging (**B**). Unique objects (**C**) that would be readily identifiable following μCT-scanning were attached to the outside of these bags, ideally close to the heads, positioned outwards (**F**, arrows), and bundled together with tape (**D**–**F**) all with the same orientation (head-up). Bundles were then wrapped in bubble wrap and other packaging material (**G**,**H**) and tightly sealed inside a plastic container, again head-up (**I**). Containers were left for at least ten minutes to settle to prevent movement during scanning (**J**) and an additional label was placed on the container to permit future identification if multiple batches were prepared together (**K**).

VGStudio Max 3.2.5 64-bit and imported into FIJI[39], a GUI for ImageJ[40]. In FIJI, individual fish were cropped out of the 16-bit stacks, which were identifiable due to the unique objects associated with each individual (see above). The brightness was adjusted by extending the distribution of pixel values to remove 0 values, and the tiff stacks were converted into 8-bit to decrease file size. Total stack file size was further decreased by removing images at the beginning and end of the exported tiff stacks that did not contain readily identifiable bone or tissue.

Segmentation and Visualisation. Reconstructed image stacks were imported into Avizo Lite (v9.3.0), a proprietary software developed by Thermo Fisher Scientific and generated either a full body volume render using the volume generation tool or manually rendered 3D models of the whole body following a rough manual segmentation of the whole body. Optimal threshold values were manually chosen based on the volume or 3D rendering and all whole-body 3D models were smoothed with a smoothing factor of 2.5. Surfaces from 3D whole-body renderings were exported from AvizoLite as Polygon File Format (.ply) files and imported into MeshLab for visualisation and manipulation. See the Usage Notes for further notes on segmenting the μCT-scans in the dataset.

Data Records

All data is freely avaliable and has been deposited into a dedicated project on Morphosource[41], which includes cropped 8-bit tiff stacks of 116 specimens[42–157], representing 56 species. Coverage of the Lake Malawi radiation by our dataset[41] is outlined in Table 1. The names of all 56 species present in the dataset, including their respective ecomorphological group, is listed in Fig. 1. Full specimen details, including scanning parameters, can be found in Supplementary Table S1. Detailed discussion of the species in the dataset, including suggestions for possible macroevolutionary and systematic studies can be found in the Usage Notes (see below).

Technical Validation

Example whole-body, scaled, 3D renderings of representatives from each ecomorphological group can be found in Fig. 4 and for every specimen (mix of volume and model renders) in the dataset in the Supplementary Material. To demonstrate the quality of 3D-models that can be segmented from specimens in our dataset we manually segmented multiple bones, including the dentary, premaxilla, lower pharyngeal jaw and multiple

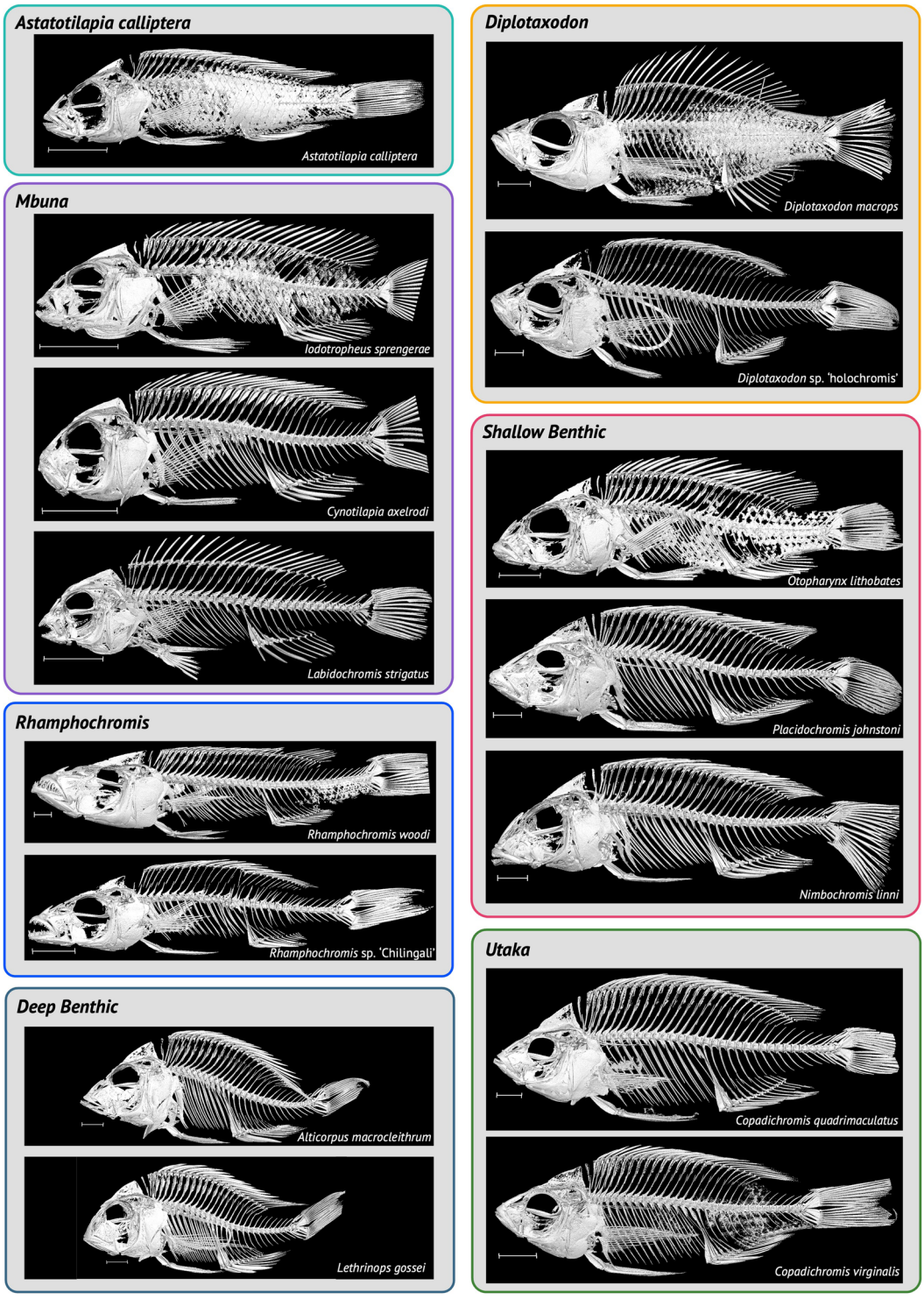

Fig. 4 Whole-body 3D models of select specimens from the dataset. Specimens are arranged according to the ecomorphological group they belong to. Species names are indicated. The ring structure in *Diplotaxodon* sp. 'holochromis' and *Lethrinops gossei* is a rubber band used for identification purposes. Scale for all images is shown as 1cm. See Supplementary Table S1 for details of the specimens used.

vertebral types in several species discussed below (see Usage Notes). This included: the 'generalist' *Astatotilapia calliptera*; the 'mbuna' and lepidophage (scale-eater), *Genyochromis mento*; the 'shallow benthic' and snail crusher, *Trematocranus placodon* (Fig. 5); the pelagic piscivores, *Rhamphochromis esox* and *Pallidochromis tokolosh* and the zooplanktivorous (utaka), *Copadichromis trimaculatus* (Fig. 6). Lower pharyngeal jaws that are highly variable among species of Lake Malawi cichlids[25] were particularly well resolved. For example, newly erupting teeth were visible on the relatively large, and dense, lower pharyngeal jaw of *Trematocranus placodon*

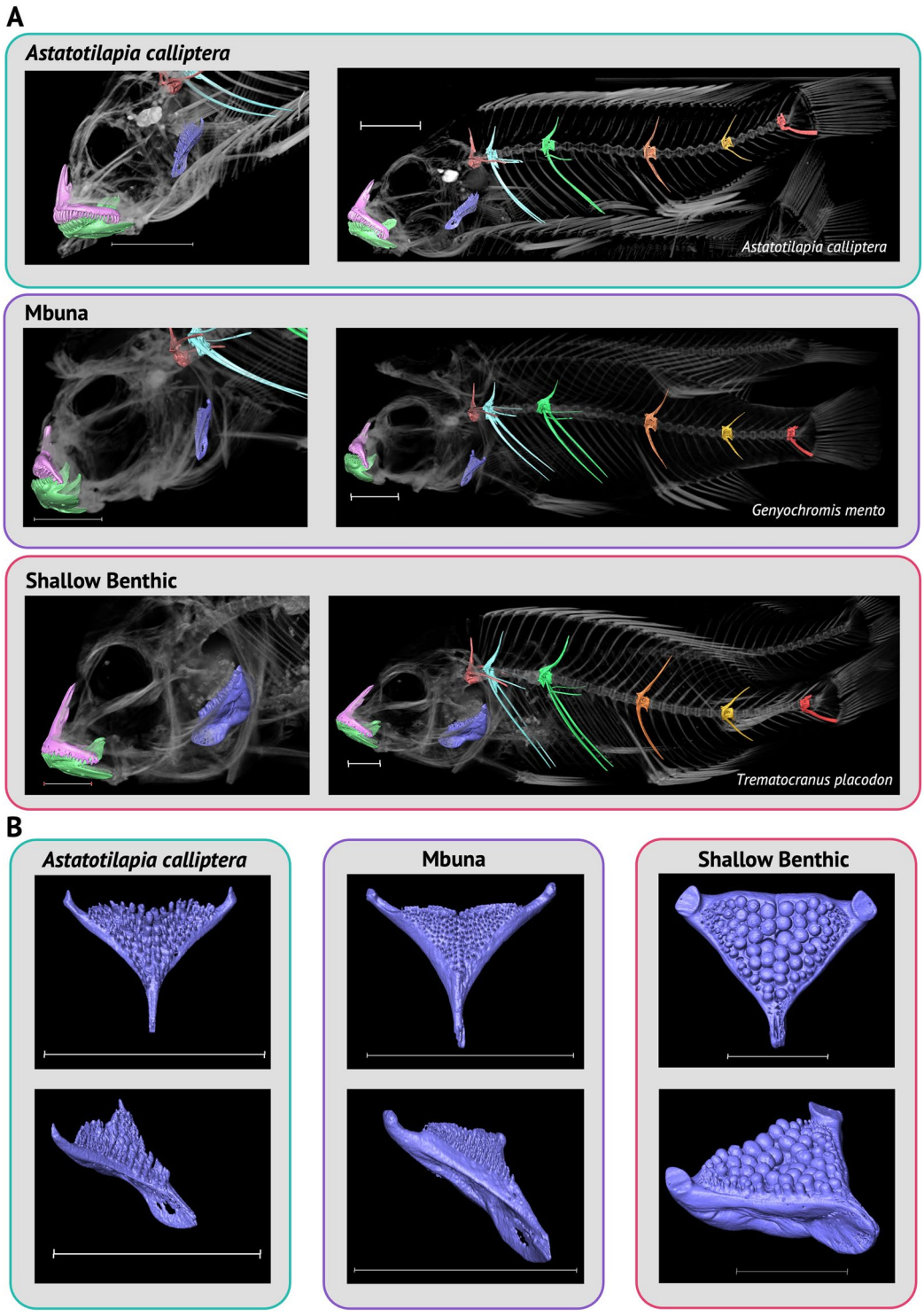

Fig. 5 Segmented Bones from *Astatotilapia calliptera*, *Genyochromis mento* (mbuna) and *Trematocranus placodon* (shallow benthic). (**A**, left) A close up, lateral view of the head of each species (species name indicated on right), showing the dentary (green), premaxilla (pink) and lower pharyngeal jaw (purple) positioned within a volume render of the head. (**A**, right) A whole body lateral view showing the aforementioned jaw bones, as well as the first non-rib-bearing vertebra (orange), the first rib-bearing (precaudal, PC) vertebrae (light blue), PC8 (green), non-rib bearing (caudal, CV), CV3 (orange), CV10 (gold) and the pre-urostyle vertebrae (red). (**B**) Anterior (top) and anterolateral (bottom) view of the lower pharyngeal jaws for each species in (A). Scale for all images is 1cm. See Supplementary Table S1 for details of the specimens used. 3D models for all segmented bones can be found in the Supplementary Material.

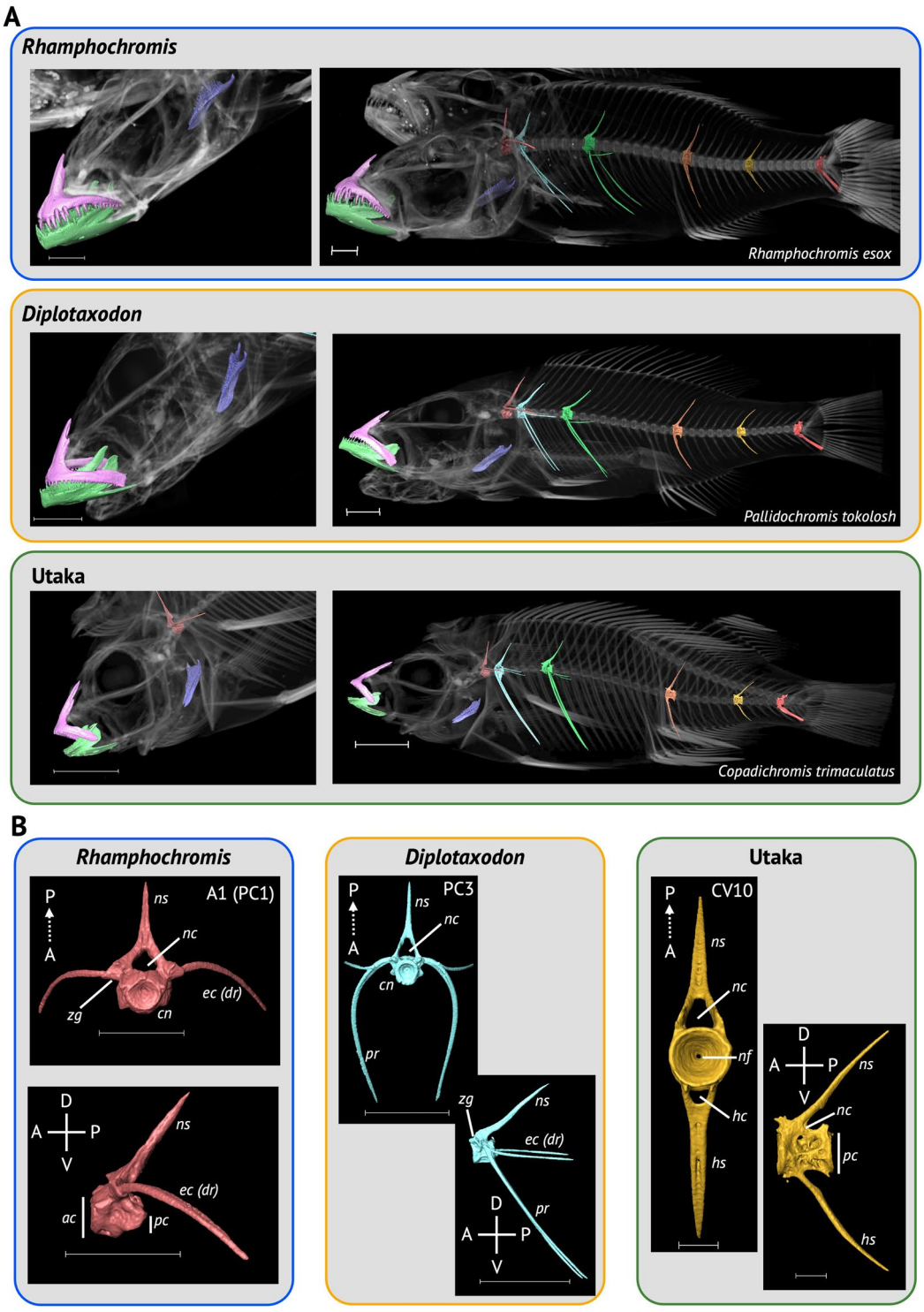

Fig. 6 Segmented Bones from *Rhamphochromis esox* (*Rhamphochromis*), *Pallidochromis tokolosh* (*Diplotaxodon*) and *Copadichromis trimaculatus* (Utaka). (**A**) Left, lateral view of the head of each species, showing the dentary (green), premaxilla (pink) and lower pharyngeal jaw (purple). Right, whole body lateral views showing aforementioned jaw bones, as well as the first non-rib-bearing vertebrae (orange), the first rib-bearing (precaudal, PC) vertebrae (light blue), PC8 (green), non-rib bearing (caudal, CV), CV3 (orange), CV10 (gold) and the pre-urostyle vertebrae (red). (**B**) Images of select vertebrae (indicated) from each species shown in (A). Axes are indicated (A, anterior; P, posterior; D, dorsal; V, ventral). Vertebral models are labelled (*ac*, anterior cone span; *cn*, centrum; *ec* (*dr*), epicentrals (dorsal ribs); *hc*, haemal canal; *hs*, haemal spine; *nc*, neural canal; *nf*, neural foramen; *ns*, neural spine; *pc*, posterior cone span; *pr*, pleural ribs; *zg*, zygapophyses). Scale for all images is 1cm, besides CV10 for Utaka which is 0.1cm. See Supplementary Table S1 for details of the specimens used. 3D models for all segmented bones can be found in the supplementary material.

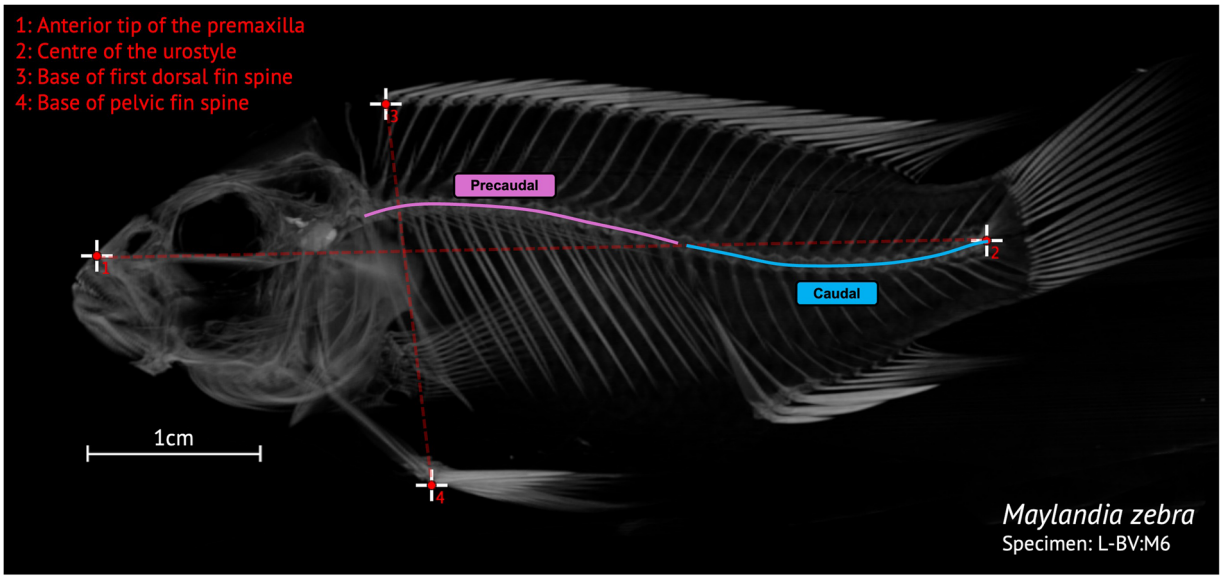

Fig. 7 Example specimen volume rendering with body aspect ratio landmarks. The number of precaudal (pink) and caudal vertebrae (blue), including the urostyle, the total number of vertebrae (sum of the precaudal and caudal vertebrae, including the urostyle) and the body aspect ratio was estimated for 113 of the 116 specimens in the dataset. The landmarks used to estimate the body aspect ratio are indicated in the figure on an example specimen (*Maylandia zebra*, L-BV:M6, see Supplementary Table S1). Landmarks 1 and 2 were used to calculate the length, and landmarks 3 and 4 the width by calculating the length of a straight line between the x,y coordinates. Landmark 1, anterior tip of the premaxilla; Landmark 2, centre of the urostyle; Landmark 3, Base of the first dorsal fin spine; Landmark 4, base of the pelvic fin spine.

(Fig. 5B). Similarly, renderings of multiple vertebral types (Figs. 5–6) were also of good quality. The zygapophyses and fine structure of the vertebral centra, sometimes including the neural foramen, were also well resolved. All 3D-renderings of these bones can be found in the Supplementary Materials as downloadable .ply files.

In addition, to demonstrate that our data will also be useful for the collection of meristic data, we also counted the number of precaudal, caudal and total number of vertebrae (including the urostyle), as well as an estimation of the body aspect ratio for 113 of the 116 specimens in Supplementary Table S2. The three remaining specimens were deformed or poorly rendered and vertebral counts or body aspect ratios could not be taken. Precaudal, caudal and total vertebral counts as all as an estimation of the body aspect ratio were estimated from 2D lateral images of either a volume rendering or 3D-model of the whole body of the specimen (Fig. 7). Lateral images of a volume or 3D whole body rendering can be found in the Supplementary Material for every specimen in the dataset. Length landmarks were placed on the anterior tip of the premaxilla and in the centre of the urostyle and width landmarks were placed at the base of the dorsal fin spine and pelvic fin spine, respectively (see Fig. 7). We note that these data could also be collected with the use of 2D radiographs. However, μCT-scanning adds the additional possibility of also generating 3D models which can be the basis of studies that consider and compare overall, complex bone shape that would otherwise be missed (3D geometric morphometrics), or undetectable with the use of 2D radiographs. Therefore, the μCT-scans in our dataset provide can both provide well resolved models for geometric morphometric studies comparing complex bone shape between Lake Malawi cichlids as well as a useful source of meristic data for macroevolutionary studies. We have included suggestions of possible macroevolutionary studies that could be conducted with these data in the Usage Notes.

Usage Notes

***Diplotaxodon* and *Rhamphochromis*.** Nine species of the *Diplotaxodon* group (47%; Table 1), including the type species *Diplotaxodon argenteus* (n=1) and *Pallidochromis tokolosh* (n=2) are present within our dataset[41]. In addition, we sampled 10 species of the *Rhamphochromis* genus (71%; Table 1), including the type species *Rhamphochromis longiceps* (n=2) and the remarkably large *Rhamphochromis woodi* (n=2, see below), that are endemic to Lake Malawi. We were also able to sample two sympatric species from the crater lake, Lake Kingiri, *Rhamphochromis* sp. 'Kingiri dwarf' (n=2) and *Rhamphochromis* sp. 'Kingiri large' (n=2), as well as *Rhamphochromis* sp. 'Chilingali' (n=4) from the satellite, Lake Chilingali (Fig. 4), which is now presumed extinct in the wild[158].

The *Diplotaxodon* and *Rhamphochromis* groups are two reciprocally monophyletic diverging lineages of Lake Malawi cichlids[4] that have adapted to the pelagic-limnetic zone of Lake Malawi[159]. The majority of species in the groups are piscivorous, although several species, including *Diplotaxodon limnothrissa* (n=2) are predominantly zooplanktivorous[160]. Large-bodied *Rhamphochromis* primarily feed on Lake Malawi sardines (usipa; *Engraulicypris sardella*) and endemic cichlids (e.g. utaka). Members of *Diplotaxodon* and *Rhamphochromis* are among the deepest-living of all Lake Malawi cichlids, with representatives of both being caught at depths exceeding 200 metres - the 'twilight zone' where light is almost completely absent[159]. Species within the *Diplotaxodon*

macrops complex, which is represented in the scanned samples by *Diplotaxodon macrops* (n=1) (Fig. 4), *Diplotaxodon* sp. 'macrops north' (n=2), *Diplotaxodon* sp. 'macrops black dorsal' (n=2) and *Diplotaxodon* sp. 'macrops ngulube' (n=2), have been found between 100 and 220m, a depth similarly reported to be occupied by *Rhamphochromis* during the day[161].

Morphological comparisons of *Diplotaxodon* and *Rhamphochromis* with Lake Malawi cichlids from other habitats could provide valuable insights into convergent adaptation of traits enabling occupation of pelagic niches. Divergence along depth gradients is associated with the evolution of reproductive isolation in many marine and freshwater species groups, likely a consequence of the strong selective pressures associated with deeper water, such as the absence of sunlight, greater hydrostatic pressure, and reduced levels of dissolved oxygen[162,163]. Morphological comparisons of *Diplotaxodon* and *Rhamphochromis*, against closely related littoral species, could be a powerful model for the study of evolution of convergent phenotypes necessary for adapting to pelagic environments. Body elongation, supported by increased vertebral counts, is a adaptive trait common in teleosts adapted to pelagic (and piscivorous) niches[164], including in *Rhamphochromis*[165]. Moreover, the evolutionary modification of vertebral morphology has been linked to changing swimming kinematics, body shape and habitat preference[166], including adapting to pelagic environments[34]. Given the remarkable depth preference and rapid divergence of the *Diplotaxodon* and *Rhamphochromis* lineages, a study of body shape, as well as vertebral count and shape could better determine the rate at which these phenotypes can become fixed and provide further insights into the role these morphological adaptations play along the benthic-pelagic speciation axis[162,163].

Remarkable size variation is present within the *Rhamphochromis* genus. *Rhamphochromis woodi* is considered to be one of the largest Lake Malawi cichlids, measuring a standard length (SL) of up to 40 cm[167]. In contrast, the smallest known member of *Rhamphochromis*, *Rhamphochromis sp. 'Kingiri dwarf'*, endemic to the crater lake Kingiri, do not exceed 7.5 cm SL in the wild[158] – a 5.33x length difference just within the same genus. Similarly, wild caught *Rhamphochromis* sp. 'Chilingali' are also small bodied, with maximum observed standard length of 10.6 cm[8], which makes them relatively amenable to laboratory study. Its elongate body, supported by relatively high vertebral counts, has made it a useful model in evolutionary developmental biology[17], particularly for the study of somitogenesis[18], the developmental process that gives rise to the vertebral precursors. Nonetheless, given the exceptional size difference in the genus *Rhamphochromis*, our dataset represents a potentially valuable resource for the study of the evolution of allometric scaling, which has not been well studied in cichlids[168].

Shallow Benthic. The shallow benthic species group is extremely speciose, comprising hundreds of species that exhibit remarkable morphological[4,169] diversity. The majority of shallow benthic species inhabit relatively shallow inshore habitats of Lake Malawi, such as the sand or mud lake floor, or sand-rock transitional zones. Our dataset[41] includes 20 shallow benthic species in 12 genera (Table 1), including several large, ambush predators, as well as a collection of trophic specialists. For a complete list of shallow benthics in our dataset[41] see Supplementary Table S1.

Large ambush predators represented in the dataset[41] include *Dimidochromis strigatus* (n=1), *Dimidochromis compressiceps* (n=1), *Tyrannochromis macrostoma* (n=1), *Nimbochromis livingstonii* (n=1) and *Nimbochromis polystigma* (n=2). *Dimidochromis compressiceps* has a generalist piscivore lifestyle, occupying the reed-beds of the Lake. *Nimbochromis livingstonii* and *N. polystigma* are both considered to be 'sleeper[s]' (Chichewa: "kaligono"), which bury themselves within the sandy substrate and snatch unsuspecting prey attracted by the disturbed sediment[169]. Another member of *Nimbochromis*, *Nimbochromis linni* (n=1) has a characteristic downward-projecting snout (Fig. 4), enabling it to extract prey from rock crevices[169,170].

We sampled several shallow-benthic predators, including *Otopharynx speciosus* (n=2), one of the few piscivores within *Otopharynx*. Males of this species have been encountered at depths exceeding 25m[169], suggesting tolerance of relatively deep water, and suggesting the species may have morphological adaptations enabling occupation of deep-water niches similar to *Rhamphochromis* and *Diplotaxodon*. Of the approximately 20 species of *Otopharynx*[171] we were able to sample an additional three species: *Otopharynx lithobates* (n=3, including the holotype NHMUK 1974.7.5.1); *Otopharynx tetrastigma* (n=2); and the undescribed *Otopharynx* sp. "brooksi nkhata" (n=1). We also sampled several specialised trophic specialists including the molluscivores *Mylochromis anaphyrmus* (n=1) and *Trematocranus placodon* (n=1) and the invertebrate picker *Placidochromis johnstoni* (n=1, Fig. 4). The diet of *T. placodon* predominately comprises the gastropods *Bulinus nyassanus* and *Melanoides tuberculata*[172]. Enlarged sensory pores and lateral lines form a sonar-like detection system that allows *T. placodon* to sense the movement of these prey within the sediment. Curiously, this strategy and associated morphological characteristics are also associated with *Aulonocara* and *Lethrinops*, both 'deep benthics', suggesting convergent evolution of lateral line phenotypes[9]. The specimens in our dataset[41] may enable morphological comparisons to further investigate differences in sensory pore characteristics among species.

'Rock-dwelling' *Mbuna*. The mbuna group dominate the rocky shores of Lake Malawi, and are used as a model system for the study of rapid speciation and adaptive radiation[25,173,174]. Similar to the shallow-benthics, there are hundreds of species, many of which are undescribed[169,174]. We aimed to maximise our coverage of the phenotypic diversity in the group by sampling multiple genera, which are largely differentiated on the basis of head, jaw and tooth morphology[174]. Our dataset[41] includes 7 species (15 individuals) of mbuna, covering 7 of the 14 described mbuna genera (Table 1).

Cynotilapia can be distinguished from other genera by the presence of unicuspid (conical) teeth[169,175,176] and is represented in our dataset by *Cynotilapia axelrodi* (n=1, Fig. 4). This is a genus of typically planktivorous species[169] and their relatively simple dentition may reflect this lifestyle[177]. By contrast, *Maylandia* (*Metriaclima*[178]), represented by *Maylandia zebra* (n=5), has closely arranged bicuspid teeth, that is uses for pulling and scraping

loose Aufwuchs (periphyton) attached to the rocks found in their preferred preferred rocky habitats[175,179]. *Tropheops* and *Iodotropheus*, represented by *Tropheops tropheops* (n=2) and *Iodotropheus sprengerae* (n=2), also have closely packed bicuspid teeth, that they use to feed on epilithic algae which they pluck with sideways, upwards head jerks, a behaviour likely supported by *Tropheops*' characteristic steeply sloped vomer (71-96°)[169]. Members of *Petrotilapia*, represented by *Petrotilapia genalutea* (n=1) have a mixed combination of tricupsid and unicupsid teeth that they use to comb loose peripyton from rock surfaces[180]. A further represented mbuna genus is the monotypic *Genyochromis*, represented by *Genyochromis mento* (n=2). Like the majority of mbuna, *G. mento* has prominent outer bicupsid teeth that are supported by smaller inner tricupsid teeth[169,175]. In contrast to most other mbuna, however, *G. mento* is a highly specialised feeder, a lepidophage (scale-eater), that targets the the caudal and anal fins of other cichlids in rocky habitats[169,175,181]. The preferred striking side of *G. mento* significantly correlates with left-right asymmetry of the dentary, with right and left-leaning individuals preferring to strike the corresponding side, respectively, of their prey. Interestingly, however, a comparison of their jaw laterality with *Perissodus microlepis*, a lepidophage endemic to Lake Tanganyika[20], showed that laterality in *G. mento* is weaker than in *P. microlepis* – likely a result of phylogenetic constraint from their shorter evolutionary history and their herbivorous ancestors[181].

The craniofacial bones commonly studied in mbuna, such as the dentary, premaxilla, pharyngeal jaws, as well as their associated teeth, can be segmented from specimens in the dataset (see *G. mento*, Fig. 5) and will be helpful for geometric morphometric analyses focused on examining craniofacial shape differences between mbuna species. Future sampling should focus on the seven remaining genera not sampled in our dataset[41]: *Abactochromis*, *Chindongo*, *Cyathochromis*, *Gepyrochromis*, *Labeotropheus*, *Melanochromis* and *Psuedotropheus*.

Astatotilapia calliptera and Ruaha Catchment. *Astatotilapia* is polyphyletic and current members of the genus are widespread across East and North Africa[6,182,183]. Only one species of *Astatotilapia* is native to Lake Malawi, *Astatotilapia calliptera*, which is also found in East African rivers flowing eastward to the Indian Ocean, from the Rovuma River in the north, to the Save River in the south. Given the wide distribution of the species, it is perhaps unsurprising that intraspecific genetic variation within the species is comparable to that of the whole Lake Malawi radiation[4,6]. Despite their wide distribution and relatively large intraspecific genetic variation, they phylogenetically cluster within the Lake Malawi radiation (Fig. 1), forming a sister clade to the mbuna, with which they share an excess of alleles[4]. This pattern, alongside a perceived riverine 'generalist' lifestyle, has led to the hypothesis that either Lake Malawi cichlids radiated from an *A. calliptera-like* ancestor or that *A. calliptera* is the sympatric ancestor of all Lake Malawi cichlids[4,6,169,183].

Given the importance of *A. calliptera* in the Lake Malawi radiation, we sampled multiple individuals from multiple populations. We scanned nine laboratory-reared individuals from the Mbaka river population, which flows into the northern end of Lake Malawi[184]. We also scanned individuals from Lake Chilwa (an endorheic lake south-east of Lake Malawi[185]; n=2), Lake 'Misoko', presumably Lake Masoko (a crater lake north of Lake Malawi[184], n=2), and wild-caught individuals from the main body of Lake Malawi (n=2). Populations of *A. calliptera* differ in life history strategies[186] and are also undergoing sympatric speciation along a depth gradient in at least one location (Lake Masoko)[8], where littoral and benthic *A. calliptera* ecomorphs have diverged in multiple characteristics, including body shape and trophic specialism, in approximately 1000 years[8]. Therefore, it is possible that morphological evaluations of more populations of *A. calliptera* will reveal further diversity, potentially providing greater insight into the role it has taken in generating the wider Lake Malawi haplochromine radiation and we would suggest increasing the sampling of *A. calliptera* populations to further investigate this.

A key part of macroevolutionary studies is the estimation of ancestral state of traits based on the morphology of their descendants[187]. This necessitates a comprehensive understanding of trait diversity across taxa, where such data is critical for the construction of models of morphological evolution, including estimating rates of phenotypic evolution. Since the genetic diversity of the Lake Malawi radiation was possibly seeded by multiple riverine species[5], we sought to add specimens to the dataset that could enable the morphological reconstruction of the common ancestor of the Lake Malawi radiation. Therefore, we sampled two additional species of *Astatotilapia*. These included *Astatotilapia gigliolli* (n=2) and *Astatotilapia* sp. 'Ruaha blue' (n=2), native to the Great Ruaha River[182,183]. Construction of a mtDNA-based phylogeny initially placed *Astatotilapia* sp. 'Ruaha blue' as a sister taxa to the Lake Malawi radiation[182]. However, a phylogeny based on variation within whole-genome sequences has shown *A. gigliolli* and *A.* sp. 'Ruaha blue', sister taxa, form a sister clade with both the Lake Malawi and Lake Victoria radiations (see Fig. 1). This topology is likely the result of an ancestral hybridisation event with the ancestors of both lineages prior to their respective adaptive radiations[5]. Therefore, the addition of species from the Ruaha catchment, may therefore enable a more robust estimation of the ancestral phenotype of Lake Malawi cichlids.

Deep Benthic and '_Utaka_'. We sampled deep-water benthic species from two genera; *Alticorpus* and *Lethrinops*[9,188] (Table 1). *Alticorpus* is characterised by the presence of greatly enlarged cranial sensory openings and lateral line canals used to detect prey in the sediment. Deep-water benthic species are found below 50m, a 'twilight' zone with very little visible light. *Alticorpus macrocleithrum* (n=3) is found between 75m and 125m, with abundance peaking above 100m[189], a depth similarly occupied by deep-water Lethrinops[190], including *Lethrinops gossei* (n=1). Several species of *Lethrinops*, however, inhabit shallower water[4,169]. We sampled two species of shallow water *Lethrinops*, including *Lethrinops auritus* (n=2), and *Lethrinops albus* (n=2), both of which phylogenetically cluster within the 'shallow benthic' lineage (Fig. 1).

Our dataset[41] also contains four species of zooplankton-feeding, shoaling cichlids which are commonly referred to as 'utaka'. Utaka is primarily made up of species belonging to *Copadichromis*[191], with a small number of species also belonging to *Mchenga* and *Nyassachromis*[192]. However, their placement within the utaka is disputed and they have not been considered in our species/genera counts (see Table 1). We sampled four

species of *Copadichromis*: *Copadichromis likomae* (n=2), *Copadichromis quadrimaculatus* (n=2), *Copadichromis trimaculatus* (n=2, see Fig. 6) and *Copadichromis virginalis* (n=2). Utaka feed in the water column, and can be commonly found close to the shore[169]. *Copadichromis* are generally characterised by their relatively small, highly protrusible mouths, that they use to suck zooplankton into their mouths, as well as numerous long gill rakers which strain plankton from the water that enters their mouths as a result of their sucking feeding mechanism[169,193].

Both the deep benthics and utaka are currently underrepresented within our dataset and future sampling should aim to add additional species of *Copadichromis*. In addition, sampling missing 'deep benthic' genera, such as *Aulonocara* and *Tramitichromis* should be prioritised for future sampling efforts. *Aulonocara stuartgranti* and *Aulonocara steveni* would be particularly interesting future additions and could offer interesting morphological comparisons with deeper living species. Moreover, given that *Lethrinops* is polyphyletic[190,194], additional sampling of *Lethrinops* species could provide morphological data to support future systematic studies.

Whilst we were able to generate relatively good models for the specimens within this group (see Fig. 4 and Fig. 6), it is clear that some of the jaw did not resolve as well as in other specimens. Given the preferred 'sucking' zooplanktivore feeding mechanism of the species within *Copadichromis* it is possible that the jaw bones of these fish species are not particularly dense. This perhaps made it difficult to image these specimens using the same scanning procedure used for all the other remaining specimens. Therefore, in future, we would recommend care when segmenting craniofacial bones from the *Copadichromis* in this dataset and future sampling efforts should increase scanning exposure time and power to optimise specimen imaging.

Processing and Segmentation Notes. The computer specifications we used for all processing steps (see Methodology) are hard to find on personal, or older machines and some users may find it difficult to work with some of our larger image stacks. To minimise memory usage during segmentation and speed up processing, cropped reconstructed stacks can be loaded in multiple increments (note that the Z-voxel size must be multiplied by said increment). We tested this and found that roughly comparable models could be generated, although it was clear that finer morphological detail was absent (data not shown). Therefore, where possible, the whole stack should be used when segmenting regions of interest. In addition, since these regions were manually segmented, many of the segmentation steps rely on the judgment of the individual segmenting and rendering the regions of interest. We found that segmenting from median-filtered reconstructed image stacks drastically lowered the quality of the rendered models (data not shown) and we suggest refraining from segmenting from a median-filtered image stack. In addition, we found that relatively low smoothing factors were best for rendering surfaces from segmented regions of interest. In Avizo Lite (v9.3.0), a smoothing factor between 0-10 (including rational intermediates) can be applied when rendering surfaces of segmented regions of interest. We rarely found it necessary to use a value above 3; indeed, all whole-body 3D models were smoothed with a factor of 2.5. Therefore, we suggest that regardless of the tool used to smooth and render segmented surfaces that smoothing be used conservatively. We also note that there are free, open access alternatives to Avizo Lite (v9.3.0) for the segmentation of 3D-image data, such as 3D-Slicer, which has a large and active community of users[195] and Dragonfly which supports the use of deep learning to automatically segment 3D image data and offers non-commercial licenses, for academic use, free-of-charge. Both of these tools could be used in place of Avizo Lite (v9.3.0) for the segmentation steps outlined in Fig. 2.

Code availability

No custom code was used in the generation of this dataset.

Received: 25 January 2024; Accepted: 26 July 2024;
Published online: 10 September 2024

References

1. Turner, G. F., Seehausen, O., Knight, M. E., Allender, C. J. & Robinson, R. L. How many species of cichlid fishes are there in African lakes? *Molecular Ecology* **10**, 793–806, https://doi.org/10.1046/j.1365-294x.2001.01200.x (2001).
2. Barlow, G. *The Cichlid Fishes: Nature's Grand Experiment In Evolution* (Hachette UK, London, 2008).
3. Sparks, J. S. & Smith, W. L. Phylogeny and biogeography of cichlid fishes (Teleostei: Perciformes: Cichlidae). *Cladistics* **20**, 501–517, https://doi.org/10.1111/j.1096-0031.2004.00038.x (2004).
4. Malinsky, M. *et al.* Whole-genome sequences of Malawi cichlids reveal multiple radiations interconnected by gene flow. *Nature Ecology I& Evolution* **2**, 1940–1955, https://doi.org/10.1038/s41559-018-0717-x (2018).
5. Svardal, H. *et al.* Ancestral hybridization facilitated species diversification in the Lake Malawi cichlid fish adaptive radiation. *Molecular biology and evolution* **37**, 1100–1113, https://doi.org/10.1093/molbev/msz294 (2020).
6. Svardal, H., Salzburger, W. & Malinsky, M. Genetic variation and hybridization in evolutionary radiations of cichlid fishes. *Annual Review of Animal Biosciences* **9**, 55–79, https://doi.org/10.1146/annurev-animal-061220-023129 (2021).
7. Ronco, F. *et al.* Drivers and dynamics of a massive adaptive radiation in cichlid fishes. *Nature* **589**, 76–81, https://doi.org/10.1038/s41586-020-2930-4 (2021).
8. Genner, M. J. *et al.* Evolution of a cichlid fish in a Lake Malawi satellite lake. *Proceedings of the Royal Society B: Biological Sciences* **274**, 2249–2257, https://doi.org/10.1098/rspb.2007.0619 (2007).
9. Genner, M. J. & Turner, G. F. Ancient hybridization and phenotypic novelty within Lake Malawi's cichlid fish radiation. *Molecular Biology and Evolution* **29**, 195–206, https://doi.org/10.1093/molbev/msr183 (2012).
10. Meier, J. I. *et al.* Ancient hybridization fuels rapid cichlid fish adaptive radiations. *Nature communications* **8**, 14363, https://doi.org/10.1038/ncomms14363 (2017).
11. Keller-Costa, T., Canário, A. V. & Hubbard, P. C. Chemical communication in cichlids: a mini-review. *General and comparative endocrinology* **221**, 64–74, https://doi.org/10.1016/j.ygcen.2015.01.001 (2015).
12. Faber-Hammond, J. J. & Renn, S. C. Transcriptomic changes associated with maternal care in the brain of mouthbrooding cichlid *Astatotilapia burtoni* reflect adaptation to self-induced metabolic stress. *Journal of Experimental Biology* **226**, jeb244734, https://doi.org/10.1242/jeb.244734 (2023).

13. Plenderleith, M., Oosterhout, C. V., Robinson, R. L. & Turner, G. F. Female preference for conspecific males based on olfactory cues in a Lake Malawi cichlid fish. *Biology Letters* **1**, 411–414, https://doi.org/10.1098/rsbl.2005.0355 (2005).
14. Morita, M. *et al*. Bower-building behaviour is associated with increased sperm longevity in Tanganyikan cichlids. *Journal of evolutionary biology* **27**, 2629–2643, https://doi.org/10.1111/jeb.12522 (2014).
15. McKaye, K. R. & Kocher, T. Head ramming behaviour by three paedophagous cichlids in Lake Malawi, Africa. *Animal Behaviour* **31**, 206–210, https://doi.org/10.1016/S0003-3472(83)80190-0 (1983).
16. Woltering, J. M., Holzem, M., Schneider, R. F., Nanos, V. & Meyer, A. The skeletal ontogeny of *Astatotilapia burtoni*–a direct-developing model system for the evolution and development of the teleost body plan. *BMC developmental biology* **18**, 1–23, https://doi.org/10.1186/s12861-018-0166-4 (2018).
17. Santos, M. E., Lopes, J. F. & Kratochwil, C. F. East African cichlid fishes. *EvoDevo* **14**, 1, https://doi.org/10.1186/s13227-022-00205-5 (2023).
18. Marconi, A., Yang, C. Z., McKay, S. & Santos, M. E. Morphological and temporal variation in early embryogenesis contributes to species divergence in Malawi cichlid fishes. *Evolution & Development* **25**, 170–193, https://doi.org/10.1111/ede.12429 (2023).
19. Navon, D., Olearczyk, N. & Albertson, R. C. Genetic and developmental basis for fin shape variation in African cichlid fishes. *Molecular Ecology* **26**, 291–303, https://doi.org/10.1111/mec.13905 (2017).
20. Ronco, F., Büscher, H. H., Indermaur, A. & Salzburger, W. The taxonomic diversity of the cichlid fish fauna of ancient Lake Tanganyika, East Africa. *Journal of Great Lakes Research* **46**, 1067–1078, https://doi.org/10.1016/j.jglr.2019.05.009 (2020).
21. Arthur, W. The emerging conceptual framework of evolutionary developmental biology. *Nature* **415**, 757–764, https://doi.org/10.1038/415757a (2002).
22. Albertson, R. C. & Kocher, T. D. Assessing morphological differences in an adaptive trait: a landmark-based morphometric approach. *The Journal of Experimental Zoology* **289**, 385–403, https://doi.org/10.1002/jez.1020 (2001).
23. Adams, D., Yamaoka, K. & Kassam, D. Functional significance of variation in trophic morphology within feeding microhabitat-differentiated cichlid species in Lake Malawi. *Animal Biology* **54**, 77–90, https://doi.org/10.1163/157075604323010060 (2004).
24. Hulsey, C. D., Alfaro, M. E., Zheng, J., Meyer, A. & Holzman, R. Pleiotropic jaw morphology links the evolution of mechanical modularity and functional feeding convergence in Lake Malawi cichlids. *Proceedings of the Royal Society B: Biological Sciences* **286**, 20182358, https://doi.org/10.1098/rspb.2018.2358 (2019).
25. Conith, A. J. & Albertson, R. C. The cichlid oral and pharyngeal jaws are evolutionarily and genetically coupled. *Nature Communications* **12**, 5477, https://doi.org/10.1038/s41467-021-25755-5 (2021).
26. Kratochwil, C. F. *et al*. Agouti-related peptide 2 facilitates convergent evolution of stripe patterns across cichlid fish radiations. *Science* **362**, 457–460, https://doi.org/10.1126/science.aao6809 (2018).
27. Gerwin, J., Urban, S., Meyer, A. & Kratochwil, C. F. Of bars and stripes: A Malawi cichlid hybrid cross provides insights into genetic modularity and evolution of modifier loci underlying colour pattern diversification. *Molecular Ecology* **30**, 4789–4803, https://doi.org/10.1111/mec.16097 (2021).
28. Clark, B. *et al*. Oca2 targeting using crispr/cas9 in the Malawi cichlid *Astatotilapia calliptera*. *Royal Society Open Science* **9**, 220077, https://doi.org/10.1098/rsos.220077 (2022).
29. DeLorenzo, L. *et al*. Genetic basis of ecologically relevant body shape variation among four genera of cichlid fishes. *Molecular ecology* **32**, 3975–3988, https://doi.org/10.1111/mec.16977 (2023).
30. Darrin Hulsey, C., Keck, B. P., Alamillo, H. & O'Meara, B. C. Mitochondrial genome primers for Lake Malawi cichlids. *Molecular Ecology Resources* **13**, 347–353, https://doi.org/10.1111/1755-0998.12066 (2013).
31. McGee, M. D. *et al*. The ecological and genomic basis of explosive adaptive radiation. *Nature* **586**, 75–79, https://doi.org/10.1038/s41586-020-2652-7 (2020).
32. Masonick, P., Meyer, A. & Hulsey, C. D. Phylogenomic analyses show repeated evolution of hypertrophied lips among Lake Malawi cichlid fishes. *Genome Biology and Evolution* **14**, evac051, https://doi.org/10.1093/gbe/evac051 (2022).
33. Price, S. A., Friedman, S. T. & Wainwright, P. C. How predation shaped fish: the impact of fin spines on body form evolution across teleosts. *Proceedings of the Royal Society B: Biological Sciences* **282**, 20151428, https://doi.org/10.1098/rspb.2015.1428 (2015).
34. Baxter, D., Cohen, K. E., Donatelli, C. M. & Tytell, E. D. Internal vertebral morphology of bony fishes matches the mechanical demands of different environments. *Ecology and Evolution* **12**, e9499, https://doi.org/10.1002/ece3.9499 (2022).
35. Haberthür, D. *et al*. Microtomographic investigation of a large corpus of cichlids. *Plos one* **18**, e0291003, https://doi.org/10.1371/journal.pone.0291003 (2023).
36. Todd Streelman, J. & Danley, P. D. The stages of vertebrate evolutionary radiation. *Trends in Ecology & Evolution* **18**, 126–131, https://doi.org/10.1016/S0169-5347(02)00036-8 (2003).
37. Gavrilets, S. & Losos, J. B. Adaptive radiation: Contrasting theory with data. *Science* **323**, 732–737, https://doi.org/10.1126/science.1157966 (2009).
38. Unknown. malawi.si. https://malawi.si/slides/MalawiCichlidsList.html (2023).
39. Schindelin, J. *et al*. Fiji: an open-source platform for biological-image analysis. *Nature methods* **9**, 676–682, https://doi.org/10.1038/nmeth.2019 (2012).
40. Schneider, C. A., Rasband, W. S. & Eliceiri, K. W. NIH Image to ImageJ: 25 years of image analysis. *Nature methods* **9**, 671–675, https://doi.org/10.1038/nmeth.2089 (2012).
41. Bucklow, C. V. *et al*. A whole body micro-ct scan library that captures that skeletal diversity of Lake Malawi cichlid fishes. Avaliable at https://www.morphosource.org/projects/000570997.
42. Bucklow, C. V. & Benson, R. *Alticorpus macrocleithrum*. media 000571119: Whole body. https://doi.org/10.17602/M2/M571119 (2024).
43. Bucklow, C. V. & Benson, R. *Alticorpus macrocleithrum*. media 000571123: Whole body. https://doi.org/10.17602/M2/M571123 (2024).
44. Bucklow, C. V. & Benson, R. *Alticorpus macrocleithrum*. media 000572736: Whole body. https://doi.org/10.17602/M2/M572736 (2024).
45. Bucklow, C. V. & Benson, R. *Astatotilapia calliptera*. media 000571193: Whole body. https://doi.org/10.17602/M2/M571193 (2024).
46. Bucklow, C. V. & Benson, R. *Astatotilapia calliptera*. media 000571197: Whole body. https://doi.org/10.17602/M2/M571197 (2024).
47. Bucklow, C. V. & Benson, R. *Astatotilapia calliptera*. media 000571202: Whole body. https://doi.org/10.17602/M2/M571202 (2024).
48. Bucklow, C. V. & Benson, R. *Astatotilapia calliptera*. media 000571206: Whole body. https://doi.org/10.17602/M2/M571206 (2024).
49. Bucklow, C. V. & Benson, R. *Astatotilapia calliptera*. media 000571211: Whole body. https://doi.org/10.17602/M2/M571211 (2024).
50. Bucklow, C. V. & Benson, R. *Astatotilapia calliptera*. media 000571215: Whole body. https://doi.org/10.17602/M2/M571215 (2024).
51. Bucklow, C. V. & Benson, R. *Astatotilapia calliptera*. media 000572497: Whole body. https://doi.org/10.17602/M2/M572497 (2024).
52. Bucklow, C. V. & Benson, R. *Astatotilapia calliptera*. media 000572494: Whole body. https://doi.org/10.17602/M2/M572494 (2024).
53. Bucklow, C. V. & Benson, R. *Astatotilapia calliptera*. media 000572503: Whole body. https://doi.org/10.17602/M2/M572503 (2024).
54. Bucklow, C. V. & Benson, R. *Astatotilapia calliptera*. media 000572508: Whole body. https://doi.org/10.17602/M2/M572508 (2024).
55. Bucklow, C. V. & Benson, R. *Astatotilapia calliptera*. media 000572522: Whole body. https://doi.org/10.17602/M2/M572522 (2024).
56. Bucklow, C. V. & Benson, R. *Astatotilapia calliptera*. media 000572517: Whole body. https://doi.org/10.17602/M2/M572517 (2024).
57. Bucklow, C. V. & Benson, R. *Astatotilapia calliptera*. media 000573224: Whole body. https://doi.org/10.17602/M2/M573224 (2024).
58. Bucklow, C. V. & Benson, R. *Astatotilapia calliptera*. media 000572527: Whole body. https://doi.org/10.17602/M2/M572527 (2024).
59. Bucklow, C. V. & Benson, R. *Astatotilapia calliptera*. media 000572539: Whole body. https://doi.org/10.17602/M2/M572539 (2024).

60. Bucklow, C. V. & Benson, R. *Astatotilapia gigliolii*. media 000572470: Whole body. https://doi.org/10.17602/M2/M572470 (2024).
61. Bucklow, C. V. & Benson, R. *Astatotilapia gigliolii*. media 000572476: Whole body. https://doi.org/10.17602/M2/M572476 (2024).
62. Bucklow, C. V. & Benson, R. *Astatotilapia sp.* 'Ruaha blue'. media 000572482: Whole body. https://doi.org/10.17602/M2/M572482 (2024).
63. Bucklow, C. V. & Benson, R. *Astatotilapia sp.* 'Ruaha blue'. media 000572488: Whole body. https://doi.org/10.17602/M2/M572488 (2024).
64. Bucklow, C. V. & Benson, R. *Copadichromis likomae*. media 000571334: Whole body. https://doi.org/10.17602/M2/M571334 (2024).
65. Bucklow, C. V. & Benson, R. *Copadichromis likomae*. media 000571338: Whole body. https://doi.org/10.17602/M2/M571338 (2024).
66. Bucklow, C. V. & Benson, R. *Copadichromis quadrimaculatus*. media 000571344: Whole body. https://doi.org/10.17602/M2/M571344 (2024).
67. Bucklow, C. V. & Benson, R. *Copadichromis quadrimaculatus*. media 000571348: Whole body. https://doi.org/10.17602/M2/M571348 (2024).
68. Bucklow, C. V. & Benson, R. *Copadichromis trimaculatus*. media 000571355: Whole body. https://doi.org/10.17602/M2/M571355 (2024).
69. Bucklow, C. V. & Benson, R. *Copadichromis trimaculatus*. media 000571359: Whole body. https://doi.org/10.17602/M2/M571359 (2024).
70. Bucklow, C. V. & Benson, R. *Copadichromis virginalis*. media 000571366: Whole body. https://doi.org/10.17602/M2/M571366 (2024).
71. Bucklow, C. V. & Benson, R. *Copadichromis virginalis*. media 000571370: Whole body. https://doi.org/10.17602/M2/M571370 (2024).
72. Bucklow, C. V. & Benson, R. *Cynotilapia axelrodi*. media 000571377: Whole body. https://doi.org/10.17602/M2/M571377 (2024).
73. Bucklow, C. V. & Benson, R. *Dimidiochromis compressiceps*. media 000572737: Whole body. https://doi.org/10.17602/M2/M572737 (2024).
74. Bucklow, C. V. & Benson, R. *Dimidiochromis strigatus*. media 000572743: Whole body. https://doi.org/10.17602/M2/M572743 (2024).
75. Bucklow, C. V. & Benson, R. *Diplotaxodon aeneus*. media 000571382: Whole body. https://doi.org/10.17602/M2/M571382 (2024).
76. Bucklow, C. V. & Benson, R. *Diplotaxodon aeneus*. media 000571386: Whole body. https://doi.org/10.17602/M2/M571386 (2024).
77. Bucklow, C. V. & Benson, R. *Diplotaxodon aeneus*. media 000572632: Whole body. https://doi.org/10.17602/M2/M572632 (2024).
78. Bucklow, C. V. & Benson, R. *Diplotaxodon aeneus*. media 000572643: Whole body. https://doi.org/10.17602/M2/M572643 (2024).
79. Bucklow, C. V. & Benson, R. *Diplotaxodon argenteus*. media 000571393: Whole body. https://doi.org/10.17602/M2/M571393 (2024).
80. Bucklow, C. V. & Benson, R. *Diplotaxodon limnothrissa*. media 000571400: Whole body. https://doi.org/10.17602/M2/M571400 (2024).
81. Bucklow, C. V. & Benson, R. *Diplotaxodon limnothrissa*. media 000571404: Whole body. https://doi.org/10.17602/M2/M571404 (2024).
82. Bucklow, C. V. & Benson, R. *Diplotaxodon macrops*. media 000571409: Whole body. https://doi.org/10.17602/M2/M571409 (2024).
83. Bucklow, C. V. & Benson, R. *Diplotaxodon sp.* 'holochromis'. media 000573144: Whole body. https://doi.org/10.17602/M2/M573144 (2024).
84. Bucklow, C. V. & Benson, R. *Diplotaxodon sp.* 'holochromis'. media 000573151: Whole body. https://doi.org/10.17602/M2/M573151 (2024).
85. Bucklow, C. V. & Benson, R. *Diplotaxodon sp.* 'macrops black dorsal'. media 000573107: Whole body. https://doi.org/10.17602/M2/M573107 (2024).
86. Bucklow, C. V. & Benson, R. *Diplotaxodon sp.* 'macrops black dorsal'. media 000573117: Whole body. https://doi.org/10.17602/M2/M573117 (2024).
87. Bucklow, C. V. & Benson, R. *Diplotaxodon sp.* 'macrops ngulube'. media 000573113: Whole body. https://doi.org/10.17602/M2/M573113 (2024).
88. Bucklow, C. V. & Benson, R. *Diplotaxodon sp.* 'macrops ngulube'. media 000573121: Whole body. https://doi.org/10.17602/M2/M573121 (2024).
89. Bucklow, C. V. & Benson, R. *Diplotaxodon sp.* 'similis white back north'. media 000573127: Whole body. https://doi.org/10.17602/M2/M573127 (2024).
90. Bucklow, C. V. & Benson, R. *Diplotaxodon sp.* 'similis white back north'. media 000573138: Whole body. https://doi.org/10.17602/M2/M573138 (2024).
91. Bucklow, C. V. & Benson, R. *Genyochromis mento*. media 000571414: Whole body. https://doi.org/10.17602/M2/M571414 (2024).
92. Bucklow, C. V. & Benson, R. *Genyochromis mento*. media 000571418: Whole body. https://doi.org/10.17602/M2/M571418 (2024).
93. Bucklow, C. V. & Benson, R. *Hemitilapia oxyrhynchus*. media 000572650: Whole body. https://doi.org/10.17602/M2/M572650 (2024).
94. Bucklow, C. V. & Benson, R. *Iodotropheus sprengerae*. media 000571423: Whole body. https://doi.org/10.17602/M2/M571423 (2024).
95. Bucklow, C. V. & Benson, R. *Iodotropheus sprengerae*. media 000571427: Whole body. https://doi.org/10.17602/M2/M571427 (2024).
96. Bucklow, C. V. & Benson, R. *Labidochromis strigatus*. media 000571434: Whole body. https://doi.org/10.17602/M2/M571434 (2024).
97. Bucklow, C. V. & Benson, R. *Labidochromis strigatus*. media 000571441: Whole body. https://doi.org/10.17602/M2/M571441 (2024).
98. Bucklow, C. V. & Benson, R. *Lethrinops albus*. media 000571443: Whole body. https://doi.org/10.17602/M2/M571443 (2024).
99. Bucklow, C. V. & Benson, R. *Lethrinops albus*. media 000571448: Whole body. https://doi.org/10.17602/M2/M571448 (2024).
100. Bucklow, C. V. & Benson, R. *Lethrinops auritus*. media 000571454: Whole body. https://doi.org/10.17602/M2/M571454 (2024).
101. Bucklow, C. V. & Benson, R. *Lethrinops auritus*. media 000571465: Whole body. https://doi.org/10.17602/M2/M571465 (2024).
102. Bucklow, C. V. & Benson, R. *Lethrinops gossei*. media 000572675: Whole body. https://doi.org/10.17602/M2/M572675 (2024).
103. Bucklow, C. V. & Benson, R. *Maylandia zebra*. media 000572545: Whole body. https://doi.org/10.17602/M2/M572545 (2024).
104. Bucklow, C. V. & Benson, R. *Maylandia zebra*. media 000572554: Whole body. https://doi.org/10.17602/M2/M572554 (2024).
105. Bucklow, C. V. & Benson, R. *Maylandia zebra*. media 000572553: Whole body. https://doi.org/10.17602/M2/M572553 (2024).
106. Bucklow, C. V. & Benson, R. *Maylandia zebra*. media 000572560: Whole body. https://doi.org/10.17602/M2/M572560 (2024).
107. Bucklow, C. V. & Benson, R. *Maylandia zebra*. media 000572569: Whole body. https://doi.org/10.17602/M2/M572569 (2024).
108. Bucklow, C. V. & Benson, R. *Astatotilapia calliptera* x *tropheops tropheops* (presumed). media 000572568: Whole body. https://doi.org/10.17602/M2/M572568 (2024).
109. Bucklow, C. V. & Benson, R. *Mylochromis anaphyrmus*. media 000572676: Whole body. https://doi.org/10.17602/M2/M572676 (2024).
110. Bucklow, C. V. & Benson, R. *Nimbochromis linni*. media 000572674: Whole body. https://doi.org/10.17602/M2/M572674 (2024).

111. Bucklow, C. V. & Benson, R. *Nimbochromis livingstonii*. media 000571459: Whole body. https://doi.org/10.17602/M2/M571459 (2024).
112. Bucklow, C. V. & Benson, R. *Nimbochromis polystigma*. media 000571468: Whole body. https://doi.org/10.17602/M2/M571468 (2024).
113. Bucklow, C. V. & Benson, R. *Nimbochromis polystigma*. media 000571473: Whole body. https://doi.org/10.17602/M2/M571473 (2024).
114. Bucklow, C. V. & Benson, R. *Otopharynx lithobates*. media 000571483: Whole body. https://doi.org/10.17602/M2/M571483 (2024).
115. Bucklow, C. V. & Benson, R. *Otopharynx lithobates*. media 000571484: Whole body. https://doi.org/10.17602/M2/M571484 (2024).
116. Bucklow, C. V. & Benson, R. *Otopharynx lithobates*. media 000571489: Whole body. https://doi.org/10.17602/M2/M571489 (2024).
117. Bucklow, C. V. & Benson, R. *Otopharynx sp.* 'Brooksi nkhata'. media 000573140: Whole body. https://doi.org/10.17602/M2/M573140 (2024).
118. Bucklow, C. V. & Benson, R. *Otopharynx speciosus*. media 000571496: Whole body. https://doi.org/10.17602/M2/M571496 (2024).
119. Bucklow, C. V. & Benson, R. *Otopharynx speciosus*. media 000571501: Whole body. https://doi.org/10.17602/M2/M571501 (2024).
120. Bucklow, C. V. & Benson, R. *Otopharynx tetrastigma*. media 000571508: Whole body. https://doi.org/10.17602/M2/M571508 (2024).
121. Bucklow, C. V. & Benson, R. *Otopharynx tetrastigma*. media 000571512: Whole body. https://doi.org/10.17602/M2/M571512 (2024).
122. Bucklow, C. V. & Benson, R. *Pallidochromis tokolosh*. media 000571517: Whole body. https://doi.org/10.17602/M2/M571517 (2024).
123. Bucklow, C. V. & Benson, R. *Pallidochromis tokolosh*. media 000571521: Whole body. https://doi.org/10.17602/M2/M571521 (2024).
124. Bucklow, C. V. & Benson, R. *Petrotilapia genalutea*. media 000571526: Whole body. https://doi.org/10.17602/M2/M571526 (2024).
125. Bucklow, C. V. & Benson, R. *Placidochromis electra*. media 000572692: Whole body. https://doi.org/10.17602/M2/M572692 (2024).
126. Bucklow, C. V. & Benson, R. *Placidochromis johnstoni*. media 000572694: Whole body. https://doi.org/10.17602/M2/M572694 (2024).
127. Bucklow, C. V. & Benson, R. *Placidochromis milomo*. media 000572687: Whole body. https://doi.org/10.17602/M2/M572687 (2024).
128. Bucklow, C. V. & Benson, R. *Placidochromis milomo*. media 000572716: Whole body. https://doi.org/10.17602/M2/M572716 (2024).
129. Bucklow, C. V. & Benson, R. *Protomelas spilopterus*. media 000572702: Whole body. https://doi.org/10.17602/M2/M572702 (2024).
130. Bucklow, C. V. & Benson, R. *Rhamphochromis esox*. media 000571531: Whole body. https://doi.org/10.17602/M2/M571531 (2024).
131. Bucklow, C. V. & Benson, R. *Rhamphochromis esox*. media 000571535: Whole body. https://doi.org/10.17602/M2/M571535 (2024).
132. Bucklow, C. V. & Benson, R. *Rhamphochromis ferox*. media 000571542: Whole body. https://doi.org/10.17602/M2/M571542 (2024).
133. Bucklow, C. V. & Benson, R. *Rhamphochromis ferox*. media 000571552: Whole body. https://doi.org/10.17602/M2/M571552 (2024).
134. Bucklow, C. V. & Benson, R. *Rhamphochromis longiceps*. media 000571550: Whole body. https://doi.org/10.17602/M2/M571550 (2024).
135. Bucklow, C. V. & Benson, R. *Rhamphochromis longiceps*. media 000571557: Whole body. https://doi.org/10.17602/M2/M571557 (2024).
136. Bucklow, C. V. & Benson, R. *Rhamphochromis sp.* 'Chilingali'. media 000573156: Whole body. https://doi.org/10.17602/M2/M573156 (2024).
137. Bucklow, C. V. & Benson, R. *Rhamphochromis sp.* 'Chilingali'. media 000573160: Whole body. https://doi.org/10.17602/M2/M573160 (2024).
138. Bucklow, C. V. & Benson, R. *Rhamphochromis sp.* 'Chilingali'. media 000572583: Whole body. https://doi.org/10.17602/M2/M572583 (2024).
139. Bucklow, C. V. & Benson, R. *Rhamphochromis sp.* 'Chilingali'. media 000572582: Whole body. https://doi.org/10.17602/M2/M572582 (2024).
140. Bucklow, C. V. & Benson, R. *Rhamphochromis sp.* 'Kingiri dwarf'. media 000573200: Whole body. https://doi.org/10.17602/M2/M573200 (2024).
141. Bucklow, C. V. & Benson, R. *Rhamphochromis sp.* 'Kingiri dwarf'. media 000573207: Whole body. https://doi.org/10.17602/M2/M573207 (2024).
142. Bucklow, C. V. & Benson, R. *Rhamphochromis sp.* 'Kingiri large'. media 000573167: Whole body. https://doi.org/10.17602/M2/M573167 (2024).
143. Bucklow, C. V. & Benson, R. *Rhamphochromis sp.* 'Kingiri large'. media 000573173: Whole body. https://doi.org/10.17602/M2/M573173 (2024).
144. Bucklow, C. V. & Benson, R. *Rhamphochromis sp.* 'longiceps blue back'. media 000573212: Whole body. https://doi.org/10.17602/M2/M573212 (2024).
145. Bucklow, C. V. & Benson, R. *Rhamphochromis sp.* 'longiceps blue back'. media 000573216: Whole body. https://doi.org/10.17602/M2/M573216 (2024).
146. Bucklow, C. V. & Benson, R. *Rhamphochromis sp.* 'longiceps grey back'. media 000573178: Whole body. https://doi.org/10.17602/M2/M573178 (2024).
147. Bucklow, C. V. & Benson, R. *Rhamphochromis sp.* 'longiceps grey back'. media 000573185: Whole body. https://doi.org/10.17602/M2/M573185 (2024).
148. Bucklow, C. V. & Benson, R. *Rhamphochromis sp.* 'yellow belly'. media 000573187: Whole body. https://doi.org/10.17602/M2/M573187 (2024).
149. Bucklow, C. V. & Benson, R. *Rhamphochromis sp.* 'yellow belly'. media 000573192: Whole body. https://doi.org/10.17602/M2/M573192 (2024).
150. Bucklow, C. V. & Benson, R. *Rhamphochromis woodi*. media 000571564: Whole body. https://doi.org/10.17602/M2/M571564 (2024).
151. Bucklow, C. V. & Benson, R. *Rhamphochromis woodi*. media 000571568: Whole body. https://doi.org/10.17602/M2/M571568 (2024).
152. Bucklow, C. V. & Benson, R. *Stigmatochromis macrorhynchos*. media 000572708: Whole body. https://doi.org/10.17602/M2/M572708 (2024).
153. Bucklow, C. V. & Benson, R. *Taeniolethrinops praeorbitalis*. media 000572717: Whole body. https://doi.org/10.17602/M2/M572717 (2024).
154. Bucklow, C. V. & Benson, R. *Trematocranus placodon*. media 000572727: Whole body. https://doi.org/10.17602/M2/M572727 (2024).
155. Bucklow, C. V. & Benson, R. *Tropheops tropheops*. media 000571573: Whole body. https://doi.org/10.17602/M2/M571573 (2024).
156. Bucklow, C. V. & Benson, R. *Tropheops tropheops*. media 000571577: Whole body. https://doi.org/10.17602/M2/M571577 (2024).

157. Bucklow, C. V. & Benson, R. *Tyrannochromis macrostoma*. media 000572724: Whole body. https://doi.org/10.17602/M2/M572724 (2024).
158. Turner, G., Ngatunga, B. P. & Genner, M. J. The Natural History of the Satellite Lakes of Lake Malawi. Preprint at https://doi.org/10.32942/osf.io/sehdq (2019).
159. Hahn, C., Genner, M. J., Turner, G. F. & Joyce, D. A. The genomic basis of cichlid fish adaptation within the deepwater "twilight zone" of Lake Malawi. *Evolution Letters* **1**, 184–198, https://doi.org/10.1002/evl3.20 (2017).
160. Turner, G. F. Description of a commercially important pelagic species of the genus *Diplotaxodon* (Pisces: Cichlidae) from Lake Malawi, Africa. *Journal of Fish Biology* **44**, 799–807, https://doi.org/10.1111/j.1095-8649.1994.tb01256.x (1994).
161. Lowe-McConnell, R. Recent research in the African great lakes: fisheries, biodiversity and cichlid evolution. Accesible here = https://aquadocs.org/handle/1834/22270 (2003).
162. Wilson, G. D. & Hessler, R. R. Speciation in the deep sea. *Annual Review of Ecology and Systematics* **18**, 185–207, https://doi.org/10.1146/annurev.es.18.110187.001153 (1987).
163. Jennings, R. M., Etter, R. J. & Ficarra, L. Population differentiation and species formation in the deep sea: the potential role of environmental gradients and depth. *PLoS One* **8**, e77594, https://doi.org/10.1371/journal.pone.0077594 (2013).
164. Neat, F. & Campbell, N. Proliferation of elongate fishes in the deep sea. *Journal of Fish Biology* **83**, 1576–1591, https://doi.org/10.1111/jfb.12266 (2013).
165. Stiassny, M. Phylogenetic versus convergent relationships between piscivorous cichlid fishes from Lakes Malawi and Tanganyika. *Bulletin of the British Museum (Natural History), Zoology* **40**, 67–101 (1981).
166. Donatelli, C. M. *et al.* Foretelling the flex-vertebral shape predicts behavior and ecology of fishes. *Integrative and Comparative Biology* **61**, 414–426, https://doi.org/10.1093/icb/icab110 (2021).
167. Turner, G., Robinson, R., Shaw, P., Carvalho, G. & Snoeks, J. *Identification and biology of Diplotaxodon, Rhamphochromis and Pallidochromis* (Cichlid Press, 2004).
168. Fujimura, K. & Okada, N. Shaping of the lower jaw bone during growth of Nile Tilapia *Oreochromis niloticus* and a Lake Victoria cichlid *Haplochromis chilotes*: A geometric morphometric approach. *Development, Growth & Differentiation* **50**, 653–663, https://doi.org/10.1111/j.1440-169X.2008.01063.x (2008).
169. Konings, A. *Malaŵi Cichlids in their Natural Habitat* (Cichlid Press, 2016), 5th edn.
170. Gatumu, E. M. Redescription of the genera *Nimbochromis* and *Tyrannochromis* (Teleostei: Cichlidae) from Lake Malawi, Africa. https://solo.bodleian.ox.ac.uk/permalink/44OXF_INST/ao2p7t/cdi_proquest_journals_305235338 (2003).
171. Oliver, M. K. Six new species of the cichlid genus *Otopharynx* from Lake Malaŵi (Teleostei: Cichlidae). *Bulletin of the Peabody Museum of Natural History* **59**, 159–197, https://doi.org/10.3374/014.059.0204 (2018).
172. Evers, B. N., Madsen, H., McKaye, K. M. & Stauffer, J. R. The schistosome intermediate host, *Bulinus nyassanus*, is a 'preferred' food for the cichlid fish, *Trematocranus placodon*, at Cape Maclear, Lake Malawi. *Annals of Tropical Medicine & Parasitology* **100**, 75–85, https://doi.org/10.1179/136485906X78553 (2006).
173. Albertson, R. C. Morphological divergence predicts habitat partitioning in a Lake Malawi cichlid species complex. *Copeia* **2008**, 689–698, https://doi.org/10.1643/CG-07-217 (2008).
174. Genner, M. J. & Turner, G. F. The mbuna cichlids of Lake Malawi: a model for rapid speciation and adaptive radiation. *Fish and fisheries* **6**, 1–34, https://doi.org/10.1111/j.1467-2679.2005.00173.x (2005).
175. Ribbink, A., Marsh, B., Marsh, A., Ribbink, A. & Sharp, B. A preliminary survey of the cichlid fishes of rocky habitats in Lake Malawi. *South African Journal of Zoology* **18**, 149–310, https://doi.org/10.1080/02541858.1983.11447831 (1983).
176. Kassam, D., Seki, S., Rusuwa, B., Ambali, A. J. & Yamaoka, K. Genetic diversity within the genus *Cynotilapia* and its phylogenetic position among Lake Malawi's mbuna cichlids. *African Journal of Biotechnology*. **4**, https://doi.org/10.4314/ajb.v4i10.71319 (2005).
177. Genner, M., Turner, G., Barker, S. & Hawkins, S. Niche segregation among Lake Malawi cichlid fishes? Evidence from stable isotope signatures. *Ecology Letters* **2**, 185–190, https://doi.org/10.1046/j.1461-0248.1999.00068.x (1999).
178. Stauffer Jr, J. R., Bowers, N. J., Kellogg, K. A. & McKaye, K. R. A revision of the blue-black *Pseudotropheus zebra* (Teleostei: Cichlidae) complex from Lake Malaŵi, africa, with a description of a new genus and ten new species. *Proceedings of the Academy of Natural Sciences of Philadelphia* 189–230, http://www.jstor.org/stable/4065053 (1997).
179. Holzberg, S. A field and laboratory study of the behaviour and ecology of *Pseudotropheus zebra* (Boulenger), an endemic cichlid of Lake Malawi (Pisces; Cichlidae). *Journal of Zoological Systematics and Evolutionary Research* **16**, 171–187, https://doi.org/10.1111/j.1439-0469.1978.tb00929.x (1978).
180. Marsh, A. A taxonomic study of the fish genus *Petrotilapia* (Pisces: Cichlidae) from Lake Malawi. *Ichthyological Bulletin of the J.L.B. Smith Institute of Ichthyology* **48**, 1–14 (1983).
181. Takeuchi, Y. *et al.* Specialized movement and laterality of fin-biting behaviour in *Genyochromis mento* in Lake Malawi. *Journal of Experimental Biology* **222**, jeb191676, https://doi.org/10.1242/jeb.191676 (2019).
182. Genner, M. J., Ngatunga, B. P., Mzighani, S., Smith, A. & Turner, G. F. Geographical ancestry of Lake Malawi's cichlid fish diversity. *Biology Letters* **11**, 20150232, https://doi.org/10.1098/rsbl.2015.0232 (2015).
183. Turner, G., Ngatunga, B. P. & Genner, M. J. *Astatotilapia* species (Teleostei, Cichlidae) from Malawi, Mozambique and Tanzania, excluding the basin of Lake Victoria. Preprint at https://doi.org/10.32942/osf.io/eu6rx (2021).
184. Malinsky, M. *et al.* Genomic islands of speciation separate cichlid ecomorphs in an East African crater lake. *Science* **350**, 1493–1498, https://doi.org/10.1126/science.aac9927 (2015).
185. Njaya, F. *et al.* The natural history and fisheries ecology of Lake Chilwa, Southern Malawi. *Journal of Great Lakes Research* **37**, 15–25, https://doi.org/10.1016/j.jglr.2010.09.008 (2011).
186. Parsons, P. J., Bridle, J. R., Rüber, L. & Genner, M. J. Evolutionary divergence in life history traits among populations of the Lake Malawi cichlid fish *Astatotilapia calliptera*. *Ecology and evolution* **7**, 8488–8506, https://doi.org/10.1002/ece3.3311 (2017).
187. Omland, K. E. The assumptions and challenges of ancestral state reconstructions. *Systematic biology* **48**, 604–611, https://doi.org/10.1080/106351599260175 (1999).
188. Joyce, D. A. *et al.* Repeated colonization and hybridization in Lake Malawi cichlids. *Current Biology* **21**, R108–R109, https://doi.org/10.1016/j.cub.2010.11.029 (2011).
189. Duponchelle, F., Ribbink, A., Msukwa, A., Mafuka, J. & Mandere, D. Depth distribution and breeding patterns of the demersal species most commonly caught by trawling in the south west arm of Lake Malawi. Available at https://malawicichlids.com/duponchelle_ch2.pdf (2000).
190. Turner, G. F. A new species of deep-water *Lethrinops* (Cichlidae) from Lake Malawi. *Journal of Fish Biology* **101**, 1405–1410, https://doi.org/10.1111/jfb.15208 (2022).
191. Anseeuw, D., Nevado, B., Busselen, P., Snoeks, J. & Verheyen, E. Extensive introgression among ancestral mtDNA lineages: Phylogenetic relationships of the utaka within the lake malawi cichlid flock. *International Journal of Evolutionary Biology* **2012**, 1–9, https://doi.org/10.1155/2012/865603 (2012).
192. Stauffer, J. & Konings, A. Review of *Copadichromis* (Teleostei: Cichlidae) with the description of a new genus and six new species. *Ichthyological Exploration of Freshwaters* **17**, 9–42 (2006).
193. Turner, G. F., Crampton, D. A., Rusuwa, B., Hooft van Huysduynen, A. & Svardal, H. Taxonomic investigation of the zooplanktivorous Lake Malawi cichlids *Copadichromis mloto* (Iles) and *C. virginalis* (Iles). *Hydrobiologia* 1–11, https://doi.org/10.1007/s10750-022-05025-1 (2022).

194. Turner, G. F., Crampton, D. A. & Genner, M. J. A new species of *Lethrinops* (Cichliformes: Cichlidae) from a Lake Malawi satellite lake, believed to be extinct in the wild. Zootaxa. **5318**(4), 515-530, https://doi.org/10.11646/zootaxa.5318.4.5 (2023).
195. Kikinis, R., Pieper, S. D. & Vosburgh, K. G. *3D Slicer: A Platform for Subject-Specific Image Analysis, Visualization, and Clinical Support* https://doi.org/10.1007/978-1-4614-7657-3_19 (Springer New York, New York, NY, 2014).

Acknowledgements
We thank Vincent Fernandez, CT facility manager at the NHMUK and Liz Martin-Silverstone at the XTM Facility at the University of Bristol for organising access to their respective imaging facilities. Thank you to the fish whose lives were sacrificed for this work. This research was partly funded by a Biotechnology and Biological Sciences Research Council (BBSRC) studentship (Grant Number: 2445747).

Author contributions
C.V.B. and B.V. conceived the study. C.V.B. and R.B. designed the data acquisition pipeline and dataset curation methodology. C.V.B. and R.B. conducted the imaging. C.V.B. performed the sample collection, processed all the raw image data, and wrote the manuscript. B.V., R.B. and M.J.G. edited the manuscript. J.M. organised specimens at the NHMUK. G.F.T. and M.J.G. contributed specimens to be imaged. All authors reviewed the manuscript.

Competing interests
The authors declare no competing interests.

Additional information
Supplementary information The online version contains supplementary material available at https://doi.org/10.1038/s41597-024-03687-1.

Correspondence and requests for materials should be addressed to R.B. or B.V.

Reprints and permissions information is available at www.nature.com/reprints.

Publisher's note Springer Nature remains neutral with regard to jurisdictional claims in published maps and institutional affiliations.

Open Access This article is licensed under a Creative Commons Attribution 4.0 International License, which permits use, sharing, adaptation, distribution and reproduction in any medium or format, as long as you give appropriate credit to the original author(s) and the source, provide a link to the Creative Commons licence, and indicate if changes were made. The images or other third party material in this article are included in the article's Creative Commons licence, unless indicated otherwise in a credit line to the material. If material is not included in the article's Creative Commons licence and your intended use is not permitted by statutory regulation or exceeds the permitted use, you will need to obtain permission directly from the copyright holder. To view a copy of this licence, visit http://creativecommons.org/licenses/by/4.0/.

© The Author(s) 2024

4.3 Vertebral Shape Analysis in Lake Malawi Cichlids

4.3.1 Motivation and Author Contributions

Owing to time constraints, it was not possible to integrate the following analysis into another manuscript. As such, it is presented here in a more traditional thesis chapter format. However, following submission and the inclusion of additional analyses, this chapter will form the basis of my next manuscript. The chapter is largely self-contained, with the methodology embedded throughout rather than forming a separate section. This structure should also make it easier to adapt the analyses and methods for future publication.

The analysis was first conceived in 2021, following a discussion between myself, Berta Verd, and Katherine (Kate) Criswell. At the time, Kate had just published a study examining vertebral regionalisation in *Leucoraja erinacea* (little skate) [Criswell et al., 2021], a follow-up to her earlier work on the embryonic development of the axial skeleton in the same species [Criswell et al., 2017a]. Our initial aim was to replicate her somitic cell-tracking experiments [Criswell et al., 2021, 2017b] in Lake Malawi cichlids, to determine which somites contribute to which vertebral precursors and to identify which *hox* genes are expressed in these cells. However, Kate had also conducted some preliminary, unpublished analyses in teleosts using geometric morphometrics to quantify vertebral shape variation. In these analyses, she identified nested domains within the precaudal and caudal regions of the vertebral column, using the same regionalisation methodology she had previously applied to describe the vertebral column of the little skate.

Inspired by these findings, as well as a shift in my own interests away from experimental embryology, we sought to replicate this analysis in Lake Malawi cichlids. In addition to investigating patterns of regionalisation, I also aimed to assess whether vertebral shape functions as an adaptive trait. The axial skeleton has been largely overlooked in African cichlid research to date [Oliver, 2024], and I was curious to explore whether vertebral shape could represent an axis of adaptive variation, as has been proposed on broader phylogenetic scales in teleosts [Donatelli et al., 2021, Baxter et al., 2022].

Due to the time required to generate a suitable μCT-scan dataset, the analyses did not begin until relatively recently, when it became clear that completing the project alone would be unfeasible. Fortunately, during my DPhil I've had the pleasure of teaching many talented MBiol students through tutorials, including a tutorial with Hannah Ugboma. Hannah joined the lab for her masters research project in September 2024 and has been instrumental in helping to bring this chapter to completion. Together, we segmented the vertebral models from the μCT-scans, and to avoid introducing bias during

landmarking, Hannah performed all the landmarking herself. I developed the necessary code for the subsequent statistical analysis, designed the analytical workflow, and was primarily responsible for interpreting the results.

4.3.2 Methodology

Species Selection

The Lake Malawi cichlid radiation was sampled broadly, including representatives from all seven ecomorphological groups [Bucklow et al., 2024]. From this dataset, I selected species that were also present on the phylogeny of McGee et al. [2020], resulting in vertebral shape data for 45 species. Full specimen details are provided in Supplementary Table S1. This subset spans all seven major ecomorphological groups described in Lake Malawi [Malinsky et al., 2018], capturing a wide range of axial skeletal variation within the radiation. For the regionalisation analysis, I focused on a smaller subset of eight species, selecting one representative from each ecomorphological group (excluding *Diplotaxodon*) and including two species from the Mbuna clade. The species included were: *Astatotilapia calliptera* (*Astatotilapia*), *Copadichromis quadrimaculatus* (utaka), *Lethrinops gossei* (deep benthic), *Placidochromis johnstoni* (shallow benthic), *Maylandia zebra* and *Tropheops tropheops* (mbuna), and *Rhamphochromis sp.* 'Chilingali' (*Rhamphochromis*). These species were deliberately chosen to span a range of total vertebral counts. Our aim was to test whether the number of vertebrae influenced the number and position of identified vertebral regions, and to evaluate whether axial domains could be considered homologous across species with differing vertebral formulas.

Segmentation of μCT-scans

For the interspecies analysis, rather than quantifying variation along the whole vertebral column, we focused on three precaudal and three caudal vertebrae. Precaudal and caudal counts varied between specimens, therefore in order to maintain the relative positions of the precaudal and caudal vertebrae and ensure comparability between species, precaudal and caudal vertebrae were segmented based on their their relative position to the first caudal vertebrae, that is, the first haemal-arch bearing vertebrae that articulates with the second anal fin spine (Figure 4.1A, B). The vertebrae immediately anterior and posterior to the first caudal vertebrae were ignored. Instead, the three vertebrae immediately anterior or posterior to this gap were segmented (Figure 4.1B). In contrast, for the regionalisation analysis i.e. the quantitative determination of the number of nested domains in the vertebral column, all vertebrae were segmented from the vertebral column of select species (Figure 4.1C). The final vertebrae (the 'urostyle'), which featured in our count data, and is a vertebrae [Woltering et al., 2018, Oliver, 2024] was ignored

as its unique morphology prevented it from being landmarked as the other vertebrae (see below). Vertebrae were manually segmented from μCT scans in Avizo Lite (v9.3.0), as previously described [Bucklow et al., 2024]. For precaudal vertebrae, where possible, both pleural ribs were segmented. Epicentrals were ignored. Models were exported as Polygon File Format (PLY) files for further analysis.

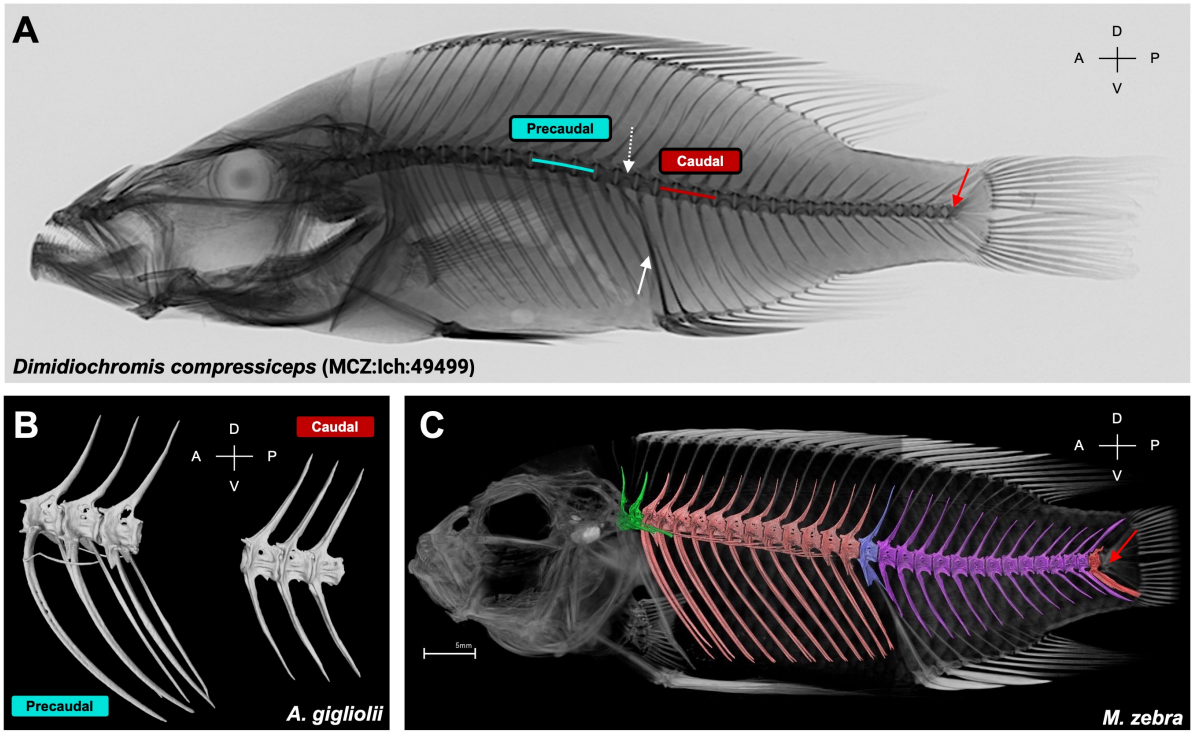

Figure 4.1: Vertebral segmentation. (A) X-ray of *Dimidiochromis compressiceps*, precaudal (blue) and caudal (red) vertebrae segmented for the interspecies analysis is indicated. Dashed arrow marks the centrum of the first caudal vertebrae and the solid white arrow shows the second anal fin spine, which projects dorsally to rest near the first haemal spine. Note that the vertebrae immediately and anterior and posterior this vertebrae were ignored. Purple arrow indicates the position of the urostyle, which was counted as a vertebrae in our count data analysis but was not segmented for regionalisation analysis. (B) Example precaudal and caudal vertebrae from *Astatotilapia* (*A.*) *gigliolii*. (C) μCT-scan of *Maylandia* (*M.*) *zebra*, all vertebrae segmented for the regionalisation analysis are indicated. Colours are not relevant to the analysis here.

Landmarking of Vertebral Models

Our landmarking scheme was based on a set of fifteen landmarks (Katherine Criswell, personal comms), based on some preliminary regionalisation analysis in teleosts following her analysis in *Leucoraja erinacea* (Little Skate) [Criswell et al., 2021]. These landmarks formed the basis of the regionalisation analysis, as it permitted the comparison of both precaudal and caudal vertebrae as all landmarks were common to both vertebral types. These landmarks are represented by the first 15 landmarks in our landmarking scheme

(Figure 4.2). For additional shape analysis, however, additional landmarks were added in order to capture features unique to precaudal and caudal vertebrae. In order to investigate pleural rib curvature, ten additional semilandmarks were equidistantly placed along the outer curve of the rightward pleural rib. Two fixed landmarks were placed on the anterior and posterior tips of the rib. To capture haemal spine placement, we added additional landmarks to the anterior fusion point of the haemal arches and the posterior tip of the haemal spine. Vertebral model files were imported into 3D-Slicer (v5.8.1) and landmarks were manually added for all the models. Coordinate data for each landmark and specimen was exported as a .JSON file and compiled into a TPS (Thin Plate Spline) file in R for further analysis.

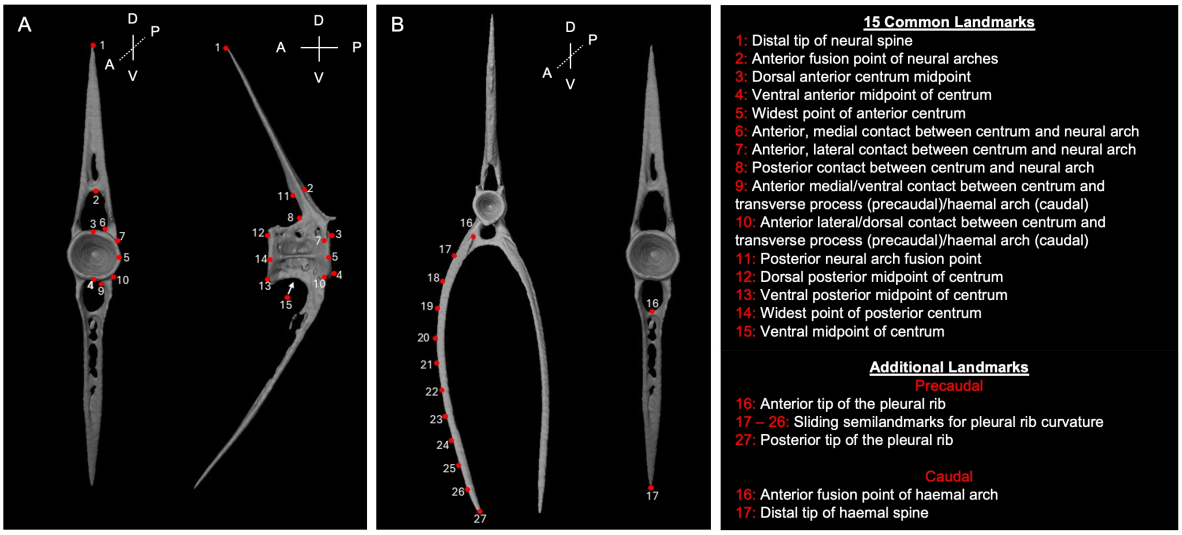

Figure 4.2: Vertebral shape landmarking scheme. (A) Caudal vertebrae landmarked with the 15 landmarks common to precaudal and caudal vertebrae, anatomical definitions for each point are shown in the inset. (B) Precaudal (left) and caudal (right) vertebrae, showing additional landmarks placed to capture shape of precaudal and caudal vertebrae. Orientations of all models is indicated with a compass (A, anterior, P, posterior, D, dorsal and V, ventral). Figure adapted with permission from Hannah Ugboma.

Extraction of Linear Measures

Whilst our primary focus was on geometric morphometric analysis, I also extracted several linear measurements to address unresolved questions from previous work. In 'African Cichlid Lake Radiations Recapitulate Riverine Axial Morphologies Through Repeated Exploration of Morphospace', I argued that body elongation in cichlids could be driven by changes in centrum aspect ratios and by increased intervertebral distances, with more elongate species evolving longer vertebral centra and longer intervertebral spacing. Therefore, I extracted two linear measurements: centrum aspect ratios, which quantify the ratio between the anteroposterior length and dorsoventral width of each vertebra; and intervertebral distances, which measure the spacing between adjacent vertebrae.

For all three precaudal and caudal vertebrae I calculated a centra aspect ratio, using the natural log-transformed anteroposterior length and dorsoventral width. To extract a length measure Euclidean distances were calculated between three pairs of landmarks that marked corresponding points on the anterior and posterior cones of the centra (landmarks 3–12, 5–14 and 4–13), respectively (see Figure 4.2). The mean ln[length] was used as the length of the centrum for each respective vertebrae. Dorsoventral widths were calculated using the Euclidean distance between landmark pairs 3–4 and 12–13, respectively (see Figure 4.2). The mean log-transformed distance was taken and the aspect ratio was calculated by subtracting the width from the length (ln[Centrum Length]-ln[Centrum Width]).

To estimate the intervertebral distances (IVDs) Euclidean distances were calculated between adjacent cone landmarks—either posterior-to-anterior or anterior-to-posterior, depending on vertebral orientation—using landmark pairs 3–12, 5–14, and 4–13. For each individual, I computed the natural logarithm of each intervertebral distance and then averaged these values within the precaudal and caudal domains separately. To obtain a single intervertebral distance value per species, the mean precaudal and mean caudal ln[IVD] values were themselves averaged. ln[IVD] scaled positively with specimen length, indicating that longer specimens had greater intervertebral distances (Figure 4.3A). To account for body size, we calculated relative IVD by subtracting ln[Specimen Length] from ln[IVD] (i.e., relative IVD = ln[IVD] - ln[Specimen Length]). However, even after this correction, relative IVD increased with body size (Figure 4.3B), suggesting positive allometry of IVD with respect to specimen length. Therefore, even after accounting for shared ancestry, larger-bodied species have disproportionately longer intervertebral distances which allometrically scale with species length. Despite this residual scaling relationship, we used relative IVD values for subsequent analyses, as they better accounted for specimen-specific body size differences.

Phylogenetic Generalised Least Squares

To evaluate the evolutionary relationships among centrum aspect ratio, intervertebral distance (IVD), total vertebral counts, and whole-body aspect ratio, and to assess whether centrum aspect ratios and IVDs contribute to body elongation, we used phylogenetic generalized least squares (PGLS) implemented via the *pgls* function in the R package *caper* (v1.0.1) [Orme et al., 2018]. We also fit additional models to test for associations between our univariate traits and multivariate shape principal components (PCs; see below). Since our shape PCs were already phylogenetically corrected, we instead accounted for phylogeny in the univariate traits by extracting residuals from intercept-only PGLS models. Residuals from these intercept only models were then used as a response variable in an ordinary least squares (OLS) model, with the multivariate space PCs as predictors. To

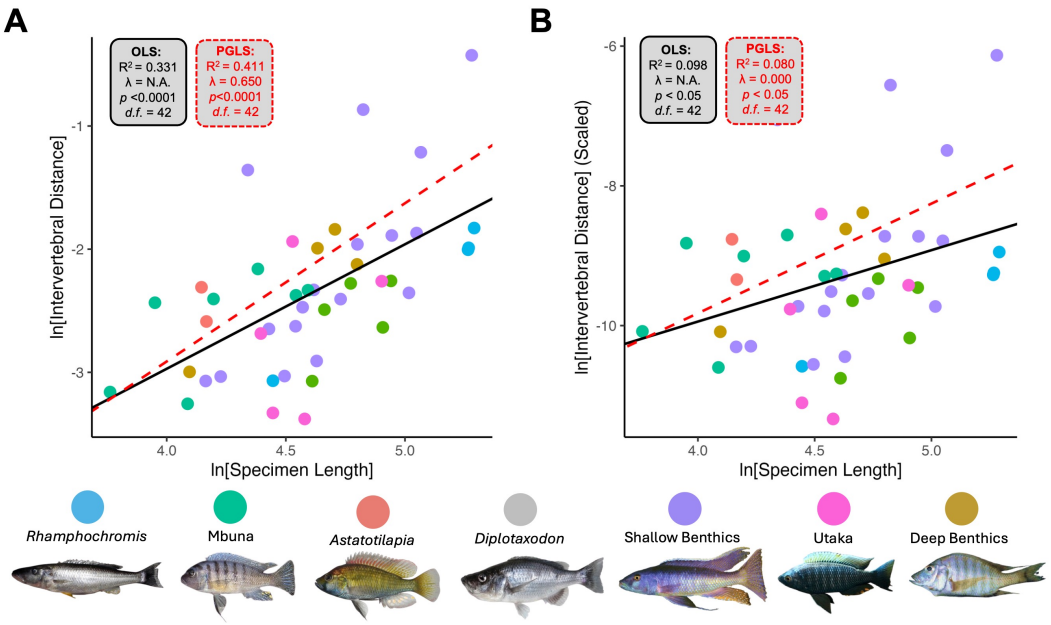

Figure 4.3: Intervertebral distances (IVDs) scale allometrically with specimen length. (A) Scatterplot of ln-transformed intervertebral distances (ln[IVD]) against ln[Specimen Length]. (B) Scatterplot of relative IVD (ln[IVD] – ln[Specimen Length]) against ln[Specimen Length]. Ordinary least squares (OLS) regressions are shown as black solid lines, and phylogenetic generalized least squares (PGLS) regressions are shown as red dashed lines. Species are grouped by ecomorphology, with representative images shown for each ecomorphological group. Image credits: *Rhamphochromis esox* (George Turner); Mbuna, *Maylandia zebra* (Callum Bucklow); *Astatotilapia calliptera* (George Turner); *Diplotaxodon Greenwoodi* (Ad Konings); Shallow Benthic, *Champsochromis caerelus* (Ad Konings); Utaka, *Copadichromis virgainlis* (Ad Konings); Deep Benthic, *Alticorpus macrocleithrum* (George Turner).

account for phylogenetic signal in the trait covariance in our PGLS models, we estimated Pagel's λ branch transformation parameter [Pagel, 1997, 1999] by maximum likelihood. Pagel's λ measures the influence of phylogeny on trait covariance, where $\lambda = 1$ suggests that the covariance evolves according to Brownian motion along the phylogenetic tree. Values between 0 and 1 indicate varying degrees of phylogenetic influence, with higher values reflecting stronger phylogenetic signal in the trait covariance.

General Procrustes Analysis

To test whether vertebral shape (i.e., geometric variation) represents a source of adaptive divergence in Lake Malawi cichlids, we first needed to quantify the shape variation and remove effects of size, orientation, and position using Generalized Procrustes Analysis (GPA). We calculated Procrustes-aligned coordinates by General Procrustes superimposition using the *gpagen* function in the R package *geomorph* (v4.0.6) [Baken et al., 2021]. Alignments were iterated 100 times and were obtained by maximizing Procrustes distance, rather than minimizing bending energy, in order to preserve biologically meaningful shape

variation across specimens. This analysis was repeated for the regionalisation analysis, albeit with just the standard 15 landmarks for all the vertebrae. For precaudal vertebrae, we defined landmarks 18-26 as semilandmarks that we defined to slide between the fixed anterior and posterior tip of the pleural rib (Figure 4.2). Aligned coordinates for each vertebrae were then used to calculate a mean precaudal and caudal vertebral shape for each specimen using the *mshape* function also in *geomorph* (v4.0.6) [Baken et al., 2021].

Phylogenetic Principal Component Analysis

To reduce the dimensionality of the aligned coordinates and identify major axes of shape variation, we performed a phylogenetic principal component analysis (PPCA) on the mean aligned precaudal and caudal coordinates. We pruned the phylogeny from McGee et al. [2020] to include only the species present in our dataset. PPCA was conducted using the *gm.prcomp* function in the *geomorph* package (v4.0.6) [Baken et al., 2021], implementing a generalized least squares (GLS) approach as described by Revell [2009]. To identify which coordinates contributed most to shape variation, we ranked all coordinate loadings for each of the top four PCs and extracted the ten with the highest absolute values (see Supplementary Table S2). We further visualised shape variation along each PC by plotting the species with the most negative and most positive PC scores against the consensus shape, allowing qualitative assessment of the morphological differences captured by each axis.

Since we had previously shown the importance of vertebral counts on adaptation along the benthic-pelagic axis and for active piscivores, we also wanted to test whether vertebral shape could be an adaptive substrate for adaptation to these niches too. To visualize the morphospace occupied by each group, we calculated convex hulls, with the area of each polygon representing the extent of morphospace occupation. Differences in occupied morphospace between groups were tested using the *procD.lm* function in the R package *geomorph* (v4.0.6) [Baken et al., 2021], which applies residual randomization as implemented in the *RRPP* package [Collyer and Adams, 2018]. Group differences were evaluated using 100,000 permutations, and effect sizes were assessed using Cohen's F. For analyses involving more than two groups, pairwise comparisons were conducted using the *pairwise* function, also implemented in *geomorph* (v4.0.6).

Quantitative Regionalisation of Vertebral Column

To determine the number of regions within the vertebral column, we used the *MorphoRegions* package [Gillet et al., 2024], an updated implementation of the earlier *regions* package developed by Jones et al. [2018a], which built on foundational work by Head and Polly [2015]. This approach identifies domains composed of serially homologous structures, such as vertebrae, by modelling them as segmented linear regressions. Regional

boundaries are inferred as breakpoints, estimated via maximum likelihood across all possible segment combinations, allowing for increasing model complexity without requiring *a priori* hypotheses.

To reduce dimensionality in the Procrustes-aligned shape data prior to regionalisation analysis, we conducted a principal components analysis using the *gm.prcomp* function in the *geomorph* package (v4.0.6) [Baken et al., 2021], without applying phylogenetic correction. The first five principal components accounted for approximately 95% of the total shape variation across specimens, and the remaining components were discarded as noise. These five PCs were used as input to the *calcregions* function in *MorphoRegions* [Gillet et al., 2024]. For each vertebral column, we fit two sets of models, specifying either a minimum of two or three vertebrae per region. The maximum number of regions tested was constrained by the total vertebral count and the minimum vertebrae per region. For instance, with 29 vertebrae and a three-vertebra minimum, the maximum number of regions possible was nine. Best-fitting models were selected based on the corrected Akaike Information Criterion (AICc).

4.4 Results

4.4.1 Relative Spine Placement and Rib Curvature Explain Most of the Shape Variation

The first principal component (PC) axis for precaudal and caudal vertebrae explains 39.23% and 45.38%, respectively (Figure 4.4). Examination of the loadings of the coordinates associated with the respective landmarks (see Supplementary Table S2) contributing to PC1 demonstrated that much of the variation in the two vertebral types was attributed to neural spine placement, with species scoring negatively having relatively posteriorly shifted neural spines (Figure 4.4A), where the tip of the neural spine is shifted posteriorly relative to the neural arch. Additionally, in caudal vertebrae, species scoring negatively on PC1 have posteriorly shifted haemal spines, overall representing what visually resembles a dorsoventral compression of the neural and haemal spines. Posterior shifts in the posterior tip of the pleural rib contributed positively to PC1 for precaudal vertebrae, suggesting a posterior shift in the curvature of the ribs in species scoring negatively in PC1. Therefore, PC1 for both precaudal and caudal vertebrae can be seen as a proxy for an anteroposterior positional shift of the neural, haemal, and pleural ribs.

PC2 accounted for 12.95% and 26.61% for precaudal and caudal vertebrae, respectively (Figure 4.4B). Similarly to PC1, neural spine placement contributes strongly for both precaudal and caudal vertebrae, with species scoring positively in PC2 having relatively posteriorly shifted neural spines. However, for precaudal vertebrae species scoring

negatively on PC2 have relatively curve spines, indicated by the relative positioning of landmarks 19–21.

PC2 for the caudal vertebrae appears to reflect relative allometric scaling of the centra. The centra of *Astatotilapia gigliolii*, which scores most positively along PC2, are relatively compressed, while *Rhamphochromis ferox*, a considerably larger species, scores low on this axis and exhibits relatively larger caudal centra. This suggests that PC2 captures shape variation associated with size differences, despite overall size having been removed through Procrustes alignment.

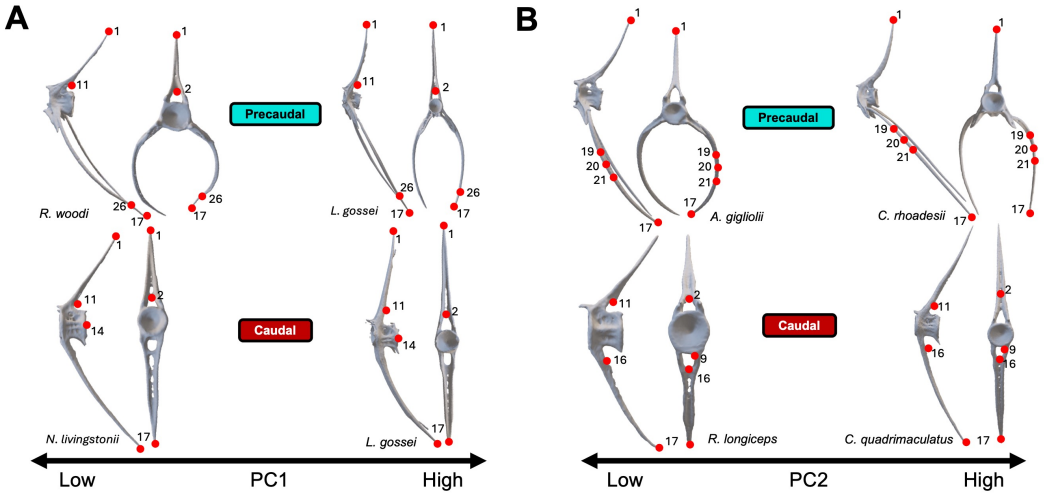

Figure 4.4: Top five landmarks contributing to PC1 and PC2 for precaudal and caudal vertebrae. A representative precaudal (top) and caudal (bottom) vertebrae is shown for each species at the extreme of the respective principal component for each vertebrae. Landmarks which contribute significantly to each PC are indicated. Note that this shows the top 5 landmarks, not the coordinate ranks. Landmarks 19-21 represent sliding landmarks and their positions have been shifted relative to their actual placement to demonstrate that the part of the shape variation being captured is curvature of the pleural rib. Some landmarks are shared between PC1 and PC2 for the same vertebral type. This is not an error but rather a consequence of different coordinates (X,Y,Z) for that landmark contributing to each PC (see Supplementary Table S2).

4.4.2 Ecomorphological Groups Segregate According to Vertebral Shape Morphology

We found significant differences in vertebral morphospace occupation in PC1 and PC2 between ecomorphological groups for both the precaudal and caudal vertebrae, respectively (Figure 4.5A, B). Both precaudal (MANOVA, $R^2 = 0.630$, $Z = 6.40$, $p < 0.0001$) and caudal (MANOVA, $R^2 = 0.449$, $Z = 5.30$, $p < 0.0001$) vertebral shape variation differed significantly between ecomorphological groups, suggesting that these groups are distinguishable, at least in part, by vertebral morphology. We found multiple signifi-

cant differences between groups in occupied vertebral shape morphospace (see Supplementary Tables S3, S4). Deep-water benthic species ("deep benthics") and members of *Rhamphochromis* occupied relatively distinct axial morphospaces for both precaudal and caudal vertebrae. Deep-water benthic species are typically found below 50 m, a "twilight" zone with very little visible light [Bucklow et al., 2024], where they associate with the substrate (hence benthic) [Malinsky et al., 2018]. For precaudal vertebrae, the deep benthics loaded positively in both PC1 and PC2, suggesting that they tend to have a relatively straight neural spine, deviating minimally from the neural arches and have relatively straight pleural ribs (see *Lethrinops gossei* in Figure 4.4A). In contrast, *Rhamphochromis* are a genus of piscivores adapted to the pelagic-limnetic zone of Lake Malawi [Hahn et al., 2017]. These contrasting ecologies suggest that evolutionary modification of vertebral shape has been important to the diversification of Lake Malawi cichlids, and may have been particularly critical in adaptation along the benthic–pelagic axis and for active, pursuit predators.

We found significant differences in occupation of vertebral shape morphospace for adapatation along the benthic-pelagic axis. Presence along the benthopelagic axis explained a small, but nonetheless significant amount of the variation in vertebral shape morphology in PC1 and PC2 for both precaudal (MANOVA, $R^2 = 0.204$, $Z = 2.86$, $p < 0.01$) and caudal ($R^2 = 0.177$, $Z = 2.82$, $p < 0.001$ vertebrae (see Supplementary Figure S1A, C). We found no difference between benthopelagic and demersal species in occupied axial morphospace (PC1 and PC2) for either precaudal or caudal vertebrae (see Supplementary Figure S1B, D). However, pelagic species were significantly different from both benthopelagic and demersal species. Pelagic species clustered in a region of morphospace relatively low in PC1 and PC2 for precaudal and caudal vertebrae, respectively. Perhaps unsurprisingly, given that all of the *Rhamphochromis* species are both pelagic and piscivorous, we found that piscivores generally score more negatively in PC1 and PC2 for precaudal (MANOVA, $R^2 = 0.235$, $Z = 3.58$, $p < 0.00001$) and caudal (MANOVA, $R^2 = 0.161$, $Z = 3.12$, $p < 0.00001$) vertebrae, respectively, than non-piscivores. Therefore, both pelagic and piscivorous species, have evolved posteriorly shifted neural spines (and haemal spines, for caudal vertebrae) and evolved curvier pleural ribs and larger allometrically scaled caudal centra.

4.4.3 Vertebral Shape Evolution Correlates With Body Elongation in Lake Malawi Cichlids

We previously showed that both pelagic and piscivorous species exhibit elongated bodies, supported by high vertebral counts. Within Lake Malawi, this is exemplified most dramatically by the genus *Rhamphochromis* which have evolved elongate bodies supported by very high total vertebral counts [Stiassny, 1981, Oliver, 2024]. Coincidentally, *Rham-*

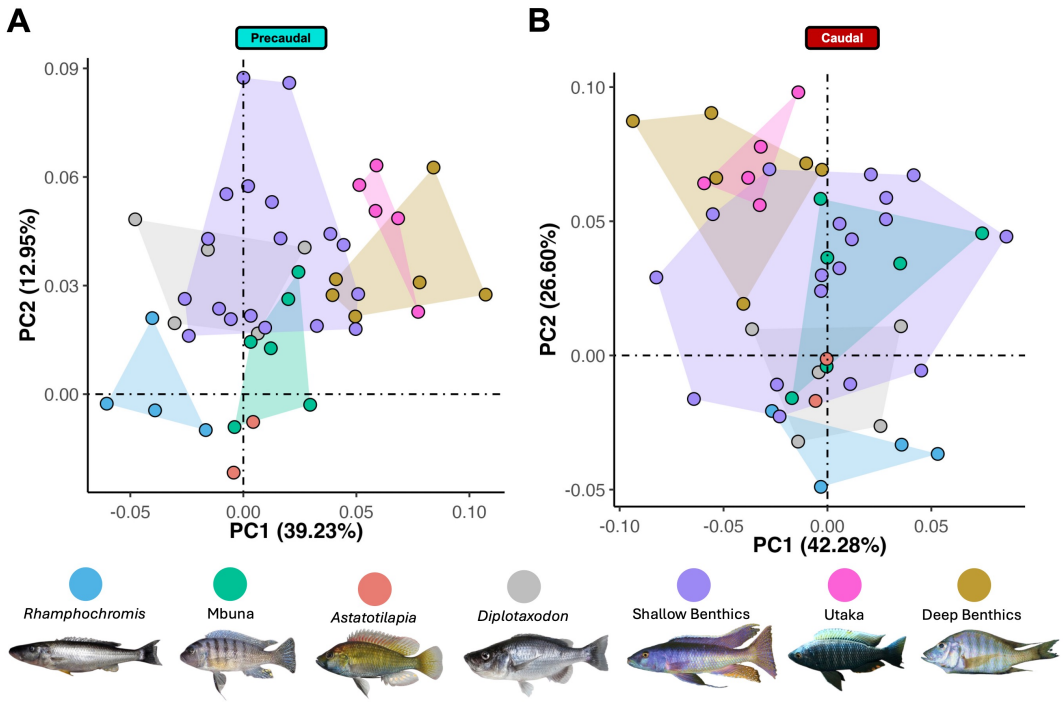

Figure 4.5: Vertebral shape morphospace occupation according to ecomorphological groupings. Phylogenetic principal component analyses of vertebral shape for (A) precaudal and (B) caudal vertebrae, showing PC1 versus PC2 for each type. The percentage of variance explained by each axis is indicated. The dotted-dashed lines denote the origin (0,0), representing the mean consensus shape across all species. Species are grouped by ecomorphological category, with convex hulls outlining the morphospace occupied by each group. Image credits: *Rhamphochromis esox* (George Turner); Mbuna, *Maylandia zebra* (Callum Bucklow); *Astatotilapia calliptera* (George Turner); *Diplotaxodon Greenwoodi* (Ad Konings); Shallow Benthic, *Champsochromis caerelus* (Ad Konings); Utaka, *Copadichromis virgainlis* (Ad Konings); Deep Benthic, *Alticorpus macrocleithrum* (George Turner).

phochromis species occupy a distinct region of vertebral shape morphospace (Figure 4.5), primarily scoring low in PC1 and PC2 for precaudal and caudal vertebrae, respectively. Therefore, we hypothesised that the evolutionary modification of vertebral shape could be driven by body elongation. Consistent with the whole subfamily (see above), residual ln[Length]-ln[Depth] values exhibited strong phylogenetic signal ($\lambda = 0.925$), indicating that variation in body elongation is highly structured by phylogeny. We found moderate negative correlations between both precaudal PC1 (Figure 4.6A, $R^2 = 0.451$, $\beta_1 = -2.71$, $p < 0.0001$, $d.f. = 44$) and caudal PC2 (Figure 4.6B, $R^2 = 0.553$, $\beta_1 = -3.11$, $p < 0.0001$, $d.f. = 44$) with the residuals of ln[Length]-ln[Depth], suggesting that negative scores in both precaudal PC1 and caudal PC2 are associated with more elongate fusiform bodies. Therefore, posterior shifts in the position of the neural spines (precaudal PC1 and caudal PC2), posterior shifts of the haemal spine and relative proportions of the caudal centra (caudal PC2), and increased curvature of the pleural ribs (precaudal PC1) are associated

with body elongation in Lake Malawi cichlids.

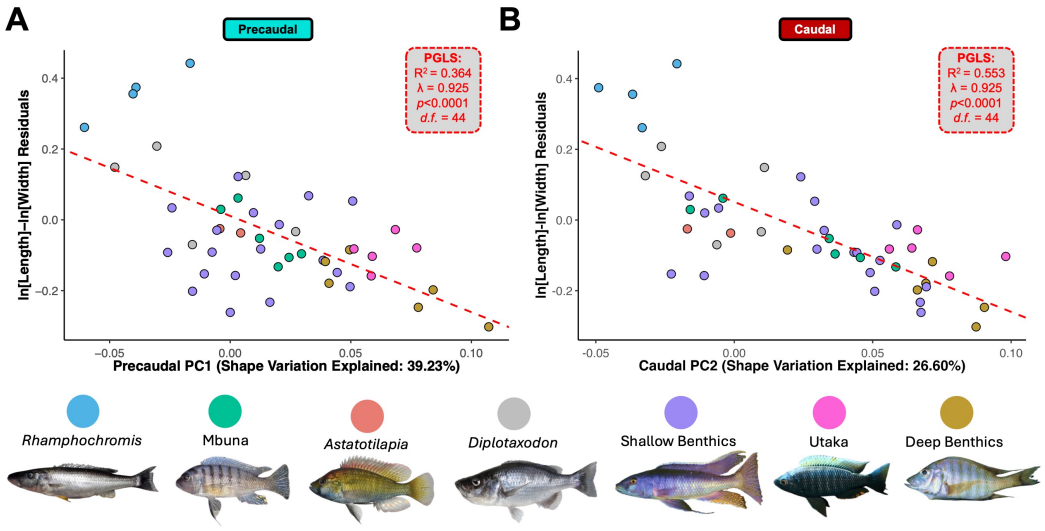

Figure 4.6: Vertebral shape is strongly associated with body elongation. Scatterplots of phylogenetically corrected residuals (from $y \sim 1$) for log-transformed body elongation (ln[Length] - ln[Depth]) plotted against precaudal PC1 (A) and caudal PC2 (B). The percentage of variance explained by each axis is indicated. Red dashed lines represent phylogenetic regression fits, with model coefficients shown in dashed red boxes. Note that λ values shown represent the value estimated for the intercept only model for log-transformed body elongation (ln[Length] - ln[Depth]). Species are coloured by ecomorphological group, with representative images provided for each group. Image credits: *Rhamphochromis esox* (George Turner); Mbuna, *Maylandia zebra* (Callum Bucklow); *Astatotilapia calliptera* (George Turner); *Diplotaxodon Greenwoodi* (Ad Konings); Shallow Benthic, *Champsochromis caerelus* (Ad Konings); Utaka, *Copadichromis virgainlis* (Ad Konings); Deep Benthic, *Alticorpus macrocleithrum* (George Turner).

4.4.4 Centra Elongation and Intervertebral Spacing Has Not Contributed to Body Elongation

Consistent with the rest of the subfamily, we found a positive correlation between ln[Total Count] and ln[Length] - ln[Depth] (Figure 4.7A, $R^2 = 0.451$, $\beta_1 = 1.848$, $\lambda = 0.516$, $p < 0.0001$, $d.f. = 42$). The slope coefficient (β_1) is greater than 1.00, suggesting that both vertebral count and body aspect have scaled non-linearly as Lake Malawi cichlids diversified, with the magnitude of the increase in body aspect ratio decreasing in lineages with already relatively high vertebral counts.

We found a weak but statistically significant negative correlation between centrum aspect ratio and ln[Total Count] (Figure 4.7B, $R^2 = 0.122$, $\beta_1 = -0.626$, $p < 0.05$, $d.f. = 42$), suggesting that lineages with increased vertebral counts have evolved more square-shaped centra. The negative slope ($\beta_1 = -0.626$) from the log-log model indicates that centrum aspect ratio decreases disproportionately as vertebral count increases. This

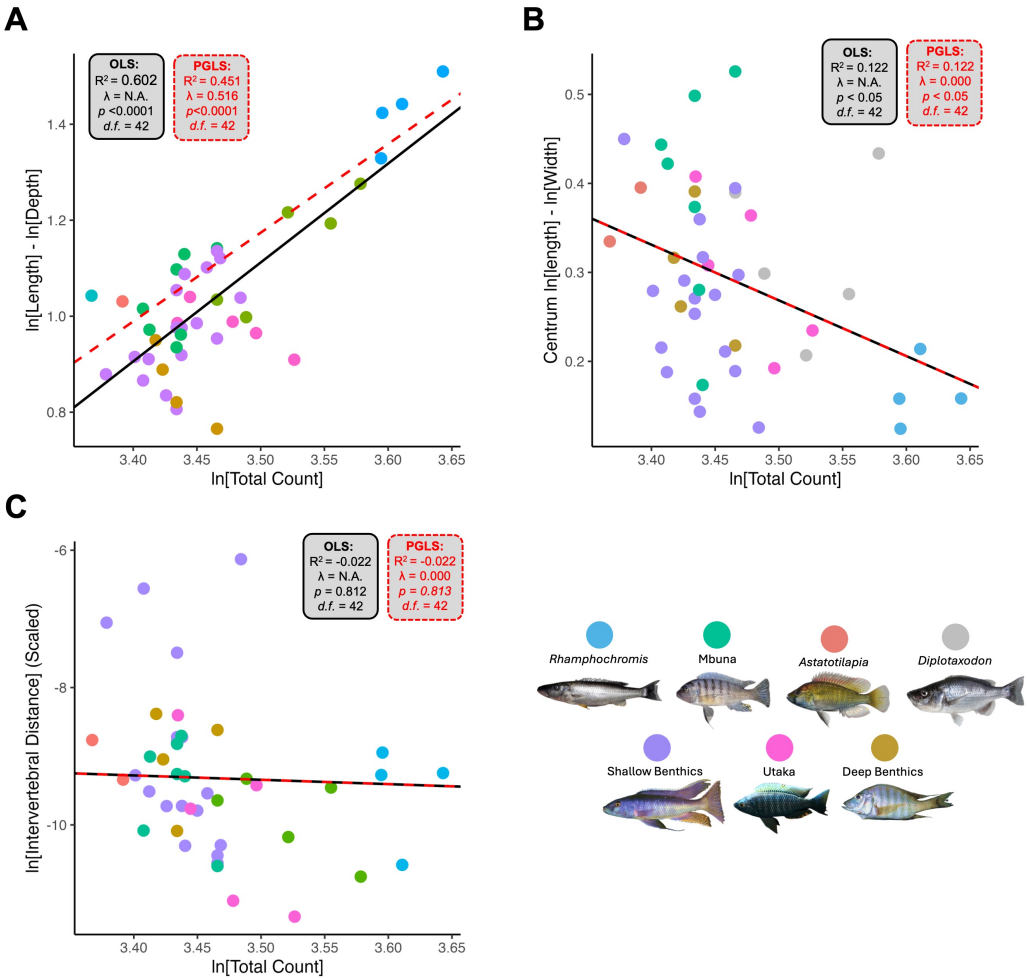

Figure 4.7: Centra elongation and intervertebral spacing have not contributed to body elongation. Scatterplots showing relationships between (A) ln[Total Count] and ln[Length]–ln[Depth] (body aspect ratio), (B) mean centra aspect ratio (calculated as centra ln[Length] – ln[Width]), and (C) mean ln[Intervertebral Distance] scaled to specimen length. Ordinary least squares (OLS) regression lines are shown in black, with coefficients in black boxes. Phylogenetic generalized least squares (PGLS) fits are shown as red dashed lines, with coefficients in dashed red boxes. For (B) and (C), OLS and PGLS fits were statistically indistinguishable (ΔAIC < 3). Species are coloured by ecomorphological group, with representative images shown for each group. Image credits: *Rhamphochromis esox* (George Turner); Mbuna, *Maylandia zebra* (Callum Bucklow); *Astatotilapia calliptera* (George Turner); *Diplotaxodon Greenwoodi* (Ad Konings); Shallow Benthic, *Champsochromis caerelus* (Ad Konings); Utaka, *Copadichromis virgainlis* (Ad Konings); Deep Benthic, *Alticorpus macrocleithrum* (George Turner).

suggests that lineages with more vertebrae have evolved not only more square vertebral centra, but that the reduction in aspect ratio increases when vertebral counts are already relatively high. Notably, however, we did not find a significant correlation between scaled intervertebral distance (IVD) and ln[Total Count] (Figure 4.7C; $R^2 = -0.022$, $\beta_1 = -0.634$, p = 0.813, d.f. = 42). In fact, ln[Total Count] performs worse as a predictor than simply using the mean of the scaled IVD ($R^2 = -0.022$). Therefore, the addition of vertebrae and, by extension, body elongation is not accompanied by an increase in intervertebral distance.

While body aspect ratio was significantly predicted by an additive linear model including ln[Total Count], scaled IVD, and centrum aspect ratio as fixed effects ($R^2 = 0.424$, $\lambda = 0.560$, $p < 0.0001$, *d.f.* = 40), only ln[Total Count] contributed significantly to the model ($\beta = 1.867$, $p < 0.0001$). The contributions of scaled IVD ($\beta = 0.0139$, $p = 0.313$) and centrum aspect ratio ($\beta = 0.051$, $p = 0.754$) were negligible. Therefore, body elongation appears to be primarily associated with an increase in vertebral number, rather than elongation of individual centra or increased spacing between vertebrae. As a result, the remaining variation in body aspect ratio not explained by vertebral count cannot be attributed to differences in centrum aspect ratios or intervertebral spacing. As a result, at least in Lake Malawi cichlids, this variation is likely driven by additional factors likely unrelated to the axial skeleton.

4.4.5 Multiple Regions are Nested Within the Precaudal and Caudal Domains

Determination of the number of regions within the vertebral column, based on vertebral shape variation, revealed the presence of multiple discrete domains along its length (Figure 4.8). The number of inferred regions ranged from four in *Tropheops tropheops* to seven in *Rhamphochromis sp.* 'Chilingali'. Across all best-fitting models, the modal number of regions was five (observed in 10 out of 14 cases), suggesting that alternative models may represent poorer fits to the data. Notably, we did not recover a strict precaudal–caudal distinction in any of the species analysed. Instead, our results indicate that both precaudal and caudal domains are composed of multiple, nested sub-regions. While the precise number of nested regions varied slightly among species, the most frequently recovered pattern consisted of two regions within the precaudal domain and three within the caudal domain. The three nested caudal regions are broadly consistent with the presence of '*true*' caudal vertebrae, pre-ural and ural vertebrae, as previously described in *Astatotilapia burtoni* [Woltering et al., 2018]. The repeated recovery of three distinct caudal sub-regions across species suggests a common pattern of regionalisation, despite variation in total vertebral count or body shape.

Curiously, however, only *Lethrinops gossei* and *Copadichromis quadrimaculatus* ex-

hibited a breakpoint at the expected precaudal/caudal boundary (see Figure 4.8, dashed black lines). This suggests that the precaudal/caudal transition is likely a genuine anatomical feature of the cichlid axial skeleton. However, variation in vertebral shape, or noise introduced in the shape data, may obscure its consistent detection in other species. This may be particularly true for *Rhamphochromis sp.* 'Chilingali', which has a notably higher vertebral count (36) compared to the other species analysed (which range from 29 to 32). The increased number of vertebrae could introduce additional shape variation, potentially inflating the number of regions inferred by the model. Including additional *Rhamphochromis* species in future analyses may help clarify whether this reflects true biological modularity or an artefact of increased axial complexity.

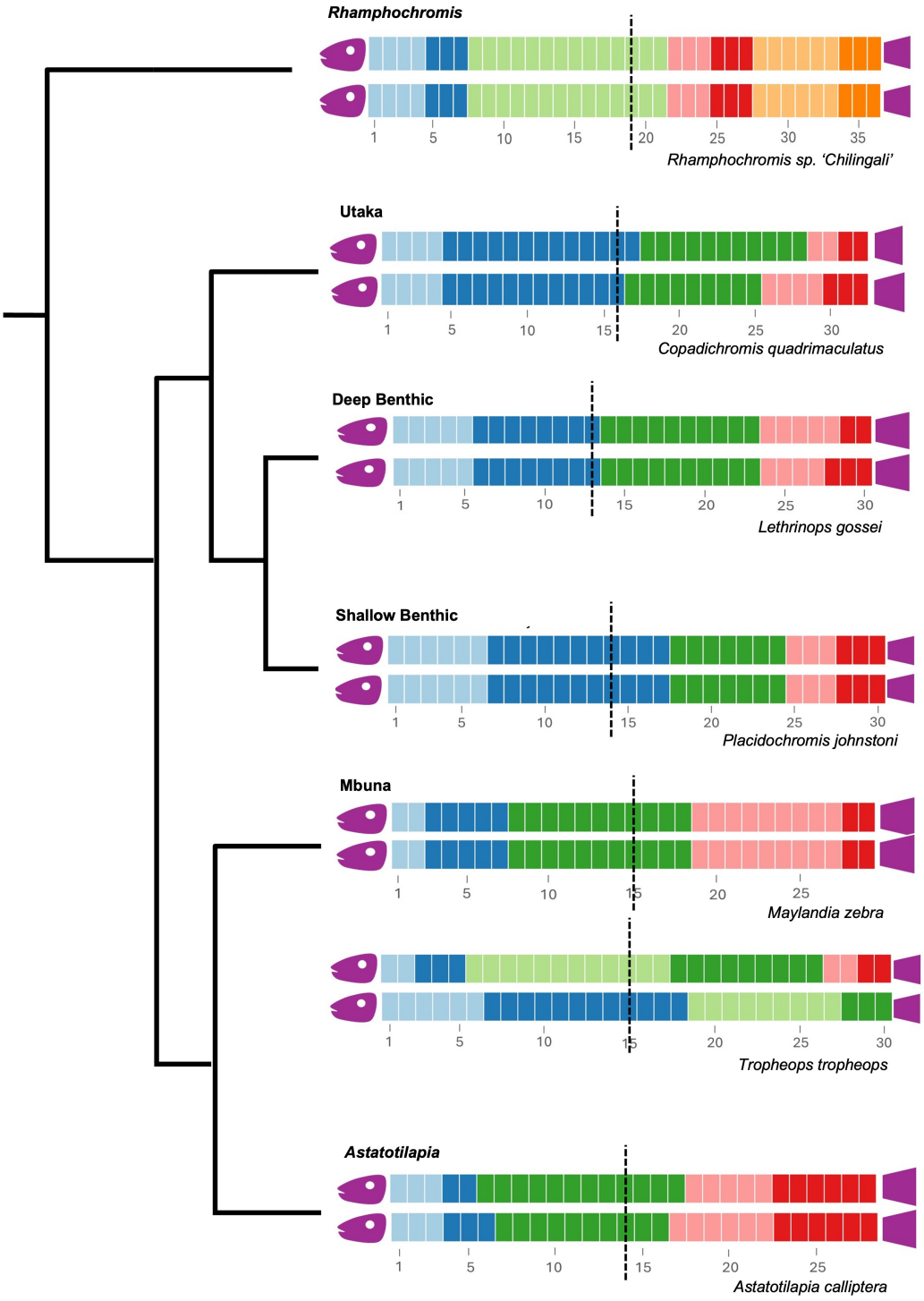

Figure 4.8: Multiple regions are nested within the broader precaudal and caudal domains. A cladogram of each ecomorphological group in Lake Malawi (excluding Diplotaxodon) is shown, based on the phylogeny published by Malinsky et al. [2018], with species names indicated for each lineage. For each lineage, a schematic representation of the vertebral column is provided, with regions colour-coded. The top row of schematics shows the best-fitting model results assuming a minimum of two vertebrae per region, while the bottom row reflects results with a three-vertebra minimum, as determined by AICc values (see Methodology). Dashed black lines indicate the expected position of the first caudal vertebra, defined as the first vertebra bearing a haemal arch.

4.5 Discussion of Geometric Morphometric Analysis

It would be pertinent to reiterate that the geometric morphometric analyses presented here is preliminary and ultimately requires a lot of additional work in order to build a convincing narrative. Nonetheless, three primary conclusions are apparent. Firstly, vertebral shape has been modified as Lake Malawi cichlids have diversified. Second, a significant proportion of the evolved vertebral shape change is correlated with elongation of the body, suggesting a role for the modification of vertebral shape changing the body aspect ratio. Finally, at least in the cichlid vertebral column, multiple domains are nested within the precaudal and caudal domains. Therefore, despite the apparent homogenisation of shape along the anterior-posterior axis, the primary distinction between precaudal and caudal domains is overly simplistic and cichlids (indeed likely teleosts [De Clercq et al., 2017]) have vertebral column regionalisation potentially as complex as tetrapods.

The next steps will seek to investigate the macroevolutionary dynamics that underpin the evolution of shape variation. Similar to our analysis of ln[Total Count] evolution, we will need to test whether vertebral shape variation has been shaped by selection during the diversification of Lake Malawi cichlids, estimate rates of evolutionary change, and evaluate whether different lineages have evolved toward distinct vertebral shape optima. These multivariate comparative analyses can be implemented using the R package *mvmorph* [Clavel et al., 2015]. Before undertaking this analysis, however, it would be prudent to increase the sample size to better represent the phylogeny. Several additional species in the μCT-scan dataset [Bucklow et al., 2024] were not segmented due to time constraints. Looking ahead, automated segmentation tools such as SPROUT (Semi-automated Parcellation of Region Outputs Using Thresholding) may help streamline this process for future analyses [He et al., 2024].

A closer examination of noise in the regionalisation analysis will be essential. It is possible that retaining 95% of the shape variation (see Methodology) may have included significant noise, which could partly explain our failure to recover a strict precaudal-caudal boundary in most species. In addition, we will need to confirm the identified regions and determine whether these regions are homologous across species. While vertebral counts are expected to vary between species—and by extension, between regions—it remains unclear how these domains relate to one another, if at all. The value of this analysis lies not only in identifying regionalisation within a given species, but in assessing whether those regions are comparable across taxa. This will require careful, comparative analysis of vertebral morphology. Once we are confident in our approach, we can extend this work to other teleostean clades to investigate broader patterns of vertebral column regionalisation.

5 General Discussion

5.1 Is Axial Evolution Constrained in Lacustrine Environments?

The elevated evolutionary rate in Lake Tanganyika suggests that increased variance in vertebral counts, and more broadly, axial morphology, is not simply a consequence of increased time available for diversification in Lake Tanganyika. In contrast to Lake Tanganyika, Lake Malawi and Victoria are young, estimates place both the lakes on the scale of several hundred thousand years [Malinsky et al., 2018], if not younger [Meier et al., 2017]. Uyeda et al. [2011] previously demonstrated that whilst rapid, short term (<1myrs) evolution can occur, and our analysis clearly indicates ln[Total Count] has evolved in Lake Malawi, the rates may be constrained, where neither of the radiations may have had sufficient time to accumulate variation. Over longer intervals (>1myrs), such as that of Lake Tanganyika, this pattern of bounded evolution capitulates to a pattern of increasing divergence with time. Therefore, the increased rate in Lake Tanganyika may suggest that sufficient time has lapsed for constraints placed on the evolution of vertebral counts (and axial morphology) to be broken. In contrast, preliminary evidence suggested that the best fitting model for ln[Total Count], ln[length]-ln[Depth] and ln[Precaudal]-ln[Caudal] evolution within Lake Malawi was the exponentially accelerating model of Blomberg et al. [2003] (data not shown), suggesting that axial morphospace in Lake Malawi is still being explored and has not yet had sufficient time to reach an equilibrium or encounter evolutionary constraints that limit diversification. It should be noted, however, that the evolutionary rate of total vertebral counts in riverine lineages is almost twice as high as in Lake Tanganyika. This indicates that variance in total counts accumulates approximately twice as fast in riverine environments. Such a pattern may suggest that axial morphological evolution is constrained in lacustrine systems, potentially due to ecological limitations, the dynamics of rapid speciation, or a combination of the two.

Lakes and rivers likely differ in the size and nature of their adaptive zones. In this context, greater variance in riverine lineages may reflect evolutionary expansion into niche spaces that are absent or reduced in lacustrine environments. Moreover, some habitats are exclusive to either rivers or lakes (e.g., pelagic habitats are restricted to lakes [Meier

et al., 2017, Malinsky et al., 2018], whereas rheophilic habitats are restricted to rivers [Stiassny and Alter, 2015]). Although we detected increased trait evolution rates in pelagic lineages, these were seven times lower than those observed in piscivores, a niche that occurs in both riverine and lacustrine systems. In simpler terms, while the vertebral column, and axial morphology more broadly, play an important role in adaptation to lacustrine niches, it may be even more critical for riverine lineages. In addition, deciphering the role that speciation may play in the evolution of axial morphology may be better disentangle the relationship between riverine and lacustrine constraints. If, for example, the evolution of total vertebral counts is associated with speciation in riverine, but not lacustrine lineages, it may suggest that axial trait evolution is more tightly linked to the diversification processes in riverine systems. Speciation rates are highest in the lacustrine radiations [McGee et al., 2020], and given the rapid divergence observed in Lakes Malawi and Victoria, it is plausible that vertebral counts are constrained by the limited number of generations that occur before species isolation is complete. Whilst we did not explicitly test whether the evolution of vertebral counts and axial morphology has increased speciation rates and/or decreased extinction rates [Beaulieu and O'Meara, 2016], we did test whether total count evolution could be explained by dynamics unique to haplochromines which are extremely speciose but found weak support for these models. Nonetheless, further work integrating trait evolution and speciation may be important to elucidate the increased rate present in riverine lineages.

5.2 Developmental Constraints on Somitogenesis Canalise Vertebral Counts

Despite the evolvability of vertebral counts, our results suggest that these traits evolve at a much slower rate than would be expected if the trait were under strong directional selection. Even within piscivorous lineages, where we demonstrated that increased vertebral counts have evolved, the estimated attraction toward a higher trait optimum was extremely weak. As a result, phylogenetic half-lives are exceptionally long ($\sim$22 Myrs), far exceeding the age of the lacustrine radiations [Ronco et al., 2021, Malinsky et al., 2018, Genner and Turner, 2012, Meier et al., 2017]. Moreover, among the hypotheses tested, our best-supported model for vertebral count evolution was one in which vertebral counts evolve under distinct, linear, stochastic rates in riverine environments and within each lacustrine radiation. This could suggest that the evolution of vertebral counts is driven by stochastic drift, stabilising selection, or by directional selection where the direction of selection fluctuates over time [Felsenstein, 1988, Harmon et al., 2010]. Our results, however, support the interpretation that developmental constraints on somitogenesis itself limit the evolutionary lability of this trait. That is, while vertebral counts are clearly

capable of evolutionary change, such changes likely require that the normal constraints of somitogenesis be circumvented or modified.

We found little intraspecific variation in vertebral counts, suggesting that the fidelity of somitogenesis has remained consistent as African cichlids have diversified, despite evolutionary changes in vertebral numbers. This indicates that vertebral and somitic counts are highly canalised, making it unlikely that plasticity within somitogenesis has been under selection. Given the expected canalisation of this trait, modifying its plasticity would likely be deleterious. An increased somitic rate in *Rhamphochromis sp.* 'Chilingali' relative to *Astatotilapia calliptera*, which forms fewer somites, has been shown to contribute to higher somite counts in *R. sp.* 'Chilingali' [Marconi et al., 2023]. However, additional evidence suggests no difference in somitic rate between the two species. In fact, somitogenesis in *R. sp.* 'Chilingali' appears to occur over a longer duration (James Hammond, in prep) than in *A. calliptera*, likely due to a longer presomitic mesoderm at the onset of somitogenesis. This difference may be driven by changes in the initial conditions, such as alterations to gastrulation (Shannon Taylor, in prep). Therefore, the addition of somites in *R. sp.* 'Chilingali' is likely a result of a relatively longer presomitic mesoderm, providing more tissue to segment rather than a fundamental change in the mechanism of somitogenesis. To further elucidate the constraints on somitic fidelity and identify the key factors maintaining its canalisation across species, construction of an *in silico* model that recapitulates this intraspecific variation could be invaluable. Not only could we determine the parameters of somitogenesis that are necessary to canalise the number of somitic pairs but also investigate which are necessary to modify in order to break this developmental constraint.

5.3 Elongation of the Body Is Complex, Requiring the Co-evolution of Multiple Axial Traits

The addition of vertebrae is a common mechanism of body elongation in teleosts [Ward and Brainerd, 2007, Mehta et al., 2010, Ward and Mehta, 2010]. As in other teleostean clades, elongation has been especially important for piscivorous and pelagic species, where a more streamlined, fusiform body likely enhances swimming efficiency [Mehta et al., 2010]. Our analyses consistently show that elongation in African cichlids has partly been achieved through the addition of vertebrae. In addition, our vertebral shape analysis in Lake Malawi cichlids suggests that changes in vertebral shape have played an important role too. A significant portion of vertebral shape variation appears to have co-evolved with elongation, likely as a biomechanical response to the spatial constraints of a more fusiform body. As the body elongates, dorsoventral compression may necessitate posterior shifts in the position of neural and haemal spines, as well as pleural ribs. This pattern is

especially evident in eels, which exhibit extreme elongation and highly posteriorly shifted skeletal elements [Thieren et al., 2012, Pfaff et al., 2016, Usui et al., 2024]. Such shifts may represent a widespread biomechanical constraint on the evolution of elongate bodies in teleosts. Therefore, rather than driving elongation, modification of vertebral shape may be a consequence of body elongation, rather than specifically driving its elongation.

In African cichlids, we have previously shown that evolutionary changes in posterior body elongation are tightly coupled to changes in cranial elongation (see Results Chapter One). However, cranial elongation appears to occur without corresponding increases in vertebral number. Therefore, body elongation in cichlids could arise through the reuse or modification of developmental programs other than those controlling axial segmentation. Curiously, however, despite previous evidence that intraspecific variation in vertebral counts could lead to advantageous phenotypic differences between individuals or populations of fish [Swain, 1992, Tibblin et al., 2016], we found no evidence that individuals with increased vertebral counts also exhibit higher body aspect ratios across the full range of body aspect ratios found in African cichlids. Therefore, intraspecific variation in vertebral counts does not scale predictably with body elongation, despite the addition of vertebrae being evolutionarily important for body elongation. Of course, it is possible that intraspecific variation does correlate with other traits that we have not considered, but it nonetheless does not explain why individuals with increased vertebral counts do not have increased body aspect ratios.

This result was particularly surprising. It suggests that intraspecific variation is decoupled from macroevolutionary patterns of body shape diversification. Therefore, at local phylogenetic scales, changes in total vertebral counts do not necessarily follow changes in body shape along long(er) branches of the phylogeny. Curiously, our data indicates that vertebral count and body aspect ratio have also scaled non-linearly: in lineages with already high vertebral counts, further increases are associated with diminishing returns in body elongation. However, even in relatively deep-bodied species with comparatively few vertebrae, individuals with increased counts show no detectable difference in the whole body aspect ratio. This implies that one of our underlying assumptions, that small incremental increases in vertebral number are sufficient to drive changes in body aspect ratio, may not always hold.

The macroevolutionary models we have applied assume these traits evolve stochastically, accumulating variation gradually over time, even if those rates differ between lineages. However, it is possible that major shifts in vertebral number and body elongation occur in larger evolutionary jumps, particularly when species colonise new niches that favour elongate morphologies. Following such shifts, the phenotype may remain stable as long as it confers sufficient fitness for that niche. These findings contribute to a broader and ongoing debate about the tempo of macroevolution, whether it is gradual and continuous or characterized by rapid shifts followed by stasis, as proposed in mod-

els of punctuated equilibrium [Pennell et al., 2014]. Regardless of its macroevolutionary plausibility, the constraint lies in whether it can occur during development. We have identified a number of species within Lake Malawi, primarily shallow benthic piscivores, such as *Champsochromis caeruleus*, that have evolved increased vertebral counts more recently than *Rhamphochromis*. Comparison of the dynamics underpinning somitogenesis in these species may further elucidate how relatively large, rapid increases in vertebral counts are developmentally feasible.

5.4 Divergent Strategies Likely Shape the Vertebrae of African Cichlids

Fast predatory fish such as barracuda or Scombriformes are known to have relatively few vertebrae compared with other similarly elongate fish [Mehta et al., 2010], opting instead to modulate the vertebral aspect ratio to generate fewer but more elongate vertebrae, which may stiffen their body axis, providing better propulsion when pursuing prey [Jimenez et al., 2023]. Notably, however, we found no evidence that more elongate vertebral centra were contributing to body elongation (at least in Lake Malawi). Indeed, vertebral centrum aspect ratios negatively correlate with the addition of vertebrae. As a consequence, *Rhamphochromis* have relatively square centra and indeed the least elongate centra within the radiation. In contrast to barracuda and Scombriformes, however, it seems unlikely that *Rhamphochromis* or indeed other ecologically similar clades such as *Bathybates* (endemic to Lake Tanganyika [Ronco et al., 2020]) might be participating in continual swimming like barracuda or Scombriformes. Instead, the decrease in centra aspect ratio may be related to adapting to pelagic depths. The modification of vertebral shape, including the evolution of shorter centra, has been correlated with adaptation to pelagic depths in teleosts [Baxter et al., 2022] and collection of depth preference data could further disentangle the relationship between depth preference and vertebral shape modification.

Curiously, however, the species with the largest centrum aspect ratio is *Chindongo elongatus*, a rock-dwelling mbuna with average vertebral counts but a surprisingly elongate body. It is possible that elongating centra is only advantageous up to a threshold number of vertebrae or beyond a certain whole-body aspect ratio. In contrast, other taxa, such as *Gobiocichla* and *Teleogramma*, are extremely elongate yet have considerably fewer vertebrae than would be predicted given their body shape. These demersal, rheophilic species inhabit the bottoms of fast-flowing rivers, often burying themselves in the substrate [Stiassny, 1990, Stiassny and Alter, 2015]. In such environments, a rigid vertebral column, for example by having elongate centra, may provide mechanical stability for substrate burial. A broader survey of centrum aspect ratios across the subfamily could

clarify the importance of this trait, as well as fitting careful and considerate interaction models between these axial traits could help disentangle their evolutionary relationships. Indeed, combining these data with biomechanical surveys of swimming performance could elucidate the relationship between the structure of the axial skeleton, body shape and swimming performance [Satterfield et al., 2023].

5.5 African Cichlids Provide a Model for Allometric Scaling in Teleosts

We did, however, find that intervertebral distances scale allometrically with specimen length. Larger individuals exhibit proportionally greater spacing between vertebrae even after correcting for overall size. This relationship is particularly notable in the genus *Rhamphochromis*, which exhibits remarkable intraspecific and interspecific size variation. *R. woodi* is among the largest cichlids in Lake Malawi, reaching standard lengths (SL) of up to 40 cm [Turner et al., 2004]. It is possible that increased body size alone confers sufficient vertebral column flexibility to facilitate the sharp twists and turns necessary for pursuing prey. However, the genus also includes much smaller taxa, such as *Rhamphochromis sp.* 'Kingiri dwarf' and *R. sp.* 'Chilingali', which are endemic to crater lakes and rarely exceed 7.5 cm and 10.6 cm SL, respectively [Turner et al., 2019, Genner et al., 2007]. Due to the limited representation of *Rhamphochromis* species in the phylogeny [McGee et al., 2020], we were unable to explore these size differences in more detail. However, it would be curious to see if this pattern is maintain in these smaller members.

Comparative work with other elongated pelagic piscivores, such as members of the genus *Bathybates* in Lake Tanganyika, which have independently evolved increased vertebral counts and body elongation [Stiassny, 1981], could further illuminate the role of axial allometry in cichlid evolution. Allometric scaling remains understudied in cichlids [Fujimura and Okada, 2008], and it is worth noting that our μCT scan dataset includes nearly all known *Rhamphochromis* [Bucklow et al., 2024], offering a strong foundation for such analyses. Nonetheless, the exceptional size disparity across both genera presents an intriguing opportunity for future studies on allometric scaling not just of axial morphology but a large breadth of traits.

6 Conclusion and Future Directions

6.1 Cichlids as Models for Axial Skeleton Evolution and Development

Remarkable diversity in vertebral counts has arisen in African cichlids, and increases in vertebral count have been important in driving evolution of elongate body forms in both riverine and lacustrine lineages in African cichlids. Interestingly, however, despite the occupation of axial morphospace broadly correlating with the age of the cichlid adaptive radiations, this divergence time alone cannot account for the diversity in total vertebral counts that have repeatedly evolved in these water systems.

Vertebral counts are highly evolvable and changes in vertebral count can occur rapidly. The addition of vertebrae has been particularly important in driving elongation of the fusiform body which has been important in adapting to multiple ecological niches. However, while vertebral addition plays a role in body elongation, additional mechanisms independent of axial elongation are also important in body elongation and despite the evolvability of vertebral counts, intraspecific variation in vertebral counts has been canalised throughout cichlid diversification, suggesting that the variability of somitogenesis has not been the source of this evolvability.

Diversification of vertebral shape, particularly in Lake Malawi cichlids, highlights the complexity of axial trait evolution, with body elongation requiring vertebral addition and necessitating vertebral shape modification. In addition, at least in the cichlid vertebral column, multiple domains are nested within the precaudal and caudal domains. Despite the apparent homogenisation of vertebral shape within the teleostean vertebral column, the primary distinction between precaudal and caudal domains is overly simplistic.

The results presented demonstrate that African cichlids serve as powerful models for understanding the evolution of the vertebral column, offering valuable insights into the complex interplay between vertebral count, shape diversification, and body elongation. By revealing how these traits co-evolve within rapidly radiating lineages, this study highlights the integrative nature of axial patterning and its evolutionary flexibility. These insights not only deepen our understanding of vertebral evolution in cichlids but also lay the groundwork for exploring the broader dynamics of axial trait evolution across teleosts

and provide a foundation for future research into the genetic mechanisms underlying these processes.

6.2 Quantitative Trait Locus (QTL) Analysis of Hybrid Crosses

Future work will focus on hybrid lines that we have generated. Unfortunately, time constraints placed on my DPhil have prevented their full inclusion in this thesis, as I had initially hoped. We have generated two interspecific—indeed, across genus—hybrid crosses of Lake Malawi cichlids: between the rock-dwelling mbuna, *Maylandia zebra*, and the riverine generalist *Astatotilapia calliptera*. Crucially, we successfully hybridised the species in both directions: *Maylandia zebra* (♂) x *Astatotilapia calliptera* (♀); *Astatotilapia calliptera* (♂) x *Maylandia zebra* (♀), see Figure 6.1 and we are currently raising the F2 offspring of both of these crosses.

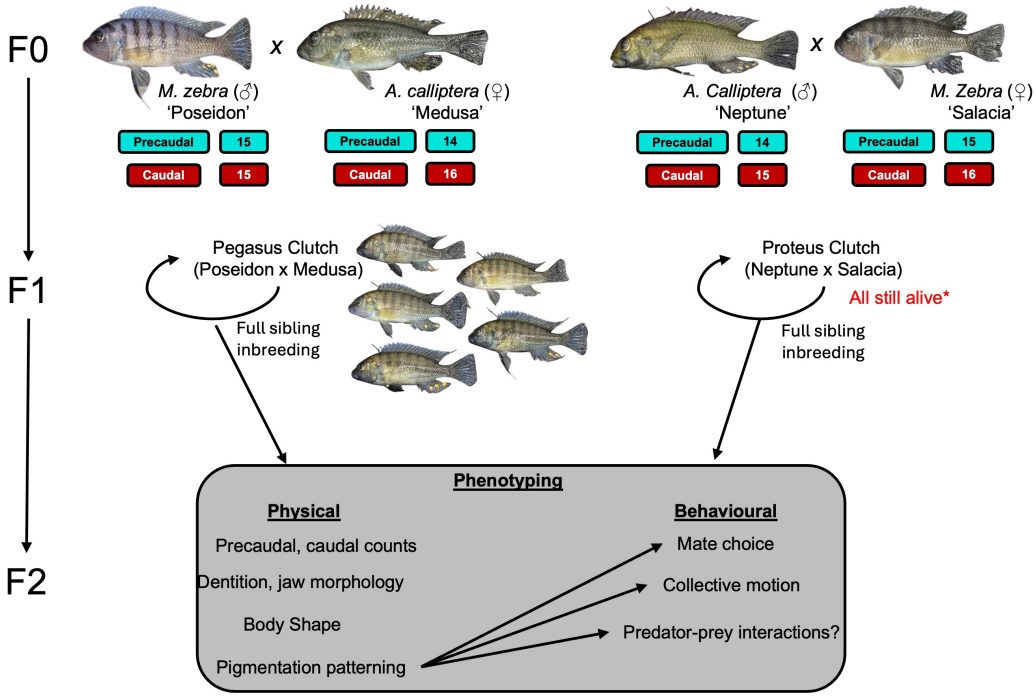

Figure 6.1: Flowchart illustrating the generations and crossing design used in our hybrid experiments. F_0 individuals from two parental species were crossed through natural mating to produce F_1 clutches. These F_1 hybrids, heterozygous at all loci (inheriting one allele from each parent), were maintained as isolated full-sibling families for inbreeding. Inbreeding among F_1 siblings generates F_2 offspring in which homozygosity is recovered at segregating loci. Phenotyping the F_2 hybrids allows us to identify individuals expressing parental traits, implying homozygosity at loci contributing to those traits. Representative images are shown for each generation, except for the Proteus clutch and F_2 hybrids, which are still alive.

Our initial motivation for generating these hybrids was the difference in axial phenotypes between the two species. They differ markedly in body shape, have overlapping distributions of total vertebral counts but differ in the proportions of precaudal and caudal vertebrae. These crosses thus present a unique opportunity to investigate the genetic basis of axial traits through quantitative trait locus (QTL) analysis—a method used to identify specific genomic regions associated with variation in quantitative traits. By analysing the hybrid offspring, we can identify genetic differences between parental species to map loci that influence traits such as vertebral number and regionalisation. This approach offers valuable insights into the genetic architecture of axial patterning and the broader question of how genetic variation contributes to phenotypic diversity [Husemann et al., 2017, DeLorenzo et al., 2023, Selz and Seehausen, 2019, Ehemann et al., 2024].

Previous work in Central American cichlids has shown that total vertebral counts, lateral line scale number, and the proportions of precaudal to caudal vertebrae not only co-vary but also map to overlapping QTL, suggesting these traits may be linked through shared genetic loci or common developmental mechanisms [Ehemann et al., 2024]. In the results presented here, we identify several axial traits that exhibit covariation—such as total vertebral count and body elongation, as well as coordinated elongation of cranial and post-cranial regions. These findings support the hypothesis that axial traits may be governed by shared genomic regions. We also note a striking pattern of co-evolution between lateral line scale counts and total vertebral number in Lake Malawi cichlids (Figure 6.2), pointing to a potentially conserved axis of trait integration not only within Pseudocrenilabrinae but across the cichlid family more broadly (see Supplementary Table S5 for count data). Interestingly, preliminary observations suggest asymmetry in lateral line scale number between the left and right sides of the body in some Lake Malawi species (George Turner, personal comms), raising the intriguing possibility of investigating the developmental basis of asymmetry in this system. As I argued in '*Intraspecific Variation and the Evolution of Vertebral Regionalisation in African Cichlids*', uncovering the genetic architecture of these traits is essential for understanding both their developmental origins and evolutionary dynamics. Therefore, our primary aim with the F2 hybrid population is to determine which axial phenotypes co-vary and whether they map to shared genomic loci that may underlie their development.

We are especially excited to have generated reciprocal crosses, which remains rare in cichlid QTL studies [Ding et al., 2014, Svensson et al., 2017]. The reciprocal nature of our crosses provides an opportunity to investigate sex-linked traits and maternal contributions to phenotypic development and evolution. There is a growing body of evidence that maternal inheritance [Alho et al., 2011, Tibblin et al., 2016] *and* maternal contributions to egg contents [Sun et al., 2005] are important for the development of multiple axial traits. Since we have generated hybrids in both directions, we can tease apart maternal

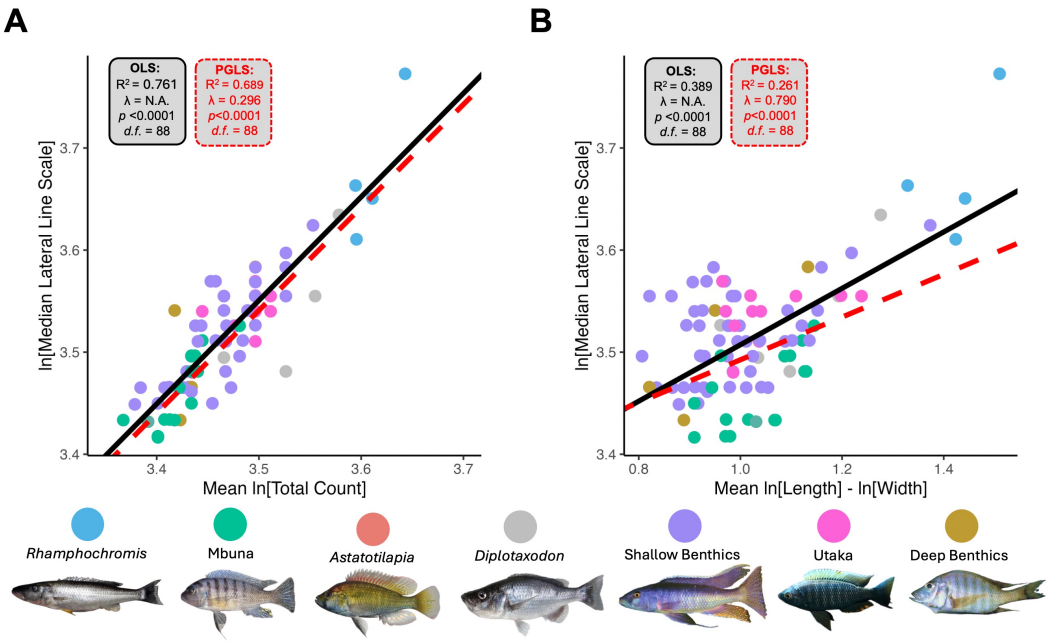

Figure 6.2: Lateral line scales, total vertebral counts and whole body aspect ratios have co-evolved in Lake Malawi cichlids. Scatterplots of ln[median lateral line scale] counts against mean ln[Total Counts] (A) and ln[Length]-ln[Depth] (whole body aspect ratio) (B). Ordinary least squares (OLS) regression lines are shown in black, with coefficients in black boxes. Phylogenetic generalised least squares (PGLS) fits are shown as red dashed lines, with coefficients in dashed red boxes. Species are coloured according to their respective ecomorphological group. Images for representative species are indicated for each group. See Supplementary Table S5 for lateral line count data. Image credits: *Rhamphochromis esox* (George Turner); Mbuna, *Maylandia zebra* (Callum Bucklow); *Astatotilapia calliptera* (George Turner); *Diplotaxodon Greenwoodi* (Ad Konings); Shallow Benthic, *Champsochromis caerelus* (Ad Konings); Utaka, *Copadichromis virgainlis* (Ad Konings); Deep Benthic, *Alticorpus macrocleithrum* (George Turner).

contributions to multiple axial phenotypes, including body shape and vertebral proportions. However, whilst our initial focus in generating these hybrids was for elucidating the mechanisms underpinning evolution of axial phenotypes, it has become increasingly apparent that our crosses provide a unique opportunity to account for sex inheritance (and maternal contributions) for a whole litany of traits. Jaw shape, dentition, fin shape and pigmentation patterning, all differ considerably between the two species and careful systematic phenotyping will be important in ensuring that the maximum number of traits can be quantified from these crosses. Thankfully, we have already defined a pipeline for μ-CT scanning multiple specimens effectively, as well as digitising the 3D models [Bucklow et al., 2024]. We were also lucky to have generated lots of large F1 specimens for the *Maylandia zebra* (♂) x *Astatotilapia calliptera* (♀) cross, that whilst we did not keep to generate F2s we did nonetheless μCT-scan to preliminarily identify traits which we could pursue. Our first short term aim will be to continue to quantify these traits and determine which traits are sufficiently different to pursue for QTL analysis, from this

preliminary analysis we can calculate the expected sample sizes of F2s required.

We were fortunate to successfully hybridise *Astatotilapia calliptera* (♂) × *Maylandia zebra* (♀), a challenging cross due to the strong mate choice preferences of *M. zebra* females, who typically favour aggressive males [Mellor et al., 2011]. While the reciprocal cross consistently produced fertilised clutches, we recovered only a single clutch from this pairing, suggesting relatively high female promiscuity in *A. calliptera*. *A. calliptera* has been hypothesised to be the sympatric ancestor of all Lake Malawi cichlids [Malinsky et al., 2018, Konings, 2016, Turner et al., 2021, Svardal et al., 2021], and is widely distributed across East African water systems, from the Rovuma River in the north to the Save River in the south. Despite this broad range and substantial intraspecific genetic diversity, the species clusters phylogenetically within the Lake Malawi radiation, forming a sister clade to the mbuna, with which it shares an excess of alleles [Malinsky et al., 2018]. An ancestral hybridisation event between the progenitors of the Lake Malawi and Lake Victoria radiations may have introduced the genetic variation necessary for these adaptive radiations [Svardal et al., 2020]. If so, the retention of promiscuous mating behaviour in *A. calliptera* may have played a role in its evolutionary success. By establishing reciprocal crosses, I aim to further investigate the role of female mate choice and its evolutionary consequences, as well as further investigate the barriers that hybridisation may have on mate choice [Svensson et al., 2017].

Anecdotally, I have noticed additional behavioural differences in the F1 crosses. Members of the 'Proteus clutch' (F1, *Astatotilapia calliptera* (♂) x *Maylandia zebra* (♀)) appear considerably more aggressive than individuals from the reciprocal cross, and also seem to spend more time shoaling. While behaviour was not the primary focus in generating these hybrids, I have nonetheless standardised rearing conditions across clutches to minimise environmental variation. Previous evidence in *Tropheus sp.* 'Caramba' (a haplochromine mouthbrooder endemic to Lake Tanganyika; [Ronco et al., 2020]) has shown that females raised without maternal mouthbrooding exhibit reduced reproductive success and lower fry survival [Novák et al., 2023]. These findings underscore the long-term, transgenerational effects of early-life social deprivation in mouthbrooding cichlids. To mitigate such effects in my study, all offspring were reared by their mothers rather than via artificial incubation ('tumbling'). The behavioural differences observed may therefore reflect underlying genetic inheritance, maternal effects via the mouthbrooding environment, or an interaction of both. My reciprocal crosses offer a valuable framework to begin disentangling how sex-specific and environmental factors shape complex behaviours. These behavioural traits could be incorporated into future phenotyping pipelines, potentially alongside variation in colour patterning [Ding et al., 2014], for which there is considerable expertise in the department and more widely in the cichlid scientific community.

6.3 Concluding Remarks

African cichlids provide an exceptionally powerful system to investigate the evolution and development of body shape, form and morphology. We have confidently demonstrated the utility of African cichlids in elucidating the macroevolutionary dynamics of vertebral column evolution, showing that the evolution of vertebral counts, shape and body elongation has been critical to the success of this remarkable subfamily. Ironically, however, the most important results presented herein have arisen as a result of their use as a model. As evolutionary biologists whilst we do become transfixed by the systems that we study, we must remember that our role is to deduce the generalisable principles, mechanisms and dynamics that underpin the evolution of life and its remarkable diversity. We must always bear this in mind.

Nonetheless, these extraordinary fish consume much of my time, passion and thought. I have been remarkably lucky to have discovered them at the beginning of my DPhil and whilst it is exceptionally naïve for me to say this: I cannot imagine my future career without them. That is not to say I will never work with different clades. There are a multitude of, primarily vertebrate, clades that I would adore to work with. Still, I suspect cichlids will always feature somewhere in this hypothetical future. What remains clear is that cichlids offer an extraordinarily powerful system for addressing a wide range of questions in evolutionary and developmental biology. And for now, at least, I have many more questions that I cannot in good conscience leave unanswered. As we attempt to understand the staggering complexity of life, it is sometimes helpful to be reminded of its enduring significance. I leave this thesis with the words of Julian of Norwich:

"*And in this he showed me a little thing, the quantity of a hazelnut, lying in the palm of my hand, as it seemed. And it was as round as any ball. I looked upon it with the eye of my understanding, and thought, 'What may this be?' And it was answered generally thus, 'It is all that is made.' I marvelled how it might last, for I thought it might suddenly have fallen to nothing for littleness. And I was answered in my understanding: It lasts and ever shall, for God loves it. And so have all things their beginning by the love of God.*" – Julian of Norwich, Revelations of Divine Love

7 Bibliography

Urara Adachi, Rina Koita, Akira Seto, Akiteru Maeno, Atsuki Ishizu, Sae Oikawa, Taisei Tani, Mizuki Ishizaka, Kazuya Yamada, Koumi Satoh, et al. Teleost hox code defines regional identities competent for the formation of dorsal and anal fins. *Proceedings of the National Academy of Sciences*, 121(25):e2403809121, 2024. doi: 10.1073/pnas.2403809121.

Dean Adams, Kosaku Yamaoka, and Daud Kassam. Functional significance of variation in trophic morphology within feeding microhabitat-differentiated cichlid species in lake malawi. *Animal Biology*, 54(1):77–90, 2004. doi: 10.1163/157075604323010060.

Eric van den Akker, Catherine Fromental-Ramain, Wim de Graaff, Hervé Le Mouellic, Philippe Brûlet, Pierre Chambon, and Jacqueline Deschamps. Axial skeletal patterning in mice lacking all paralogous group 8 hox genes. *Development*, 128(10):1911–1921, 2001. doi: 10.1242/dev.128.10.1911.

R. C. Albertson and T. D. Kocher. Assessing morphological differences in an adaptive trait: a landmark-based morphometric approach. *The Journal of Experimental Zoology*, 289(6):385–403, 2001. doi: 10.1002/jez.1020.

R Craig Albertson. Morphological divergence predicts habitat partitioning in a lake malawi cichlid species complex. *Copeia*, 2008(3):689–698, 2008. doi: 10.1643/CG-07-217.

Jussi S Alho, Tuomas Leinonen, and Juha Merilä. Inheritance of vertebral number in the three-spined stickleback (gasterosteus aculeatus). *PLoS One*, 6(5):e19579, 2011. doi: 10.1371/journal.pone.0019579.

Melanie Altner, Bernhard Ruthensteiner, and Bettina Reichenbacher. New haplochromine cichlid from the upper miocene (9–10 mya) of central kenya. *BMC Evolutionary Biology*, 20:1–26, 2020. doi: 10.1186/s12862-020-01602-x.

Dieter Anseeuw, Bruno Nevado, Paul Busselen, Jos Snoeks, and Erik Verheyen. Extensive introgression among ancestral mtDNA lineages: Phylogenetic relationships of the utaka

within the lake malawi cichlid flock. *International Journal of Evolutionary Biology*, 2012:1–9, 2012. ISSN 2090-8032, 2090-052X. doi: 10.1155/2012/865603.

Alexander Apschner, Stefan Schulte-Merker, and P Eckhard Witten. Not all bones are created equal–using zebrafish and other teleost species in osteogenesis research. In *Methods in cell biology*, volume 105, pages 239–255. Elsevier, 2011. doi: 10.1016/B978-0-12-381320-6.00010-2.

Viviana Astudillo-Clavijo, Melanie LJ Stiassny, Katriina L Ilves, Zuzana Musilova, Walter Salzburger, and Hernán López-Fernández. Exon-based phylogenomics and the relationships of african cichlid fishes: tackling the challenges of reconstructing phylogenies with repeated rapid radiations. *Systematic Biology*, 72(1):134–149, 2023. doi: 10.1093/sysbio/syac051.

Erica K Baken, Michael L Collyer, Antigoni Kaliontzopoulou, and Dean C Adams. geomorph v4. 0 and gmshiny: Enhanced analytics and a new graphical interface for a comprehensive morphometric experience. *Methods in Ecology and Evolution*, 12(12): 2355–2363, 2021. doi: 10.1111/2041-210X.13723.

Dana Baxter, Karly E Cohen, Cassandra M Donatelli, and Eric D Tytell. Internal vertebral morphology of bony fishes matches the mechanical demands of different environments. *Ecology and Evolution*, 12(11):e9499, 2022. doi: 10.1002/ece3.9499.

Jeremy M Beaulieu and Brian C O'Meara. Detecting hidden diversification shifts in models of trait-dependent speciation and extinction. *Systematic biology*, 65(4):583–601, 2016. doi: 10.1093/sysbio/syw022.

Simon P Blomberg, Theodore Garland Jr, and Anthony R Ives. Testing for phylogenetic signal in comparative data: behavioral traits are more labile. *Evolution*, 57(4):717–745, 2003. doi: 10.1111/j.0014-3820.2003.tb00285.x.

L. M. Blumer, V. Burskaia, I. Artiushin, J. Saha, J. Camacho Garcia, F. Campuzano Jiménez, A. Hooft van der Huysdynen, J. Elkin, B. Fischer, N. Van Houtte, C. Zhou, S. Gresham, M. Malinsky, T. Linderoth, W. Sawasawa, G. Vernaz, I. Bista, A. Hickey, M. Kucka, S. Louzada, R. Zatha, F. Yang, B. Rusuwa, M. E. Santos, Y. F. Chan, D. A. Joyce, A. Böhne, E. A. Miska, M. Ngochera, G. F. Turner, R. Durbin, and H. Svardal. Introgression dynamics of sex-linked chromosomal inversions shape the malawi cichlid radiation. *Science*, 388(6752):eadr9961, 2025. doi: 10.1126/science.adr9961. URL `https://www.science.org/doi/abs/10.1126/science.adr9961`.

Christine Böhmer, Oliver WM Rauhut, and Gert Wörheide. Correlation between hox code and vertebral morphology in archosaurs. *Proceedings of the Royal Society B: Biological Sciences*, 282(1810):20150077, 2015. doi: 10.1098/rspb.2015.0077.

Ralf Britz and G David Johnson. Occipito-vertebral fusion in ocean sunfishes (teleostei: Tetraodontiformes: Molidae) and its phylogenetic implications. *Journal of Morphology*, 266(1):74–79, 2005. doi: 10.1002/jmor.10366.

Callum V Bucklow, Martin J Genner, George F Turner, James Maclaine, Roger Benson, and Berta Verd. A whole-body micro-ct scan library that captures the skeletal diversity of lake malawi cichlid fishes. *Scientific Data*, 11(1):984, 2024. doi: 10.1038/s41597-024-03687-1.

Marta Carapuço, Ana Nóvoa, Nicoletta Bobola, and Moisés Mallo. Hox genes specify vertebral types in the presomitic mesoderm. *Genes & development*, 19(18):2116–2121, 2005. doi: 10.1101/gad.338705.

Rory T Cerbus, Ichiro Hiratani, and Kyogo Kawaguchi. Homeotic and nonhomeotic patterns in the tetrapod vertebral formula. *Proceedings of the National Academy of Sciences*, 121(47):e2411421121, 2024. doi: 10.1073/pnas.2411421121.

Bodo Christ and Charles P Ordahl. Early stages of chick somite development. *Anatomy and embryology*, 191:381–396, 1995. doi: 10.1007/BF00304424.

Julien Clavel, Gilles Escarguel, and Gildas Merceron. mvmorph: an r package for fitting multivariate evolutionary models to morphometric data. *Methods in Ecology and Evolution*, 6:1311–1319, 2015. doi: 10.1111/2041-210X.12420.

Thomas Claverie and Peter C Wainwright. A morphospace for reef fishes: elongation is the dominant axis of body shape evolution. *PloS one*, 9(11):e112732, 2014. doi: 10.1371/journal.pone.0112732.

Andrew S Cohen, Michael J Soreghan, and Christopher A Scholz. Estimating the age of formation of lakes: an example from lake tanganyika, east african rift system. *Geology*, 21(6):511–514, 1993. doi: 10.1130/0091-7613(1993)021<0511:ETAOFO>2.3.CO;2.

Martin J Cohn and Cheryll Tickle. Developmental basis of limblessness and axial patterning in snakes. *Nature*, 399(6735):474–479, 1999. doi: 10.1038/20944.

Michael L Collyer and Dean C Adams. Rrpp: An r package for fitting linear models to high-dimensional data using residual randomization. *Methods in Ecology and Evolution*, 9(7):1772–1779, 2018. doi: 10.1111/2041-210X.13029.

Andrew J Conith and R Craig Albertson. The cichlid oral and pharyngeal jaws are evolutionarily and genetically coupled. *Nature Communications*, 12(1):5477, 2021. doi: 10.1038/s41467-021-25755-5.

J. Cooke and E.C. Zeeman. A clock and wavefront model for control of the number of repeated structures during animal morphogenesis. *Journal of Theoretical Biology*, 58 (2):455–476, 1976. doi: 10.1016/s0022-5193(76)80131-2.

Katharine E Criswell, Michael I Coates, and J Andrew Gillis. Embryonic development of the axial column in the little skate, leucoraja erinacea. *Journal of Morphology*, 278 (3):300–320, 2017a. doi: 10.1002/jmor.20637.

Katharine E Criswell, Michael I Coates, and J Andrew Gillis. Embryonic origin of the gnathostome vertebral skeleton. *Proceedings of the Royal Society B: Biological Sciences*, 284(1867):20172121, 2017b. doi: 10.1098/rspb.2017.2121.

Katharine E Criswell, Lucy E Roberts, Eve T Koo, Jason J Head, and J Andrew Gillis. hox gene expression predicts tetrapod-like axial regionalization in the skate, leucoraja erinacea. *Proceedings of the National Academy of Sciences*, 118(51):e2114563118, 2021. doi: 10.1073/pnas.2114563118.

Karen D Crow, Peter F Stadler, Vincent J Lynch, Chris Amemiya, and Günter P Wagner. The "fish-specific" hox cluster duplication is coincident with the origin of teleosts. *Molecular Biology and Evolution*, 23(1):121–136, 2006. doi: 10.1093/molbev/msj020.

Adelbert De Clercq, Matthew R Perrott, Peter S Davie, Mark A Preece, Ben Wybourne, Nicole Ruff, Ann Huysseune, and Paul Eckhard Witten. Vertebral column regionalisation in chinook salmon, oncorhynchus tshawytscha. *Journal of anatomy*, 231(4): 500–514, 2017. doi: 10.1111/joa.12655.

Leah DeLorenzo, Destiny Mathews, A Allyson Brandon, Mansi Joglekar, Aldo Carmona Baez, Emily C Moore, Patrick J Ciccotto, Natalie B Roberts, Reade B Roberts, and Kara E Powder. Genetic basis of ecologically relevant body shape variation among four genera of cichlid fishes. *Molecular ecology*, 32(14):3975–3988, 2023. doi: 10.1002/ece3.2823.

Ayas Deniz and Gülsemin ŞEN Ağilkaya. New record of the slender snipe eel, nemichthys scolopaceus (richardson, 1848), from the north-eastern mediterranean sea (büyükeceli coast). *Mediterranean Fisheries and Aquaculture Research*, 1(2):87–91, 2018. doi: 10.32582/aa.63.1.8.

Kristin Dietrich, Imke AK Fiedler, Anastasia Kurzyukova, Alejandra C López-Delgado, Lucy M McGowan, Karina Geurtzen, Chrissy L Hammond, Björn Busse, and Franziska Knopf. Skeletal biology and disease modeling in zebrafish. *Journal of Bone and Mineral Research*, 36(3):436–458, 2020. doi: 10.1002/jbmr.4256.

Baoqing Ding, Daniel W Daugherty, Martin Husemann, Ming Chen, Aimee E Howe, and Patrick D Danley. Quantitative genetic analyses of male color pattern and female mate choice in a pair of cichlid fishes of lake malawi, east africa. *PLoS One*, 9(12):e114798, 2014. doi: 10.1371/journal.pone.0114798.

Cassandra M Donatelli, Alexus S Roberts, Eric Scott, Kylene DeSmith, Dexter Summers, Layanne Abu-Bader, Dana Baxter, Emily M Standen, Marianne E Porter, Adam P Summers, et al. Foretelling the flex—vertebral shape predicts behavior and ecology of fishes. *Integrative and Comparative Biology*, 61(2):414–426, 2021. doi: 10.1093/icb/icab110.

Andreas R Dunz and Ulrich K Schliewen. Molecular phylogeny and revised classification of the haplotilapiine cichlid fishes formerly referred to as "tilapia". *Molecular Phylogenetics and Evolution*, 68(1):64–80, 2013. doi: 10.1016/j.ympev.2013.03.015.

Fabrice Duponchelle, Emmanuel Paradis, Anthony J Ribbink, and George F Turner. Parallel life history evolution in mouthbrooding cichlids from the african great lakes. *Proceedings of the National Academy of Sciences*, 105(40):15475–15480, 2008. doi: 10.1073/pnas.0802343105.

Nicolas Ehemann, Paolo Franchini, Axel Meyer, and C Darrin Hulsey. Meristic co-evolution and genomic co-localization of lateral line scales and vertebrae in central american cichlid fishes. *Ecology and Evolution*, 14(9):e70266, 2024. doi: 10.1002/ece3.70266.

B. N. Evers, H. Madsen, K. M. McKaye, and J. R. Stauffer. The schistosome intermediate host, bulinus nyassanus, is a 'preferred' food for the cichlid fish, trematocranus placodon, at cape maclear, lake malawi. *Annals of Tropical Medicine & Parasitology*, 100(1):75–85, 2006. ISSN 0003-4983. doi: 10.1179/136485906X78553.

Ken BR Ewan and Alan W Everett. Evidence for resegmentation in the formation of the vertebral column using the novel approach of retroviral-mediated gene transfer. *Experimental cell research*, 198(2):315–320, 1992. doi: 10.1016/0014-4827(92)90385-l.

Izeni P Farias, Guillermo Ortí, Iracilda Sampaio, Horacio Schneider, and Axel Meyer. Mitochondrial dna phylogeny of the family cichlidae: monophyly and fast molecular evolution of the neotropical assemblage. *Journal of Molecular Evolution*, 48:703–711, 1999. doi: 10.1007/PL00006514.

Joseph Felsenstein. Phylogenies and quantitative characters. *Annual Review of Ecology and Systematics*, pages 445–471, 1988. doi: 10.1146/annurev.es.19.110188.002305.

Angeleen Fleming, Marcia G Kishida, Charles B Kimmel, and Roger J Keynes. Building the backbone: the development and evolution of vertebral patterning. *Development*, 142(10):1733–1744, 2015. doi: 10.1242/dev.118950.

E Ford. Vertebral variation in teleostean fishes. *Journal of the marine biological association of the United Kingdom*, 22(1):1–60, 1937.

Matt Friedman, Benjamin P Keck, Alex Dornburg, Ron I Eytan, Christopher H Martin, C Darrin Hulsey, Peter C Wainwright, and Thomas J Near. Molecular and fossil evidence place the origin of cichlid fishes long after gondwanan rifting. *Proceedings of the Royal Society B: Biological Sciences*, 280(1770):20131733, 2013. doi: 10.1098/rspb.2013.1733.

Catherine Fromental-Ramain, Xavier Warot, Sudhakar Lakkaraju, Bertrand Favier, Herbert Haack, Céline Birling, Andrée Dierich, Pascal Dollé, and Pierre Chambon. Specific and redundant functions of the paralogous hoxa-9 and hoxd-9 genes in forelimb and axial skeleton patterning. *Development*, 122(2):461–472, 1996. doi: 10.1242/dev.122.2.461.

Koji Fujimura and Norihiro Okada. Development of the embryo, larva and early juvenile of nile tilapia oreochromis niloticus (pisces: Cichlidae). developmental staging system. *Development, growth & differentiation*, 49(4):301–324, 2007. doi: 10.1111/j.1440-169X.2007.00926.x.

Koji Fujimura and Norihiro Okada. Shaping of the lower jaw bone during growth of nile tilapia oreochromis niloticus and a lake victoria cichlid haplochromis chilotes: A geometric morphometric approach. *Development, Growth & Differentiation*, 50(8):653–663, 2008. doi: 10.1111/j.1440-169X.2008.01063.x.

Sergey Gavrilets and Jonathan B. Losos. Adaptive radiation: Contrasting theory with data. *Science*, 323(5915):732–737, 2009. doi: 10.1126/science.1157966.

Martin J Genner and George F Turner. The mbuna cichlids of lake malawi: a model for rapid speciation and adaptive radiation. *Fish and fisheries*, 6(1):1–34, 2005. doi: 10.1111/j.1467-2679.2005.00173.x.

Martin J Genner and George F Turner. Ancient hybridization and phenotypic novelty within lake malawi's cichlid fish radiation. *Molecular Biology and Evolution*, 29(1):195–206, 2012. doi: 10.1093/molbev/msr183.

Martin J Genner, Paul Nichols, Gary R Carvalho, Rosanna L Robinson, Paul W Shaw, Alan Smith, and George F Turner. Evolution of a cichlid fish in a lake malawi satellite lake. *Proceedings of the Royal Society B: Biological Sciences*, 274(1623):2249–2257, 2007. doi: 10.1098/rspb.2007.0619.

Martin J Genner, Benjamin P Ngatunga, Semvua Mzighani, Alan Smith, and George F Turner. Geographical ancestry of lake malawi's cichlid fish diversity. *Biology Letters*, 11(6):20150232, 2015. doi: 10.1098/rsbl.2015.0232.

Amandine Gillet, Katrina E Jones, and Stephanie E Pierce. Repatterning of mammalian backbone regionalization in cetaceans. *Nature Communications*, 15(1):7587, 2024. doi: 10.1002/jez.b.21029.

Céline Gomez, Ertuğrul M Özbudak, Joshua Wunderlich, Diana Baumann, Julian Lewis, and Olivier Pourquié. Control of segment number in vertebrate embryos. *Nature*, 454 (7202):335–339, 2008. doi: 10.1038/nature07020.

David Haberthür, Mikki Law, Kassandra Ford, Marcel Häsler, Ole Seehausen, and Ruslan Hlushchuk. Microtomographic investigation of a large corpus of cichlids. *Plos one*, 18 (9):e0291003, 2023. doi: 10.1371/journal.pone.0291003.

Christoph Hahn, Martin J Genner, George F Turner, and Domino A Joyce. The genomic basis of cichlid fish adaptation within the deepwater "twilight zone" of lake malawi. *Evolution Letters*, 1(4):184–198, 2017. doi: 10.1002/evl3.20.

Luke J Harmon, Jonathan B Losos, T Jonathan Davies, Rosemary G Gillespie, John L Gittleman, W Bryan Jennings, Kenneth H Kozak, Mark A McPeek, Franck Moreno-Roark, Thomas J Near, et al. Early bursts of body size and shape evolution are rare in comparative data. *Evolution*, 64(8):2385–2396, 2010.

Albert G Hayward, Piyush Joshi, and Isaac Skromne. Spatiotemporal analysis of zebrafish hox gene regulation by cdx4. *Developmental Dynamics*, 244(12):1564–1573, 2015. doi: 10.1002/dvdy.24343.

Yichen He, Marco Camaiti, Lucy E Roberts, James M Mulqueeney, Marius Didziokas, and Anjali Goswami. Introducing sprout (semi-automated parcellation of region outputs using thresholding): an adaptable computer vision tool to generate 3d segmentations. *bioRxiv*, pages 2024–11, 2024. doi: 10.1101/2024.11.22.624847.

Jason J Head and P David Polly. Evolution of the snake body form reveals homoplasy in amniote hox gene function. *Nature*, 520(7545):86–89, 2015. doi: 10.1038/nature14042.

Simone Hoegg, Jeffrey L Boore, Jennifer V Kuehl, and Axel Meyer. Comparative phylogenomic analyses of teleost fish hox gene clusters: lessons from the cichlid fish astatotilapia burtoni. *BMC genomics*, 8:1–16, 2007. doi: 10.1186/1471-2164-8-317.

S Holzberg. A field and laboratory study of the behaviour and ecology of pseudotropheus zebra (boulenger), an endemic cichlid of lake malawi (pisces; cichlidae). *Journal of*

Zoological Systematics and Evolutionary Research, 16(3):171–187, 1978. doi: 10.1111/j.1439-0469.1978.tb00929.x.

Sirkka Liisa Hostikka, Jun Gong, and Ellen M Carpenter. Axial and appendicular skeletal transformations, ligament alterations, and motor neuron loss in hoxc10 mutants. *International journal of biological sciences*, 5(5):397, 2009. doi: 10.7150/ijbs.5.397.

Zongshan Hu, Zhen Zhang, Zhihui Zhao, Zezhang Zhu, Zhen Liu, and Yong Qiu. A neglected point in surgical treatment of adolescent idiopathic scoliosis: variations in the number of vertebrae. *Medicine*, 95(34):e4682, 2016. doi: 10.1097/MD.0000000000004682.

C. Darrin Hulsey, Michael E. Alfaro, Jimmy Zheng, Axel Meyer, and Roi Holzman. Pleiotropic jaw morphology links the evolution of mechanical modularity and functional feeding convergence in lake malawi cichlids. *Proceedings of the Royal Society B: Biological Sciences*, 286(1897):20182358, 2019. doi: 10.1098/rspb.2018.2358.

Martin Husemann, Michael Tobler, Cagney McCauley, Baoqing Ding, and Patrick D Danley. Body shape differences in a pair of closely related malawi cichlids and their hybrids: Effects of genetic variation, phenotypic plasticity, and transgressive segregation. *Ecology and Evolution*, 7(12):4336–4346, 2017. doi: 10.1002/ece3.2823.

Tadahiro Iimura, Nicolas Denans, and Olivier Pourquié. Establishment of hox vertebral identities in the embryonic spine precursors. *Current topics in developmental biology*, 88:201–234, 2009. doi: 10.1016/S0070-2153(09)88007-1.

Iker Irisarri, Pooja Singh, Stephan Koblmüller, Julián Torres-Dowdall, Frederico Henning, Paolo Franchini, Christoph Fischer, Alan R Lemmon, Emily Moriarty Lemmon, Gerhard G Thallinger, et al. Phylogenomics uncovers early hybridization and adaptive loci shaping the radiation of lake tanganyika cichlid fishes. *Nature communications*, 9 (1):3159, 2018. doi: 10.1038/s41467-018-05479-9.

Laith A Jawad, Fawziah Sh Habbeb, and Mustafa A Al-Mukhtar. Some osteological studies of coptodon zillii (gervais 1848) and oreochromis aureus (steindachner 1864) collected shatt al-arab river, basrah, iraq. *International Journal of Marine Science*, 8 (4):26, 2018. doi: 10.5376/ijms.2018.08.0004.

Yordano E Jimenez, Kelsey N Lucas, John H Long Jr, and Eric D Tytell. Flexibility is a hidden axis of biomechanical diversity in fishes. *Journal of Experimental Biology*, 226 (Suppl_1):jeb245308, 2023. doi: 10.1242/jeb.245308.

Katrina E Jones, Kenneth D Angielczyk, P David Polly, Jason J Head, Vincent Fernandez, Jacqueline K Lungmus, Sarah Tulga, and Stephanie E Pierce. Fossils reveal the

complex evolutionary history of the mammalian regionalized spine. *Science*, 361(6408): 1249–1252, 2018a. doi: 10.1126/science.aar3126.

Katrina E Jones, Lorena Benitez, Kenneth D Angielczyk, and Stephanie E Pierce. Adaptation and constraint in the evolution of the mammalian backbone. *BMC evolutionary biology*, 18:1–13, 2018b. doi: 10.1186/s12862-018-1282-2.

Daud Kassam, Shingo Seki, Bosco Rusuwa, Aggrey JD Ambali, and Kosaku Yamaoka. Genetic diversity within the genus cynotilapia and its phylogenetic position among lake malawi's mbuna cichlids. *African Journal of Biotechnology*, 4(10), 2005. doi: 10.4314/ajb.v4i10.71319.

Benjamin P Keck and C Darrin Hulsey. Continental monophyly of cichlid fishes and the phylogenetic position of heterochromis multidens. *Molecular Phylogenetics and Evolution*, 73:53–59, 2014. doi: 10.1016/j.ympev.2014.01.011.

Stephan Koblmüller, Ulrich K Schliewen, Nina Duftner, Kristina M Sefc, Cyprian Katongo, and Christian Sturmbauer. Age and spread of the haplochromine cichlid fishes in africa. *Molecular Phylogenetics and Evolution*, 49(1):153–169, 2008. doi: 10.1016/j.ympev.2008.05.045.

Ad Konings. *Malawi Cichlids in their Natural Habitat*. Cichlid Press, 5th edition, 2016. ISBN 978-1-932892-23-9.

Nikesh M Kumar, Taylor L Cooper, Thomas D Kocher, J Todd Streelman, and Patrick T McGrath. Large inversions in lake malawi cichlids are associated with habitat preference, lineage, and sex determination. *bioRxiv*, pages 2024–10, 2025. doi: 10.7554/eLife.104923.2.

Pierre Le Pabic, Edmund J Stellwag, Shelby N Brothers, and Jean-Luc Scemama. Comparative analysis of hox paralog group 2 gene expression during nile tilapia (oreochromis niloticus) embryonic development. *Development genes and evolution*, 217:749–758, 2007. doi: 10.1007/s00427-007-0182-z.

Karel F Liem and S Laurie Sanderson. The pharyngeal jaw apparatus of labrid fishes: a functional morphological perspective. *Journal of Morphology*, 187(2):143–158, 1986. doi: 10.1002/jmor.1051870203.

Maria C Malabarba, Luiz R Malabarba, and Hernán López-Fernández. On the eocene cichlids from the lumbrera formation: additions and implications for the neotropical ichthyofauna. *Journal of Vertebrate Paleontology*, 34(1):49–58, 2014. doi: 10.1080/02724634.2013.830021.

Milan Malinsky, Hannes Svardal, Alexandra M Tyers, Eric A Miska, Martin J Genner, George F Turner, and Richard Durbin. Whole-genome sequences of malawi cichlids reveal multiple radiations interconnected by gene flow. *Nature ecology & evolution*, 2 (12):1940–1955, 2018. doi: 10.1038/s41559-018-0717-x.

Aleksandra Marconi, Cassandra Zie Yang, Samuel McKay, and M Emília Santos. Morphological and temporal variation in early embryogenesis contributes to species divergence in malawi cichlid fishes. *Evolution & Development*, 25(2):170–193, 2023. doi: 10.1111/ede.12429.

Ryan D Marek, Peter L Falkingham, Roger BJ Benson, James D Gardiner, Thomas W Maddox, and Karl T Bates. Evolutionary versatility of the avian neck. *Proceedings of the Royal Society B*, 288(1946):20203150, 2021. doi: 10.1098/rspb.2020.3150.

Miguel Maroto, Robert A Bone, and J Kim Dale. Somitogenesis. *Development*, 139(14): 2453–2456, 2012. doi: 10.1242/dev.069310.

A.C. Marsh. A taxonomic study of the fish genus petrotilapia (pisces: Cichlidae) from lake malawi. *Ichthyological Bulletin of the J.L.B. Smith Institute of Ichthyology*, 48(3): 1–14, 1983.

Paul Masonick, Axel Meyer, and Christopher Darrin Hulsey. Phylogenomic analyses show repeated evolution of hypertrophied lips among lake malawi cichlid fishes. *Genome Biology and Evolution*, 14(4):evac051, 2022. doi: 10.1111/jfb.15848.

Michael Matschiner. Gondwanan vicariance or trans-atlantic dispersal of cichlid fishes: a review of the molecular evidence. *Hydrobiologia*, 832:9–37, 2019. doi: 10.1007/s10750-018-3686-9.

Michael Matschiner, Astrid Böhne, Fabrizia Ronco, and Walter Salzburger. The genomic timeline of cichlid fish diversification across continents. *Nature communications*, 11(1): 5895, 2020. doi: 10.1038/s41467-020-17827-9.

Matthew D McGee, Samuel R Borstein, Joana I Meier, David A Marques, Salome Mwaiko, Anthony Taabu, Mary A Kishe, Brian O'Meara, Rémy Bruggmann, Laurent Excoffier, et al. The ecological and genomic basis of explosive adaptive radiation. *Nature*, 586(7827):75–79, 2020. doi: 10.1038/s41586-020-2652-7.

Rita S Mehta, Andrea B Ward, Michael E Alfaro, and Peter C Wainwright. Elongation of the body in eels. *Integrative and Comparative Biology*, 50(6):1091–1105, 2010. doi: 10.1111/bij.12098.

Joana I Meier, David A Marques, Salome Mwaiko, Catherine E Wagner, Laurent Excoffier, and Ole Seehausen. Ancient hybridization fuels rapid cichlid fish adaptive radiations. *Nature communications*, 8(1):14363, 2017. doi: 10.1038/ncomms14363.

David Thomas Mellor, CM Tarsiewicz, and RC Jordan. Female maylandia zebra prefer victorious males. *Journal of Fish Biology*, 78(2):680–687, 2011. doi: 10.1111/j.1095-8649.2010.02884.x.

Britta S Meyer, Michael Matschiner, and Walter Salzburger. Disentangling incomplete lineage sorting and introgression to refine species-tree estimates for lake tanganyika cichlid fishes. *Systematic Biology*, 66(4):531–550, 2017. doi: 10.1093/sysbio/syw069.

Elizabeth M Morin-Kensicki, Ellie Melancon, and Judith S Eisen. Segmental relationship between somites and vertebral column in zebrafish. *Development*, 2002. doi: 10.1242/dev.129.16.3851.

Alison M Murray. Eocene cichlid fishes from tanzania, east africa. *Journal of Vertebrate Paleontology*, 20(4):651–664, 2001a. doi: 10.1671/0272-4634(2000)020[0651:ECFFTE]2.0.CO;2.

Alison M Murray. The oldest fossil cichlids (teleostei: Perciformes): indication of a 45 million-year-old species flock. *Proceedings of the Royal Society of London. Series B: Biological Sciences*, 268(1468):679–684, 2001b. doi: 10.1098/rspb.2000.1570.

Sundar Ram Naganathan and Andrew Charles Oates. Patterning and mechanics of somite boundaries in zebrafish embryos. In *Seminars in cell & developmental biology*, volume 107, pages 170–178. Elsevier, 2020. doi: 10.1016/j.semcdb.2020.04.014.

Yuichi Narita and Shigeru Kuratani. Evolution of the vertebral formulae in mammals: a perspective on developmental constraints. *Journal of Experimental Zoology Part B: Molecular and Developmental Evolution*, 304(2):91–106, 2005. doi: 10.1002/jez.b.21029.

Thomas J Near and Christine E Thacker. Phylogenetic classification of living and fossil ray-finned fishes (actinopterygii). *Bulletin of the Peabody Museum of Natural History*, 65(1):3–302, 2024. doi: 10.3374/014.065.0101.

Jindřich Novák, Daniel Frynta, Daniela Nováková, and Jiří Patoka. Social deprivation in maternal mouthbrooders tropheus sp.“caramba”(teleostei: Cichlidae) decreases the success rate of reproduction and survival rate of fish fry. *Scientific Reports*, 13(1):8284, 2023. doi: 10.1038/s41598-023-35467-z.

Michael K Oliver. African cichlid fishes: morphological data and taxonomic insights from a genus-level survey of supraneurals, pterygiophores, and vertebral counts (ovalentaria,

blenniiformes, cichlidae, pseudocrenilabrinae). *Biodiversity Data Journal*, 12:e130707, 2024. doi: 10.3897/BDJ.12.e130707.

David Orme, Rob Freckleton, Gavin Thomas, Thomas Petzoldt, Susanne Fritz, Nick Isaac, and Will Pearse. *caper: Comparative Analyses of Phylogenetics and Evolution in R*, 2018. URL `https://CRAN.R-project.org/package=caper`. R package version 1.0.1.

Mark Pagel. Inferring evolutionary processes from phylogenies. *Zoologica Scripta*, 26(4): 331–348, 1997. doi: 10.1111/j.1463-6409.1997.tb00423.x.

Mark Pagel. Inferring the historical patterns of biological evolution. *Nature*, 401(6756): 877–884, 1999. doi: 10.1038/44766.

Isabel Palmeirim, Domingos Henrique, David Ish-Horowicz, and Olivier Pourquié. Avian hairy gene expression identifies a molecular clock linked to vertebrate segmentation and somitogenesis. *Cell*, 91:639–648, 1997. doi: 10.1016/s0092-8674(00)80451-1.

Paul J Parsons, Jon R Bridle, Lukas Rüber, and Martin J Genner. Evolutionary divergence in life history traits among populations of the lake malawi cichlid fish astatotilapia calliptera. *Ecology and evolution*, 7(20):8488–8506, 2017. doi: 10.1002/ece3.3311.

Colin Patterson and G David Johnson. The intermuscular bones and ligaments of teleostean fishes. *Smithsonian Contributions to Zoology*, 559:1–83, 1995. doi: 10.5479/si.00810282.559.

Matthew W Pennell, Luke J Harmon, and Josef C Uyeda. Is there room for punctuated equilibrium in macroevolution? *Trends in ecology & evolution*, 29(1):23–32, 2014. doi: 10.1016/j.tree.2013.07.004.

Cathrin Pfaff, Roberto Zorzin, and Jürgen Kriwet. Evolution of the locomotory system in eels (teleostei: Elopomorpha). *BMC Evolutionary Biology*, 16:1–11, 2016. doi: 10.1186/s12862-016-0728-7.

Nadine Piekarski and Lennart Olsson. Muscular derivatives of the cranialmost somites revealed by long-term fate mapping in the mexican axolotl (ambystoma mexicanum). *Evolution & development*, 9(6):566–578, 2007. doi: 10.1111/j.1525-142X.2007.00197.x.

Nadine Piekarski and Lennart Olsson. Resegmentation in the mexican axolotl, ambystoma mexicanum. *Journal of Morphology*, 275(2):141–152, 2014. doi: 10.1002/jmor.20204.

Max Poll. Classification des cichlidae du lac tanganika. tribus, genres et espèces. *Acad R Belg Mem Cl Sci*, 45:1–163, 1986.

SA Price, ST Friedman, and PC Wainwright. How predation shaped fish: the impact of fin spines on body form evolution across teleosts. *Proceedings of the Royal Society B: Biological Sciences*, 282(1819):20151428, 2015. doi: 10.1098/rspb.2015.1428.

Liam J Revell. Size-correction and principal components for interspecific comparative studies. *Evolution*, 63(12):3258–3268, 2009. doi: 10.1111/j.1558-5646.2009.00804.x.

A.J. Ribbink, B.A. Marsh, A.C. Marsh, A.C. Ribbink, and B.J. Sharp. A preliminary survey of the cichlid fishes of rocky habitats in lake malawi. *South African Journal of Zoology*, 18(3):149–310, 1983. doi: 10.1080/02541858.1983.11447831.

Filippo M Rijli, Robert Matyas, Massimo Pellegrini, Andree Dierich, Peter Gruss, Pascal Dollé, and Pierre Chambon. Cryptorchidism and homeotic transformations of spinal nerves and vertebrae in hoxa-10 mutant mice. *Proceedings of the National Academy of Sciences*, 92(18):8185–8189, 1995. doi: 10.1073/pnas.92.18.8185.

Fabrizia Ronco, Heinz H Büscher, Adrian Indermaur, and Walter Salzburger. The taxonomic diversity of the cichlid fish fauna of ancient lake tanganyika, east africa. *Journal of Great Lakes Research*, 46(5):1067–1078, 2020. doi: 10.1016/j.jglr.2019.05.009.

Fabrizia Ronco, Michael Matschiner, Astrid Böhne, Anna Boila, Heinz H Büscher, Athimed El Taher, Adrian Indermaur, Milan Malinsky, Virginie Ricci, Ansgar Kahmen, et al. Drivers and dynamics of a massive adaptive radiation in cichlid fishes. *Nature*, 589(7840):76–81, 2021. doi: 10.1038/s41586-020-2930-4.

Walter Salzburger. Understanding explosive diversification through cichlid fish genomics. *Nature Reviews Genetics*, 19(11):705–717, 2018. doi: 10.1038/s41576-018-0043-9.

Walter Salzburger, Tanja Mack, Erik Verheyen, and Axel Meyer. Out of tanganyika: genesis, explosive speciation, key-innovations and phylogeography of the haplochromine cichlid fishes. *BMC evolutionary biology*, 5:1–15, 2005. doi: 10.1186/1471-2148-5-17.

Murugesan Sankar, Harald Kryvi, Thomas WK Fraser, Antony J Prabhu Philip, Sofie Remø, Tom J Hansen, Paul Eckhard Witten, and Per Gunnar Fjelldal. A new method for regionalization of the vertebral column in salmonids based on radiographic hallmarks. *Journal of Fish Biology*, 105(4):1189–1199, 2024. doi: 10.1111/jfb.15873.

M Emília Santos, João F Lopes, and Claudius F Kratochwil. East african cichlid fishes. *EvoDevo*, 14(1):1, 2023.

Darien R Satterfield, Thomas Claverie, and Peter C Wainwright. Body shape and mode of propulsion do not constrain routine swimming in coral reef fishes. *Functional Ecology*, 37(2):343–357, 2023. doi: 10.1111/1365-2435.14227.

Jean-Luc Scemama, Jamie L Vernon, and Edmund J Stellwag. Differential expression of hoxa2a and hoxa2b genes during striped bass embryonic development. *Gene expression patterns*, 6(8):843–848, 2006. doi: 10.1016/j.modgep.2006.02.004.

Christopher Scharpf. Scantily clad but not naked: an analysis of the metriaclima vs. maylandia (teleostei: Cichlidae) debate. *Zootaxa*, 5620(3):461–469, 2025. doi: 10.11646/zootaxa.5620.3.5.

Frederic Dieter Benedikt Schedel, Zuzana Musilova, and Ulrich Kurt Schliewen. East african cichlid lineages (teleostei: Cichlidae) might be older than their ancient host lakes: new divergence estimates for the east african cichlid radiation. *BMC Evolutionary Biology*, 19:1–25, 2019. doi: 10.1186/s12862-019-1417-0.

Ralf F Schneider, Joost M Woltering, Dominique Adriaens, and Olivia Roth. A comparative analysis of the ontogeny of syngnathids (pipefishes and seahorses) reveals how heterochrony contributed to their diversification. *Developmental Dynamics*, 252(5):553–588, 2023. doi: 10.1002/dvdy.551.

Oliver Martin Selz and Ole Seehausen. Interspecific hybridization can generate functional novelty in cichlid fish. *Proceedings of the Royal Society B*, 286(1913):20191621, 2019. doi: 10.1098/rspb.2019.1621.

Maja Slijepčević, Frietson Galis, Jan W Arntzen, and Ana Ivanović. Homeotic transformations and number changes in the vertebral column of triturus newts. *PeerJ*, 3:e1397, 2015. doi: 10.7717/peerj.1397.

CM Small, S Bassham, J Catchen, A Amores, AM Fuiten, RS Brown, AG Jones, and WA Cresko. The genome of the gulf pipefish enables understanding of evolutionary innovations. *Genome biology*, 17:1–23, 2016. doi: 10.1186/s13059-016-1126-6.

Kersten M Small and S Steven Potter. Homeotic transformations and limb defects in hox a11 mutant mice. *Genes & development*, 7(12a):2318–2328, 1993. doi: 10.1101/gad.7.12a.2318.

Paolo Sordino, Frank van der Hoeven, and Denis Duboule. Hox gene expression in teleost fins and the origin of vertebrate digits. *Nature*, 375(6533):678–681, 1995. doi: 10.1038/375678a0.

M Alejandra Sosa and Carolina Acosta Hospitaleche. Vertebral formula and numerical variations in the spine of the antarctic and southern south american penguins (aves: Sphenisciformes). *Vertebrate Zoology*, 74:209–219, 2024. doi: 10.3897/vz.74.e114112.

Laura C Soul and Roger BJ Benson. Developmental mechanisms of macroevolutionary change in the tetrapod axis: a case study of sauropterygia. *Evolution*, 71(5):1164–1177, 2017. doi: 10.1111/evo.13217.

Jay Stauffer and Ad Konings. Review of copadichromis (teleostei: Cichlidae) with the description of a new genus and six new species. *Ichthyological Exploration of Freshwaters*, 17(1):9–42, 03 2006.

Jay R Stauffer Jr, Nancy J Bowers, Karen A Kellogg, and Kenneth R McKaye. A revision of the blue-black pseudotropheus zebra (teleostei: Cichlidae) complex from lake malaŵi, africa, with a description of a new genus and ten new species. *Proceedings of the Academy of Natural Sciences of Philadelphia*, pages 189–230, 1997. doi: http://www.jstor.org/stable/4065053.

Melanie Stiassny. Phylogenetic versus convergent relationships between piscivorous cichlid fishes from lakes malawi and tanganyika. *Bulletin of the British Museum (Natural History), Zoology*, 40:67 – 101, 01 1981.

Melanie LJ Stiassny. Cichlid familial intrarelationships and the placement of the neotropical genus cichla (perciformes, labroidei). *Journal of Natural History*, 21(5):1311–1331, 1987. doi: 10.1080/00222938700770811.

Melanie LJ Stiassny. Tylochromis: relationships and the phylogenetic status of the african cichlidae. american museum novitates; no. 2993. *American Museum of Natural History*, 1990.

Melanie LJ Stiassny and S Elizabeth Alter. Phylogenetics of teleogramma, a riverine clade of african cichlid fishes, with a description of the deepwater molluskivore—teleogramma obamaorum—from the lower reaches of the middle congo river. *American Museum Novitates*, 2015(3831):1–18, 2015. doi: 10.1206/3831.1.

Todd J Streelman and P Danley. The stages of vertebrate evolutionary radiation. *Trends in Ecology & Evolution*, 18(3):126–131, 2003. doi: 10.1016/S0169-5347(02)00036-8.

Yong-Hua Sun, Shang-Ping Chen, Ya-Ping Wang, Wei Hu, and Zuo-Yan Zhu. Cytoplasmic impact on cross-genus cloned fish derived from transgenic common carp (cyprinus carpio) nuclei and goldfish (carassius auratus) enucleated eggs. *Biology of reproduction*, 72(3):510–515, 2005. doi: 10.1095/biolreprod.104.031302.

Hannes Svardal, Fu Xiang Quah, Milan Malinsky, Benjamin P Ngatunga, Eric A Miska, Walter Salzburger, Martin J Genner, George F Turner, and Richard Durbin. Ancestral hybridization facilitated species diversification in the lake malawi cichlid fish adaptive radiation. *Molecular biology and evolution*, 37(4):1100–1113, 2020. doi: 10.1093/molbev/msz294.

Hannes Svardal, Walter Salzburger, and Milan Malinsky. Genetic variation and hybridization in evolutionary radiations of cichlid fishes. *Annual Review of Animal Biosciences*, 9:55–79, 2021. doi: 10.1146/annurev-animal-061220-023129.

Ola Svensson, Katie Woodhouse, Cock van Oosterhout, Alan Smith, George F Turner, and Ole Seehausen. The genetics of mate preferences in hybrids between two young and sympatric lake victoria cichlid species. *Proceedings of the Royal Society B: Biological Sciences*, 284(1849):20162332, 2017. doi: doi.org/10.1098/rspb.2016.2332.

Douglas P Swain. The functional basis of natural selection for vertebral traits of larvae in the stickleback gasterosteus aculeatus. *Evolution*, 46(4):987–997, 1992. doi: 10.1111/j.1558-5646.1992.tb00614.x.

Yuichi Takeuchi, Hiroki Hata, Atsushi Maruyama, Takuto Yamada, Takuma Nishikawa, Makiko Fukui, Richard Zatha, Bosco Rusuwa, and Yoichi Oda. Specialized movement and laterality of fin-biting behaviour in genyochromis mento in lake malawi. *Journal of Experimental Biology*, 222(3):jeb191676, 2019. doi: 10.1242/jeb.191676.

Els Thieren, Wim Wouters, Wim Van Neer, and Anton Ervynck. Body length estimation of the european eel anguilla anguilla on the basis of isolated skeletal elements. *Cybium*, 36(4):551–562, 2012.

Petter Tibblin, Hanna Berggren, Oscar Nordahl, Per Larsson, and Anders Forsman. Causes and consequences of intra-specific variation in vertebral number. *Scientific Reports*, 6(1):26372, 2016. doi: 10.1038/srep26372.

G. F. Turner. Description of a commercially important pelagic species of the genus diplotaxodon (pisces: Cichlidae) from lake malawi, africa. *Journal of Fish Biology*, 44 (5):799–807, 1994. ISSN 1095-8649. doi: 10.1111/j.1095-8649.1994.tb01256.x.

George Turner, Benjamin P Ngatunga, and Martin J Genner. The natural history of the satellite lakes of lake malawi. *EcoEvoRxiv*, 2019. doi: 10.32942/osf.io/sehdq.

George Turner, Benjamin P Ngatunga, and Martin J Genner. Astatotilapia species (teleostei, cichlidae) from malawi, mozambique and tanzania, excluding the basin of lake victoria. *EcoEvoRxiv*, 2021. doi: 10.32942/osf.io/eu6rx.

George F. Turner, Ole Seehausen, Mairi E. Knight, Charlotte J. Allender, and Rosanna L. Robinson. How many species of cichlid fishes are there in african lakes? *Molecular Ecology*, 10(3):793–806, 2001. ISSN 1365-294X. doi: 10.1046/j.1365-294x.2001.01200.x.

George F Turner, Denise A Crampton, B Rusuwa, A Hooft van Huysduynen, and H Svardal. Taxonomic investigation of the zooplanktivorous lake malawi cichlids co-

padichromis mloto (iles) and c. virginalis (iles). *Hydrobiologia*, pages 1–11, 2022. doi: 10.1007/s10750-022-05025-1.

GF Turner, RL Robinson, PW Shaw, GR Carvalho, and J Snoeks. Identification and biology of diplotaxodon, rhamphochromis and pallidochromis. In *The Cichlid Diversity of Lake Malawi/Nyasa/Niassa: Identification: Distribution and Taxonomy*, pages 198–251. Cichlid Press, 2004.

Yuu Usui, Naoki Yamane, Akira Hanashima, Ken Hashimoto, Yuji Kanaoka, and Satoshi Mohri. Precaudal vertebrae in the postcranial region of moray eels form ventral processes. *Journal of Morphology*, 285(10):e21776, 2024. doi: 10.1002/jmor.21776.

Josef C Uyeda, Thomas F Hansen, Stevan J Arnold, and Jason Pienaar. The million-year wait for macroevolutionary bursts. *Proceedings of the National Academy of Sciences*, 108(38):15908–15913, 2011. doi: 10.1073/pnas.1014503108.

Andrea B Ward and Elizabeth L Brainerd. Evolution of axial patterning in elongate fishes. *Biological Journal of the Linnean Society*, 90(1):97–116, 2007. doi: 10.1111/j.1095-8312.2007.00714.x.

Andrea B Ward and Nathan J Kley. Effects of precaudal elongation on visceral topography in a basal clade of ray-finned fishes. *The Anatomical Record: Advances in Integrative Anatomy and Evolutionary Biology*, 295(2):289–297, 2012. doi: 10.1002/ar.21491.

Andrea B Ward and Rita S Mehta. Axial elongation in fishes: using morphological approaches to elucidate developmental mechanisms in studying body shape. *Integrative and Comparative Biology*, 50(6):1106–1119, 2010. doi: 10.1093/icb/icq029.

Lizzy Ward, Susan E Evans, and Claudio D Stern. A resegmentation-shift model for vertebral patterning. *Journal of anatomy*, 230(2):290–296, 2017. doi: 10.1111/joa.12540.

Juliane D Weiss, Fenton PD Cotterill, and Ulrich K Schliewen. Lake tanganyika—a'melting pot'of ancient and young cichlid lineages (teleostei: Cichlidae)? *PLoS One*, 10(4):e0125043, 2015. doi: 10.1371/journal.pone.0125043.

Joost M Woltering, Freek J Vonk, Hendrik Müller, Nabila Bardine, Ioana L Tuduce, Merijn AG de Bakker, Walter Knöchel, I Ovidiu Sirbu, Antony J Durston, and Michael K Richardson. Axial patterning in snakes and caecilians: evidence for an alternative interpretation of the hox code. *Developmental biology*, 332(1):82–89, 2009. doi: 10.1016/j.ydbio.2009.04.031.

Joost M Woltering, Michaela Holzem, Ralf F Schneider, Vasilios Nanos, and Axel Meyer. The skeletal ontogeny of astatotilapia burtoni–a direct-developing model system for

the evolution and development of the teleost body plan. *BMC developmental biology*, 18(1):1–23, 2018. doi: 10.1186/s12861-018-0166-4.

Shifeng Xue, Thanh Thao Nguyen Ly, Raunak S Vijayakar, Jingyi Chen, Joel Ng, Ajay S Mathuru, Frederique Magdinier, and Bruno Reversade. Hox epimutations driven by maternal smchd1/lrif1 haploinsufficiency trigger homeotic transformations in genetically wildtype offspring. *Nature Communications*, 13(1):3583, 2022. doi: 10.1038/s41467-022-31185-8.

Kazunori Yamahira, Thomas E Lankford Jr, and David O Conover. Intra-and interspecific latitudinal variation in vertebral number of menidia spp.(teleostei: Atherinopsidae). *Copeia*, 2006(3):431–436, 2006. doi: 10.1643/0045-8511(2006)2006[431:IAILVI]2.0.CO;2.

Zhi Ye and David Kimelman. Hox13 genes are required for mesoderm formation and axis elongation during early zebrafish development. *Development*, 147(22):dev185298, 2020. doi: 10.1242/dev.185298.

8 Supplementary Data

8.1 Species Selection for Geometric Morphometric Analysis

Table S1: Specimen Table of Lake Malawi Cichlids

Species Name	**Ecomorphology**	**Reference**
Alticorpus macrocleithrum	Deep Benthic	Bucklow et al., 2024
Astaotilapia calliptera	*Astatotilapia*	Bucklow et al., 2024
Astatotilapia gigliolii	*Astatotilapia*	Bucklow et al., 2024
Aulonocara nyassae	Deep Benthic	ark:/87602/m4/M123649
Cheliochromis euchilus	Shallow Benthic	Durbin Lab
Chilotilapia rhoadesii	Shallow Benthic	Durbin Lab
Chindongo elongatus	Mbuna	Durbin Lab
Copadichromis chrysonotus	Utaka	Durbin Lab
Copadichromis likomae	Utaka	Bucklow et al., 2024
Copadichromis quadrimaculatus	Utaka	Bucklow et al., 2024
Copadichromis trimaculatus	Utaka	Bucklow et al., 2024
Copadichromis virginalis	Utaka	Bucklow et al., 2024
Cynotilapia afra	Mbuna	Durbin Lab
Dimidiochromis compressiceps	Shallow Benthic	Bucklow et al., 2024
Diplotaxodon aeneus	*Diplotaxodon*	Bucklow et al., 2024
Diplotaxodon argenteus	*Diplotaxodon*	Bucklow et al., 2024
Diplotaxodon limnothrissa	*Diplotaxodon*	Bucklow et al., 2024
Genyochromis mento	Mbuna	Bucklow et al., 2024
Hemitilapia oxrhynchus	Shallow Benthic	Bucklow et al., 2024
Iodotropheus sprengerae	Mbuna	Bucklow et al., 2024
Lethrinops albus	Shallow Benthic	Bucklow et al., 2024
Lethrinops auritus	Shallow Benthic	Bucklow et al., 2024

Continued on next page

Species Name	**Ecomorphology**	**Reference**
Lethrinops gossei	Deep Benthic	Bucklow et al., 2024
Maylandia zebra	Mbuna	Bucklow et al., 2024
Mylochromis anaphyrmus	Shallow Benthic	Bucklow et al., 2024
Nimbochromis linni	Shallow Benthic	Bucklow et al., 2024
Nimbochromis livingstonii	Shallow Benthic	Bucklow et al., 2024
Nimbochromis polystigma	Shallow Benthic	Bucklow et al., 2024
Otopharynx lithobates	Shallow Benthic	Bucklow et al., 2024
Otopharynx speciosus	Shallow Benthic	Bucklow et al., 2024
Otopharynx tetrastigma	Shallow Benthic	Bucklow et al., 2024
Pallidochromis tokolosh	*Diplotaxodon*	Bucklow et al., 2024
Petrotilapia genalutea	Mbuna	Bucklow et al., 2024
Placidochromis electra	Shallow Benthic	Bucklow et al., 2024
Placidochromis johnstoni	Shallow Benthic	Bucklow et al., 2024
Placidochromis milomo	Shallow Benthic	Bucklow et al., 2024
Protomelas spliopterus	Shallow Benthic	Bucklow et al., 2024
Rhamphochromis esox	*Rhamphochromis*	Bucklow et al., 2024
Rhamphochromis ferox	*Rhamphochromis*	Bucklow et al., 2024
Rhamphochromis longiceps	*Rhamphochromis*	Bucklow et al., 2024
Rhamphochromis woodi	*Rhamphochromis*	Bucklow et al., 2024
Stigmatochromis macrorhynchos	Shallow Benthic	Bucklow et al., 2024
Trematocranus placodon	Shallow Benthic	Bucklow et al., 2024
Tropheops tropheops	Mbuna	Bucklow et al., 2024
Tyrannochromis macrostoma	Shallow Benthic	Bucklow et al., 2024

8.2 Principal Component Coordinate Loadings for Vertebral Landmarks

Table S2: Principal Component Coordinate Loadings for Vertebral Landmarks

Vertebrae	Rank	PC	Landmark	Coordinate	Loading
Precaudal	1	1	1	Y	0.693
Precaudal	2	1	1	X	0.205
Precaudal	3	1	17	Y	0.201
Precaudal	4	1	11	Y	0.185
Precaudal	5	1	2	Y	0.154
Precaudal	6	1	27	Y	0.153
Precaudal	7	1	18	Y	-0.147
Precaudal	8	1	17	X	-0.143
Precaudal	9	1	27	X	-0.142
Precaudal	10	1	4	Y	-0.138
Precaudal	1	2	1	Y	-0.323
Precaudal	2	2	17	Y	0.265
Precaudal	3	2	17	Z	-0.256
Precaudal	4	2	17	X	-0.245
Precaudal	5	2	21	Y	-0.221
Precaudal	6	2	1	Z	-0.218
Precaudal	7	2	20	Y	-0.200
Precaudal	8	2	19	Y	-0.195
Precaudal	9	2	16	Z	0.186
Precaudal	10	2	22	Y	-0.179
Precaudal	1	3	1	Z	-0.372
Precaudal	2	3	17	Z	0.354
Precaudal	3	3	20	Z	-0.239
Precaudal	4	3	21	Z	-0.232
Precaudal	5	3	19	Z	-0.221
Precaudal	6	3	13	Z	0.208
Precaudal	7	3	27	Z	0.198
Precaudal	8	3	22	Z	-0.196
Precaudal	9	3	23	Z	-0.171
Precaudal	10	3	15	Z	0.171

Continued on next page

Vertebrae	Rank	PC	Landmark	Coordinate	Loading
Precaudal	1	4	1	X	-0.775
Precaudal	2	4	1	Y	0.250
Precaudal	3	4	10	X	0.177
Precaudal	4	4	9	X	0.173
Precaudal	5	4	8	X	0.164
Precaudal	6	4	4	X	0.155
Precaudal	7	4	5	X	0.134
Precaudal	8	4	3	X	0.133
Precaudal	9	4	16	Z	-0.128
Precaudal	10	4	18	Z	-0.126
Caudal	1	1	1	Y	0.674
Caudal	2	1	17	Y	0.529
Caudal	3	1	17	X	0.242
Caudal	4	1	1	X	-0.195
Caudal	5	1	14	Y	-0.141
Caudal	6	1	12	Y	-0.139
Caudal	7	1	11	X	-0.130
Caudal	8	1	2	X	-0.130
Caudal	9	1	15	Y	-0.117
Caudal	10	1	13	Y	-0.113
Caudal	1	2	17	X	-0.435
Caudal	2	2	16	X	0.334
Caudal	3	2	11	X	-0.297
Caudal	4	2	2	X	-0.263
Caudal	5	2	9	X	0.236
Caudal	6	2	10	X	0.224
Caudal	7	2	13	Y	-0.221
Caudal	8	2	4	X	0.220
Caudal	9	2	14	Y	-0.178
Caudal	10	2	17	Y	0.174
Caudal	1	3	1	X	-0.453
Caudal	2	3	7	X	0.306
Caudal	3	3	6	X	0.283
Caudal	4	3	17	X	-0.283
Caudal	5	3	1	Y	-0.280
Caudal	6	3	3	X	0.264

Continued on next page

Vertebrae	Rank	PC	Landmark	Coordinate	Loading
Caudal	7	3	8	Y	0.261
Caudal	8	3	12	X	0.216
Caudal	9	3	8	X	0.190
Caudal	10	3	16	X	-0.161
Caudal	1	4	1	X	-0.445
Caudal	2	4	2	X	0.397
Caudal	3	4	11	X	0.379
Caudal	4	4	17	Y	0.293
Caudal	5	4	12	X	-0.203
Caudal	6	4	14	X	-0.193
Caudal	7	4	8	Y	-0.187
Caudal	8	4	8	Z	-0.180
Caudal	9	4	9	X	0.159
Caudal	10	4	17	X	-0.148

8.3 Pairwise Comparisons of Vertebral Shape Morphospace Occupation Between Ecomorphological Groups

Table S3: Pairwise comparisons of vertebral shape morphospace occupation among ecomorphological groups (Precaudal).

	Astatotilapia	Deep Benthic	*Diplotaxodon*	Mbuna	*Rhamphochromis*	Shallow Benthic	Utaka
Astatotilapia	1.000	**0.007**	0.175	0.474	0.292	0.071	**0.004**
Deep Benthic	**0.007**	1.000	**0.000**	**0.012**	**0.000**	**0.002**	0.700
Diplotaxodon	0.175	**0.000**	1.000	0.210	0.143	0.325	**0.001**
Mbuna	0.474	**0.012**	0.210	1.000	**0.032**	0.192	**0.009**
Rhamphochromis	0.292	**0.000**	0.143	**0.032**	1.000	**0.002**	**0.000**
Shallow Benthic	**0.071**	**0.002**	0.325	0.192	**0.002**	1.000	**0.006**
Utaka	**0.004**	0.700	**0.001**	**0.009**	**0.000**	**0.006**	1.000

Table S4: Pairwise comparisons of vertebral shape morphospace occupation among ecomorphological groups (Caudal).

	Astatotilapia	Deep Benthic	*Diplotaxodon*	Mbuna	*Rhamphochromis*	Shallow Benthic	Utaka
Astatotilapia	1.000	**0.020**	0.992	0.485	0.663	0.416	**0.022**
Deep Benthic	**0.020**	1.000	**0.001**	**0.006**	**0.000**	**0.008**	0.932
Diplotaxodon	0.992	**0.001**	1.000	0.298	0.545	0.139	**0.001**
Mbuna	0.485	**0.006**	0.298	1.000	**0.053**	0.709	**0.013**
Rhamphochromis	0.663	**0.000**	0.545	**0.053**	1.000	**0.006**	**0.000**
Shallow Benthic	0.416	**0.008**	0.139	0.709	**0.006**	1.000	**0.020**
Utaka	**0.022**	0.932	**0.001**	**0.013**	**0.000**	**0.020**	1.000

8.4 Benthic-Pelagic Axis Occupation Correlates with Vertebral Shape Change

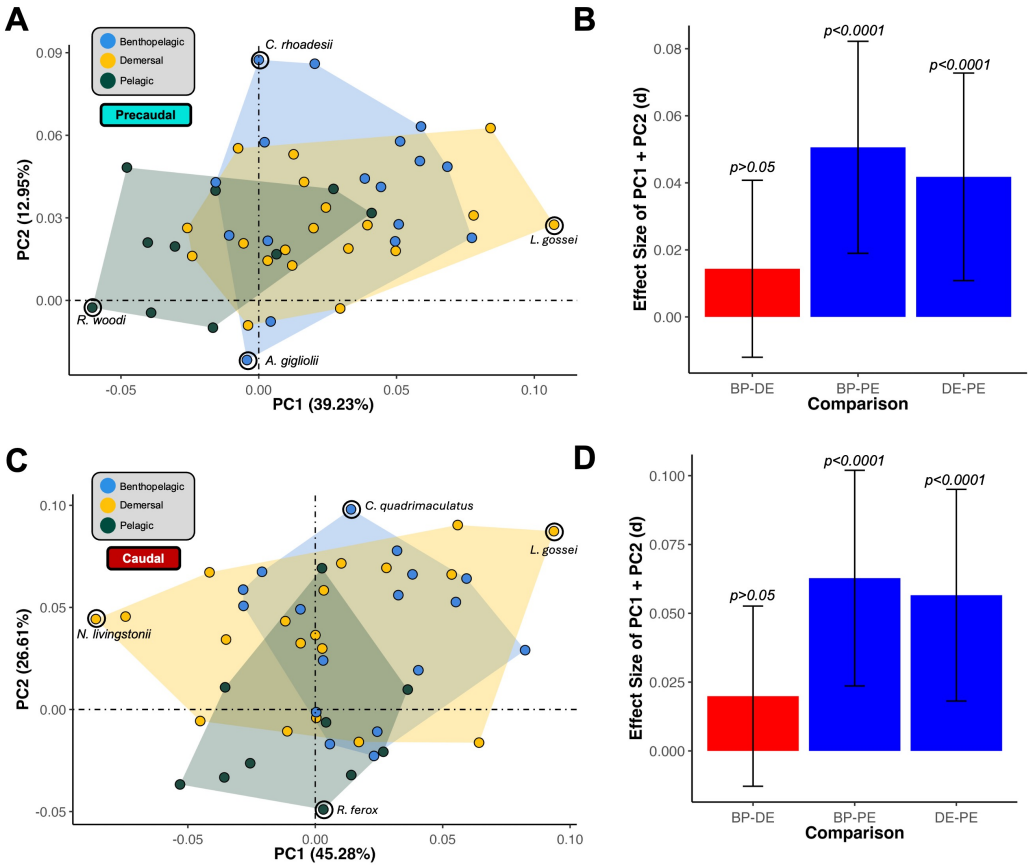

Figure S1: Vertebral shape morphospace occupation across the benthic–pelagic axis. Phylogenetic principal component analyses of vertebral shape for (A) precaudal and (C) caudal vertebrae, showing PC1 versus PC2 for each type. The percentage of variance explained by each axis is indicated. The dotted-dashed lines denote the origin (0,0), representing the mean consensus shape across all species. Species are grouped by benthic-pelagic preference, with convex hulls outlining the morphospace occupied by each group. Species at the extreme of each PC axis are identified. Effect sizes (d) from a MANOVA on PC1 and PC2 for occupation of species along the benthic-pelagic axis are shown for precaudal (B) and caudal vertebrae (D). Significant effects are shown in blue, while non-significant effects are shown in red. Error bars represent the 95% confidence intervals for the effect sizes. P-values for each effect are indicated.

8.5 Piscivores Occupy a Distinct Region of Vertebral Shape Morphospace

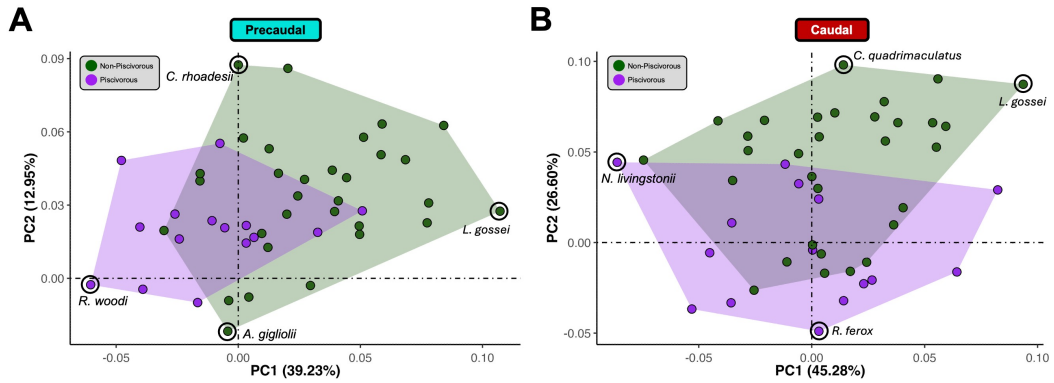

Figure S2: Vertebral shape morphospace occupation across according to piscivory. Phylogenetic principal component analyses of vertebral shape for (A) precaudal and (C) caudal vertebrae, showing PC1 versus PC2 for each type. The percentage of variance explained by each axis is indicated. The dotted-dashed lines denote the origin (0,0), representing the mean consensus shape across all species. Species are grouped piscivory, with convex hulls outlining the morphospace occupied by each group. Species at the extreme of each PC axis are identified.

8.6 Lateral Line Scale Counts in Lake Malawi Cichlids

Table S5: Lateral Line Scale Counts in Lake Malawi Cichlids

Species Name	Min	Max	Median	Reference
Abactochromis labrosus	30	32	31	Oliver and Arnegard 2010
Alticorpus macrocleithrum	30	32	31	Stauffer 1985
Astatotilapia calliptera	29	33	31	Regan 1922
Aulonocara trematocephalum	36	36	36	Eccles and Trewavas 1989
Buccochromis atritaeniatus	33	35	34	Eccles and Trewavas 1989
Buccochromis heterotaenia	35	36	35.5	Eccles and Trewavas 1989
Buccochromis nototaenia	35	37	36	Eccles and Trewavas 1989
Buccochromis oculatus	34	36	35	Eccles and Trewavas 1989
Buccochromis spectabilis	35	37	36	Eccles and Trewavas 1989
Champsochromis caeruleus	37	38	37.5	Eccles and Trewavas 1989
Champsochromis spilorhynchus	36	37	36.5	Eccles and Trewavas 1989
Cheilochromis euchilus	32	32	32	Eccles and Trewavas 1989
Chilotilapia rhoadesii	32	34	33	Regan 1922
Copadichromis chrysonotus	31	34	32.5	Eccles and Trewavas 1989
Copadichromis quadrimaculatus	35	36	35.5	Eccles and Trewavas 1989
Copadichromis trimaculatus	33	35	34	Eccles and Trewavas 1989
Copadichromis virginalis	33	36	34.5	Iles 1960
Ctenopharynx intermedius	34	36	35	Eccles and Trewavas 1989
Ctenopharynx nitidus	32	35	33.5	Eccles and Trewavas 1989
Ctenopharynx pictus	32	34	33	Eccles and Trewavas 1989
Cynotilapia afra	33	33	33	Regan 1922
Cyrtocara moorii	34	36	35	Eccles and Trewavas 1989
Dimidiochromis compressiceps	33	35	34	Eccles and Trewavas 1989
Dimidiochromis kiwinge	34	35	34.5	Eccles and Trewavas 1989
Dimidiochromis strigatus	32	34	33	Eccles and Trewavas 1989
Diplotaxodon argenteus	34	36	35	Trewavas 1935
Diplotaxodon ecclesi	32	33	32.5	Eccles and Trewavas 1989
Diplotaxodon greenwoodi	34	34	34	Stauffer and McKaye 1985
Diplotaxodon limnothrissa	35	41	38	Stauffer, Phiri and Konings 2018
Diplotaxodon macrops	31	35	33	Stauffer, Phiri and Konings 2018

Continued on next page

Species Name	Min	Max	Median	Reference
Docimodus evelynae	34	37	35.5	Eccles and Trewavas 1989
Genyochromis mento	32	33	32.5	Trewavas 1935
Hemitaeniochromis urotaenia	32	33	32.5	Eccles and Trewavas 1989
Hemitilapia oxyrhynchus	33	35	34	Regan 1922
Iodotropheus sprengerae	31	31	31	Oliver and Loiselle 1972
Labeotropheus fuelleborni	31	33	32	Fryer 1956
Labeotropheus trewavasae	33	35	34	Fryer 1956
Labidochromis freibergi	30	31	30.5	Lewis 1982
Labidochromis pallidus	30	31	30.5	Lewis 1982
Labidochromis strigatus	30	32	31	Lewis 1982
Lethrinops albus	34	35	34.5	Eccles and Trewavas 1989
Lethrinops auritus	32	32	32	Regan 1922
Maylandia lanisticola	29	32	30.5	Stauffer 1991
Maylandia zebra	31	31	31	Regan 1922
Mchenga eucinostomus	35	35	35	Regan 1922
Mchenga inornata	34	36	35	Regan 1922
Melanochromis chipokae	32	33	32.5	Konings and Stauffer 2012
Melanochromis loriae	32	34	33	Konings and Stauffer 2012
Melanochromis robustus	31	32	31.5	Konings and Stauffer 2012
Mylochromis guentheri	33	35	34	Regan 1922
Mylochromis melanonotus	34	35	34.5	Regan 1922
Mylochromis plagiotaenia	31	33	32	Regan 1922
Mylochromis sphaerodon	31	32	31.5	Regan 1922
Nimbochromis linni	33	34	33.5	Eccles and Trewavas 1989
Nimbochromis livingstonii	33	35	34	Eccles and Trewavas 1989
Nimbochromis venustus	32	34	33	Eccles and Trewavas 1989
Nyassachromis breviceps	34	36	35	Eccles and Trewavas 1989
Nyassachromis leuciscus	33	36	34.5	Eccles and Trewavas 1989
Nyassachromis microcephalus	35	35	35	Eccles and Trewavas 1989
Nyassachromis nigritaeniatus	33	36	34.5	Eccles and Trewavas 1989
Nyassachromis purpurans	32	35	33.5	Eccles and Trewavas 1989
Otopharynx argyrosoma	34	36	35	Eccles and Trewavas 1989
Otopharynx lithobates	32	35	33.5	Eccles and Trewavas 1989
Otopharynx ovatus	32	34	33	Eccles and Trewavas 1989
Otopharynx speciosus	33	34	33.5	Eccles and Trewavas 1989
Otopharynx tetrastigma	30	33	31.5	Eccles and Trewavas 1989

Continued on next page

Species Name	Min	Max	Median	Reference
Petrotilapia genalutea	29	35	32	Marsh 1983
Placidochromis hennydaviesae	31	33	32	Eccles and Trewavas 1989
Placidochromis johnstoni	31	33	32	Eccles and Trewavas 1989
Placidochromis milomo	31	33	32	Eccles and Trewavas 1989
Placidochromis phenochilus	34	34	34	Eccles and Trewavas 1989
Placidochromis subocularis	32	35	33.5	Eccles and Trewavas 1989
Protomelas annectens	33	36	34.5	Eccles and Trewavas 1989
Protomelas fenestratus	32	32	32	Eccles and Trewavas 1989
Protomelas insignis	33	34	33.5	Eccles and Trewavas 1989
Protomelas kirkii	31	33	32	Eccles and Trewavas 1989
Protomelas spilopterus	31	32	31.5	Eccles and Trewavas 1989
Protomelas taeniolatus	33	33	33	Eccles and Trewavas 1989
Protomelas triaenodon	32	33	32.5	Eccles and Trewavas 1989
Rhamphochromis esox	43	44	43.5	Regan 1922
Rhamphochromis ferox	38	39	38.5	Regan 1922
Rhamphochromis longiceps	36	38	37	Regan 1922
Rhamphochromis woodi	38	40	39	Regan 1922
Sciaenochromis ahli	33	34	33.5	Eccles and Trewavas 1989
Stigmatochromis modestus	32	32	32	Eccles and Trewavas 1989
Taeniolethrinops praeorbitalis	35	36	35.5	Regan 1922
Trematocranus placodon	31	33	32	Eccles and Trewavas 1989
Tropheops tropheops	33	33	33	Regan 1922
Tyrannochromis macrostoma	33	34	33.5	Eccles and Trewavas 1989
Tyrannochromis nigriventer	34	35	34.5	Eccles and Trewavas 1989

"It seems to be a rule, as remarked by Geoffroy Saint-Hilaire, both in varieties and in species, that when any part or organ is repeated many times in the structure of the same individual (as the vertebrae in snakes, and the stamens in polyandrous flowers) the number is variable; whereas the number of the same part or organ, when it occurs in lesser numbers, is constant."

— Charles Darwin, On the Origin of Species